The Current Deflecting Wall

in a Tidal Harbour with Density Influences

Final Report

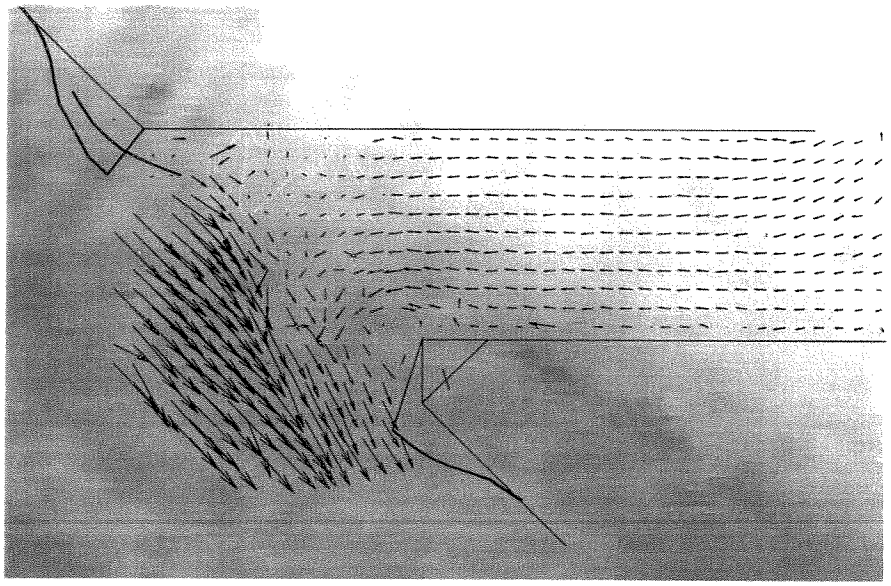

Stijn van Leeuwen
Bas Hofland

November 1999

TU Delft

The Current Deflecting Wall

in a Tidal Harbour with Density Influences

Final Report

C.W. van Leeuwen
B. Hofland

Prepared for WL | Delft Hydraulics

Submitted as a M.Sc.thesis

Thesis Committee:
prof. dr ir J.A. Battjes
dr ir J.C. Winterwerp
dr ir W. Uijttewaal
dr ir C. Kranenburg
ir G.J. Schiereck

Sectie Vloeistofmechanica
Afdeling Waterbouwkunde en Geotechniek
Subfaculteit der Civiele Techniek
Faculteit Civiele Techniek en Geowetenschappen
Technische Universiteit Delft

In the framework of the European Community's
Large Scale Installations and Facilities Programme III

TU Delft

Preface

This final report marks the end of an era, speaking for the two of us. A lifetime ago, August 1993 to be exact, we met during an introduction weekend and started studying Civil Engineering at Delft University of Technology. We were in good company, life was simple & getting good grades did not come too hard. Since we had time to spare, we spent a year as members of the board of the students union in Delft, the Vereniging voor Studie- en Studentenbelangen te Delft. Towards the end of our studies we started to look for a final thesis project. We had developed different interests and were heading off in different directions, only to end up together again. The investigating on the effect of a Current Deflecting Wall under tidal conditions with density influences became our mutual concern. In Dutch there is a saying: 'Samen uit, samen thuis', and we guess there was no avoiding it.

Bas Hofland & Stijn van Leeuwen
Delft, November '99

Abstract

Background

Siltation is a serious problem for harbours situated on tidal rivers and estuaries. Maintenance dredging is necessary on a regular basis to guarantee safe navigation and is often a large cost factor. A means to prevent sediment from entering a harbour is the Current Deflecting Wall (CDW), which passively alters the water exchange at the harbour entrance. The established beneficiary effects of the CDW during rising tide under tidal conditions with homogeneous density are:

- The mixing exchange between harbour and river is reduced.
- The water needed for tidal filling is captured by the CDW from the top layer of river water, which contains less sediment.
- An over-capture of water by the CDW pushes the mixing layer away from the harbour basin.

This final thesis presents the findings of the experiments on the effect of a Current Deflecting Wall on siltation reduction in harbours. The experiments were executed in the tidal flume at Delft Hydraulics. The experiments were conducted in the framework of the European Community's LIP III program.

Aim of the study

The thesis work had the following objectives:

- Quantification of the effect of a CDW on water exchange between harbour and river under quasi-tidal flow and homogeneous conditions (constant water density, constant discharges through the flume and the harbour). These tests were performed during Phase 1.
- Investigation of the influence of a CDW on water exchange between harbour and river under tidal flow and inhomogeneous conditions (salinity gradients). These tests were performed during Phase 2.
- Development of the experimental measurement techniques Dye Concentration Measurements (DCM) and Particle Tracking Velocimetry (PTV) for quantification of water exchange between harbour and river.

The emphasis of the current study was on the second objective because the CDW had not been studied under inhomogeneous conditions before.

Phase 1 experiments

General

The Phase 1 experiments were designed to investigate the effect of a CDW on water exchange between harbour and river for a harbour in a homogeneous environment. Under these conditions the two exchange mechanisms that are responsible for bringing sediment into the harbour are tidal filling and exchange due to turbulent mixing.

All experiments of Phase 1 were executed during the flood period when most exchange between harbour and river occurs. During Phase 1 harbours with a 45° and a 90° angle to the flow direction were investigated. For the 45°-harbour angle the effect of an entrance corner modification was tested as well. Each harbour configuration was tested with and without a CDW present. Two different tidal filling discharges were applied.

Besides the measurements with the experimental techniques velocities, water levels and the extracted discharge from the harbour basin were measured.

Effects of CDW
The CDW used for Phase 1 had a small effect on exchange of water between harbour and river. The flow pattern however does change drastically when a CDW is applied. Velocities in the harbour decrease, and the primary eddy elongates.

With higher sediment concentrations near the bed and the presence of a combination of a CDW and a sill an unaltered (or maybe even increased) exchange of water can still lead to less siltation in the harbour basin. Then only water from the upper water layer, which contains less sediment, is captured and led into the harbour. This effect was not investigated during this research.

Recommendations
For a harbour with tidal movement and a homogeneous environment further research is needed into the possible siltation reduction by a CDW in combination with a sill.

Phase 2 experiments

General
The Phase 2 experiments were designed to investigate the effect of a CDW on water exchange between harbour and river for a harbour in an inhomogeneous environment. Three main exchange mechanisms are responsible for bringing sediment into the harbour under such conditions. Although the magnitudes of the different mechanisms vary continuously over a tidal cycle, and the site-specific circumstances are important, a general order of the relative importance is as follows: exchange due to salinity-induced density currents, exchange due to tidal filling and exchange due to turbulent mixing in the mixing layer. A possible fourth exchange mechanism, density currents due to highly concentrated mud suspensions, was not taken into account.

During Phase 2 only a harbour with a 45° angle to the flow direction was investigated. Besides the measurements with the experimental techniques velocities, water levels, densities (conductivity and temperature) and bottom flow directions were measured.

Flow pattern without a CDW present
A density difference over the harbour entrance is the driving force behind the density current into the harbour. The density current has strong variations over the depth, so the flow pattern in the harbour is three-dimensional. The density current causes flow in opposite directions in the upper and lower water layer of the harbour. The density current is directed into the harbour at the bed from the first half of rising tide to the first half of falling tide.

The largest sediment influx takes place when tidal filling is present and the density current near the bottom is directed into the harbour. This is to a large extent the same period as the period when the CDW operates (flood with high velocities at river).

CDW design for inhomogeneous environment
For the present study H. Christiansen developed a CDW for inhomogeneous conditions. The downstream CDW covered the top half of the water depth, capturing water during the main part of the flood period in order to stop/slow down the outgoing density current through the upper water layer in the harbour. A sill at the bottom of the downstream harbour corner was designed to deflect the near-bed density current away from the harbour. An upstream sill for deflection of near-bed flow during falling tide was studied as well.

Effect of a downstream CDW (downstream sill included)
During rising tide the CDW creates a vertical vortex near the bed with its axis across the harbour entrance width. The vortex is the main cause for the reduction of near bed water influx during rising tide.

The vortex is created by a pressure gradient over the vertical behind the CDW: captured water creates an over-pressure in the upper layer and water deflected by the sill creates an under-pressure in the lower layer.

The CDW and the downstream sill deflect near-bed water, which flows past the harbour entrance. During flood the average decrease of the in-going discharge through the lower 25% of the water column was 40% (calculated from DCM results). Similar results were derived from the density measurements. EMS and PTV measurements show that the total inflow of water does not change much when a CDW is present. This leads to the conclusion that with a CDW present most water flowing into the harbour during rising tide originates from the upper layer in the flume, which is less dense and contains less sediment. A mathematical model confirmed this.

During flood the reduced near-bed exchange, which is caused by the CDW, creates a larger density gradient over the harbour entrance. This causes a slight increase of the density exchange. PTV results and results from the mathematical model confirm this. These results indicate an estimated increase of the density exchange of approximately 5%. This extra exchange starts around the time of high slack water, at the end of the period that the CDW operates, and continues until the average density in the harbour is equal to the level that was present without CDW.

Effect of a CDW with a downstream & an upstream sill
The DCM results show that during flood an additional upstream sill further decreases the average in-going discharge through the lower 25% of the water column to 70%. The maximum decrease of the in-going near-bed discharge through the lower 25% of the water column is 90%. The exact reason for the additional exchange reduction caused by the upstream sill is not yet understood.

During falling tide flow near the bed is deflected by the upstream sill. Salinity and PTV measurements indicate that the over-all effect of the upstream sill during falling tide is an increased exchange.

The density measurements show that with an upstream sill present, the depth-averaged density in the harbour is lower during the entire tidal cycle.

Conclusion from experiments with inhomogeneous flow
A CDW with or without an upstream sill cannot produce enough force to counter the density current. However, a substantial reduction of the influx of near-bed water into the harbour is possible. When sediment concentrations in the lower water layer of the river are higher than in the higher part of the river, this will lead to a decrease in sediment influx. The reduction of the influx of near-bed water was most substantial for the configuration with CDW and upstream sill.

Recommendation
The results show that a reduction of siltation in an estuarine harbour is possible. But for a conclusive answer on the magnitude of this siltation reduction the site-specific conditions of a prototype harbour must be taken into account.

Experimental measurement techniques

The main conclusions that can be drawn from the development of the experimental measuring techniques DCM and PTV are the following:

- DCM is a useful aid in quantifying the effect of a CDW on exchange. However in combination with the software package LOOK&C it is also a laborious method and careful investigation into the effect of the various parameters on the DCM results is essential.
- PTV is a reliable and robust way of measuring velocity distributions. Even in an experiment that was not always set up optimally, because of time pressure and other experiments that had to be taken, good results were obtained.

Table of contents

1. Introduction

1.1. Background

Sedimentation is a serious problem for all harbours around the globe. Especially where harbours are situated on tidal rivers and estuaries, the yearly deposited quantities of sediment deposited in harbour basins can be large. For instance, for the harbour basins of Hamburg, Germany, the sedimentation rate is in the order of 2 million cubic metres per year. The main problem is that sedimentation decreases the depth of the harbour basin, so maintenance dredging is necessary on a regular basis to guarantee safe navigation. When the dredged material is contaminated this can greatly increase the dredging costs. In Hamburg for instance, polluted sediment has to be stored in special areas within the city boundaries.

Maintenance dredging is often a large cost factor in harbour maintenance. A reduction in these maintenance costs would allow the harbour industry in question to be more competitive. Instead of taking the deposited material out of the harbour basin, it would be preferable to prevent the sediment from entering the harbour.

To achieve a reduction in the annual sedimentation rate the causes for the sedimentation have to be known. Sediment is transported into a harbour by various transport mechanisms. The flow patterns are highly complex and of a three-dimensional nature. Extensive research has been carried out in this field. However, detailed knowledge of water motion, needed for a reliable prediction of sedimentation of harbour basins, is still a matter of concern. It is therefore difficult to come up with measures to prevent sedimentation.

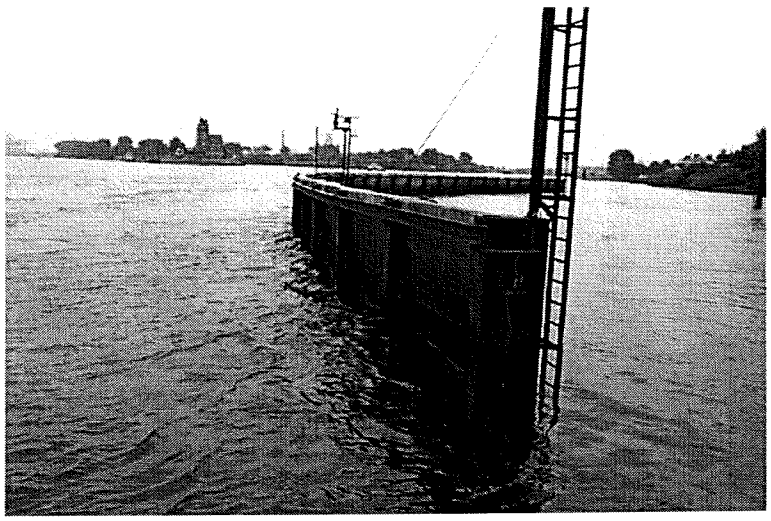

Figure 1.1. The prototype Current Deflecting Wall in the Köhlfleet harbour in Hamburg (C. Kuijper)

A relatively new and promising means to reduce harbour sedimentation is the Current Deflecting Wall (CDW). A CDW controls the entrance flow and alters the flow pattern in such a way that the penetration of suspended sediments into the harbour is substantially reduced. So far the CDW has only been studied under homogeneous conditions, non-tidal and tidal, where the density of the water has been kept constant. A full-scale prototype installed in the port of Hamburg in 1990 has shown the benefits of the CDW in a tidal basin. A hydraulic model study of a second basin in Hamburg gave similar results. Figure 1.1 shows the CDW that was built in the port of Hamburg.

A broader understanding of the effects of entrance flow control by means of a CDW was gained by a study that was part of the European "Large scale facilities and Installations Programme, part II" (LIP II). The experiments were undertaken in the large tidal flume at Delft Hydraulics.

1.2. Aim and scope of the present study

The effects of a CDW under homogeneous conditions have been studied and visualised but still needed quantification. New techniques have been developed recently to quantify the effect of a CDW on sedimentation reduction and were used in the present study.

Secondly, the CDW has until now been studied under steady or tidal flow with homogeneous conditions only, while many harbours around the world have to cope with salinity-induced density currents as well. It is worth investigating whether the CDW can reduce sedimentation under these conditions.

Part of the present study has been carried out as a fulfilment of final thesis work. This thesis work has the following objectives:

- Quantification of the effect of a CDW on water exchange between harbour and river under quasi-tidal flow and homogeneous conditions (constant density of the water, constant discharges through the flume and the harbour);
- Investigation of the influence of a CDW on water exchange between harbour and river under tidal flow and inhomogeneous conditions (salinity gradients);
- Development of the methods Dye Concentration Measurements and Particle Tracking for quantification of water exchange between harbour and river.

The ultimate aim of research on the CDW was the investigation of the effect of a CDW on *siltation* reduction in harbour basins. This siltation is mostly due to mud. The use of mud in a physical model would determine the exact effect of a CDW on siltation. Unfortunately the use of sediment in flume studies or model studies is difficult. Therefore only the exchange of water was determined in this research. For the tests with tidal inhomogeneous conditions a distinction was made between the total exchange of water between harbour and river, and the exchange of near-bed water between harbour and river. This will help to relate the water exchange to the actual sediment exchange in real harbour and river systems. The first three exchange mechanisms mentioned in 2.1 can be linked to the water movement and will be investigated.

The third phase of the European Union's Large scale facilities and Installations Programme (LIP III) has provided the means to work on both quantification of CDW-effects and to study the performance of a CDW with a density driven current present.

This report presents the final thesis work as the joint effort of two master students, B. Hofland and C.W. van Leeuwen of Delft University of Technology, who performed the LIP III studies on the CDW in close co-operation with R.A. Crowder, Ph.D. student at Bradford University. Each student carried the main responsibility for one of the major measuring techniques. In particular: B. Hofland for Particle Tracking and C.W. van Leeuwen for Dye Concentration Measurements.

1.3. Approach of the present study

Laboratory experiments were carried out at the Tidal Flume of Delft Hydraulics to study the effect of a CDW under various conditions. The study looked into the different mechanisms of exchange, their interactions, their relative importance, and the influence of a CDW on them.

The experiments were carried out in two phases:

- Phase 1: tests with several CDWs under quasi-tidal homogeneous conditions;
- Phase 2: tests with a particular CDW under tidal inhomogeneous conditions.

The set-upof this report is as follows. The mechanisms of exchange of water and matter between harbour and river are discussed in chapter 2. Chapter 3 gives a full description of the CDW in general, the various modifications for different circumstances and their (supposed) effect on exchange between harbour and river. In chapter 4 the flume and its facilities are described and the measurement program is given.

The chapters 5, 6 and 7 deal with the measurement techniques that have been used. Chapter 5 elaborates on the measurement techniques in general, followed by chapters 6 and 7 on the development of the Dye Concentration Measurement technique and the Particle Tracking Velocimetry technique respectively.

The results, conclusions and recommendations of the present study can be found in the last part of the report. Chapter 8 handles the results of the phase 1 tests with homogeneous conditions. Chapter 9 follows with the results of the phase 2 tests with inhomogeneous conditions. The conclusions, discussion and the recommendations for further research are given in chapter 10.

2. Exchange Mechanisms and Siltation

2.1. Introduction

The combined flow mechanisms in a harbour entrance may result in a net transport of sediment into the harbour and sedimentation of the harbour basin. Four main flow mechanisms can be distinguished that induce an exchange of matter between harbour and river; see Schlichting (1965), Booij (1986), Langendoen (1992):

- Exchange in consequence of a velocity difference between flow in the river along the harbour entrance and flow in the harbour (mixing layer);
- Exchange in consequence of a net flow through the harbour entrance (tidal filling);
- An exchange flow driven by a density difference between water in the harbour and river-water.
- Gravity currents generated by near-bed, high concentrations of suspended solids or fluid mud.

In sections 2.2 to 2.4 the first three main mechanisms of exchange of matter between river and harbour are discussed. Each section describes one mechanism that is not being influenced by another. Expressions of the magnitudes of the exchange are given as found in the literature. In section 2.5 the interactions between the three mechanisms are considered. The fourth exchange mechanism, a sediment-induced gravity current, is not discussed, as it was not present in the physical model that was investigated. Section 2.6 deals with mud.

2.2. Flow in the harbour entrance

2.2.1. The mixing layer

When the angle between harbour entrance and river bank exceeds about 6° (away from the orientation of flow in the flume, flow separation occurs at the harbour entrance corner (Booij, 1986). See the left side of figure 2.1 for an illustration. The flow separation is due to the fact that the flow in the river is not able to follow the sudden increase in width of the river profile at the location of the harbour entrance. The flow velocity in the harbour is usually smaller than that in the river. Because a system of two parallel streams with different flow velocities is subject to Kelvin-Helmholtz instability, wave-like disturbances arise that grow in the positive x-direction and roll-up to become vortices that form the mixing layer.

It is found that a plane mixing layer between two uniform parallel streams spreads linearly. Brown & Roshko (1974) give for a two-dimensional mixing layer (assuming infinite depth):

$$\frac{d\delta}{dx} = 0.181\frac{u_r - u_h}{u_r + u_h} = 0.181\lambda \qquad \text{Equation 2.1}$$

where x is the co-ordinate in the direction of the flume, u_r the water velocity in the river, u_h the water velocity in the harbour, λ the relative velocity difference and δ the width of the mixing layer. It should be mentioned that the spreading of a mixing layer is very sensitive to the conditions present at the origin of flow separation.

In a harbour entrance, part of the mixing layer is blocked by the opposite harbour wall. See figure 2.1 for an illustration at the right hand side of the harbour. In the figure the resulting flow pattern in a harbour entrance (averaged over time) is illustrated.

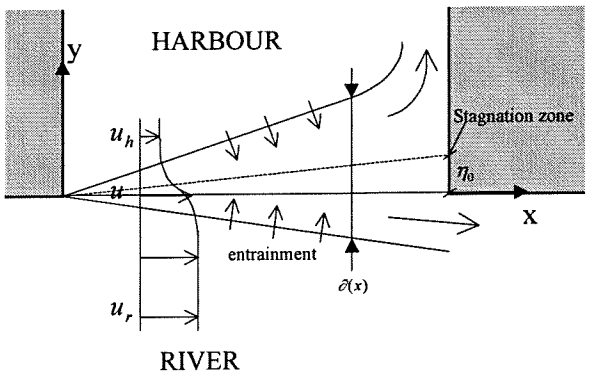

Figure 2.1. The mixing layer in the harbour entrance

Assuming that the flow velocity in the river is constant outside the mixing layer and the flow velocity in the mixing layer is smaller than that of the river, conservation of momentum implies that the separation streamline is directed into the harbour. This results in the location of a stagnation zone into the harbour (see figure 2.1).

Part of the water of the mixing layer flows into the river and the other part into the harbour. This happens from the point of flow separation up to the stagnation zone, where the separation streamline encounters the side wall, on the right hand side of the harbour in the figure. The location of the stagnation point is determined by the amount of river-water and harbour-water that is entrained in the mixing layer. A wider mixing layer, as a consequence of higher entrainment of river-water and harbour-water, brings the stagnation point even further into the harbour (e.g. Langendoen, 1992).

2.2.2. Flow in the harbour

In the harbour a circulating flow, a gyre or eddy, arises as a result of the entrainment of harbour-water into the mixing layer and the supply of water from the mixing layer into the harbour at the wall on the right hand side of figure 2.1. Conservation of mass for steady flow requires that the amount of water entrained in the mixing layer is equal to that transported back into the harbour again. Several gyres and dead zones can be present in a harbour. The pattern and number of gyres depend strongly on the geometry of the harbour.

In a rectangular harbour the primary gyre is the driving force behind a possible second gyre. Whether more than one gyre occurs depends on the ratio harbour width – harbour length, B/L. For harbours where ½ < B/L < 2 only one gyre occurs but when B/L < ½ a primary and a secondary gyre are formed (Dursthoff, 1970 and Booij, 1986). Even more gyres can occur when water velocities of the second eddy, water depth and the harbour geometry permit. For an impression of how gyres are created, see figure 2.2.

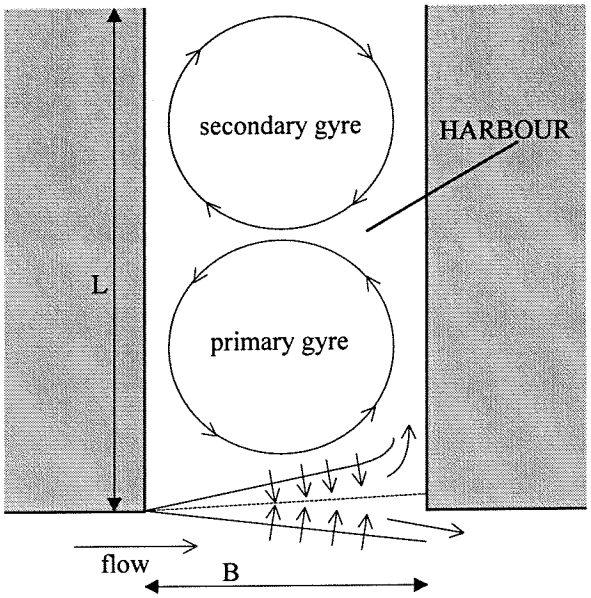

Figure 2.2. Flow pattern in a long harbour, with steady flow in river

2.2.3. Water exchange

The exchange discharge (Q_{ex}) is the rate of flow from the river to the harbour. As the volume of water in the harbour does not change for steady flow, this is equal to the amount of water that flows from the harbour to the river. The water exchange discharge through the harbour mouth is given in the form:

$$Q_{ex,0} = Cu_r B_e h \qquad \text{Equation 2.2}$$

where $Q_{ex,0}$ is the exchange discharge between river and harbour when the mixing exchange is not influenced by another exchange mechanism, C is a coefficient that depends on the geometry of the harbour, B_e is the width of the harbour entrance and h is the water depth at the harbour entrance.

Values for the coefficient C are in the order of magnitude of 0.03 to 0.05 for harbours with a rectangular entrance, depending on the angle of the harbour to the river (Booij, 1986). Lower values were found in scale models because of a different geometry: 0.0018 and 0.013 (Van Schijndel, 1998). Changing the geometry of the entrance yielded even lower values of about 0.0004. The lower values for the scale models are probably caused by the sloping side walls of the model, which cause a less abrupt detachment of flow. The fact that the values of C can vary by a factor 100 shows that the geometry of the harbour entrance can influence the exchange to a large extent.

2.3. Net flow through the harbour entrance

A net flow through the entrance is caused by water level variations at the river or through withdrawal of water from or discharge of water in the harbour basin. Variations in tidal level are usually the most significant cause of a net flow through the harbour entrance. During rising tide the increasing water level results in filling of the basin and during falling tide the opposite occurs, see figure 2.3.

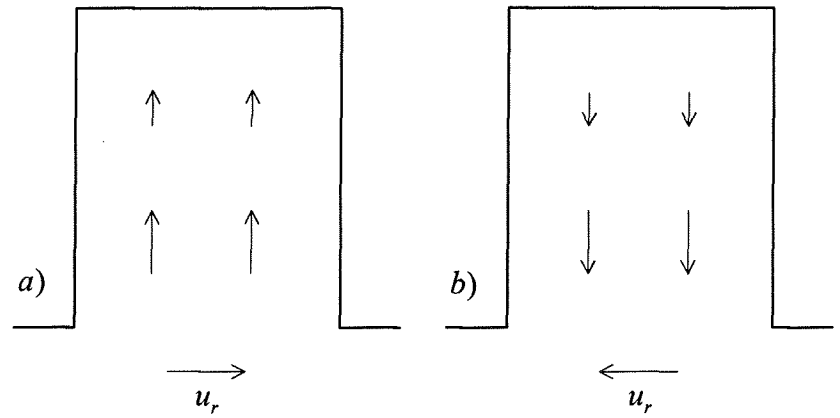

Figure 2.3. Flow pattern in the harbour due to tide level changes at the river a) during rising tide, and b) during falling tide.

The tidal motion in a harbour can be computed by the one-dimensional shallow water equations:

$$B\frac{\partial \zeta}{\partial t}+\frac{\partial Q}{\partial x}=0 \qquad \text{Equation 2.3}$$

$$\frac{\partial Q}{\partial t}+\frac{\partial}{\partial x}\left[\frac{Q^2}{A}\right]+gA\frac{\partial \zeta}{\partial x}+c_g\frac{Q|Q|}{AR}=0 \qquad \text{Equation 2.4}$$

where ζ is the local water elevation, Q is the flow rate, A is the area of the cross-section of the harbour, x is the direction parallel to the harbour axis, g is the acceleration of gravity, c_g is a dimensionless friction coefficient and R is the hydraulic radius.

If the length of the harbour is smaller than about 5% of the tidal wave length, as is usually the case, equation 2.4 becomes $d\zeta / dx = 0$. Integrating equation 2.3 to x over the length of the harbour, and using the boundary condition $Q = 0$ at the back of the harbour, yields for the flow rate through the entrance due to tide level changes:

$$Q_{tf}=A_h\frac{d\zeta}{dt} \qquad \text{Equation 2.5}$$

where A_h is the surface area of the harbour (after Langendoen, 1992).

When a harmonic tide is assumed ($\zeta=\hat{\zeta}\sin(2\pi/T\cdot t)$), the magnitude of the tidal filling (or emptying) can be calculated easily:

$$\textbf{a: } Q_{tf,\max}=\frac{2\pi\hat{\zeta}A_h}{T} \qquad \textbf{b: } Q_{tf,average}=\frac{4\hat{\zeta}A_h}{T} \qquad \text{Equation 2.6}$$

where T is the period of the tidal cycle and $\hat{\zeta}$ is the amplitude of the water elevation.

2.4. Density driven currents

A density driven current is an exchange flow between harbour and river that is driven by density differences between harbour-water and river-water. These differences are associated with differences in salinity, temperature, sediment content or a combination of the three factors. Generally, the difference in salinity is the most important factor that induces the exchange flow. Measurements of Roelfzema & Van Os (1978) showed that, when the three

flow mechanisms occur simultaneously, the exchange due to density differences can be 75 % of the total exchange of water between harbour and river. This percentage is very site specific.

If the density of the river-water is larger than that of the harbour, river-water enters the harbour along the bottom, while water from the harbour leaves the harbour near the surface. The process is reversed if the density of the river water is lower than that of the water in the harbour, see figure 2.4.

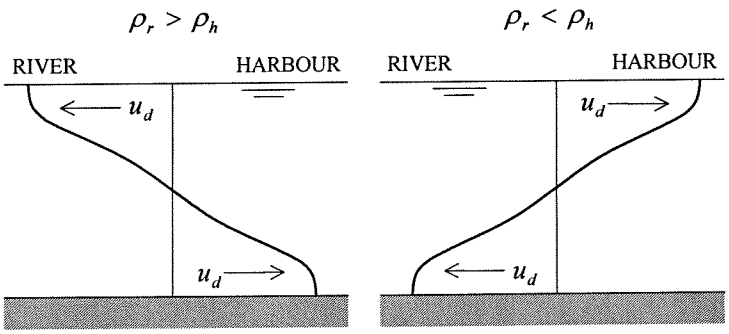

Figure 2.4. Density-driven exchange flow in the harbour entrance

At the transition from harbour to river often double-critical flow establishes itself. Neglecting friction losses at the interface between fresh and salt water, the flow velocity in both layers is (Kranenburg 1996):

$$u_d = \tfrac{1}{2}\sqrt{\varepsilon g h} \qquad \text{Equation 2.7}$$

where ε is the relative density: $|\rho_r - \rho_h| / \rho_h$. The exchange discharge for a rectangular harbour entrance is given by:

$$Q_d = \tfrac{1}{4} B_e h \sqrt{\varepsilon g h} \qquad \text{Equation 2.8}$$

Usually, the exchange discharge will be smaller because of energy losses due to circulating flow in the fresh and the salt layers, friction between the layers, mixing between the layers and contraction of the flow into the harbour. Empirically determined exchange velocities are about 10% smaller than given in equation 2.7.

For a constant density of the river-water, the density of the harbour-water approaches the density of the river-water. The density difference between harbour-water and river-water then decreases in time. Consequently, the exchange discharge decreases. The exchange discharge also decreases because the flow at the transition from harbour to river does not remain double-critical after the reflections of internal waves in the harbour. The flow at the transition from harbour to river is then just critical.

However, the densities in the harbour and the river are in general not constant in space and time. For harbours on estuaries the density of the river-water changes as a consequence of the tide. Relatively fresh water is present in front of the harbour during ebb, whereas salt water is present in front of the harbour during rising tide. As a result, the direction of the density-driven exchange flow in the harbour entrance continually reverses. The degree of mixing between salt and fresh water in the river, and thus the density distribution in the river in space and time, is also determined by the tide. (After Langendoen 1992)

There will be a phase lag between the variations in density of harbour-water and in the density of river-water. The density of harbour-water follows that of the river-water, see figure 2.9. The magnitude of the time lag is determined by the rate at which harbour-water is

exchanged by river-water. This depends on the length and width of the harbour, the surface area and depth of the harbour, the velocity of the exchange flow and the period of the tide. Consequently, the density variation of harbour-water is smaller than that of river-water.

The tide averaged density in the harbour is about equal to the local tide averaged river density. So when the volume in the harbour is big in comparison to the density exchange volume, $|\rho_r - \overline{\rho}_r| / \overline{\rho}_r$ can be used as the relative density difference in equation 2.7. This gives the following exchange volume over a tidal cycle (see appendix L):

$$V_{d,o} \approx 0.172 \cdot \overline{h} B \sqrt{\frac{\hat{\rho}_r}{\overline{\rho}_r} g \overline{h} T} \qquad \text{Equation 2.9}$$

where $\overline{h}$ is the average water depth, $\overline{\rho}_r$ is the average density of the river-water and $\hat{\rho}_r$ is the amplitude of the density in the river over a tidal cycle.

When the harbour volume is small, the density exchange will be smaller. The ratio of the harbour volume to the undisturbed density discharge ($V_h/V_{d,0}$) is a measure for the decrease of the density discharge (Eysink, 1989).

The level of mixing in the river influences the exchange in the harbour. This was found in tests done at Delft Hydraulics (1977). An illustration is given in figure 2.5. When a river is totally stratified, only a part of the river depth has density changes over time. Exchange will take place in this part of the vertical only.

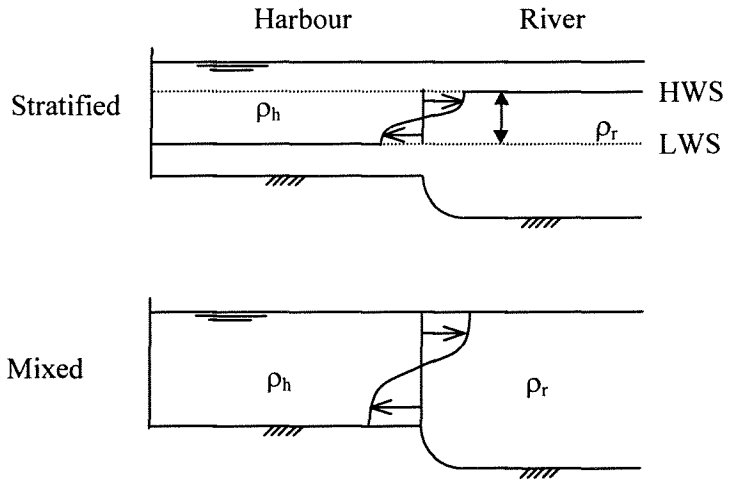

Figure 2.5. Difference in exchange between a completely stratified, and a completely mixed river.

2.5. Interactions of the flow mechanisms

Almost always a harbour is not only subject to one of the three water exchange mechanisms. Two or three can occur simultaneously, and they interact when they do (Booij, 1986; Langendoen, 1992). It is sometimes assumed that the flow pattern is simply the sum of all the flow patterns as caused by the separate phenomena. Figure 2.6. gives an illustration of this assumption. The assumption is not entirely correct. The different mechanisms interact. These interactions are described in the next sections.

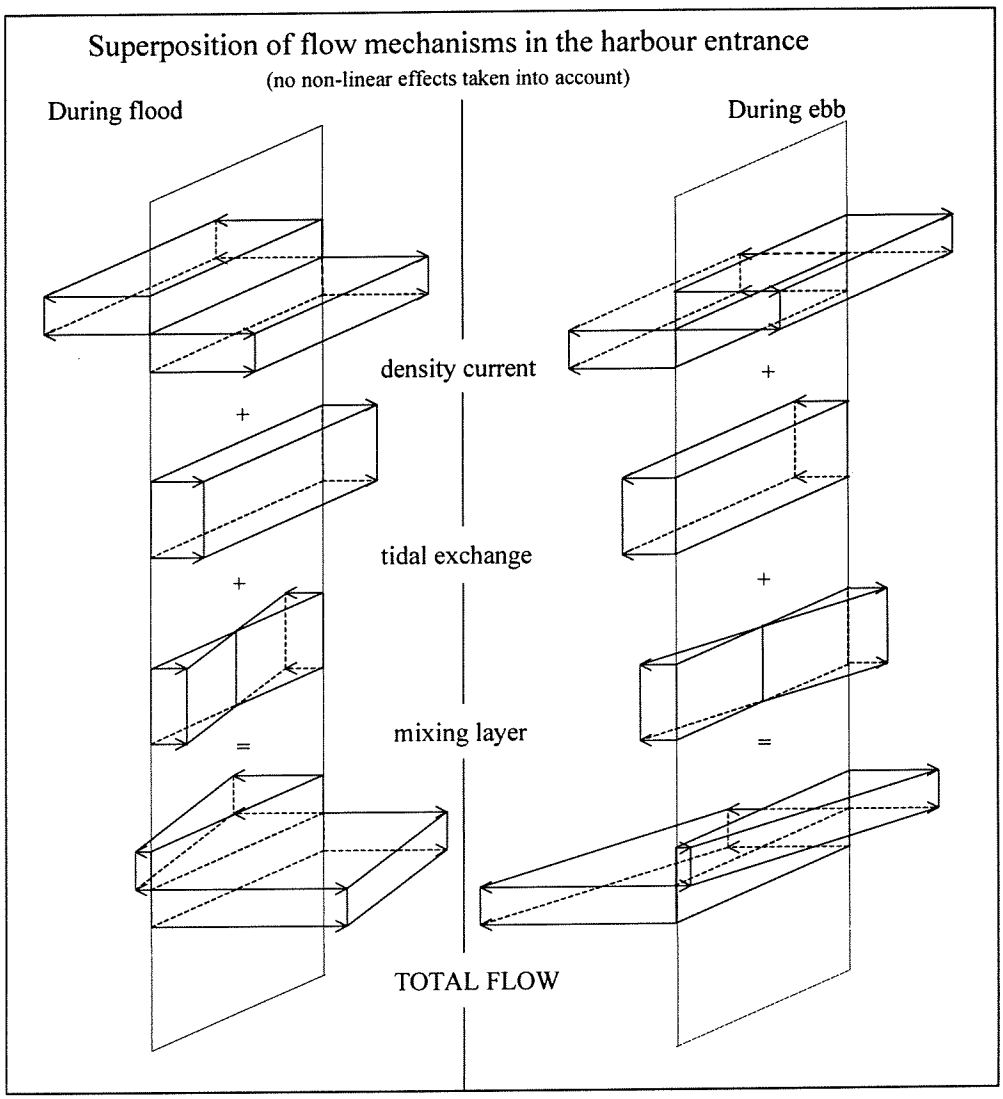

Figure 2.6. Superposition of flow patterns caused by three exchange processes

2.5.1. Mixing and tidal filling

A net flow across the harbour entrance influences the exchange discharge due to mixing, as can be seen from measurements done by Booij (1986) and Van der Graaff (1977). For both experiments a combination of flow along the harbour entrance and a net flow through the harbour entrance was used. To create a net flow across the harbour entrance, water was drawn from the harbour basin or discharged into the harbour basin. The mixing layer is shifted towards the river when water is discharged into the harbour. Less river-water flows into the harbour, which results in a weaker gyre. Withdrawal of water from the harbour results in a stronger gyre. This indicates that pure superposition of the gyre and tidal filling velocities is not correct. See figure 3.1 for an illustration of the shifted mixing layer. Van der Graaff found a linear relation between the extraction discharge and the amount of mixing. This relation is given as a correction on equation 2.2.

$$Q_{ex} = Q_{ex,0} - C_2 \frac{Q_{tf}}{Q_{ex,0}} \qquad \text{Equation 2.10}$$

in which $Q_{ex,0}$ is the undisturbed exchange as computed by equation 2.2. C_2 is an empirical constant that is in the order of 0.15-0.3.

2.5.2.Mixing and density current

A density current interacts with the mixing layer in a similar way as a net current, although it interacts differently at different depths. Measurements of Langendoen (1992) showed that qualitatively the superposition of velocities was correct, as can be seen in figure 2.7. Here a gyre and a density driven current are present at the same time. The ingoing density current near the bottom shifts the eddy to the left, and the outgoing density current near the surface shifts the eddy to the right. The figure shows the flow during high water, so the tidal filling is negligible. It is unknown to what extent the exchange in consequence of turbulent mixing is changed due to the density driven current.

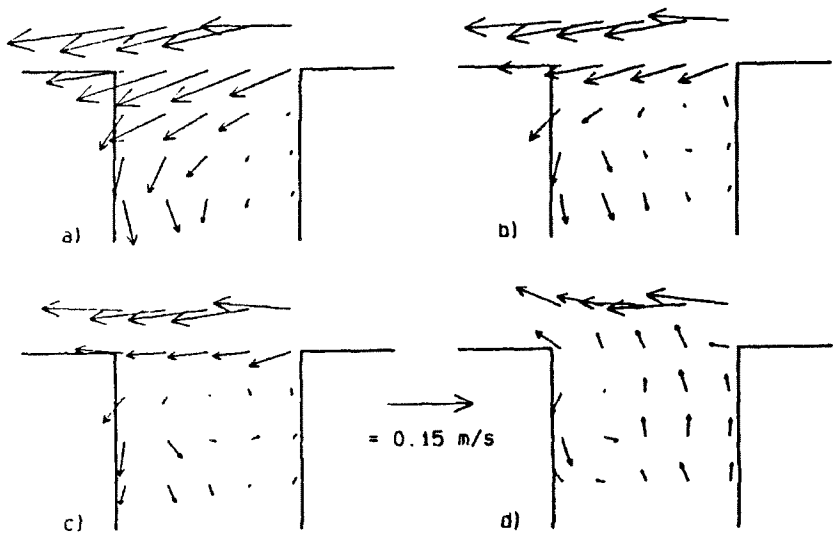

Figure 2.7. Flow at high tide in harbour entrance at four depths: a) 4cm, b) 8cm, c) 10cm, and d) 14cm from the bottom (depth = 22.5cm) (Langendoen, 1992).

The density current not only influences the gyre, but the gyre also influences the density current. Dursthoff (1970) stated that if a gyre and a density-driven exchange flow occur simultaneously, the gyre causes mixing (i.e. friction) between the upper and lower layers, through which the density-driven exchange flow can be reduced. Langendoen (1992) concluded from tidal flume experiments that a gyre reduces exchanges due to density differences, because of a decreased effective entrance width.

2.5.3. Tidal filling and density current

The layer thickness of the density-driven exchange flow changes when a net flow is present in the harbour entrance. Assuming that the flow at the transition from harbour to river is critical, the layer thickness can be determined (equations are given in chapter 9).

If the density current is stronger than the tidal filling current, it can be assumed that the layer thickness remains half the water depth. Superposition of the two flow profiles is now possible. The inflow due to the density exchange decreases due to both tidal emptying and tidal filling, as can be seen in figure 2.8. The magnitude of this reduction is half the tidal filling discharge.

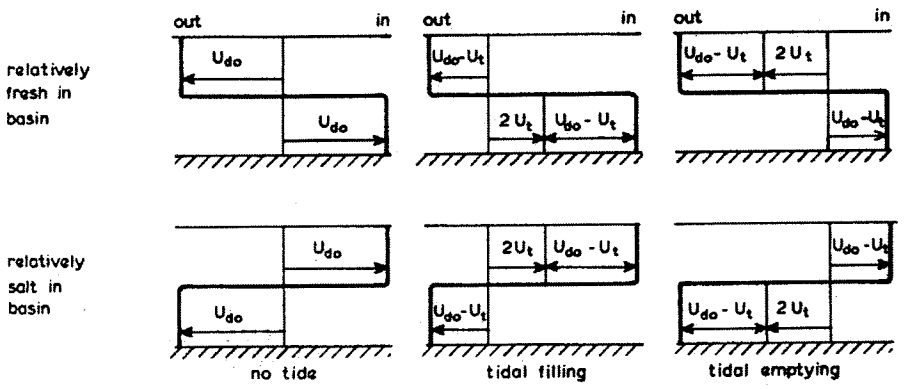

Figure 2.8. Interaction of density current and tidal filling (Eysink, 1989)

Both tidal filling and the direction of the density-driven current change during a tidal cycle. The phase lag between the two cyclic processes determines the total exchange caused by the two mechanisms. This is illustrated in figure 2.9.

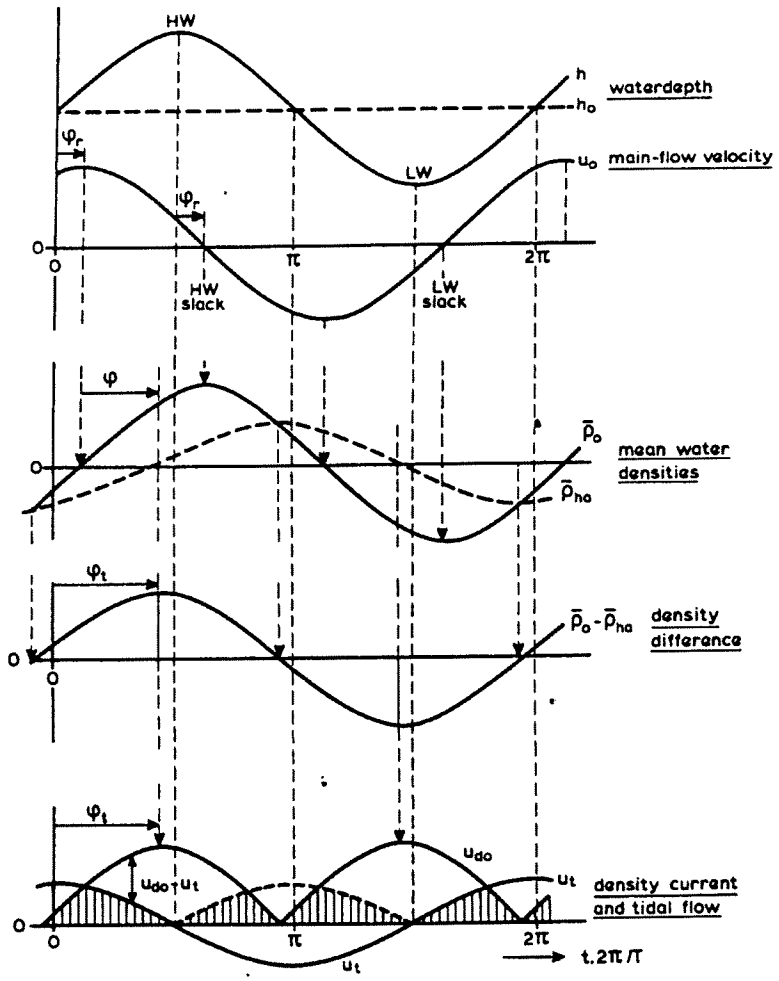

Figure 2.9. Effect of phase lag between tidal and density currents on the density induced exchange flow (Eysink, 1989)

2.5.4. All three mechanisms

Eysink (1989) developed an empirical model (SILTHAR), which can be used to calculate the sedimentation due to all three exchange mechanisms in a harbour. Approximations were made for the interaction between the different mechanisms (mainly equations 2.5, 2.8, and 2.9). He assumed linear harmonic fluctuations of the several parameters, and integrated the various equations analytically. This is no more than a crude estimation of the total exchange. Some assumptions were made in order to integrate the equations. The interaction of turbulent mixing and the density current is not taken into account. Also the water level is assumed to be constant when integrating the exchange due to the density current over a tidal cycle.

As was indicated in the previous sections, not all phenomena have the same strength. In many studies (e.g. Roelfzema, 1977; Langendoen, 1992; Headland, 1994; Eysink, 1989) it was concluded that, with all three conditions present, the influence of density currents forms the biggest obstacle in reducing accretion in harbour basins. Although the magnitudes of the different mechanisms vary constantly over a tidal cycle, and the site-specific circumstances are important, a general order of the relative importance is as follows:

1. exchange due to density currents;
2. exchange due to tidal filling;
3. exchange due to turbulent mixing in the mixing layer.

The density current transports river-water further into the basin than other mechanisms, and the influence of salinity on mud, making particles flocculate and settle, may further aggravate the already major effect of density currents on accretion.

2.6. Mud and siltation in harbour basins

2.6.1. Sedimentation of harbour basins

Where accretion of harbour basins is concerned, mud is often the main problem as a result of its complex behaviour and its ability to remain suspended for a longer period of time when compared to sand. This enables mud to be transported easily into harbour basins where it can settle in areas with small flow velocities.

Sediment laden water is exchanged between river and harbour and because the sediment concentration of river water is in general much higher than that in the harbour, there is a net transport of sediment directed into the harbour. The quantity that eventually settles in the harbour basin is mainly dependent on the following (Booij, 1986):

- Exchange discharge between river and harbour;
- Concentration of sediment in the river-water and the harbour-water;
- Fall velocity of the sediment particles;
- Exchange time of water entering the harbour system;
- Residence time.

The exchange discharge is described in earlier sections. This exchange discharge renders S, the mass of sediment entering the harbour per unit time through the following expression:

$$S = Q_{ex} \Delta c \qquad \text{Equation 2.11}$$

where Δc is the difference in sediment mass concentration between river-water and harbour-water. Not all of S will be deposited in the harbour basin. Water flowing out of the harbour also contains some sediment. The part of the sediment that settles and remains in the harbour

is dependent on the trapping efficiency, e_t. This is defined as the relation between the time a particle needs to settle to the rotation time of the eddy. The expression for the trapping efficiency thus becomes:

$$e_t = \frac{h/w_s}{T_{eddy}} \qquad \text{Equation 2.12}$$

in which h is the water depth, w_s is the fall velocity of the particles, and T_{eddy} the rotation time of the eddy. When the trapping efficiency decreases, a larger part of the sediment coming into the harbour settles. The net influx of sediment will be larger. When a density current is present, using T_{eddy} is not very useful anymore. The rotation time of the density current may be a better time to use.

To come up with measures against sedimentation of the harbour one will have to go into the many factors that are responsible for sediment entering and staying in the harbour system.

2.6.2. Deposition of sediment in the harbour

The sediment that is transported into the harbour is transported further into the harbour by the gyre system. Rohr (1933) and Vollmers (1963) studied the sedimentation of harbours as a consequence of a steady river-flow along the harbour entrance. Figure 2.10 gives an illustration of the deposition patterns of coarse (bed-load transport) and fine (suspended transport) sediment in the case of one single gyre (after Rohr, 1933).

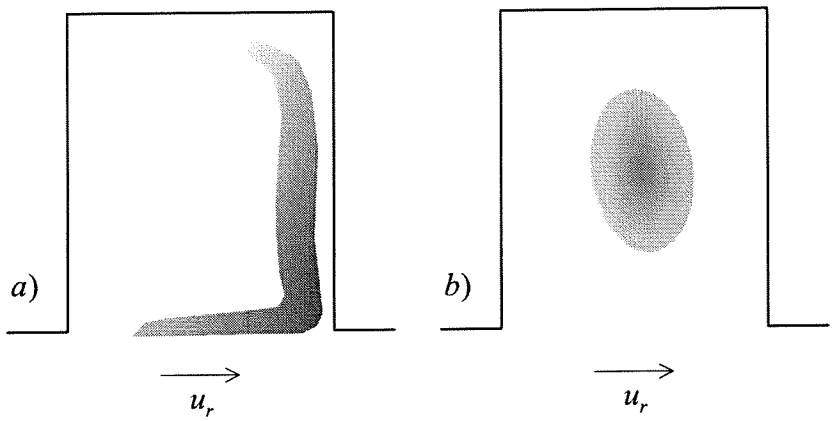

Figure 2.10. Deposition patterns of sediments in a harbour as a consequence of a) bed-load transport, and b) suspended transport, in the case of a single gyre

From experiments performed by Rohr (1933) and Langendoen (1992) it was concluded that coarse sediment settles at the edges of the harbour basin while the finer sediment is deposited in the middle. This is explained by the fact that the coarser material has a higher fall velocity and is deposited at an earlier stage, while being brought into the harbour by the gyre. The flow velocities in the gyre system are highest near the surface. This causes water at the surface to be flung to the sidewalls of the basin while water at the bed is transported to the centre of the basin. Because of torridoial movements, the finer sediment which was not deposited just yet, settles here in the middle of the eddy where the flow velocities are smallest.

Christiansen (1987) states that a gyre in the harbour entrance narrows the stream filling the basin during rising tide, see figure 2.11, which results in a higher flow velocities transporting more sediment into the harbour. After high water slack the gyre is pushed out of the harbour by the emptying of the basin. The emptying of the basin during ebb suppresses the gyre, see

figure 2.11. The low velocities in the harbour basin are not sufficient to re-suspend all the deposited material. Continuous sedimentation of the harbour then ensues.

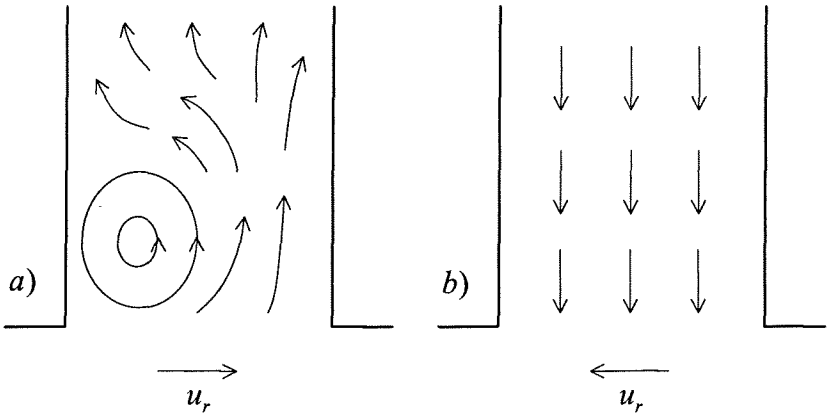

Figure 2.11. Currents in a tidal harbour a) during rising tide and b) during ebb

2.6.3. Mud and physical modelling

Mud is a very general expression for a very diverse set of mixtures with different properties. The mixture can consist of clay particles, fine sand, lime parts, organic material, gas and water with many dissolved substances like salts. The properties are determined by the exact composition of the sediment mixture, its surrounding conditions and its history.

All mud-mixtures are to some extent a cohesive substance, depending on the fraction of smaller particles. A larger fraction of smaller particles makes it easier for the particles to flocculate. Particles interlock and form flocks. Their diameter can be 10 to a few 100 times the diameter of the separate particles. The flocks have a greatly increased fall velocity. Flocculation is greatly enhanced by an increased salinity. The flocculation caused by an increased salinity is only partially reversible. Another important aspect of changing properties of sediment over time is its ability to consolidate under its own weight. After sedimentation, bottom layers are formed with increasing densities at greater depth.

The properties mentioned make it difficult to use real mud for physical modelling. First of all because the properties and surrounding circumstances are different for each harbour basin. A second reason is that it is virtually impossible to create reproducible conditions for every test series. It is also difficult to determine the differences between test conditions. These reasons would make it difficult to draw general conclusions from the test results.

3. The Current Deflecting Wall

3.1. Introduction

In chapter 2 the main exchange mechanisms that cause sedimentation have been described. In this chapter a means of influencing them is described: the Current Deflecting Wall (CDW). The CDW is a curved screen that is placed at the downstream corner and sometimes at the upstream corner of the harbour entrance. The aim of the CDW, reducing sedimentation in a harbour basin, is accomplished by changing the flow regime in the harbour entrance in such a way that the water exchange is decreased and/or that the net inflow from the river into the harbour basin contains less sediment.

Section 3.2 of this chapter describes the previous research done on CDWs. In section 3.3 some important expressions are defined. The principles of a CDW are described in section 3.4 for tidal flow and homogeneous conditions, because most research has been done under these conditions. The functioning and design of a CDW fully depends on the kind of flow conditions in front of the harbour entrance. Therefore the CDW is separately described for the different flow conditions. Section 3.5 deals with the application of a CDW under tidal inhomogeneous conditions. No research had been done on the CDW under these conditions until now and this section only contains some preliminary calculations and argumentation on the possible effect of a CDW. Section 3.6 describes the CDW under steady flow and homogeneous conditions.

3.2. Background of the CDW

Because of the huge costs for depositing contaminated dredged material in Hamburg, Strom- und Hafenbau of the Freie und Hansestadt Hamburg stimulated the development of measures to mitigate sedimentation. Consulting various experts and institutions resulted in the invention of the Current Deflecting Wall, which is a patented device.

One full-scale prototype CDW has been built at the Köhlfleet harbour in Hamburg in 1990. A second wall will probably be built in the Parkhafen basin, also in Hamburg. Monitoring over several years showed that the CDW in the Köhlfleet harbour reduced siltation by approximately 40%. This proved the beneficiary effects of a CDW on sedimentation reduction under tidal homogeneous conditions (Winterwerp et al, 1994).

Extensive research on the CDW has been done in the previous LIP II project. In this study many aspects of CDW-design have been investigated. Various shapes, positions, and slight modifications were tested. Site specific modelling has been done for the design of the CDWs at the Parkhafen basin in Hamburg (Delft Hydraulics, 1992) and for the use at river harbours (Van Schijndel, 1998 and Van den Berge, 1997).

3.3. Definition of expressions

In this section several expressions that are used in this report are defined.

Upstream & downstream

The expressions upstream and downstream are defined according to the average flow direction during a tide. This means that the downstream side is the side at the seaward side of the harbour, and the upstream side is the other side of the harbour. According to this definition, the flow during flood is directed upstream. This can be confusing, but other

definitions of the various directions may also cause confusion. Because the flow in phase 1 simulates the flow in the flood period, the flow during these experiments is only directed upstream. In all the figures that are used in this report the right hand side of the figure is upstream, except when mentioned otherwise.

Exchange discharge

The exchange discharge is a term that is not easy to define. The exchange discharge is the smallest of the two discharges that are flowing in and out of the harbour simultaneously. So it is the amount of water that enters the harbour basin, beyond the mixing layer, at a certain time, but which is not part of the net flow. The exchange discharge that enters the harbour is equal to the exchange discharge that leaves the harbour. The exchange discharge is caused by density currents and mixing, although both effects are of a different nature. A CDW can possibly introduce an extra exchange discharge.

Inside & outside of the CDW

The inside of the CDW is defined as the space (or channel) between the CDW and the flume side wall closest to the CDW. With 'outside of the CDW' the other side is meant.

Capturing water

The amount of water that is captured by the CDW is the amount of water that flows through the inside of the CDW during flood. This discharge is an important design criterion of a CDW.

3.4. The CDW under tidal flow and homogeneous conditions

The largest influx of sediment takes place during rising tide. The tidal filling causes water (and sediment) to enter the basin. During ebb the tidal flow is mostly directed outward and the mixing layer is pushed out as well, so that sediment influx is smaller or nil (Booij, 1986). The CDW is therefore placed at the downstream side of the harbour, so that it is active during flood. Figure 3.1 illustrates the effects described here.

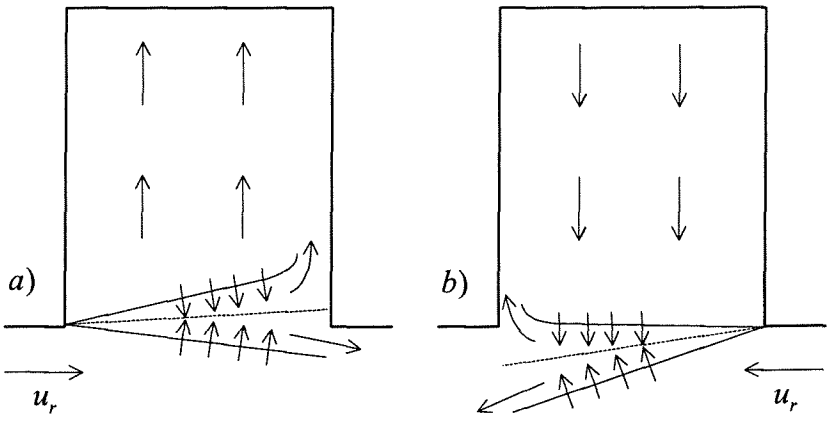

Figure 3.1. Flow pattern in the harbour as a consequence of tide level changes at the river a) during rising tide, and b) during falling tide.

3.4.1. The parts of the CDW

The various parts of a typical CDW design can be seen in figure 3.2. To give an indication of the length of an actual CDW: The CDW that was built in the Köhlfleet harbour in Hamburg had a length of 150m. The CDW that was first designed for the Park harbour consisted of two segments and had a total length of around 350m.

1 Main CDW

The main part of a CDW is designed to control the entrance flow and to let more water flow into the harbour basin than is needed for tidal filling (over-capture). The main part of the CDW has a curved shape, which is to prevent shedding and separation of the flow.

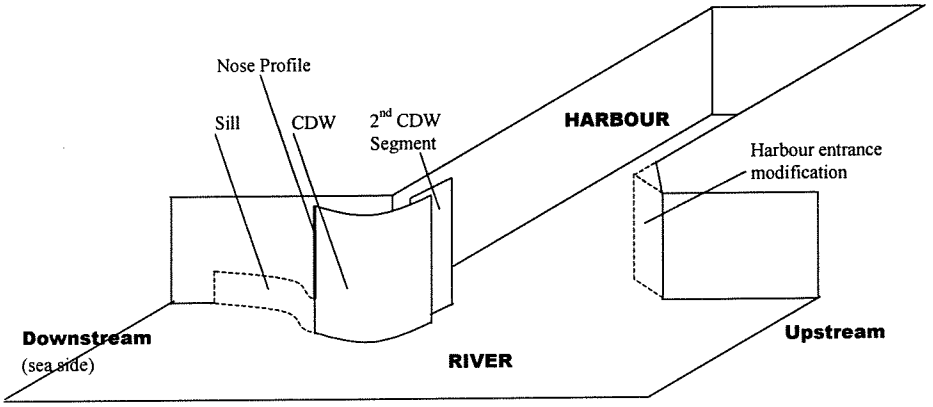

Figure 3.2. The components of a typical CDW design

Not all river water in front of the opening between CDW and river embankment will flow through this opening because it is partly blocked by the CDW. Thus the flow that approaches the CDW will make an angle with the main flow direction. From the downstream corner the CDW must be given this angle in order to keep the flow attached. With LIP II experiments this angle was around 16° away from the flume side wall, but could also vary with flow velocity. The curvature of the CDW must be such that the flow stays attached.

2 Segments

The CDW that functioned best during the LIP II research consisted of two segments: the main part and a second segment. The second segment or vane at the end of the main CDW guided the inflow of water even more. This second segment is not used for every CDW design. The CDW with a second segment is designed in such a way that the over-capture was flowing through the slot between the main part and second part of the CDW.

3 Sill

A sill is placed in front of the CDW in order to catch water from the upper layer of the river instead of from the entire water column. This prevents the water with the highest sediment concentration in the lower part of the water column and the bed load to enter the harbour. The typical height of the sill is about 25% of the water depth.

4 Shape of upstream harbour entrance corner

The shape of the upstream harbour entrance corner was found to influence the exchange during LIP II. It serves to fix the stagnation point in a certain position. Without it the stagnation point has the tendency to waver along the harbour entrance wall at the upstream side, thus further disturbing the flow pattern. Various shapes were tested in the LIP II research.

5 Nose profile

A profile on the leading edge of the CDW helped to keep the flow attached to the CDW, thus decreasing the width of mixing layer. This profile, the nose profile, was applied to the downstream corner of the CDW. A similar nose profile was applied to the second segment of the CDW. This nose profile had been used for the LIP II studies as well.

3.4.3. Functions of the CDW during rising tide

The CDW functions during rising tide. At this time water flows up-river, part of which is captured by the CDW and directed into the harbour basin. This is depicted in figure 3.3. Flow in the harbour basin is practically two dimensional, so a plan view of the harbour basin is presented. During falling tide the water exchange is often negligible, so this is a period in the tidal cycle that is not considered in the analysis.

At present, complete consensus among all researchers on the precise functions and effects of the CDW during rising tide does not exist. The following functions are mentioned (Winterwerp et al, 1994; Delft Hydraulics, 1992; Crowder, 1996):

- The separation of flow at the curved end of the CDW is less abrupt than flow separation at the sharp corner of the harbour entrance. This reduces the width of the mixing layer.
- Because the start of the mixing layer is moved to a point beyond the corner of the harbour entrance, the stagnation point/zone moves more out of the harbour, thus the exchange is decreased.
- All the water that is needed for tidal filling is captured by the CDW. With the use of a sill this amount of water stems from the top layer of water, which contains less sediment.
- In addition to the water needed for tidal filling, a small over-capture takes place by the CDW (10%). This results in an extra pressure gradient out of the harbour. This pushes the mixing more into the flume.
- (Because eddy velocities are suppressed, the "tea cup effect" is less, so the sedimentation takes place with a more even spread. Whether this is an advantage or a disadvantage depends on the wishes of individual harbour authorities.)

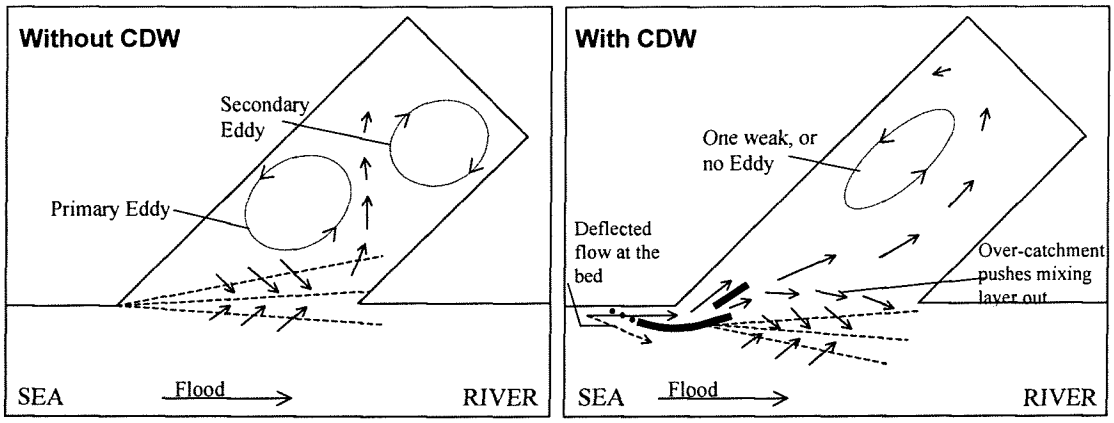

Figure 3.3. Idealised functions of CDW during rising tide after Crowder (1996)

The water exchange could not be quantified exactly during LIP II. The criteria used for designing a properly functioning CDW were:

- Less abrupt separation of flow at the upstream corner of the CDW, which reduces the size of the mixing layer.
- No or little flow separation at the flume side of the CDW until the upstream corner of the CDW is realised.
- A small mixing layer (preferably outside the harbour basin, more in the flume);
- The required volume of water for tidal filling plus approximately 10% is captured by the CDW.

- Favourable eddy configuration and flow configuration in the harbour, i.e. with a minimal eddy structure and preferably a smooth flow pattern in the basin.
- Enable safe navigation in vicinity of harbour entrance.

3.4.3. Capture efficiency

When designing a CDW the area between the CDW and the river side must be large enough to capture the water that is required for the tidal filling plus over-capture. This is called the capture efficiency of the CDW, which must be known for determining the distance of the CDW from the river bank. The capture efficiency is defined as the ratio of the actual flow rate inside the CDW to the flow rate through an area equal to the minimum cross-sectional area between the CDW and the channel wall, at a speed equal to the mean velocity in the main river upstream of the CDW (Crowder, 1999). This gives the formula:

$$e = \frac{\int_{A_{CDW}} u_{CDW}(A)dA}{\overline{u}_r A} \qquad \text{Equation 3.1.}$$

$\overline{u}$ = undisturbed mean flume velocity

u_{CDW} = velocity at entrance of CDW

A = wetted area of cross section of the CDW entrance

This ratio was found to be in the interval of 31% and 43%. It was found to be independent of the net flow through the harbour entrance.

3.5. The CDW under tidal flow and inhomogeneous conditions

Until the LIP III experiments, on which this thesis is based, no experiments had been done with a CDW under inhomogeneous conditions. So only ideas about the possible effect of the CDW on the density exchange were developed beforehand (Winterwerp, 1999).

The CDW that was developed by H.Christiansen for LIP III is schematically depicted figure 3.4.

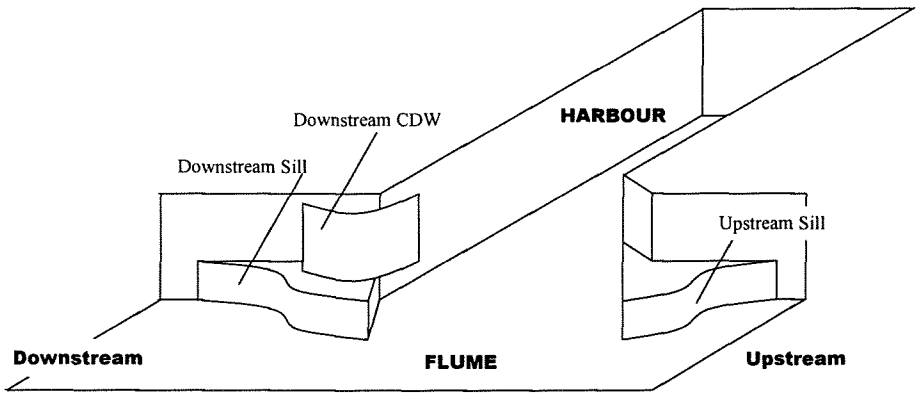

Figure 3.4. The CDW in inhomogeneous water, and its components.

The downstream CDW now only covers the top half of the water depth, in order to stop/slow down the outgoing density current that mainly takes place at the top half of the water depth during rising tide. The sill is extended outwards beyond the CDW in order to deflect the in-going density flow at the bottom. The CDW is also placed at such a distance of the flume wall, that the discharge needed for the tidal filling plus an extra 10% is captured.

As the downstream CDW now forms an obstacle, which could cause extra exchange during falling tide, an upstream sill was studied as well.

3.5.1. Possible functions of a CDW

The functions of the "classical" CDW for homogeneous tidal flow can be described in two horizontal dimensions. Because the density exchange current has strong variations over the depth, the expected flow pattern will be 3-dimensional, so the functions of a CDW will also be different.

A priori there were some ideas of the possible functions of the CDW. Only the possibility of reducing the exchange during rising tide is discussed in this section. During flood the exchange of sediment is at its maximum, and the driving force of the CDW as well. The influence that the CDW has on the mixing layer can no longer decrease the siltation, as mixing is mostly a small contribution to the total exchange. A CDW could possibly still reduce the ingoing density current at the bed in a few ways:

1. The flow of water that is captured by the CDW could possibly create extra pressure, against the pressure of the density current, which could decrease the density current.
2. The CDW decreases the effective width of the harbour entrance and therefore decreases the density current.
3. The CDW increases the friction between the layers, thereby reducing the density exchange.
4. Flow is captured from layers with a lower sediment concentration.

The first mechanism was concluded a priori not to be effective enough to obtain a substantial reduction in exchange of water. The CDW cannot produce enough force to counter the whole density current. This is presented in the next calculation with numbers of the CDW that was tested during LIP III. Winterwerp (1999) also calculated this possibility for a harbour in Antwerp, and concluded it could not help much via this mechanism. The flow through the CDW only has a force of 5% of the force of the density gradient, so no real reduction can be expected.

Exchange discharge due to a density current:

$$Q_{ex} \approx 0.45 \cdot \tfrac{1}{2} h \cdot B \cdot \sqrt{\frac{\Delta\rho}{\rho} gh} \quad ,$$

with: h = 0.25 m; B = 0.56 m; $\Delta\rho$ = 3.5 kg/m^3; ρ = 1000 kg/m^3; g = 9.81 m/s
This results in an exchange discharge of **2.9 l/s**, and a force of: F = ½Q^2ρ/A=**0.03N**

Discharge due to a CDW:

$$Q_{CDW} \approx A_{CDW} \overline{u}_r e \quad ,$$

with: A = 7.8 10^{-3} m^2; $\overline{u}$ = 0.2 m/s; e = 0.37 (capture efficiency)
This results in a CDW discharge of **0.6 l/s**, and a force of: F = ½Q^2ρ/A=**0.001N**

The second mechanism is also expected to have a minor influence, because the momentum of the discharge captured by the CDW is small.

The third mechanism can probably only be effective near the entrance of the harbour, therefore it will increase only a small part of the friction that is present over the total interface between the layers in the harbour. It is concluded that this cannot have a significant influence.

The fourth mechanism could be achieved, but no knowledge is available.

3.6. The CDW under steady flow conditions

When the river in front of a harbour has steady flow, water exchange will take place through the mixing layer. This means that the CDW should not have to capture water needed for the tidal filling. The rest of the functions as mentioned in the previous section still hold.

In a non-tidal river, the CDW is placed at the upstream side of the harbour in order to decrease mixing. Research at river harbours (Van Schijndel, 1997; Van den Berge, 1997) showed that the CDW did function, but that other measures were more effective. These other measures for sedimentation reduction were e.g. permeable- and non-permeable groins, a sill in the harbour entrance, a dam in part of the harbour entrance, and combinations of these measures. It might be that a CDW is less effective under steady homogeneous conditions, but it is also possible that the optimal CDW configuration was not found during these tests. Small changes in the configuration of a CDW have substantial influence on its effectiveness (Crowder, 1996). Much experience is still needed when designing a CDW.

4. Measurement Program

4.1. Introduction

In this chapter the experimental set-up and the measurement program will be described. First of all the tidal flume is described in section 4.2. In the sections 4.3 and 4.4 the harbour configurations and CDW configurations that were tested are described for both phases. Because the two phases had two different goals and the respective test conditions differ, both phases are dealt with separately. The last section, section 4.5, gives an overview of all tests executed.

4.2. Description of the Delft Tidal Flume

The LIP III experiments were executed in the tidal flume at Delft Hydraulics (see figure 4.1). The tidal flume consists of a basin (model sea) with a surface area of 120 m^2. Water level and salinity in the basin can be controlled, so that any tidal movement can be simulated. Attached to the sea basin is the actual flume (model river) of 130 x 1 x 1 m^3. The flume discharge can be varied in time in such a way that the length of the flume seemingly increases. Roughness elements at the bed in large parts of the flume contributed to the quick establishment of a logarithmic velocity profile, and control the position of the salt wedge. The fresh water from the flume, that flows in a thin layer on top of the sea water, is removed from the sea basin by a skimmer. These features make it possible to model a wide range of estuarine systems. A detailed description of the tidal flume is given in (Delft Hydraulics, 1986).

For the LIP III experiments a rectangular harbour basin was located twenty-two metres upstream of the sea, basin with a surface area of 10 m^2. In this basin, several harbour layouts were tested.

The flume has a control room where system signals and measurement signals are monitored, recorded and processed.

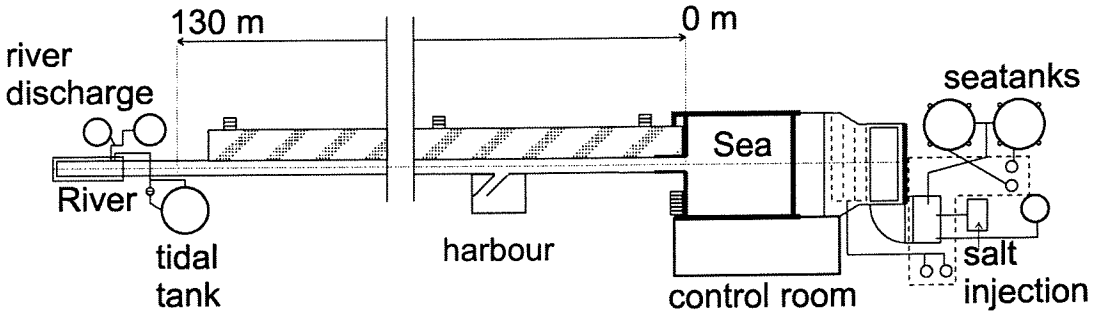

Figure 4.1. Plan of the Delft Tidal Flume with harbour

4.3. Phase 1 - homogeneous conditions

4.3.1. Harbour geometry and flow conditions

The performance of the CDW at harbours with different orientation to the river was the main research topic for phase1. The original goal was to test the harbour angles 45°, 67.5° and 90° (sharp angle at the upstream side). Due to time shortage only the 45° and 90° harbour angles were tested.

The values of some important dimensionless parameters for the model harbours are as follows:

B/L	=	-
B_e/B	=	1.0
h/B	=	0.31
Re	=	$5*10^4$
α	=	45° / 90°
$\hat{u}TB_e/B^2$	=	∞ (T = ∞ , steady flow)
$\frac{2\pi\hat{\zeta}A/T}{hB_e\hat{u}}$	=	0.025 / 0.050

where B is the width of the harbour (parallel to the flume), B_e is the width of the harbour entrance, L is the length of the harbour; h is the average water depth, $\hat{u}$ is the amplitude of the tidal current velocity, T is the characteristic time scale (tidal period) of the tide, Re is the Reynolds number and α is the angle between the harbour entrance orientation and the flume (at the upstream side). The expression $2\pi\hat{\zeta}A/T$ is equal to the maximum tidal filling discharge which is taken equal to the extraction discharge.

The layouts of the model harbours that were tested are given in figure 4.2.

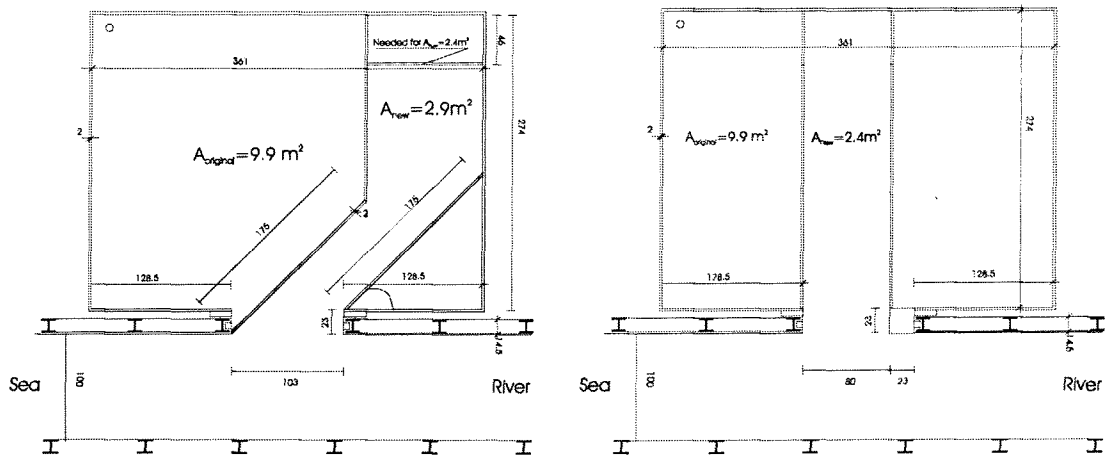

Figure 4.2. Harbour layouts for LIP III tests

The flow conditions were kept equal to those of the LIP II tests as much as possible. Tidal filling was simulated by extracting water from the harbour basin, which creates a comparable net current through the harbour entrance. Both a 1 l/s and 2 l/s discharge were extracted from the basin. Different extraction rates can be explained as different harbour surface areas or different tidal amplitudes. This can be deduced from equations 2.5 and 2.6.

Other parameters of the model are:

Average flume discharge	50 l/s
Extracted discharge (tidal filling)	1 or 2 l/s
Flume velocity	0.20 m/s
Water depth	0.25 m

4.3.2. Description of CDW configurations

The CDW that was used at the 45° harbour was based on the optimal CDW of the LIP II project (CDW 8). One difference was that the curvature was increased slightly. Secondly, the gap between the CDW and the flume side was increased by 3 cm. No sill was placed in front of the main CDW. The length of the main CDW is 78.5 cm, and the length of the second segment is 20 cm. The modification of the upstream harbour entrance corner that was developed at the LIP II tests was used as well.

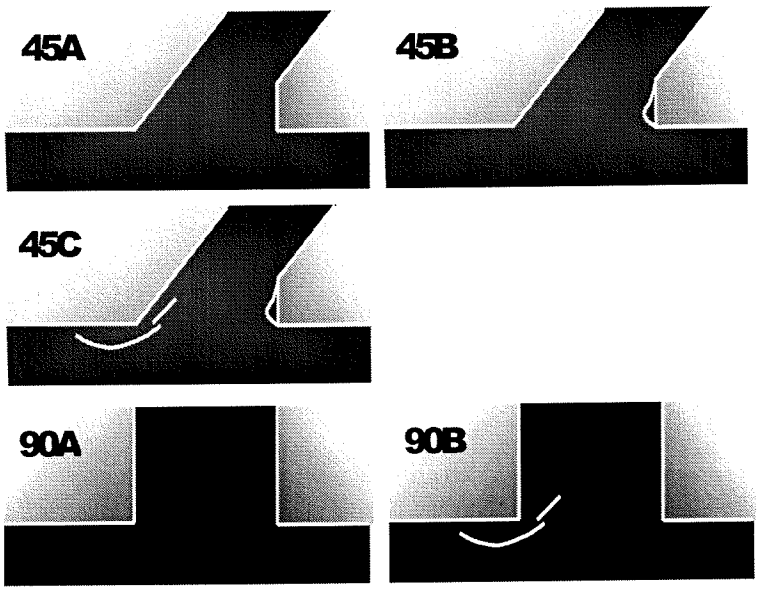

Figure 4.3. Overview of the CDW configurations used during phase 1

No 90° harbour was tested in LIP II, so a new CDW configuration had to be developed. The CDW that was used was the same as for the 45° harbour, but the positions were different. The CDW configurations that were tested can be seen in figure 4.3. The actual co-ordinates of the CDW configurations are given in appendix A.

4.3.3. Measurements taken

The following measurement techniques were applied during the phase 1:

- Electro Magnetic Velocity measurement (EMS) in the flume;
- Water level measurements (WAVO) in harbour and at various positions in the flume;
- Measurements of extracted discharge;
- Dye Concentration Measurements (DCM): dye was injected in the flume/harbour, and the colour (concentration) was monitored by video camera;
- Particle Tracking Velocimetry (PTV): particles were applied to the water surface, and the positions (movement) were recorded by video camera.

The EMS and the WAVO signals were recorded continuously to check the boundary values for the tests. Further information about the measurements can be found in chapters 5 to 7.

4.3.4. Testing procedures

Flow in the harbour adjusted quickly to changed circumstances. Therefore the CDWs could be changed often. The CDW was positioned according to the criteria mentioned in chapter 3. Dye injection was used to check the flow pattern around the CDW, see figure 4.4. Before every recording (EMS, PTV, or DCM) the extracted discharge, the flume discharge and the CDW position were checked, in order to obtain constant flow conditions.

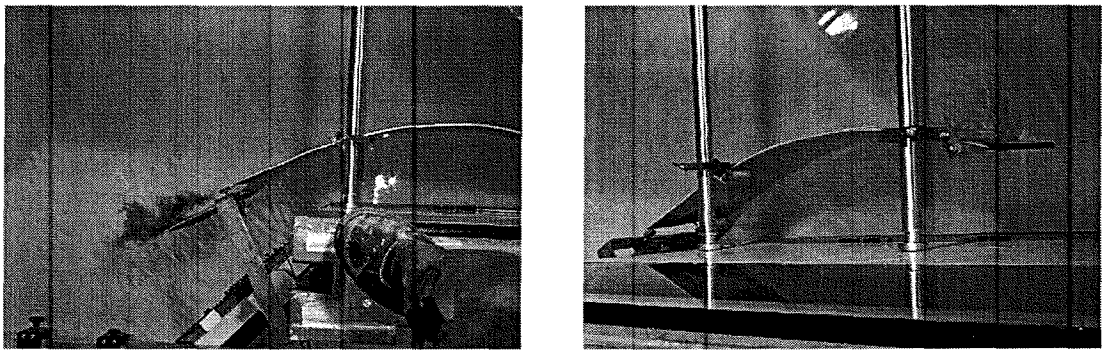

Figure 4.4. Top view of the model CDW in the flume during phase 1

4.4. Phase 2 – inhomogeneous conditions

4.4.1. Harbour geometry and flow conditions

The harbour that was tested during the second phase had an angle of 45° with the flume (upstream corner). The harbour basin had the same layout as the harbour basin used for phase 1, except for the fact that a part of the basin was closed (see figure 4.2). This was necessary to shorten the time needed for the system to reach an equilibrium state (the signals were then reproduced to a large extent in the following cycle). The surface area of the harbour was now 3 m^2 because of this alteration. The reduction of the harbour surface area decreased the tidal filling effect substantially.

During phase 2 the flow and tidal characteristics were:

Tidal period	1000 s
Average flume discharge	3.8 l/s
Amplitude of flume velocity	0.20 m/s
Average water depth	0.25 m
Tidal range	0.05 m
Density at sea	1007 kg/m^3
Density of river water	1000 kg/m^3
Ri_E	0.1

The upstream flume discharge was varied in order to influence of the tidal movement in the flume. The tidal range caused by the tidal movement was measured in the sea basin. At the location of the harbour the amplitude of the tidal movement was virtually the same as that of the sea basin. The density of the water in the sea basin was kept constant.

4.4.2. Description of CDW configurations

The CDW that was developed during phase 2 was entirely different from the "classic" CDW that is used under tidal homogeneous conditions. As no experience existed with this kind of CDW, two full days were used to test various CDWs. This resulted in two promising CDW-configurations. The three configurations that were tested are shown in figure 4.5. The reference situation had a slightly altered upstream harbour entrance corner, the second configuration had a short CDW in the top half of the water column and a large sill in the lower half of the water column. The CDW was placed at the downstream harbour entrance corner. For the third configuration a second sill was applied at the upstream harbour entrance corner, also with a height equal to half the average water depth.

It should be mentioned that some additional PTV measurements were done for a configuration with a blunt upstream harbour entrance corner and no CDW (configuration 45A of phase 1).

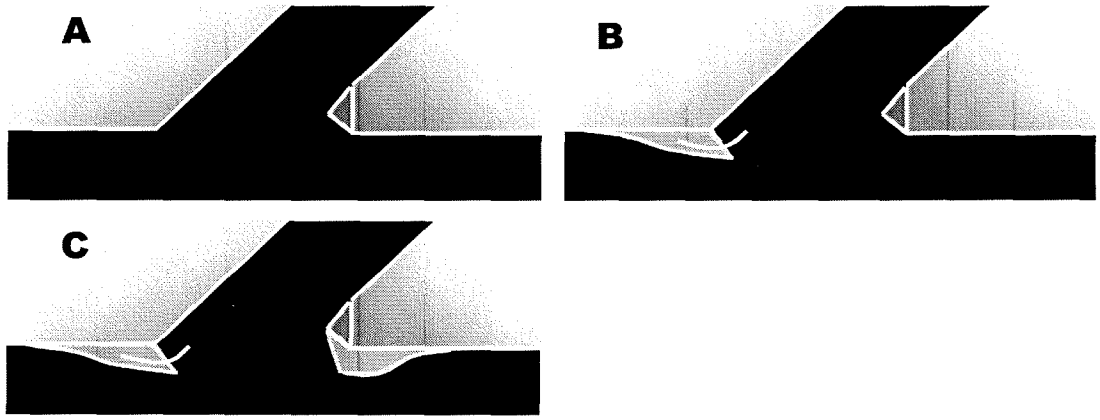

Figure 4.5. Plan of CDW configurations used during phase 2

4.4.3. Measurements taken

The following measurement techniques were applied during the second phase:

- Electro Magnetic Velocity measurement (EMS) in the flume and at several positions in the harbour.
- Water level measurements (WAVO) at various positions in the flume.
- Salinity measurements at fixed positions (VAZO).
- Moving salinity probes (BEZO) were placed at several positions in the harbour.
- Dye Concentration Measurements (DCM): dye was injected in the flume/harbour, and the colour (concentration) was monitored by video camera;
- Particle Tracking Velocimetry (PTV): particles were applied to the water surface, and the positions (movement) were recorded by video camera.
- Bottom Flow Pattern Visualisation: Metal white plates with black woollen threads were placed on the bottom of the harbour entrance, and recorded by video in order to determine the flow direction at the bottom.

As for phase 1, some measurement techniques were used continuously to check the boundary values for the tests. These were the EMS, the WAVO and the BEZO measurements. The same camera was used as for phase 1.

Further information about the measurements can be found in the chapters 5, 6 and 7.

4.4.4. Testing procedures

Creating reproducible tidal flow under inhomogeneous conditions and doing research with various instruments at the same time is a complex operation. In this section the procedures that were followed during a typical test day are described. Both the actions of the Delft Hydraulics staff and the LIP III project members are mentioned.

At the beginning of a testing day, the DH-staff started the Tidal Flume. First thing to be done was calibrating the WAVO and EMS devices. The water in the flume was used as a reference, so it had to be undisturbed. This was no problem because after each test day the flume was shut down and had approximately 10 to 12 hours rest. After calibration of the instruments, the flume could be started up. When a harbour configuration had to be changed (e.g. placing a new CDW), this was done after the calibration, and preferably before starting up the flume.

The upstream discharge and the tidal movement in the sea basin were initiated while the sea and the flume were still separated by a gate. At low slack water in the sea basin (t=800s of the first tidal cycle) this separation was removed. The reason for separation up until this moment was to prevent too much salt water from entering the flume at once. After having opened the gate the flume only needed handling by computerised controls.

The next stage was the calibration of the salt probes as well as a check of the measured signals by DH-staff. When this was concluded the automated measurement program was started. Usually this was around the third tide in the basin.

From the density data it was concluded that the system took 4 to 6 tidal cycles to reach an equilibrium state, so from the beginning of tidal cycle 7 measurements could be taken.

Two computers were used for collecting measurement data. One computer was operated by DH-staff and collected data that was needed for controlling the flume. The second computer collected the measurement data. It collected 39 measurement signals, which contained amongst others the output of 6 WAVOs (water height), 7 thermometers, 3 EMS's (flow velocity), 3 BEZOs (moving salinity probes), and 3 VAZOs (salinity probes at a fixed position). The measurements of every tidal cycle was recorded as a single file with a sample frequency of 20Hz (8.6MB).

During the day water levels and the salinity of the sea basin were checked regularly to ensure that everything was functioning properly. This was not always the case, and also not always detected at once which led to a loss of usable data. The flume control system sounds an alarm when certain values are outside the permitted boundaries but this was not the case for the other sets of measurement signals.

After the tests for the day were finished, the flume was shut down by DH-personnel. The sea and flume were again separated around 10:00h tidal time (LSW at the sea basin), when most salt water had re-entered the sea. Upstream discharge and tidal movement were switched off now. Most of the remaining salt water in the flume was then pumped into the sea to prevent the saline water from polluting the flume and spreading out over the entire length of the flume. When Particle Tracking measurements had been taken, the particles were collected from the sea basin and from the harbour.

4.5. Overview of all tests executed

The number of configurations that were tested, combined with the different measurement techniques that were applied, resulted in quite a number of tests. The following diagram gives an overview.

Project	Phase	Harbour Angle	Discharge	Configuration	Measurement
LIP III	Phase 1 Quasi-Tidal	45 degree	1 l/s	reference	Dye PTV EMS
				harbour entrance mod	Dye PTV EMS
				CDW	Dye PTV EMS
			2 l/s	reference	Dye PTV EMS
				harbour entrance mod	Dye PTV EMS
				CDW	Dye PTV EMS
		90 degree	1 l/s	reference	Dye PTV EMS
				CDW	Dye PTV EMS
			2 l/s	reference	Dye PTV EMS
				CDW	Dye PTV EMS
	Phase 2 Tidal Inhomogeneous	45 degree	-	reference	Dye PTV EMS BEZO Video Threads
				DS CDW & DS sill	Dye PTV EMS BEZO Video Threads
				DS CDW & DS sill & US sill	Dye PTV EMS BEZO Video Threads

Figure 4.6. Tests undertaken during LIP III

Although the number of configurations tested for phase 1 is larger than for phase 2, the emphasis for the LIP III project was on the tidal inhomogeneous tests. Phase 1 tests lasted only 2 weeks while seven weeks were available for phase 2. A more detailed description of the time-investment needed per measurement technique and for other test activities is given in appendix I.

5. Standard Measurement Techniques and Procedures

5.1. Introduction

For the LIP III project several measurement techniques were used. The execution of the measurements and the processing of the data are described in this chapter. Section 5.2 describes the density measurements taken with the BEZO. The EMS measurements of flow velocity are described in section 5.3, and section 5.4 describes the water level measurements by means of the WAVO devices. A fourth measurement technique, the visualisation of flow patterns at the bottom with the aid of woollen threads, is described in section 5.5.

The Dye Concentration Measurement technique and the Particle Tracking Velocimetry method will be clarified in the chapters 6 and 7 respectively.

5.2. Density measurements

Density measurements were only taken during phase 2 of the LIP III project. Salinity differences were not present during the phase 1 experiments under homogeneous conditions. For phase 2 the density was one of the most important parameters to measure because it was the driving force behind the density current. This is the most important exchange mechanism. In addition, the density measurements were used as the major check to see if the boundary conditions were constant for all tests. They also showed whether the measurements that were taken influenced the flow.

During all tests the density was measured up- and downstream of the harbour, as well as at the head of the harbour. In addition the density was measured at other locations for some tests. The positions of the density measurements in and around the harbour are depicted in figure 5.1.

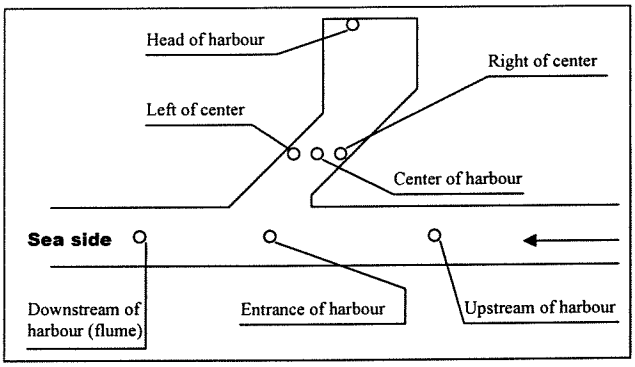

Figure 5.1. Position of BEZO measurements during phase 2.

Density measurements were taken in two different ways:

- At fixed horizontal and vertical positions with VAZO devices (fixed salinity probe);
- At fixed horizontal positions, with a changing vertical position with BEZO devices (moving salinity probe).

5.2.1. Moving salinity probe: BEZO

The moving density probe technique was developed at WL| Delft Hydraulics. It consists of a measuring unit, a control unit, and a tube pump, see figure 5.2.

A plateau supports the measuring unit. Conductivity and temperature probes are attached to a movement unit (elevator) that is attached to the measuring unit. The electronics of the measuring unit contain a position meter, and the control of the elevator engine. The control unit consists of a conductivity range amplifier and a control oscillator, which control the movement of the probe. A fixed discharge through the conductivity probe is maintained by a tube-pump.

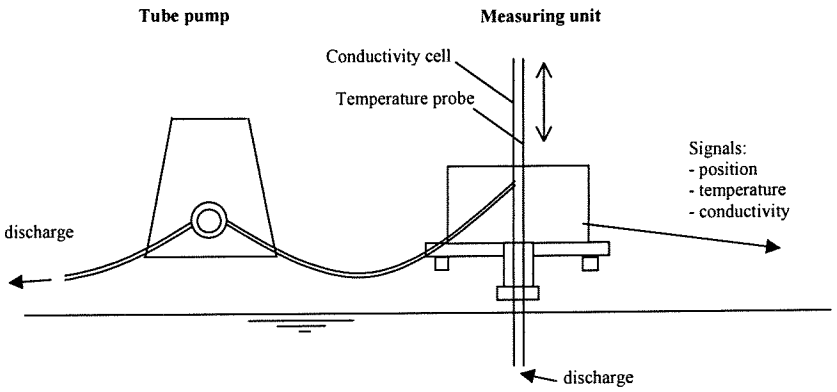

Figure 5.2. BEZO set up

5.2.2. BEZO measurements

During each tidal cycle 11 vertical salinity profiles were measured. Each vertical is measured in nine steps. The probe stays at one depth for 10s. This way the probe can adjust to the salinity at each depth. Each step the elevation is increased by 25mm. From the top position the probes are moved back to the bottom position in one step. The position of the probes in time is the same for each tidal cycle and is plotted in the next figure.

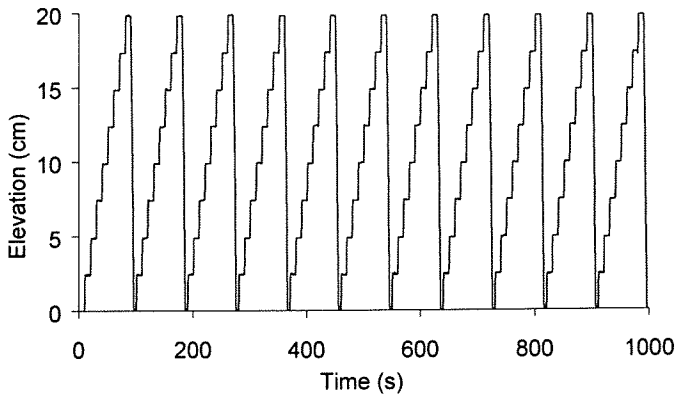

Figure 5.3. Position of BEZO as a function of time.

5.2.3. Processing of BEZO data

The basic assumption in processing the data was that each tidal cycle was an independent realisation of the same experiment. The average density distribution can now be obtained by averaging the signals of the different tides that were recorded.

Processing the density data had to be automated because of the vast amount of data that was involved. A program was written in FORTRAN 90 that first calculated the density for all samples, using the temperature and conductivity data. The next step was to average the density over the last nine seconds of the ten seconds that the probe stayed at a particular level. The first second was taken as the adjustment period of the BEZO to the new level. The density profiles that were obtained this way are skewed in time, with the point at the top recorded 80 seconds later than the point at the bottom of the profile.

For obtaining a density profile that is representative for a certain time the software package *Surfer* was used. First, all measurements that were made of the same harbour configuration were collected in one file. From this file a grid with the density values as a function of place and time is created by interpolation. The interpolating method that was used is called Kriging. This grid can be plotted as a graph with three axes. These axes give the values for the parameters height from the bed (z), time (t) and water density (ρ).

It is possible to take 'slices' from the z-t-ρ-grid. When a 'slice' with a constant time is taken from the grid, then this represents the density profile at a specific time. This way it becomes easy to obtain an approximation of the real density profile at a certain time. The corrected profiles were compared to the skewed profiles to check the final outcome. The results are shown in chapter 9.

5.3. Electromagnetic velocity measurements

Electromagnetic velocity measurements (EMS) were taken during phase1 and phase 2 of the LIP III tests. The EMS measurements give information about the velocity variation over the depth. In addition, the velocity measurements near the surface were used to validate the Particle Tracking results. EMS measurements give 2 dimensional, horizontal velocity information at only one point, but with a higher accuracy than Particle Tracking.

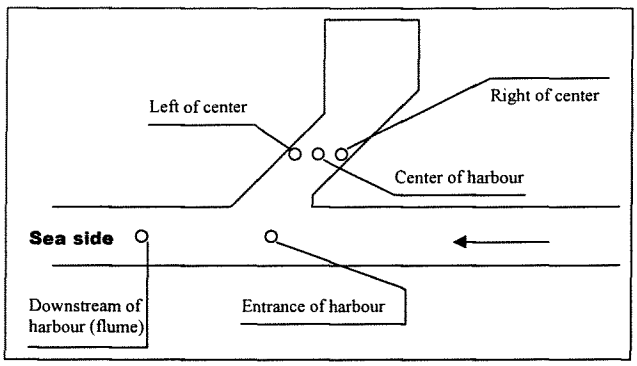

Figure 5.4. Position of EMS measurements during phase 2

5.3.1. Set up phase 1

During phase 1 measurements were taken at several positions of the harbour area. Originally three measurement depths were intended for each position, but when it became clear that 600 seconds of data was necessary for a dependable average, it was decided to take measurements at only one depth (10 cm elevation from bottom). Only one configuration was measured at three depths.

For the 45° harbour 37 positions were measured, and 29 for the 90° harbour. The value of the velocity was determined by taking the median value of 600s EMS data. The EMS measurement data are to be used for validation of a computer model. The use of this data for this thesis project was limited. See appendix B for the exact positions.

5.3.2. Set up phase 2

During phase 2 EMS measurements were taken at several positions in the harbour and the flume. Figure 5.4 shows the positions and the corresponding names.

For all harbour configurations EMS measurements were taken at three depths: 5cm, 8cm, and 18cm from the bottom. Each of these measurements lasted at least three tidal cycles.

5.3.3. Processing EMS data, phase 2

Three tidal cycles worth of data is not much for an accurate average at a certain moment in the tidal cycle. The following processing technique has been applied to increase the accuracy. First the ensemble average was taken for the available tidal cycles. Then the amplitudes of the Fourier components were determined. Next a low low-pass filtering with a cut off at 0.01 Hz was applied. The remaining signal gave an approximation of the average flow velocities during a tidal cycle. Figure 5.5 shows a raw signal (x and y), an average over three tides, the amplitude spectrum of the Fourier components and the signal after filtering out the higher frequencies.

From the amplitudes of the Fourier components it can be seen that the components with a frequency higher than 0.01Hz hardly contribute to the total signal. Sharp bends and discontinuities are not reproduced accurately.

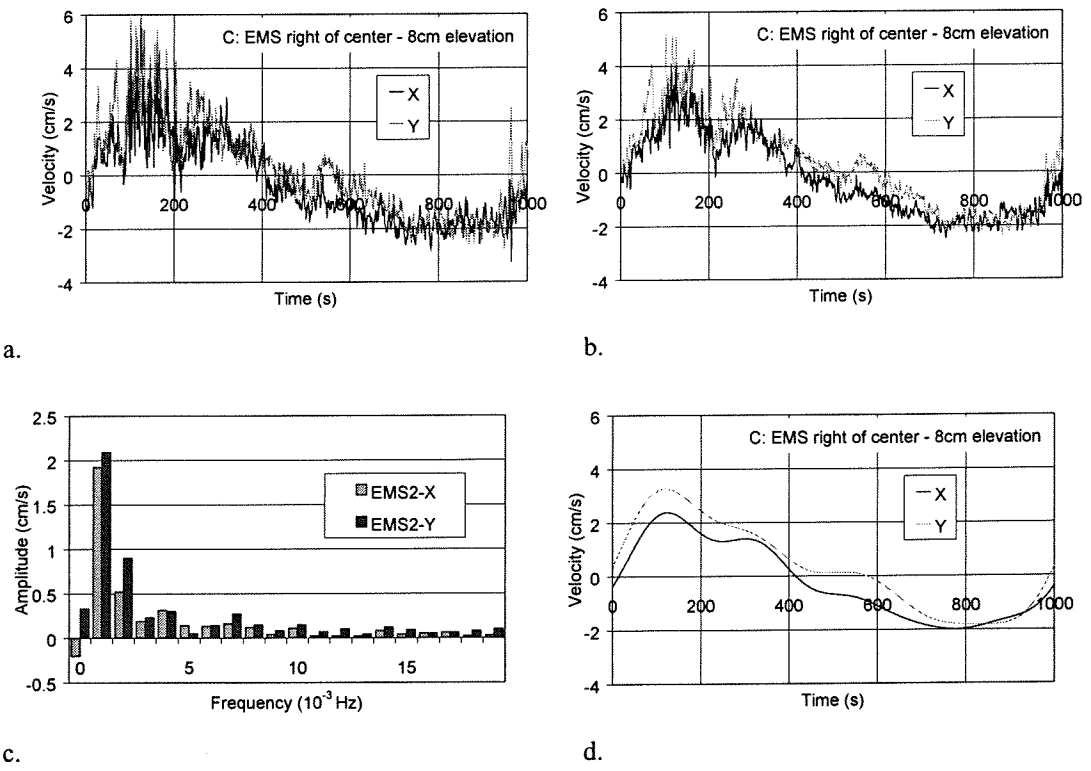

Figure 5.5. a) Measured signal of one tide, b) Signals averaged over three tides, c) Amplitude spectrum, d) Low-pass filtered signals

5.4. Water level measurements

5.4.1. Water level measurements and processing

The water level measurements were taken with the WAVO. This device has a needle that follows the water surface. The position of the needle indicates the level of the water surface. The WAVO signal from the model sea is used to control the flume.

The water level did not change during the experiments under homogeneous conditions, so except for checking the water level from time to time they were not important during phase 1. During phase 2, however, the tidal movement in the sea made continuous measurements of the water level necessary. For phase 2, measurements of the water level were taken at five positions in the flume and at one position in the harbour. The WAVO devices just upstream, downstream and in the harbour were most important. The differences between the water levels at these three locations are very small.

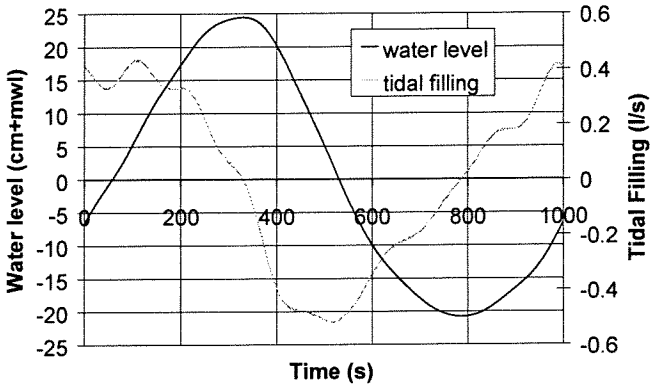

Figure 5.6. Water level in harbour basin and tidal filling discharge through entrance

The WAVO signal is processed in the same way as the EMS signal. A low-pass filter of the Fourier components was the best way to process the WAVO results because of the absence of discontinuities or sharp bends in the water level over time. When the higher frequencies are filtered out, it is possible to take the derivative of the waterlevel in time, withour obtaining large errors in the results. The exchange discharge can now be calculated with equation 2.5.

5.5. Bottom flow pattern visualisation (Threads)

5.5.1. Thread method

In addition to the planned testing methods an experimental method was put to use for phase 2. White plates with black woollen threads, positioned in a grid pattern, were placed in the flume. The woollen threads, containing minuscule air bubbles, stand up in stagnant water and are pressed towards the bottom when flow at the bottom occurs. This way both flow direction and flow velocities at the bed can be visualised. First a test plate was put in to see whether the technique was of additional value for the LIP III project. Throughout the tidal cycle the threads gave a good indication of the flow pattern (see figure 5.7). More and bigger thread plates were made to cover the entire area around the harbour entrance.

5.5.2. Use of the threads during tests

The first function of the threads was to visualise the effect of a CDW on flow at the bottom near the harbour entrance. This was of vital importance when optimising the position of the CDW. At a later stage it served as an easy method of comparison between the harbour

configurations. For presentation purposes a video-tape was made of the harbour configurations with the threads in place.

Although the threads give a very rough indication of flow patterns, it proved a good means for simultaneously visualising the differences in flow pattern between the surface (particle tracking) and the bed. Video recordings were made that give a good general idea of what is happening. The large, relatively heavy threads can be trusted to level out turbulent variations. Some video recordings show dye injected near the entrance every 40 seconds. This gives additional information about mixing, exchange and flow velocities.

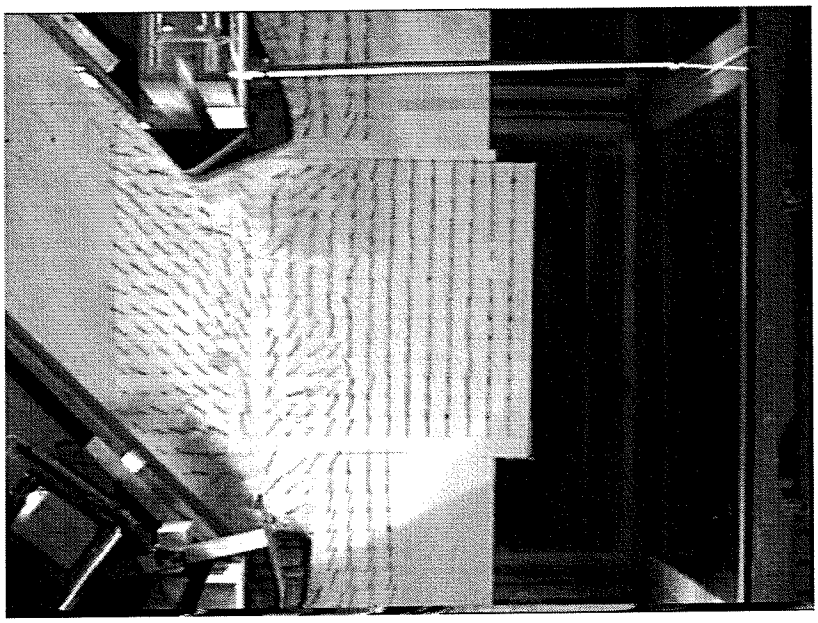

Figure 5.7. Threads for visualising the near-bottom flow pattern at t=120s (conf. C)

Putting into place the plates with threads disturbed the flow regime in the flume to a large extent. Surface waves occurred and the salinity profile was out of the ordinary range. Only after two tidal cycles a test recording could again be made of the equilibrium conditions.

5.5.4. Thread software

Software was developed at WL | Delft Hydraulics in order to quantify the differences between harbour configurations. The program obtains the direction of the threads in relation to the direction of the flume. It searches for the pixels in a picture that differ from the background grey-scale value with more than the threshold value. These pixels are assumed to be part of a thread. The directions found over the entire area can be used to obtain flow lines and to assess the effect of a CDW on the near-bed flow pattern. The program was tested during the LIP III project but was not applied, in consequence of a lack of time.

6. Dye Concentration Measurements

6.1. Introduction

6.1.1. Using the Dye Concentration Measurement technique

This chapter explains how the exchange of water between harbour and river is measured with the Dye Concentration Measurement technique (DCM). A DCM technique measures the change in dye concentration in a harbour basin. After dye is injected in the system the change in dye concentration in the harbour basin is caused by the flow mechanisms described in chapter 2.

In Phase 1, under homogeneous conditions, a fresh dye solution was evenly distributed over the harbour basin. With DCM the decrease of dye concentration in the harbour over time is measured. See figure 6.1 for an impression.

For Phase 2, under inhomogeneous conditions, dye solution was injected upstream or downstream of the harbour basin. With DCM the increase of dye solution in the harbour over time is now measured. For Phase 2 a saline dye solution was used in order to focus on exchange of water in the lower half of the water column.

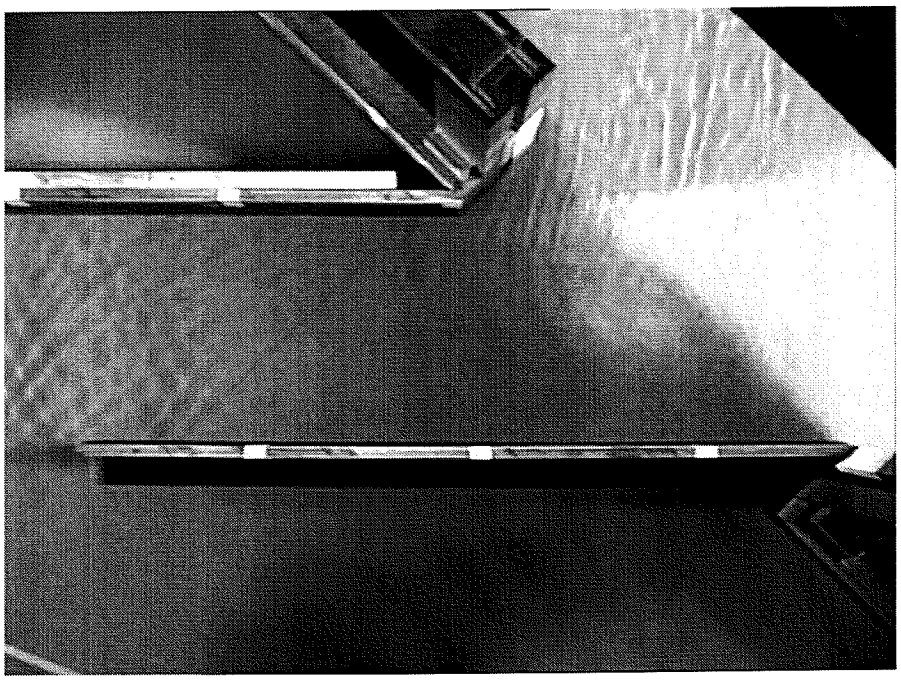

Figure 6.1. Exchange of dye between harbour and river during Phase 1

6.1.2. Aim and scope of DCM in the experiments

The use of the DCM technique is to quantify the effect of a CDW on exchange between river and harbour. The quantification is done with the aid of the software package LOOK&C of Delft University of Technology.

The DCM technique had not yet been applied to inhomogeneous conditions. Both the application of the DCM method and adapting LOOK&C to these conditions needed attention.

Developing and optimising the combination of performing tests and applying the software has been made part of the present study.

6.2. Quantifying exchange with DCM

6.2.1. Use of dye to replace sediment

As was explained in section 2.6.3 real sediment or a sediment-like substitute cannot be used for the present study. For the relation between dye exchange and sediment exchange the following comparison can be drawn. Sediment exchange between harbour and river can be related to the exchange of water between harbour and river at the start of the sediment exchange. For the short time interval at the beginning of sediment exchange, factors like trap-coefficient and fall velocities can be neglected. Then the extent to which harbour-water is replaced by river-water is a measure for the sedimentation of the harbour area. The use of dye for determination of exchange discharges is based on this principle because exchange of water is taken equal to the exchange of (water with) dye. It must be stressed that this approach tells something about exchange of sediment at the beginning of exchange and not about exchange in a later stage or about actual sedimentation.

For the comparison of dye exchange and sediment exchange the use of dye instead of sediment has two additional disadvantages. The first disadvantage is that sediment-laden water behaves differently from water with a certain dye solution. At high concentrations sediment can change the flow characteristics, where dye does not alter these characteristics at all. Secondly, for both homogeneous and the inhomogeneous conditions the highest concentration of sediment appears in the lower half of the water column. Dye can be injected near the bed and will remain dissolved in the lower half of the water column but the actual sediment distribution over the water depth cannot be simulated.

The conclusion is that using dye to replace sediment one will have to be careful in relating the results back to actual harbour-river systems.

6.2.2. Quantifying exchange for Phase 1

For Phase 1, under quasi-tidal homogeneous conditions, a certain amount of dye is spread evenly over the harbour basin at the beginning of each test. To be able to quantify the exchange under quasi-tidal homogeneous conditions it is helpful to consider the mass balance of the system (see figure 6.2.).

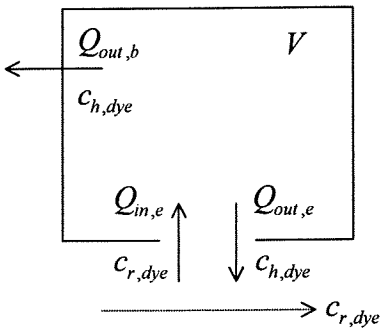

Figure 6.2. First order mass balance for Phase 1

The symbols used are: V for the recorded control volume in the harbour basin, $c_{h,dye}$ is the changing dye concentration in the harbour, $c_{r,dye}$ is the constant dye concentration in the river, $Q_{out,b}$ is the extracted harbour discharge that simulates tidal filling, $Q_{in,e}$ is the inflow through

the harbour entrance and $Q_{out,e}$ is the outflow through the harbour entrance. For the control volume only part of the total harbour area was used.

The extracted discharge at the head of the harbour, $Q_{out,b}$, is an over-simplification of the actual flow pattern schematised in figure 6.3. Because of the gyre system some of the harbour water flowing out of the recorded harbour area, flows back into the area a moment later. This water takes some of the dye back into the recorded harbour area as well. A more accurate term for $Q_{out,b}$ would be the exchange discharge in the head of the harbour, $Q_{exchange\ back}$, with a net outflow of either 1 or 2 l/s. Dye exchange at the head of the harbour would then have to be taken into account. The maximum velocity in the primary gyre is about 1/4 of the velocity in the river and the same proportion is valid for the maximum velocity in the secondary gyre in relation to the velocity in the primary gyre (Booij, 1986). The assumption is made that the velocities in the second gyre are negligible and that the flow back into the control volume at the head of the harbour can be neglected.

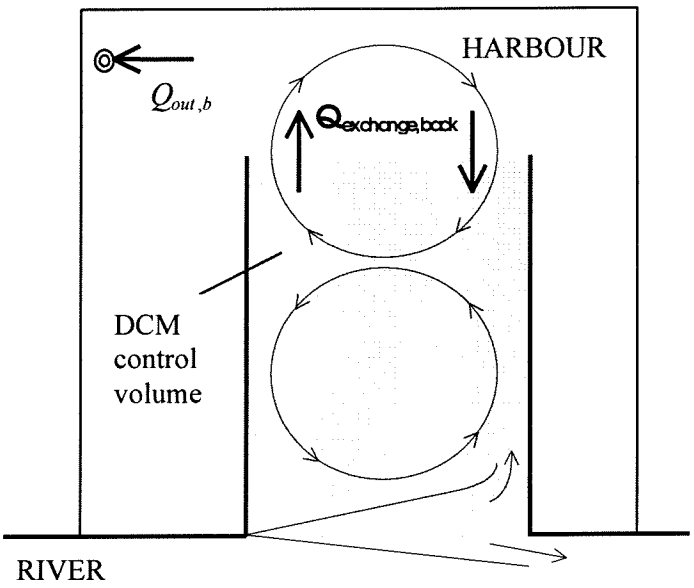

Figure 6.3. Schematic flow pattern, emphasising exchange in the head of the harbour

Before any dye is injected, the system already has a background colour or background concentration, $c_{bg,dye}$, which is about equal to the concentration on the river, $c_{r,dye}$, which remains virtually constant over one test series. This means:

$$c_{r,dye} = c_{bg,dye} = \textbf{\textit{constant}} \qquad \text{Equation 6.1.}$$

The added dye solution in the harbour basin raises the dye concentration in the basin with the input concentration $c_{in,dye}$ so:

$$c_{h,dye}(t=0) = c_{bg,dye} + c_{i,dye} = c_{r,dye} + c_{i,dye} \qquad \text{Equation 6.2.}$$

Taking the model shown in figure 6.2 with

$$\frac{dV}{dt} = 0 \qquad \text{Equation 6.3.}$$

conservation of mass then reads as follows:

$$\frac{dc_{h,dye}}{dt} = c_{r,dye}\frac{Q_{in,e}}{V} - c_{h,dye}\frac{(Q_{out,b} + Q_{out,e})}{V} \qquad \text{Equation 6.4.}$$

and:

$$Q_{in,e} = Q_{out,b} + Q_{out,e}$$ Equation 6.3.

When $Q_{in,e}$ is substituted for $Q_{out,b} + Q_{out,e}$, the solution for this equation is ($t > 0$):

$$c_{h,dye}(t) = c_{bg,dye} + c_{i,dye} e^{-\frac{Q_{in,e} t}{V}}$$ Equation 6.4.

The use of the exponential function is possible when the control volume is considered to be homogeneously mixed. This implies that all diffusion of dye takes place at the harbour entrance and that there is a negligible gradient in dye concentration over the harbour area of interest. See figure 6.4 for an illustrative graph of the decrease in dye concentration over time, based on equation 6.4.

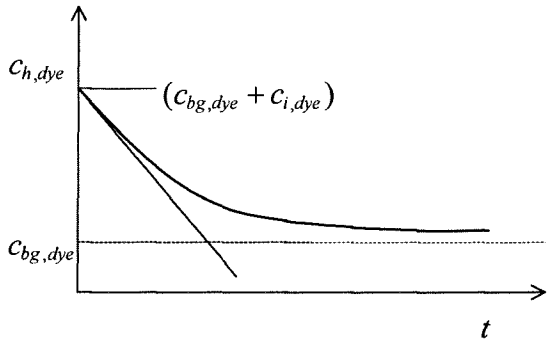

Figure 6.4. Graph of the concentration in the harbour, $c_{h,dye}$, against time

Exchange of dye can be compared to exchange of sediment (section 6.2.2) and with the exponential function fitted through the Phase 1 results, the in-flowing discharge can be determined, $Q_{in,e}$, With $Q_{in,e} = Q_{out,b} + Q_{out,e}$ and $Q_{out,b}$ and V known, the exchange discharge through the mixing zone can be computed. The calculated discharges for the different configurations are given in section 8.3.

6.2.3. Quantifying exchange for Phase 2

During Phase 2, under tidal inhomogeneous conditions, dye solution was injected in the flume, either upstream or downstream of the harbour. An increase in dye concentration in the harbour now occurs in contrast to the decrease in concentration during Phase 1 tests. The mass balance is studied for a better insight in the exchange under tidal inhomogeneous conditions (figure 6.4).

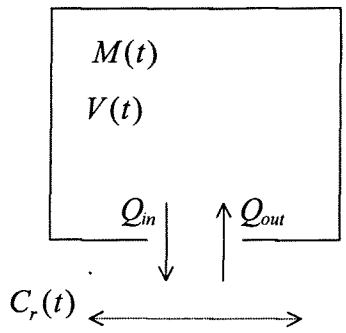

Figure 6.5. First order mass balance for Phase 2

The symbols used are: V for the recorded control volume in the harbour basin, $c_{h,dye}$ is the changing dye concentration in the harbour, $c_{r,dye}$ is the constant dye concentration in the river, Q_{out} is the discharge flowing out the harbour entrance and Q_{in} is the inflow through the harbour entrance.

Before any dye is injected, the system already has a background colour or background concentration $c_{bg,dye}$. For the Phase 2 experiments, with dye injected in the river instead of in the harbour this meant that at t = 0 when dye was being injected until the moment that dye entered the harbour at about t = 15 seconds:

$$c_{h,dye} = c_{bg,dye} = \textbf{\textit{constant}} \qquad \text{Equation 6.5.}$$

and

$$c_{r,dye,t=0} = c_{bg,dye} + c_{i,dye} = c_{h,dye} + c_{i,dye} \qquad \text{Equation 6.6.}$$

Taking the model shown in figure 6.5, conservation of mass reads as follows:

$$\frac{dc_{h,dye}}{dt} = c_{r,dye}\frac{Q_{in}(t)}{V(t)} - c_{h,dye}\frac{Q_{out}(t)}{V(t)} \qquad \text{Equation 6.7.}$$

For the tidal inhomogeneous conditions it is not possible to solve this equation with a rather simple exponential function. The flow processes keep on changing as well as the influence of the flow mechanisms on the exchange of dye. However, it is still possible to make a comparison between the different harbour configurations and their effect on the exchange of dye. This will be explained in the next section.

Dye exchange rate

When dye is injected near the bed, the assumption can be made that the input rate of dye into the harbour is proportional to exchange of saline water into the harbour near the bed.

Only a short time interval after the beginning of dye exchange between harbour and river can be used for determining the exchange because of several reasons. The first reason is that in the harbour entrance there is substantial mixing over the vertical. Part of the dye flowing into the harbour at the bed can therefor immediately flow out at through the top layer again. The more dye has entered the harbour, the more substantial this outflow becomes. The second reason is that after a certain time interval dye flows out of the control volume towards the head of the harbour.

The moment dye is present in front of the entire harbour entrance is taken as the beginning of dye exchange because then dye is exchanged over the full entrance width (see figure 6.6). This is usually approximately 40s after the beginning of each test. Then the dye has arrived at the harbour and is present across the full entrance width. The time interval can usually be taken no longer than 30 to 40s.

Comparing the exchange rates of dye for the different configurations gives an indication of the effect of each harbour modification on the exchange of saline flow near the bed.

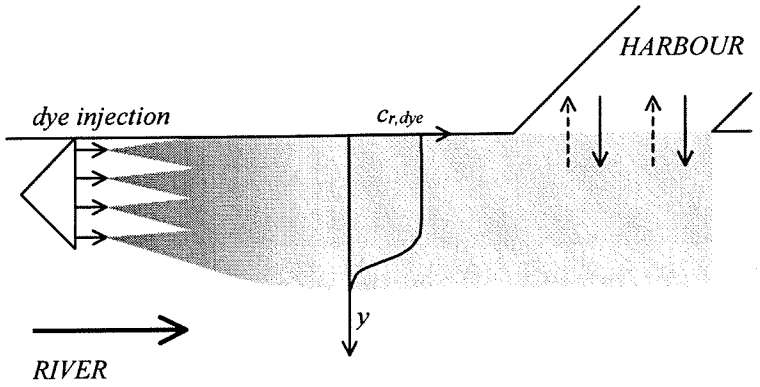

Figure 6.6. Dye injection at the beginning of a test during Phase 2

Determining the exchange discharge

Up till now only the rate of dye concentration increase in $(g/m^3)/s$ is determined. The next step is to try and determine the actual density exchange discharge by using the following approach.

The assumption is made that for a short time interval the discharge in the river is constant and that it can directly be linked to a mass of dye. This is possible because the input rate of dye solution is kept constant. The dye solution is assumed to be totally mixed over a certain area. This area, or in other words the spread of dye over the height and the width, can be determined from top view pictures and side view pictures of the flume.

This approach renders a ratio between the injected dye mass and the volume of (dyed) water flowing past the harbour per second (discharge). With this ratio the volume of (dyed) water that entered the harbour over the time interval can be calculated from the increase of dye mass in the harbour over the time interval. This gives an in-flow discharge that originated from part of the water layer near the bed. The fraction of the total amount of injected dye that enters the harbour is now a direct measure for this in-flow discharge.

6.3. DCM method LOOK&C

6.3.1 Introduction

LOOK&C is a DCM method with which the exchange between harbour and river is measured in the present study. The Laboratory of Fluid Mechanics at Delft University of Technology had originally designed the program for one specific final thesis project: Exchange of dissolved matter between groin field and river (Wallast, 1998). At a later stage LOOK&C was applied for further studies. All studies with LOOK&C were performed at the Laboratory of Fluid Mechanics.

At the beginning of the present study, the first concern was to start up LOOK&C at Delft Hydraulics. This took some time as the application of the program continued to give problems. Because of the strict time schedule attention was shifted towards the gathering of data. Data processing was postponed until the test period had ended and the problems were solved.

LOOK&C defines a grid area in the harbour basin and a reference area. The grid serves as the control volume. LOOK&C calculates the dye mass for each cell of the grid separately. The intensity of external incoming light is taken into account with the reference area. The reference area is one grid cell of adjustable size placed in an area where no change in dye concentration takes place.

General set-up DCM test

Setting up the system for DCM tests was done with great care. The general set of procedures for both Phase 1 and Phase 2 were as follows:

- Maintaining constant base conditions as light intensities, camera position and dye solution concentrations etc;
- Waiting for the flow conditions to stabilise after the (necessary) disturbances;
- Avoiding external disturbance to the flow conditions;
- Keeping a log and report, also on the incidents that might influence the eventual results.
- Performing the test. Usually, one test was taken after the other in random order until three recordings were obtained for each harbour configuration and each test moment.

For the dye testing methylene blue was used which gives a blue colour. However, LOOK&C only works with the grey scale image of the recordings. The grey scale image contains grey values ranging from 0 (black) to 256 (white). The grey value is a measure for the amount of dye in the water. The correlation between grey value and concentration is not linear. That is why it is not possible to calculate the average dye concentration from the average grey value of the area. Instead, an exponential function is made to fit through the reference concentration points. When processing the data LOOK&C can link every grey value it encounters to the exponential function.

In the actual test series dye is added to the system with flow present. The camera takes digital images of the changing concentrations after which the data is processed and the changing concentrations are calculated with the aid of the reference concentrations. The graph of these calculated dye masses against time gives the rate at which the dye concentration increases (or decreases) for the different harbour configurations.

Number of tests

The assumption was made that three tests per harbour configuration would be sufficient because the first test results were to a large extent reproducible. The first graphs confirmed this assumption as can be seen in figures 6.9 and 6.12 for both Phase 1 and 2 respectively.

Calculation of dye concentrations

Before being able to calculate dye masses from the test data, a range of known calibration concentrations must be created and recorded by camera. They form the reference concentrations for the eventual dye concentrations during the tests. Since the calibration forms the basis for the end result, this part of the DCM method should be processed with great care.

When the control volume in the harbour basin is determined, this area is closed off and known quantities of dye are added to form the reference concentrations. After having performed the calibration an attempt was made each time to remove some of the dyed calibration water before the area was opened again. This was done to prevent a higher background value of dye in the system. For this reason the closed-off area should not be much bigger than the control volume.

Per calibration six to ten reference concentrations were recorded including the zero concentration with no dye added. Also part of the calibration was one recording with flow to be able to take these zero conditions into account as well.

Closing off the calibration area from the rest of the flume influences the light intensities that normally occur in the area. To avoid too much variation in these light intensities, transparent Perspex plates were used on either side of the area of interest.

6.3.2. Data processing

LOOK&C works with a pre-processing program, Blue Mean, and three Modules to further handle the processing. These modules and the input parameters of LOOK&C are discussed in the this section.

Blue Mean

Before being processed by Blue Mean all frames of the digital camera recordings (*.AVI files with a frequency of 1 Hz) of each calibration and of the test series had to be converted into separate greyscale files (*.TIF file series).

Blue Mean, or BM in short, puts a rectangular grid over every frame (*.TIF file series) and creates a reference area (see figure 6.7). BM then converts all frames that belong to one data set as a group and stores them into one file (*.RTF format). This file is the basis for all further steps to be taken. On this file all the grey values of each grid cell and of the reference area are stored.

The parameters of BM are:

- Co-ordinates (and size) of the rectangular grid;
- Partitioning of the grid in x- and y-direction;
- Co-ordinates of the reference-area.

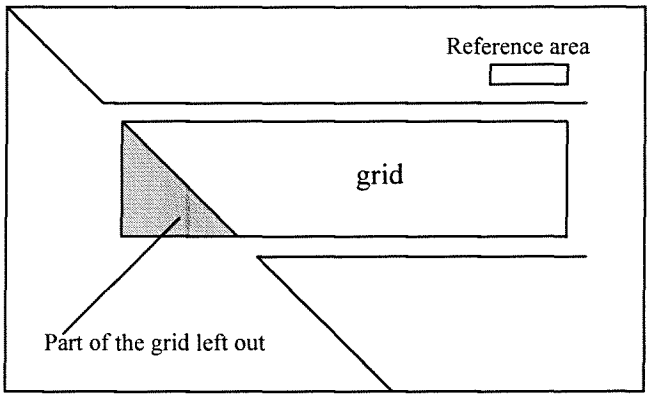

Figure 6.7. Example of a control area used in LOOK&C (without the grid partitioning)

Module 1

Module 1 (MOD1) takes the basic light conditions at the test site into account. The input for Module 1 consists of two image series: one without dye and without flow and the other also without dye but with flow. These form the background values for the actual test series.

The average grey value of the reference area is converted into a zero grey value for each grid cell. That zero grey value is subtracted in MOD3 from the grey values found in the actual test series. This renders the grey value difference between water without dye and water with an unknown quantity of dye.

Module 2

Module 2 (MOD2) establishes the relation between grey value and dye concentration for each grid cell separately. For determining this exponential relation, the concentration fit, the calibration concentrations are used. Figure 6.8 gives an impression of the relation between grey values and dye concentrations. The accuracy of this fit is discussed in section 6.7 and to more detail in appendix H.

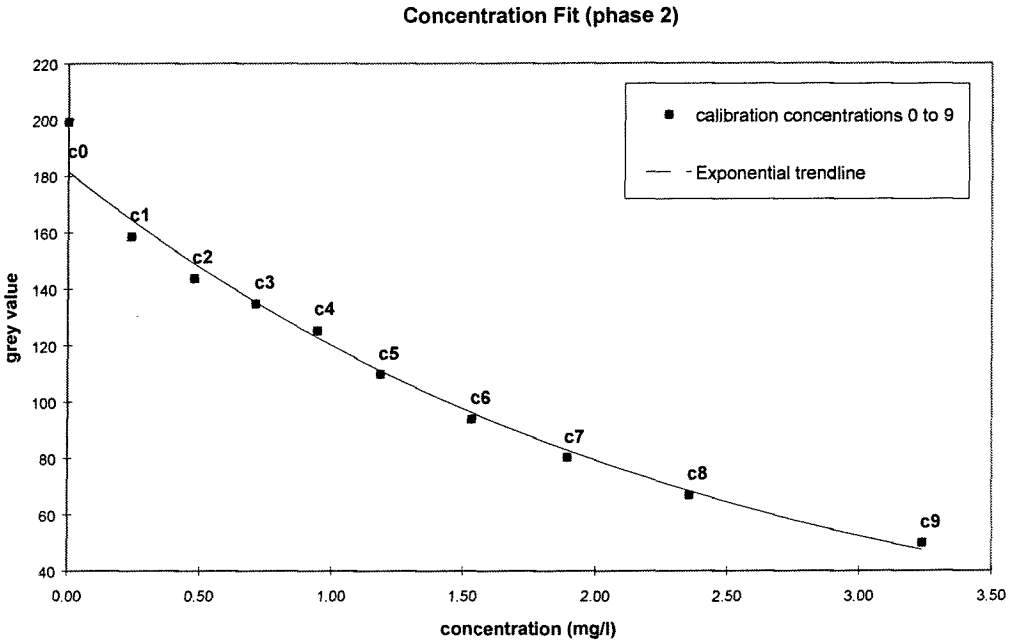

Figure 6.8. Relation between grey values and dye concentration in the control volume

Module 3

Module 3 (MOD3) calculates the dye mass for each test series.

The outcome of MOD1 and MOD2 is first read into MOD3. Them the dye masses are calculated from the test series (after all series were pre-processed by BM). The sum of all dye masses per grid cell (and per frame) are put into the output file (also *.RTF format).

When the calibration concentrations are processed by mod3, the raw mass data in the output files of the test series can be scaled back to dye masses in grams.

Amount of data

Processing the data is a time consuming matter. For instance, when investigating the influence of one of the LOOK&C parameters, not only the test data itself has to be adjusted. The calibration recordings have to be adjusted in the same manner and Module 1, 2 and 3 have to be run again, as well as the post-processing to visualise the effect. The same succession has to be followed for each of the parameters investigated.

A disadvantage of using LOOK&C is the huge amount of data that has to be collected and soon fills up memory space. For the present study three test recordings were made per harbour configuration, per discharge (Phase 1) and per moment in the tidal cycle (Phase 2). In total about 100 data series were recorded, including the calibrations, with on average 400 image frames per data set. With all this data converted into greyscale *.tif format, this comes down to almost 18 Giga Bite of memory space that had to be stored. The memory space needed for programs to run and the space needed for conversion with LOOK&C is not included.

Because of this amount of data it is very important to optimise the use of LOOK&C at an early stage. Then there is no need to store all the greyscale images for later use.

6.4. Phase 1 tests

6.4.1. Performing the tests

For the quasi-tidal homogeneous tests of Phase 1 the difference in exchange of water between harbour configurations with and without CDW had to be visualised and quantified.

Performing DCM tests during Phase 1 was not difficult. The flow conditions remained the same at all times without delicate tidal profiles to worry about. For the Phase 1 tests one litre of dye solution was poured out over the harbour basin just above the surface which caused visible surface waves. The visible disturbance due to this method of dye input had virtually disappeared after about 30 to 50 seconds. Therefore the first 50 seconds are left out for data processing. Injecting the dye evenly over the harbour area in a short time interval without causing disturbances was not possible. Experience learned that the injected dye solution was no longer visible in the harbour after about 300 to 500 seconds, depending on the harbour configuration and the extracted harbour discharge.

6.4.2. Response signal for Phase 1 tests

This section deals with the basic response signal, for all harbour configurations in general, in order to check if the DCM technique was functioning properly. For Phase 1 tests the basic signal was expected to have the following features:

- Because dye was added at the beginning of a test, the signal should start at a high concentration that would decrease quickly because of the exchange processes;
- The response signal should show a more or less exponential decrease in concentration as was discussed in section 6.2.2.

Figure 6.9 shows the first results indicating that the DCM technique gave the expected response signal.

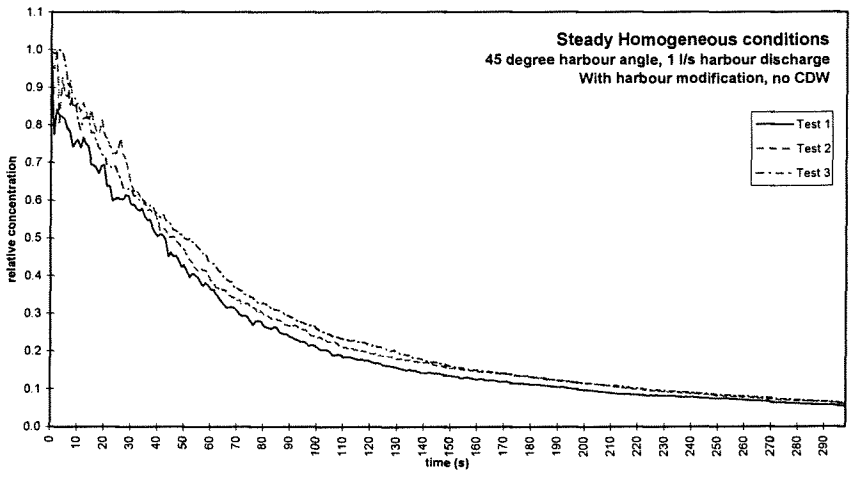

Figure 6.9. Basic response signal for the quasi-tidal homogeneous tests

6.5. Phase 2 tests

6.5.1. Performing the tests

Exchange near the bed was the focus of the DCM tests. Particle tracking data gave information about flow at the surface and DCM was to do the same for flow at the bottom.

The method of dye input used for Phase 1 could not be used because the equilibrium flow situation was easily disturbed. Salinity profiles and velocity profiles would be disturbed to such an extent that the test results would not properly represent the situation at that phase of the tidal cycle. The disturbance caused by placing the dye injection plate into the flume was comparable to moving the EMS or BEZO instruments to different positions. The amount of dye solution added with the injection plate was 3.6 ml/s, which was small compared to the discharge in the flume. Saline water with the same density as seawater was used for the dye solution in an effort to further minimise the influence of the solution on the surrounding flow and to keep the injected dye in the lower half of the water column. The resulting dye pattern during tests is shown in figure 6.10.

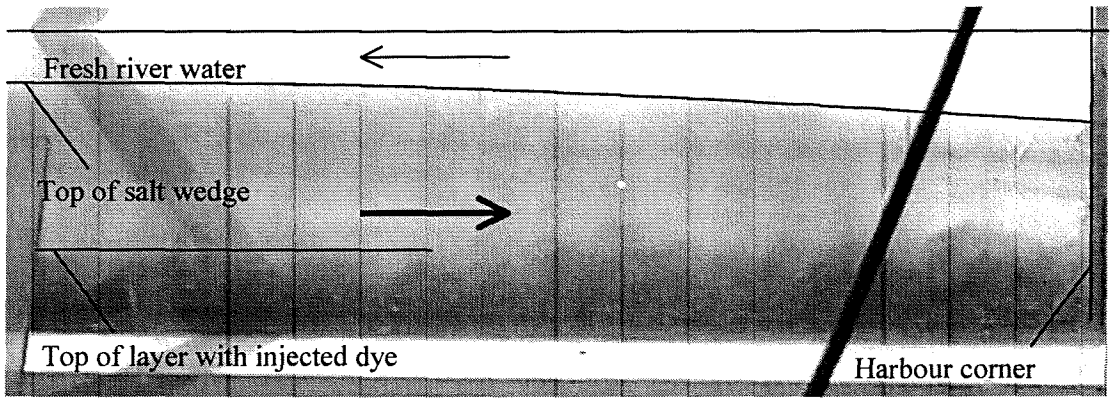

Figure 6.10. Side view of the flume during rising tide at t=980s

Until the injected dye solution reaches the mixing zone, it did not spread any higher than approximately 0.10 to 0.15m from the bed. After the dye has reached the harbour corner, the dye solution spread more over the depth. Visual observations confirm that even here the highest concentration of dye remains near the bed. Above about half the water depth virtually no dye is visible.

The input of dye solution per unit of time and the input time was kept constant. The effect of the dye technique on the flow conditions was checked. The new way of injecting dye caused no noticeable disturbance to either flow velocities or salinity profiles.

A choice had to be made which parts of the tidal cycle to analyse. It was established that bottom flow during rising tide was of most interest because then the CDW was supposed to work. Five injection moments in the rising tide period were chosen for which dye was injected just downstream of the harbour (see figure 6.11). Injection of dye solution at the beginning of rising tide could not start until t=900s. At that moment the flow in the flume near the bed was just capable of taking the injected dye towards the harbour. The latest moment that dye could be injected during rising tide was at t=280s. Just after that moment dye solution started accumulating before the flow reversed. Between the injection time at the beginning and the injection point at the end of rising tide, three more time sections were investigated.

In addition dye was injected just upstream of the harbour at moment 6 in figure 6.11 during falling tide to further establish the effect of the upstream CDW on water exchange between harbour and river.

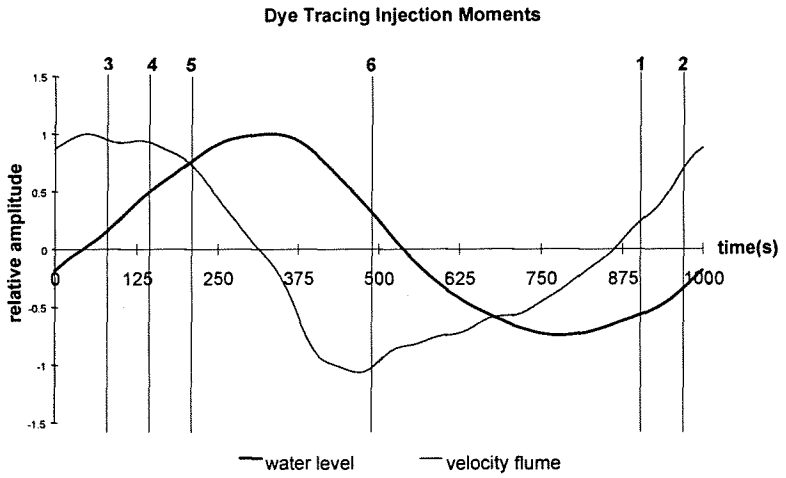

Figure 6.11. Moments during the tidal cycle when dye was injected just up- or downstream of the harbour.

6.5.2. Response signal for Phase 2 tests

This section deals with the basic response signal for Phase 2, for all harbour configurations and moments in general, to check if the DCM technique was functioning properly. The expected features of the response curve were as follows:

- At the beginning of the recording the injected dye would not yet have reached the harbour entrance so the concentration in the control volume was expected to be constant over this period;
- Next, part of the dye solution would enter the harbour system resulting in a significant increase of dye concentration;
- After the dye injection had stopped, no more dye would enter the harbour system and the graph should show a sharp decline in concentration.

Figure 6.12 shows a general result indicating that the DCM technique gave the expected response signal. The moment with a sharp increase in dye concentration corresponds with the visual observation of the moment that the injected dye had reached the harbour corner.

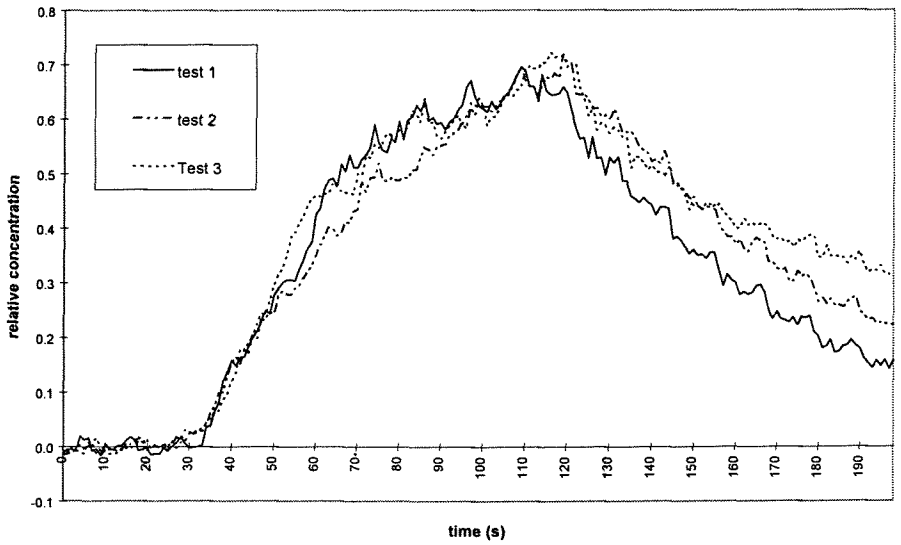

Figure 6.12. Example of results for Phase 2: Tidal Inhomogeneous tests

6.6. Accuracy of the DCM results

6.6.1. Introduction

This section deals with the accuracy of the dye results. A test protocol was followed to be able to create similar conditions for all configurations to have an equal level of accuracy for all results. The influence of many factors and parameters was investigated with this objective in mind. Not every variable could be kept the same. The over-all accuracy of the results is discussed in general in this section. See appendix H for more detailed information.

6.6.2. Factors of influence

Dye input

Some influence of performing the dye tests on the flow conditions could not be avoided. This differed for the two phases.

During Phase 1 tests the influence of the dye tests on the flow regime was substantial at the time of input of dye solution. Studying the Phase 1 data with a different DCM program, KLEUR (developed by Delft Hydraulics), indicated that the disturbance of the flow at the time of dye input was still present at the end of the test. This could not be detected with LOOK&C. The effect of this disturbance cannot be quantified.

During Phase 2 the influence of dye input was negligible.

Parameters LOOK&C

Moet nog tekst

Colour components used for LOOK&C

Another matter with influence on the accuracy is the difference in response between the colours components red, blue and green during tests. These three colour components together form the basis for the grey colour response with which LOOK&C works. From analysis of Phase 1 data it appeared that the colour components red and blue of the full colour image disturbed the averaged grey scale response. The red colour component shows an increase in dye concentration until about t=100s while the concentration should decrease from t=0s onwards. The colour component blue shows a sharp decrease in dye concentration until the dye concentration is zero at t=100s while the recording still shows a substantial dye concentration in the control volume. The error introduced this way cannot be quantified.

Background concentration & accuracy calculated dye mass

It was assumed that the methylene blue (C16H18ClN3S.3H20) would loose its colour after a couple of days but it did not. With each test more dye accumulated in the system and the water in the flume turned gradually more blue. An extra factor creating a larger background value was that the dye also stuck to the walls and the bottom.

The added dye solution gave less contrast with the flume water when the background value was raised. More importantly, the error introduced by the calibration is substantially different for different levels of concentration. A test performed without a raised background concentration and a dye increase in the control volume of 0.04g the error in the dye mass as calculated with LOOK&C is in the order of +34%. The same test with a background concentration of about 0.16g has an error level of -17%. These varying error levels have a negative effect on the accuracy and the reproducibility of test results, which was instantly visible. With only a slightly varying background concentration, the test results were reproducible to a very large extent. When background concentrations varied, the results were less similar.

The background value was checked with every set of tests that was performed for Phase 1 and did not turn out to be a significant problem. For Phase 2 it was a different matter because larger quantities of dye were used over a shorter period of time.

6.7.2. Conclusion on accuracy

The Phase 1 results show (very) little difference between configurations for the same harbour angle and the same extracted discharge. The Phase 1 results were reproducible to a large extent so the effect of the LIP III CDW and/or the modification is most probably negligible. The differences are however not substantial enough to say anything conclusive about a possible small positive or negative effect of the CDW and/or the modification on exchange between harbour and river.

The Phase 2 results were less reproducible. This was mainly caused by the different levels of background dye concentration during tests, together with different error levels for different levels of concentration. This combination makes the average error level fluctuate between approximately –10% and +10%.

6.7. Recommendations for improving the use of DCM

6.7.1 General recommendations DCM method

- The team performing DCM tests should have prior experience with DCM. Getting experience with DCM during tests takes up too much valuable test time.
- A detailed manual for the DCM program LOOK&C would greatly facilitate the use of the software package.
- The effect of using separate colour components for DCM processing should be studied. For the LIP III Phase 1 experiments, especially the effect of the colour component red on the test result was worrisome.

6.7.2. Practical recommendations DCM method

- For CDW investigations it might be useful to first perform the DCM calibration before trying to apply a CDW and determine its optimal position. A limited series of preliminary DCM tests can quickly determine the effect of a particular CDW-configuration on exchange.
- Before commencing with the data processing after testing, a thorough investigation should be made into the influence of various LOOK&C parameters and different colour component responses.
- Avoid a difference in background concentration between test series. An increase in background concentration has a negative influence on the concentration fit.
- Taking more than three tests per harbour configuration is recommended. The dye tests were less reproducible than was expected on account of the very first test results. The confidence in the DCM results would increase with a higher number of tests per harbour configuration.
- When performing the calibration, most calibration concentrations should be taken with low dye concentrations because LOOK&C is most vulnerable at lower concentrations.
- Leaving out higher calibration concentrations, which are not found in the control volume during tests, increases the accuracy of the result.
- Newly made saline dye solution should be made for every day to avoid clotting of dye solution, which disturbs a constant input of dye.

- During the calibration, take at least 5 minutes to let the calibration area settle after injecting dye solution for the next concentration before recording. Not doing this disturbs the calibration and has a negative impact on the results.

Recommendations Phase 2

- Since only the very beginning of the response signal is of importance, short injection intervals per test are recommended to avoid a substantial increase of the background concentration.
- More time in between DCM test series to avoid a substantial increase of the background concentration. With time between tests, the dye will slowly disappear from the system.

7. Particle Tracking Velocimetry

7.1. Introduction

7.1.1. Particle tracking in general

Particle Tracking Velocimetry (PTV) is one of the measurement techniques that were used during LIP III.

Particle tracking is an old technique for examining flow patterns. It is based on the assumption that particles follow the fluid motion (exactly). Until some years ago it used to be done visually or with photographs with a large exposure time (streak image velocimetry). To determine the displacements of a large number of particles (i.e. velocities) involved much labour, and mistakes were easily made. Nowadays velocities can be calculated digitally, and large numbers of vectors can be processed. This has greatly improved the applicability of the technique.

During the LIP III experiments *2-dimensional, low density Particle Tracking Velocimetry* (PTV) was used. The principle of this technique is to follow the displacement of the separate floating particles and to determine the flow velocity and flow direction from these. Only particles on the surface of the water are used, so this gives a two-dimensional flow field. When using three or four cameras, and particles over the entire depth, three-dimensional flow fields can be examined, but until now this has only been done with simple flow fields. The technique is still being developed, and is not yet suited for complex flow fields like the flow fields in the harbours at the LIP III project.

There are also other techniques (e.g. high density particle image velocimetry) that do not track a single particle, but use correlation techniques. For a classification of particle tracking techniques see Westerweel (1993).

7.1.2. Aim and scope

Using Particle Tracking Velocimetry on digital images, with algorithms that are executed by computer programs, is relatively new. It became possible with the development of faster computers. The technique was never used under the conditions that were present during the LIP III research before at Delft Hydraulics or Delft University of Technology. This chapter will elaborate on the use of PTV in the Delft Tidal Flume. In the research it was used as a tool. The development of the measurement technique itself was not the primary goal. Not all the circumstances were therefore perfect for the technique. Also other measurements had to be done, and only limited time in the flume was available. The use of PTV at LIP III can be regarded as a "practical" test of the PTV technique.

First the general goal of the PTV tests will be described. Then the main program, which was used for the processing, is described. After that the processing of the information is explained, and next the set up of the experiments is explained. Then the use of the technique is evaluated, followed by a section that deals with the accuracy of the results. The conclusions about the use of the technique itself are mentioned last. In chapters 8 and 9 the results are discussed.

7.2. Quantifying exchange with PTV

7.2.1. Why surface floats?

Most sediment is present in the lower layers of a river, so flow velocities near the bottom should be used for quantifying exchange. Particles near the bottom would be suitable for measuring the velocities there. Still surface floats were used during the tests, giving the flow field at the surface. This was mainly because of practical reasons. Particles at the bottom were tried, but they hardly moved due to the bottom friction, so good measurements could not be obtained. Also semi-submerged floats, with the largest flow-resistant area near the bottom, were tested. The use of semi-submerged floaters was not given priority, because there was not much experience with this technique, the floaters were not available and no time was available to experiment with these. Only some tests have been done.

The surface velocities that were measured do however give information about the velocities and water exchange at the bottom. When certain assumptions are made, and when the PTV results are analysed together with other measurements, the exchange can be quantified. The way the PTV results are used differs for both phases of the project, so the goals are described per phase in the next paragraphs.

7.2.2. Homogeneous situation: tidal and diffuse exchange (phase 1)

Exchange due to tidal filling is generally larger than the diffusive exchange through the mixing layer. The tidal exchange is easily determined by using the measured water level variation. The diffusive exchange can be a substantial part of the total exchange in the harbours with homogeneous water of phase 1. This diffusive exchange is impossible to measure directly with PTV. An indirect way of quantification is however possible. Booij (1986) derived the following equations with which the exchange discharge can be calculated:

$$Q_{ex} = 0.018 \cdot h u_r B_e \frac{\delta}{\delta_{theor.}} \qquad \text{Equation 7.1}$$

$$\delta_{theor.} = 0.10 \cdot (1 - u_r/u_h)(1 + u_r/u_h) \cdot x$$

where $\delta_{theor.}$ is the theoretical width of the mixing layer, and δ is the measured width of the mixing layer. See chapter 2 for the meaning of the other parameters.

Equation 7.1 indicates that the width of the mixing layer is proportional to the exchange discharge. The width of the mixing layer can be obtained from the PTV measurements. There are however some difficulties when using this method. First of all, surface velocities were used, so this will not be very reliable. Secondly the accuracy of the PTV measurements is not very high. Furthermore some assumption had to be made in order to derive equation 7.1. These uncertainties, together with the facts that phase 2 was given a higher priority, and a better way of quantifying exchange was available (DCM), made that this indirect way of quantifying exchange was not applied.

PTV is however a good means of quantifying the flow field in the harbour. The place, strength, and shape of the various eddies can be determined. The influence of a CDW on the flow field in the harbour can also be demonstrated.

In the homogeneous situation (phase 1), one can assume a vertical velocity profile (except in the mixing layer). This way the velocities near the bottom can be regarded to be proportional to the surface velocities, so the surface flow can be regarded as being representative for the depth averaged flow field. Secondary currents can of course not be measured.

7.2.3. Inhomogeneous situation: density current and tidal filling (phase 2)

During phase 2 the major exchange mechanisms (tidal filling and density driven currents) are of an advective nature. Advection can be measured well by means of PTV.

In order to determine the exchange of water, still some assumptions have to be made, as only the surface velocities are known from PTV. The simplest assumption (see 1. in figure 7.1) is that the outgoing density current at the surface has the same magnitude, but opposite direction, as the in going near bed current. The layer depths are assumed as being half the water depth. The tidal filling must also be taken into account.

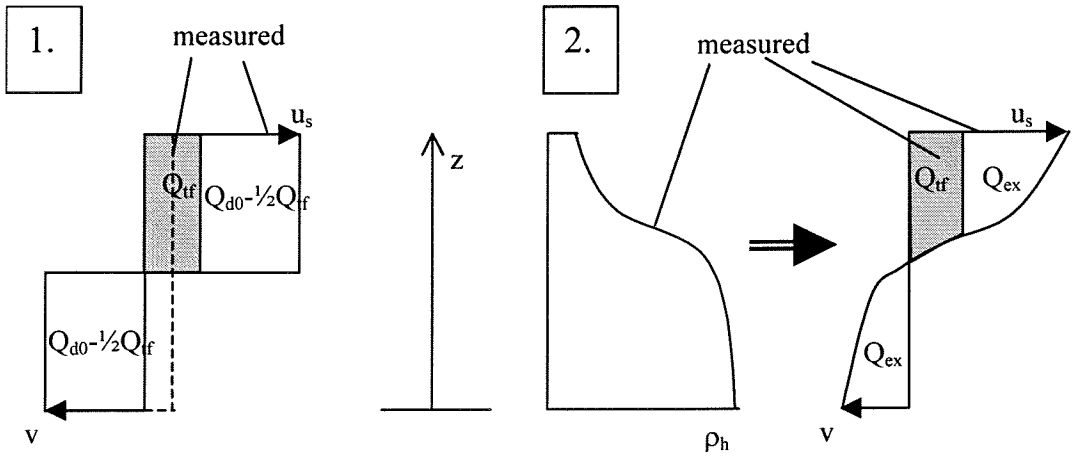

Figure 7.1. Two ways of quantifying the density exchange discharge in stratified flow from the vertical velocity profile

A better approximation of the discharge can be obtained, as the layer depths do not have to be half the water depth, and the velocity is not distributed uniformly over the layer depth. A better assumption could be made for the layer depths, using the density measurements. The position of the layer-interface can be determined by finding the z-coordinate with the highest density gradient. A uniform flow profile per layer can be shown to be present when the flow is (almost) internally critical, and there is an almost sudden transition from one density to another.

Using the density measurements of the whole vertical may even give a better determination of the exchange current (see 2. in figure 7.1). The velocity profile can be related to the density profile. This is discussed further in appendix M.

The EMS measurements can also be used to determine the velocity profile. The execution of the analysis will be described in detail in chapter 9.

7.3. FPTV

At the LIP III project the program FPTV, developed at the TU Eindhoven, was used (Van der Plas, 1998). This program executes low density particle tracking, so individual particles are followed in order to determine the flow field. The program converts gray-scale image files of .PGM format into vector fields. The .PGM files have 768 x 576 pixels, and each pixel has one of the 256 grey values. The FPTV program searches for white blobs on a black background

The program goes through the following steps to obtain the vector field:

- Filtering (dynamic tresholding)
  The background information is subtracted from the images.
- Detection
  The "blobs" -as the images of separate particles are called- are detected by searching for a group of pixels with certain characteristics (size, grey value, etc.) in the digital images. The position can be found with sub pixel accuracy (i.e. more accurate than the size of a pixel) by taking the weighted average of the various grey values in the pixels that are regarded as being part of a blob.
- Mapping
  The dimensions (pixels, and pixels/frame) are scaled to physical units (m, and m/s), and the angle of the camera is corrected.
- Matching
  On consecutive frames the same particles have to be matched. The sample frequency has to be taken small enough, so that the displacement per frame is not more than the distance between particles. This would cause spurious vectors.
  From an average flow field that is based on the previous displacements of a particle, a prediction is made for the future position of this particle. The particle that is closest to this spot on the next image is the best match.
- Path storage. Now the velocities can be calculated, and stored.

The output file of the program contains a list of vectors that were matched. A large part of the post-processing still has to be done after this. See 7.5.2.

7.3.1. Using FPTV

A script was used (Uijttewaal) to let the FPTV program process a series of pictures. This made it possible to process large series of images of one recording at once. However, the FPTV program contains an error, which hindered a quick progress of the processing of results. When processing a large number of pictures the program crashed, after having processed only part of the pictures. The program had to be restarted on average two times per series of 100 pictures. No scripts could be written in order to allow several series to be processed automatically, because the program was not dependable. This cost a lot of time. It was possible to start the program for a few series at one moment, which made processing time shorter.

7.3.2. Factors influencing outcome of FPTV

Several parameters have to be chosen when using the program. The most important are mentioned in this paragraph. Also the choice of the value is explained.

Particle (blob) size on image

The size of the blob that is searched for on the image was set at a minimum of 1 and a maximum of 20 pixels. A pixel covered 2.7 mm of the water surface so a particle creates a blob of 1 to 3 pixels (depends on the threshold) on the image.

Due to surface tension, the particles tend to floc together. The particle clusters that formed were also recognised as blobs, because of the large upper limit, and the velocities of these were used. When the small-scale surface velocity is wanted, and not a time-averaged velocity, the maximum amount of particles should be set to a value close to the actual particle size, so the big groups of particles are not detected.

Threshold value

The threshold value for the difference in grey-scale between blob and background is another important parameter. This was chosen at 50 mostly. This is very high on a scale of 256 grey-scale values. When the flume was coloured because of the dye tests, or the lighting was insufficient a threshold of 30 was used. This resulted in a higher number of matched vectors. The range of this parameter in which about the same number of particles are detected was found to be rather large. It was easy to get the program to detect the particles.

Number of frames

The number of consecutive images on which a particle had to be detected before it was accepted was set at 3 during all the tests, so the influence of changing this parameter was not examined.

Sample frequencies

Different sample frequencies were tested. First a frequency of 20 Hz was used but after comparing results of different frequencies, it was decided to use a frequency of 10 Hz. The sample frequency can be based on the following criteria:

- The required accuracy of the velocity at a specific time
- The amount of mistaken matches that can occur
- The amount of data that can be handled

Only average velocities were needed for the research, so small-scale velocity fluctuations did not have to be measured. The sample frequency could be low according to the first criterion.

To see whether a certain sample frequency will cause mistaken matches, the displacement of a particle per frame must be compared to the distance between particles. When the displacement of a particle is more than the distance to a neighbouring particle, no distinction can be made anymore between the separate particles. There will always be a finite chance on mistaken matches, but the number is low when the average distance between particles is smaller than the maximum displacement of a particle between consecutive frames.

Now a calculation follows for the sample frequency of 10 Hz that was used. On average about 150 particles were present per frame. That would mean that the average distance between particles would be approximately (in a surface area of the harbour of 0.56m x 2m):

$$\sqrt{(0.56 \times 2.00)/150} \approx 8.5cm\,.$$

With a flow velocity in the flume of maximum 20 cm/s only a displacement of 2 cm could be expected per frame, so for the second criterion of mistaken matches the sample frequency was rather high.

The sample frequency should have been taken lower, or more particles should have been put on the surface in order to decrease the amount of data.

7.4. Processing

Processing the PTV data required a large amount of processing steps of which an oversight is presented below. The pre-processing comprises all the processing steps that are undertaken

before the FPTV program is used. The post-processing comprises the processing steps that are undertaken after the FPTV has determined the flow field.

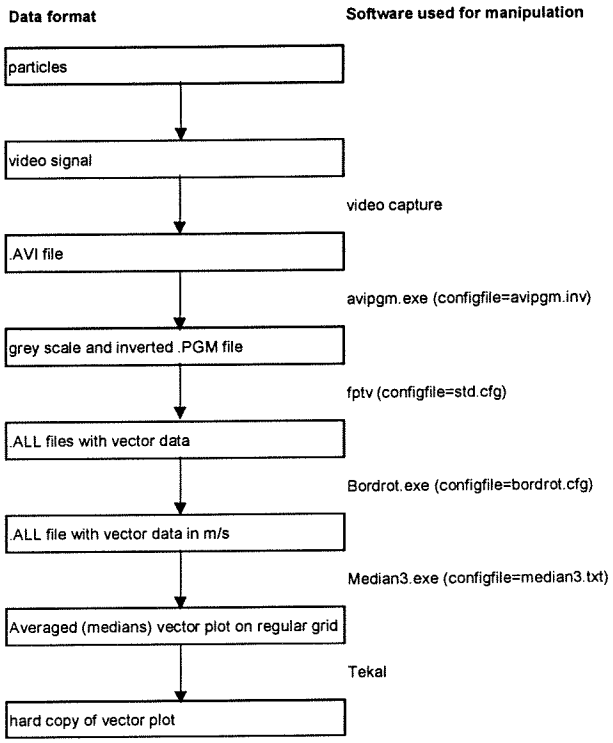

Figure 7.2. Information path for Particle tracking

7.4.1. Pre-processing

The video pictures that were recorded on tape are first turned into .AVI video files. The .AVI files have to be turned into separate .PGM files for the FPTV program. The .PGM files were first made in two stages: A batch program was used that steered the *Video Capture* program. This program could make images in .TIF format. These images were turned into .PGM files by a second program, called *image robot*, which is especially made for repeating graphical manipulations. The batch program could not handle the large amount of data, so some images were faulty, and sometimes the program broke down.

During phase 2 a FORTRAN-program was available that converted the .AVI files directly into .PGM files. This was dependable, and rather quick. Now it was also possible to start several series of processing, and the program would run by itself. The limiting factor now was only the amount of memory on hard disk. The .PGM files were transferred to data files (.ALL) which contained columns with vector data.

7.4.2. Post-processing

After all vectors have been found by FPTV the information is not yet presentable, as can be seen in figure 7.3. There are still spurious vectors present. These problems can be solved by projecting a grid over the area of interest. One vector is now allocated to the centre of each cell. This vector is determined by taking an average of all vectors in a cell. This vector represents the flow of the entire the cell.

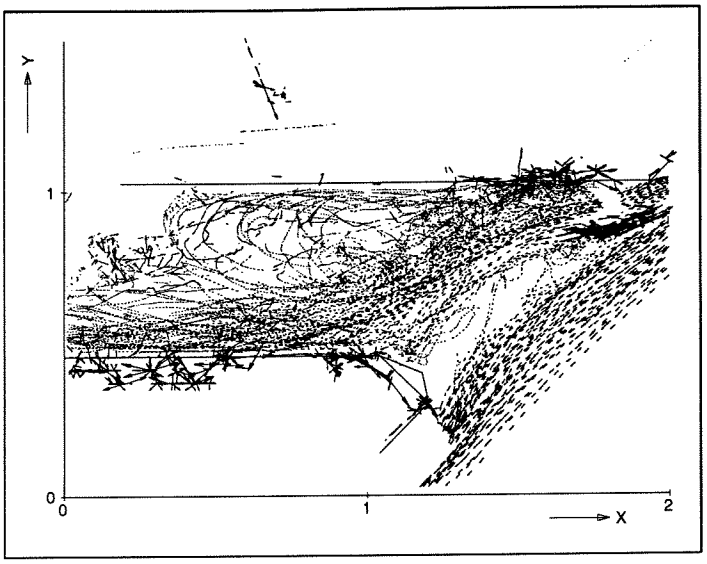

Figure 7.3. All vectors that are detected and matched by FPTV program in the harbour, during quasi-tidal tests, with a CDW present

There are several possibilities for determining this vector. One can take the average or the median. The median has the advantage that spurious vectors, which are either very large or very small, hardly influence the result. The magnitude of a spurious vector does influence the average. When using the average value, one can remove the vectors that exceed the value of the average +/- three times the standard deviation (Van Prooijen, 1999). This procedure does however involve an extra manipulation. It was chosen to use the median technique. For PIV post-interrogation (a slightly different technique to find the velocities) this was also found to be the best method (Westerweel, 1993).

Two programs were written in PASCAL for executing the post processing. The first one, BORDERS, rotates and scales the vectors found by FPTV. It also removes the vectors that lay outside the harbour area (appendix G). A second program, MEDIAN, (appendix H) determines the vectors on a regular grid. First it removes all single vectors that are physically unrealistically large. Then, for each grid cell, it finds the medians of the separate velocity components u and v of all vectors that are found in this cell, and allocates these values a vector that is placed on the centre of the cell.

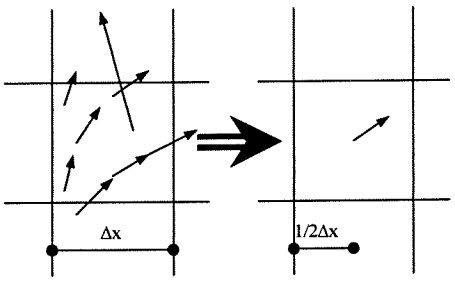

Figure 7.4. Per grid cell the median vector is determined The entire area is divided in grid cells.

When only one or two vectors were found in a grid cell the resultant median vector is unreliable. A spurious vector will now always influence the final result. When a low number of vectors is found in a grid cell the chance that these vectors are spurious is also bigger. The area can be situated near a shadow, or another disturbance, which is the cause for the low number of vectors, and can also very well be the cause of spurious vectors. The vectors that are based on a low number of original vectors are checked by comparing them to the average of all the neighbouring vectors that are based on enough original vectors. When the

difference is too large the vector is being regarded as unreliable, and is discarded. When two neighbouring vectors are reliable, and there is a gradient over the grid cell, the average should be an estimation of the real value. When only one neighbouring vector is reliable, a vector will be discarded sooner. In that case there is not enough information present.

Making the vectors presentable requires one more step. The program TEKAL was used for this. The vector information is combined with a plot of the harbour and flume borders, and a possible CDW and an image file (.EPS) of the flow field in the harbour is made.

A few parameters that must be chosen for the post processing are described next, and the choice of the value is explained:

Grid size

During the post processing also some choices have to be made. The most important parameter was the grid size. This was set to 5cm, because it would give a good visual representation of the flow field. With on average 26 vectors per cell, the information was also thought to be reliable. It was not changed.

Maximum allowable velocity

Those vectors that are unrealistically large are not taken into account. The maximum velocity is the velocity in the flume. The surface velocity in the flume will be about 10% higher than the average flume velocity, turbulent fluctuations may give about 20% higher flow velocities, so a value of $1.5u_r$ can be used as a safe estimate of the maximum possible vector size.

Maximum difference between unreliable vector and neighbours

Unreliable vectors (low number of samples) are compared to the average values of the adjacent vectors. They are discarded when the difference exceeds a certain absolute value. 1 cm/s was chosen. As the average velocity in the harbour is about 5 cm/s this will give the vectors that are checked an accuracy of 20%.

7.5. Number of matched vectors

An indication of the number of vectors that was found during the tests is given in the table below:

Phase	Time of recor-ding	Number of vectors used for one image			Average number of vectors used per cell in one image		
		Average	Min	Max	Average	Min	Max
Phase 1	60s	11,500	6,700	21,000	26	13	40
Phase 2	30s(/40s)	13,000	8,000	19,000	26	18	37

Table 7.1. Information used for PTV images

More particles were present in the harbour during phase 2. The same amount of vectors per cells found, while the duration of the recordings was half that of phase 1. More particles were detected because there were simply more particles available during phase 2. Also less experience was present with the project members during phase 1, so they were too careful when applying the particles. Even during phase two rather a few particles were used.

Originally three minutes were recorded during phase 1, but when processing was found to take long, and the results of one minute seemed to suffice, only one minute was processed.

7.6. Set-up of the tests

7.6.1. General

The model harbour was painted white, and black wooden beads (5 mm diameter) were used as particles, giving a high contrast. Lighting was set up on several sides, in such a way that no light reflected directly into the camera, and no sharp shadows were present in the area of interest.

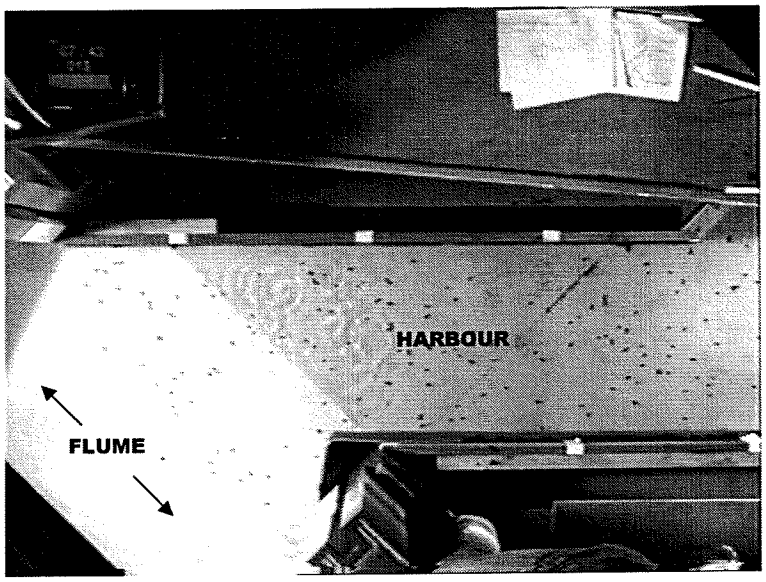

Figure 7.5. Plan view of model harbour during phase 2 with particles present

The camera was fixed at a point 3.26 m above the water surface. When measurements were made the video was recording constantly. A monitor that showed the time in the tide was placed in view of the camera, so the time that each image was made was visible on the image itself. At the harbour edges markings were placed, which were used to scale the images. First everything was taped on video, after that the .AVI files were made from the video tapes. All tests could be done without having to bother with starting or stopping the recording computer. This way the execution of the tests became quicker and easier. When using the video recordings instead of direct recordings, the number of matched vectors decreased by 14%. A lot of the vectors that were lost were spurious vectors, so the decrease of vectors was not regarded as a big problem.

7.6.2. Homogeneous conditions

During the experiments with quasi-tidal and homogeneous conditions, recordings were made for one minute per configuration, and these were repeated for three times. The particles were distributed over the water surface by hand just before the recording started. This was relatively easy. Because the flow was steady, recording could start at any moment. The particles did not have to be on the surface at a specific time. During the time recordings were taken, particles were put to the flume, upstream of the harbour. This way new particles would get into the harbour, as a net inflow was going into the harbour. Particles would now also be present in front of the harbour entrance.

Taking measurements for a long time with a relatively low number of particles, instead of a short time span with a large number of particles causes the measurements to be statistically more independent, which yields better average velocities.

7.6.3. Inhomogeneous conditions

During the tests with inhomogeneous conditions, the flow was not steady, so a different strategy was followed. Eight sample periods with a duration of 10 seconds per tidal cycle were selected to execute the PTV measurements (see figure 7.6). During these ten seconds the flow was assumed to be steady. Just before the beginning of a sample period, two persons distributed the particles uniformly over the water surface.

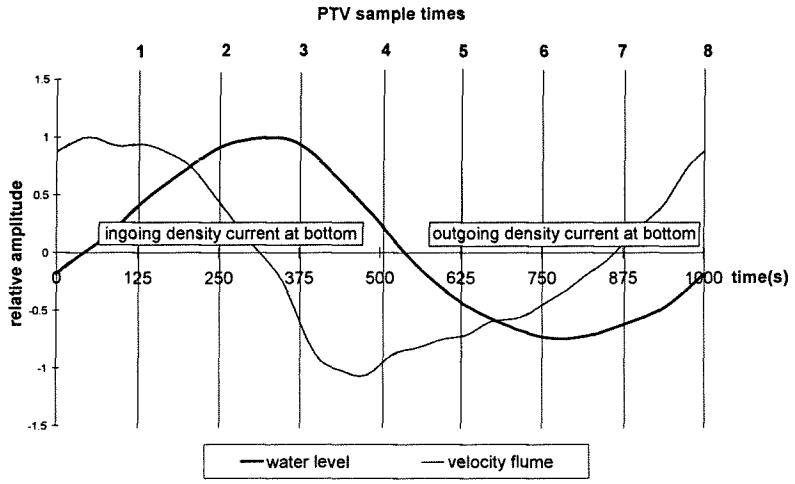

Figure 7.6. Times at which PTV recordings were made, together with water level and flow velocities in the flume

During a sample period particles were put either at the back of the harbour, or upstream or downstream in the flume, depending on the flow direction, so that the particles would enter the view of the camera.

At some areas in the harbour, particles were not present. Upwelling flow caused a diverging flow at the surface, so no particles would enter this area. During the sample period, particles were put in the harbour at those places by hand. The hand and sleeve were lighter than the harbour bottom, so they were not detected as particles. This way also velocities at these areas were detected.

Each sample period was recorded 3 to 4 times (independent realisations), so 30 or 40 seconds of data was collected. 2000 particles were available for phase 2. This was not enough to record all the flow patterns for all the sample times in one go. Two times the particles had to be gathered from the sea basin. This had to be done carefully, in order to leave the stratified system undisturbed.

7.6.4. Computer facilities needed

Several computers were dedicated for the several steps in the process. The pictures are made on a *Pentium II PC* with a *Windows 95* operating system. Also the processing of images is done on this computer. Memory on the hard disk of this computer should 2 to 3 times the amount of memory that is needed to only store the image data. This way processing is not hindered. Only one series of 100 colour pictures is 120 MB. Using FTP the information is sent to a *Linux* environment, where the vector fields are created. The information is sent back to another *Windows* computer where the post-processing is executed.

7.7. Accuracy

The accuracy of the PTV measurements is discussed in this section. No specific experiments

were done to obtain the accuracy, so existing data was used. Several sources of errors are discussed. A distinction must be made between the error in one single measured vector and the error in a median vector that represents the average velocity in a grid cell.

7.7.1. Accuracy of measurement

The first source of errors is the error of the measurement technique itself. An estimation of the magnitude is made next: A pixel is 0.27 cm in diameter. For the determination of the position, an accuracy of approximately 10% of the pixel diameter can be assumed to be present. This value of the sub-pixel accuracy is known from experience. For the determination of a velocity two positions are needed, so an error of ±0.055 cm is then present per sample, which gives an error of ±0.55 cm/s per sample (frequency = 10 Hz). In the harbour basin velocities are 1 to 5 cm/s. The inaccuracy now is 50% down to 10% of the velocity. Flow velocities in the flume can be higher (20 cm/s), and the errors on these velocities will be smaller (3%).

The error on a median vector is smaller due to the averaging. The error decreases approximately with the square root of the number of samples. The formula for a normal distribution can be used for approximating (samples are not independent) this:

$$\Delta x = t_v \frac{s}{\sqrt{n}} \qquad \text{Equation 7.2}$$

In which t_v is the student-t factor, s the standard deviation, and n the number of particles.

7.7.2. Inaccuracy of average flow velocity

The flow velocity has time dependent fluctuations on the mean value, and in the measurement volume (grid cell) a velocity gradient is present. These variations cause an error when the average (or median) velocity is determined. The velocity differences that can be expected due to bottom shear induced turbulence are in the order of 10% in normal steady flow. In the mixing layer velocities in the range of $v_{harbour}$ - v_{flume} can occur.

For 27 grid cells with relatively steady and homogeneous flow[1] the average value and standard deviation of the velocity components were determined (with rejection of the outlyers). The standard deviation per grid cell was on average 0.5 cm/s (approximately 12% of the flow velocity). Based on the estimates that were made earlier this error is thought to be caused for about a half by turbulence and for a half by the inaccuracy of the measurement. For 9 grid cells in the mixing layer the standard deviation was found to be 3.5 cm/s. This means that 95% of the vectors will be in a range of +/- 7 cm/s, which is approximately $v_{harbour}$ - v_{flume}. The influence of the measurement inaccuracy is now negligible.

Because only a small amount of particles was used, the number of particles that is matched in a grid cell can vary, and the accuracy of the velocity can vary a lot per grid cell.

[1] In the back of the harbour of phase 2 when an outgoing density current was present at the surface.

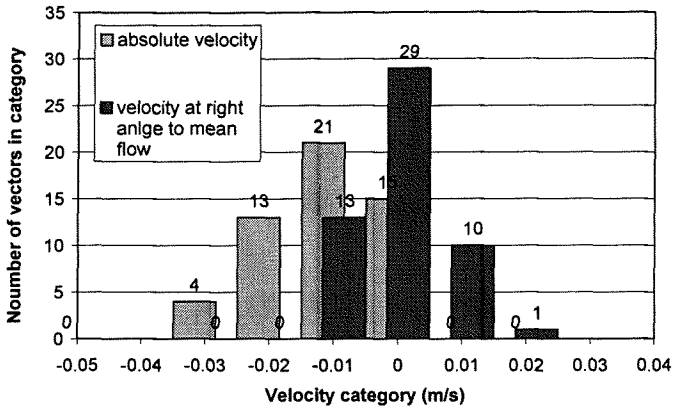

Figure 7.7. Example of the velocity distribution for one grid cell of 5x5 cm^2

7.7.3. Mistaken matches

Mistaken matches form a third source of errors. No indication can be given on the error caused by mistaken matches, although the expected influence on the median vector is small. The most extreme mistaken matches are easily removed, and the number is relatively low (approx. 1%).

At some places there are obstacles (e.g. border of harbour) or dirt in the field of view. When these are matched as a particle, this can also be regarded as a mistaken match. When too many wrong vectors are obtained this way, no useful information can be obtained at these places. It is difficult to remove these vectors automatically.

7.7.4. Comparison to other measurements

During phase 1 the discharge through a few cross sections was determined by summing the velocities that were found by PTV at one cross section, and multiplying that by the grid width. The discharge was obtained by multiplying this total by the water depth. This discharge was multiplied by a factor of 0.9. This factor takes into account that the surface velocities are higher than the depth averaged velocities. This discharge should be an estimate of the discharge from the harbour basin (1 or 2 l/s). This was found to be correct within about 20%, so the order of magnitude of the flow, as found by the PTV, was concluded to be correct.

Not a lot of EMS measurements are available. During phase 2 EMS measurements were done at a depth that varied from 4 to 9 cm. The PTV measurements are compared to the EMS measurements for the moments when the EMS was at a 4 cm depth, and flow in the flume was weak. The PTV results are of the same order of magnitude, but some deviate considerably from the EMS results. It cannot be said whether it is because of inaccuracy or the different depth.

7.8. Semi-submerged floats

Semi-submerged floats were made in order to try and measure velocities at different depths using PTV. Several designs were tried, and the one as shown in figure 7.8 was chosen. The floaters are white, except for the black tip, which was made of cork, and of the same size as the beads that were used as surface floaters. The white parts of the floats are not detected on the white background.

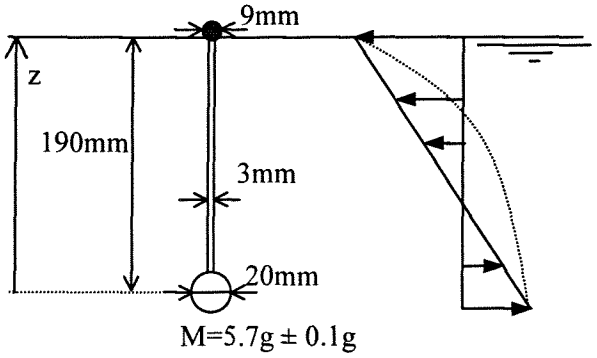

Figure 7.8. Semi-submerged floats that were used for determining velocities at different levels

The idea was that when the surface velocities and the velocity of the float are known, the velocity at the bottom of the float can also be determined. For this the resistance of the floats has to be known. Also the velocity profile over the depth of the float needs to be known. Because the bottom part has a large area, the influence of the part in between is small. The flow profile is assumed to be linear.

For the resultant force on the float the following equations are used:

$$\sum F_x = \tfrac{1}{2} C_{w,m}(\mathrm{Re})\rho D_m \cdot \int_{z=0}^{surface} \left(u_x'(z)\cdot|\vec{u}'|(z)\right)dz + \tfrac{1}{2} C_{w,s}(\mathrm{Re})\rho \frac{\pi}{4} D_s^2 \cdot u_x'(0)\cdot|\vec{u}'|(0) = 0$$

$$\sum F_y = \tfrac{1}{2} C_{w,m}(\mathrm{Re})\rho D_m \cdot \int_{z=0}^{surface} \left(u_y'(z)\cdot|\vec{u}'|(z)\right)dz + \tfrac{1}{2} C_{w,s}(\mathrm{Re})\rho \frac{\pi}{4} D_s^2 \cdot u_y'(0)\cdot|\vec{u}'|(0) = 0$$

$$\vec{u}'(z) = \vec{u}_f - \vec{u}$$

Equation 7.3

where:

z = vertical co-ordinate

ρ = density of water = 1000 kg/m3

u = flow velocity

$u_x(z)$, $u_y(z)$ = flow velocity components

u_f = velocity of float

C_c = drag coefficient for cylinder = 1.2 (2e4<Re<2e5)(Battjes, 1990)

C_s = drag coefficient for sphere = 0.5 (2e4<Re<1e5)

D_c = diameter cylinder = 0.003 m

D_s = diameter of sphere = 0.02 m

The velocity at the bottom end can be solved, because only u(0) (velocity at the bottom of the float) is unknown.

The floats were used at one time in a tide, for two configurations. At the places where EMS velocity measurements were taken, the values were computed. The floats were floating almost straight up in the basin, so only a small deviation due to an oblique orientation can be expected. Only in the mixing layer the floats were not floating straight, so they can not be used there. During the presence of a density current the floats moved very slowly (a few

mm/s). Inertia effect can therefore be neglected.

7.8.1. Results of semi-submerged floats

Velocities in the right order of magnitude were found when using the PTV measurements of both the floats and the beads. Because the accuracy was not expected to be very large, the measurements were not processed further. The influence of the vertical shaft on the total resistance was larger than expected.

The technique might be useful for obtaining flow fields at different depths where not a large accuracy is required. When velocity fields of the surface and of the floats are available, a computer program could determine the flow field at the depth of the bottom of the float. No time was available for this.

7.9. Conclusions and recommendations

7.9.1. Conclusions

- PTV is a reliable and robust way of measuring two dimensional velocity distributions. Even in an experiment that was not always set up optimally, because of time pressure and other experiments that had to be taken, good results were obtained.
- Particles can be put on the water surface by hand during recording; this way also in diverging flow (upwelling) the flow field can be recorded.
- The time needed for processing PTV results can be decreased drastically when also the pre- and post processing are combined in one program.
- 2-D particle tracking cannot be used for measuring discharges in a complex flow field like the one that was examined in the LIP III research. Additional measurements are still required.
- The accuracy of the measurement technique is approximately ±0.55 cm/s per matched vector with a sample frequency of 10 Hz.
- The variation in flow velocity is the main source of the errors in the median vector.
- The accuracy of the vector fields made during LIP III is 10-15% of the flow velocity for the parts where flow is relatively steady. In the mixing layer it is approximately ±3.5 cm/s.

7.9.2. Recommendations

- The sample frequency can be taken lower at approximately 5 Hz, when only average velocities are required. The amount of data decreases proportionally with the sample frequency, so attention should be given to the right choice of this value.
- Three dimensional Particle Tracking should be applied for obtaining a clear picture of the complex three dimensional flow structure in the harbour entrance.

8. Results Phase 1: Homogeneous Conditions

8.1. Introduction

In this chapter the results of the phase 1 experiments are described. These tests were performed with a steady flow in the flume and an extracted discharge from the harbour basin. The extraction causes a net flow through the harbour entrance, which resembles the tidal filling discharge. This is the reason that the steady flow is called quasi-tidal.

The flow patterns that occur for the various configurations that were tested are described in section 8.2. Section 8.3 presents the PTV results and in section 8.4 the exchange discharges that were measured with DCM are presented. The conclusions of phase 1 are presented in chapter 10.

8.2. Description of flow

8.2.1. Definitions

In the following section the sizes and velocities of the various eddies are described. In figure 8.1 the definitions that are used in this report to characterise an eddy are given.

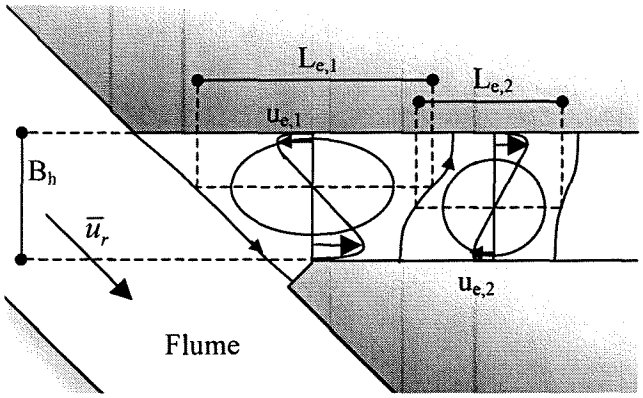

Figure 8.1. Definitions of sizes and velocities of gyres

The eddy closest to the flume is the primary eddy. The width of an eddy (B_h) is taken as the width of the harbour basin (after Booij, 1986). The length of an eddy is determined by the separating flow lines on both sides of the eddy (see figure 8.1). This length is measured over the middle of the eddy, parallel to the orientation of the harbour.

The eddy velocity that is used for comparing different eddies is the maximum velocity of the return current (in opposite direction of the net flow). For the primary eddy (figure 8.1) this is the maximum velocity at the sea side of the harbour, flowing towards the flume. For the secondary eddy this is the maximum velocity at the upstream side of the harbour, flowing towards the flume. The reason for taking the return current is that the influence of the tidal filling discharge would be too large when the maximum velocity in the eddy was taken for the comparison between eddies.

The EMS measurements give information about the flow variation over the depth. The flow profiles over the depth in both the flume and the harbour were not studied in great detail in the present study. The results of the EMS measurements are given in appendix B.3. They show that the flow velocities in lower layers of the harbour basin have generally the same direction as the surface velocities. This makes it possible to examine the eddy configuration with just the use of the surface velocities. All velocities that are mentioned in this chapter are surface velocities, unless mentioned otherwise.

8.2.2. Extracted discharge versus tidal filling discharge

The discharge caused by tidal filling can be compared to the extraction discharge from the harbour basin. In the case of an extraction, the net discharge at the head of the harbour is equal to the extracted discharge. The tidal filling discharge however, decreases in the direction of the end of the harbour, and is nil at the head of the harbour. The difference between a real tidal harbour with a small basin and a harbour with extraction from the basin is schematically drawn in figure 8.2.

For both situations in the figure the discharge caused by the extraction is about equal to the tidal filling discharge near the harbour entrance. Therefore the flow patterns are also comparable near the entrance. Towards the head of the harbour the net discharge differs and therefore the flow pattern differs as well.

The harbour used for the experiments can also be regarded as the first section of a harbour with a larger basin. In that case the flow patterns caused by the tidal filling discharge and the extracted discharge in this first harbour section are similar.

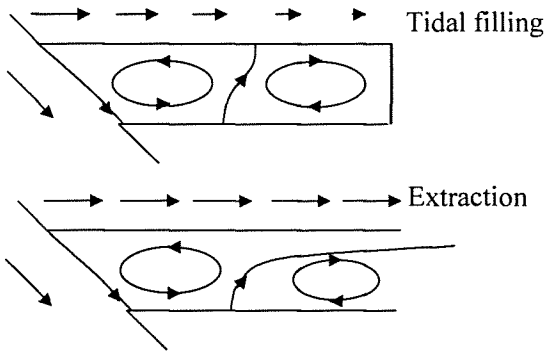

Figure 8.2. Flow pattern with tidal filling and extraction from basin

8.2.3. Harbour with 45° angle

The harbour with a 45° angle to the flow direction in the flume without CDW or modification of the upstream corner was chosen as the reference harbour. A stagnation point is present at the blunt end at the upstream corner (see figure 8.3). On the harbour side of this stagnation point, flow is directed into the harbour basin. The blunt upstream harbour corner makes an angle of 45° with the adjacent harbour wall. Because of this relatively sharp angle flow separates there. The flow that separates at the upstream corner resembles a plane jet, which is directed towards the middle of the harbour basin. High turbulence intensity was clearly visible in this region. At each side of this plane jet an eddy is present. The position and size of the primary eddy is the same for both extraction discharges, because the plane jet dominates the flow near the entrance. The secondary eddy in the reference harbour does change when the extraction discharge is increased to 2 l/s.

The velocity in the primary eddy is 0.25 to 0.3 $\overline{u}_r$, which is a common value. However, the velocity in the secondary eddy, which was found to be 0.25 to 0.3$u_{e,1}$ in previous research, has velocities in the same order of magnitude as the primary eddy. This is caused by the jet at the blunt end, which results in a direct exchange of momentum between the river and the secondary eddy. This blunt end was not present in harbours in other research (e.g. Langendoen, 1992). Normally, there is only transfer of momentum to the secondary eddy via the primary eddy.

Influence of modification of upstream harbour entrance corner

The modification of the upstream harbour entrance corner does not influence the flow pattern when 1 l/s is extracted.

The flow pattern does change when 2 l/s is extracted (modification present). Then there is no flow separation at the corner between the blunt end and the upstream side wall of the harbour. Now only one eddy is present in the harbour basin (see appendix B.2.).

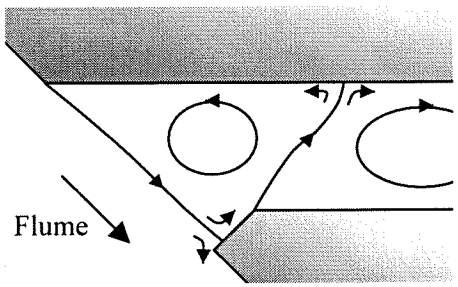

Figure 8.3. Indication of flow pattern in 45° harbour

CDW influence

The CDW influences the flow in the harbour basin considerably. This is visible in figure 8.4. Most water needed for tidal filling is coming in through the CDW. Between the main flow in the flume and the over-capture through the CWD, a zone with low flow velocities and a high turbulent intensity is present. The amount of exchange through this zone is small. Only few particles enter the harbour from the flume via the flume side of the CDW.

One very long eddy is present in the harbour over the full width of the harbour basin. This eddy has very low (return) flow velocities. The flow pattern can be regarded as being an eddy but is probably better described as two parallel flows, flowing in opposite directions. The flow pattern caused by the flow through the CDW is similar for both extraction discharges.

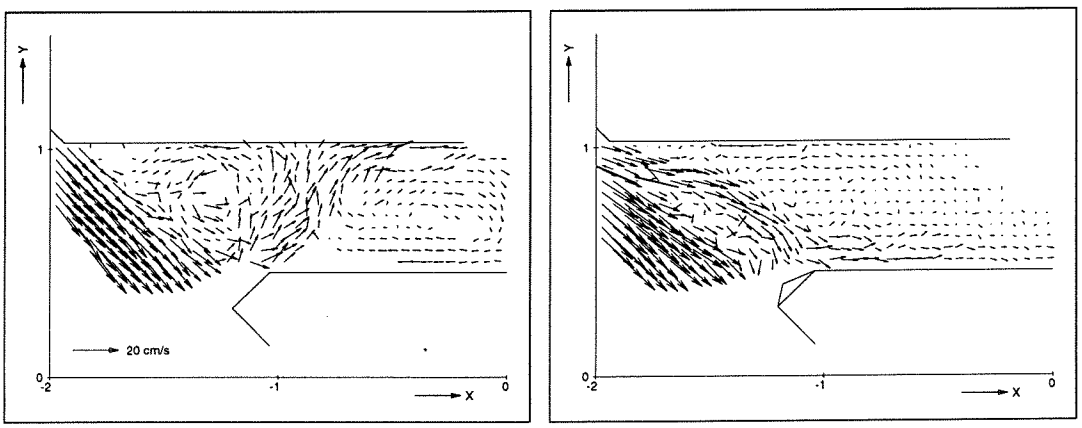

Figure 8.4. Flow in harbour basin without (left) and with (right) CDW with 1l/s extraction from basin

8.2.4. Harbour with 90° angle

In the 90° harbour only one eddy is present for all configurations and extractions. The length/width ratio of this eddy is large.

Influence extracted discharge

When the extracted discharge is increased the length of the eddy remains about the same but the shape alters a little. With the 2 l/s extracted discharge the eddy is less symmetrical. This follows from superposition of a net flow and an eddy, but can also be due to averaging the velocities of a less stable, moving eddy. For the configuration without CDW and a 2 l/s extraction, some small fluctuating eddies are present between the mixing layer and the large eddy.

CDW influence

The CDW increases the length of the eddy for both extracted discharges. With a tidal filling of 1 l/s the CDW hardly decreases the flow velocity in the eddy. The CDW decreases the flow velocity in the eddy drastically for the tidal filling of 2 l/s.

8.3. Eddy characteristics

An oversight of the sizes and velocities in the eddies as determined from the PTV results is given next in table 8.1.

Angle	Discharge	Configuration	Eddy no.	$L_e : B_h$ (error ±0.1)	$u_e / \overline{u}_r$ (error ±0.03)
45°	1 l/s	Reference	1	1.4	0.31
			2	1.6	0.27
		With modification	1	1.4	0.32
			2	1.6	0.24
		With CDW & mod	1	3.0	0.15
	2 l/s	Reference	1	1.4	0.30
			2	>1.6	0.13
		With modification	1	2.8	0.23
		With CDW & mod	1	3.0	0.14
90°	1 l/s	Reference	1	2.0	0.26
		With CDW	1	2.4	0.24
	2 l/s	Reference	1	2.2	0.26
		With CDW	1	>2.8	0.12

Table 8.1. Sizes and velocities of the eddies for all configurations tested during phase 1

8.4. Determination of exchange discharge

8.4.1. Estimation of exchange discharge

An estimate of the exchange discharge can be obtained from earlier research on the combination of a net extracted discharge and diffusive exchange in the mixing layer. The exchange discharge can be calculated using equations 2.2 and 2.10. This results in the following exchange discharges:

For a tidal filling of 1 l/s: Q_{tot} = 1.95 to 2.85 l/s, Q_{ex} = 0.95 to 1.85 l/s
For a tidal filling of 2 l/s: Q_{tot} = 2.70 to 3.50 l/s, Q_{ex} = 0.7 to 1.5 l/s

Where Q_{tot} is the total in-going discharge through the harbour entrance and Q_{ex} is the exchange discharge between harbour and flume.

8.4.2. Determination of exchange discharge with DCM

The approach with the exponential fits was used to determine the order of magnitude of the exchange discharges. This gave unsatisfactory results that were in general too low because many of the calculated discharges did not even approach the extracted discharges. This in turn rendered negative exchange discharges, which is impossible. The calculated discharges are given in table 8.2. A calculation example of an exponential fit leading to negative exchange discharges is given in appendix H section H.4.2.

Harbour angle	Extracted discharge	Configuration	Q_{tot} (l/s)
45°	1 l/s	Reference	1.123
		With modification	1.733
		With CDW & mod	1.447
	2 l/s	Reference	1.560
		With modification	1.676
		With CDW & mod	1.866
90°	1 l/s	Reference	0.885
		With CDW	0.946
	2 l/s	Reference	1.070
		With CDW	1.070

Table 8.2. Calculated discharges from the exponential fits through phase 1 results

It was not thought worthwhile to try a 3^d degree polynomial fit (with the tangent at t=0s for determining the exchange rates) instead of the exponential. The calculated discharges are not expected to be much larger. Other reasons are the minimal differences and the emphasis within LIP III on phase 2.

9. Results Phase 2: Inhomogeneous Conditions

9.1. Introduction

In this chapter an analysis of the measurements that were taken during phase 2 will be given. First an overview of the magnitude of the various processes during a tidal cycle is given in section 9.2. This divides the tidal cycle in periods in which the exchange processes and their interactions are relatively constant. The sections 9.3 and 9.4 give a description of the flow patterns in the harbour (entrance) for the configuration without CDW and with CDW respectively. These sections are followed by an estimate of the exchange discharges over the tidal cycle in section 9.5, as measured by several techniques. In section 9.6 a theoretical description of the influence of a CDW on the exchange during a tidal cycle is presented. The last section presents an overview of the phase 2 results as discussed in this chapter.

The time indication that is used in this chapter is based on the tide as generated in the sea basin (control signal). A tidal cycle starts at t=0s when the water elevation is equal to the mean water level during rising tide. This moment occurs about 80 seconds later at the harbour. The expressions rising tide and falling tide in this section indicate the occurrence at the harbour site. The duration of a tidal cycle is 1000 seconds. Rising tide is defined as the period between low water and the subsequent high water. At the site of the harbour this period is approximately from t=805s to t=320s in the next tidal cycle. The small graphs within the thread images give the water level that was measured in the harbour.

9.2. Division of a tidal cycle according to exchange processes

The intensity of the several exchange processes that were described in chapter 2 can roughly be described by sine functions. A phase lag is present between these processes. The tidal cycle will be divided in periods in which the exchange processes have a constant direction. In figure 9.1, the measurement results are depicted that indicate the magnitude of the processes in the harbour.

In the first graph the water level in the harbour is shown. The tangent of the water level is proportional to the tidal filling. Tidal filling occurs from about -200 to 300s and tidal emptying (negative tidal filling) from about 300 to 800s. The amplitude is approximately 0.5 l/s.

The second graph of figure 9.1 shows the flow velocity near the bed that was measured in the flume, just downstream of the harbour at an elevation of 0.10 m from the bottom. This flow velocity is an indication of the magnitude of the mixing exchange. It is not possible to get the actual mixing exchange out of these velocity measurements because the mixing exchange is influenced greatly by the other exchange mechanisms. The flow is directed up-river from 900 to 1300s. This period is approximately the time that the CDW should function.

In the third graph the depth-averaged densities that were measured in the harbour and river are depicted. The difference between those two densities is the driving force behind the density current. The direction of the density current approximately changes when the density difference is nil.

In the fourth graph the surface velocity that was measured in the harbour basin is depicted. The tidal filling velocity is subtracted, so this is also an indication of the magnitude of the

density discharge. The density-induced discharge flows in at the bottom and out at the top from about 950 to 1450s. From about 450 to 950s the flow directions are reversed.

The directions of the several exchanges processes in the harbour are depicted in table 9.1. The horizontal axis corresponds to the time scale of figure 9.1. A plus or minus sign indicates whether the exchange mechanism is present or not. A zero indicates the period when the influence of the mechanism is negligible. The minus sign at the tidal filling bar indicates tidal emptying. The plus sign at the density current indicates that the flow of the bottom layer is directed inward. A minus sign at the density current indicates that the flow of the bottom layer is directed outward.

In the last row of table 9.1 an indication of the overall effects of all exchange directions on flow in the harbour is presented. In this row seven separate periods are defined. The reason for doing this is that in each of the defined periods the directions of the exchange processes are constant. This will give a better insight into the various stages during the tidal cycle. The working of the CDW over the tidal cycle will be easier to comprehend. The exact time-spans of the periods are arbitrary. The various periods in relation to the flow processes in the harbour are:

Period 1 (t=0-300s): Rising tide & in-going density current near the bottom

The density current at the bottom and the tidal filling are directed inward. Flume velocities directed upstream decrease from the maximum value to almost zero at t = 300 s.

Period 2 (t=250-350s): High water slack

The density current still flows in at the bottom. The tidal filling and flume velocities are negligible.

Period 3 (t=350-475s): Falling tide & in-going density current near bottom

The tidal emptying is commencing, flume velocities directed downstream are high but the density current is still going in at the bottom.

Period 4 (t=475-525s): Falling tide & slack density current

A short time without a density current in the harbour and with high flume velocities directed downstream.

Period 5 (t=525-800s): Falling tide & outgoing density current near the bed

The density current is now flowing out at the bottom and in at the surface. Rather high flume velocities directed downstream are still present in the flume.

Period 6: (t=800-900s): Low water slack and beginning of rising tide

The exchange discharge due to the density current flowing out near the bed is still high, the flume velocity and the tidal emptying are negligible.

Period 7: (t=900-1000s): Rising tide with slack density current

Flume velocities directed upstream are increasing and the density current is starting to flow in again at the bottom.

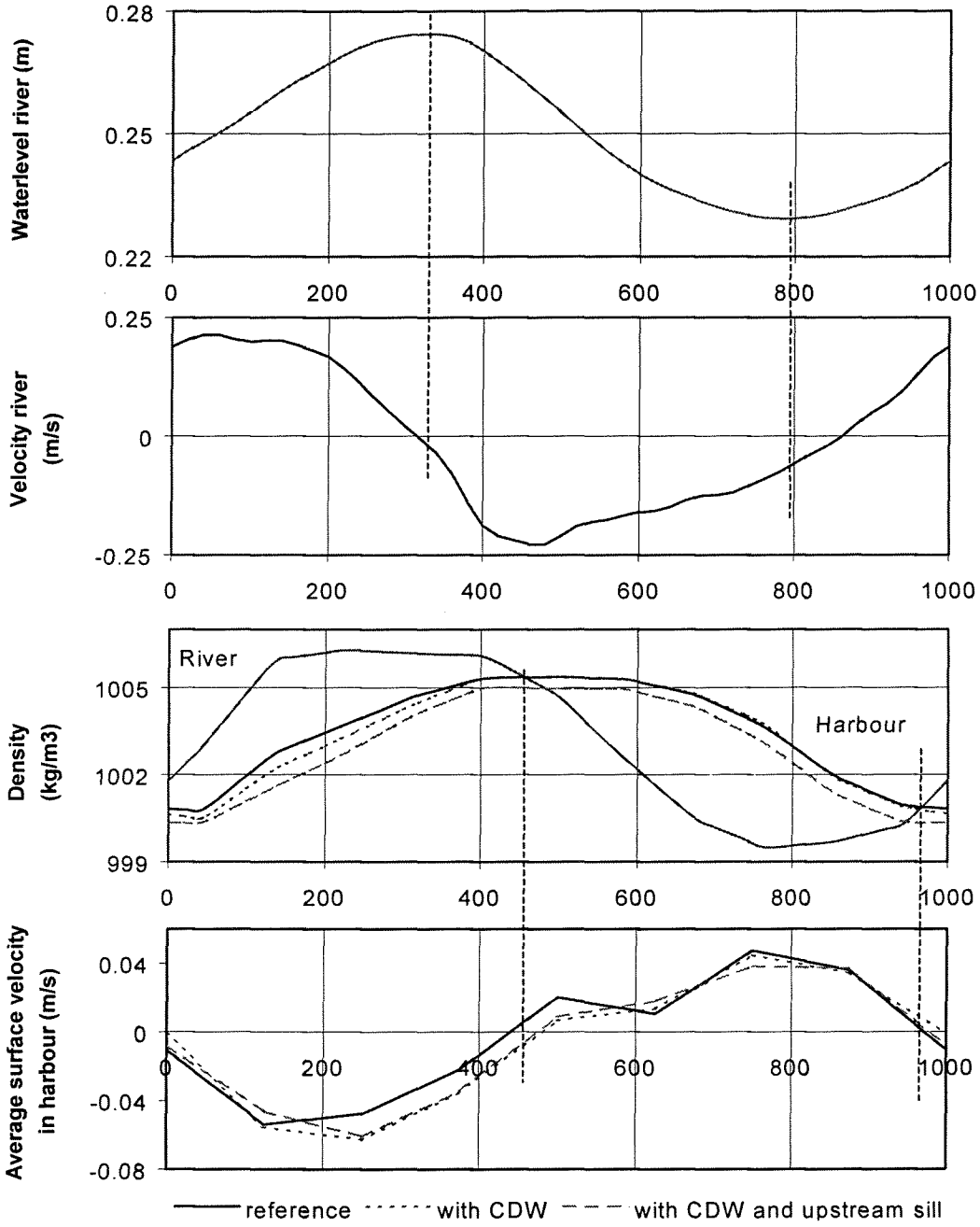

Figure 9.1. Flow characteristics during tidal cycle

Eddy / mixing	+	0	+			0	+
Tidal Filling	+	0	-			0	+
Density current	+			0	-		0
Sediment conc.	?						
CDW	+	0					+
Upstream sill	0		+			0	
Period	1	2	3	4	5	6	7

Table 9.1. Subdivision of tidal cycle in periods in which flow is relatively constant

9.3. Description of flow without CDW during a tidal cycle

Period 1 (t=0-300s): Rising tide & in-going density current near the bottom

Around t=120s the water in the flume still has its highest velocity. The density current near the bed in the harbour is directed into the harbour, as is shown in figure 9.2.b. At the same time water is flowing out of the harbour at the surface (figure 9.2.a). The PTV recordings show a decrease of approximately 30% of the effective entrance width due to the water from the bottom layer that flows up. This is explained in more detail in the next section.

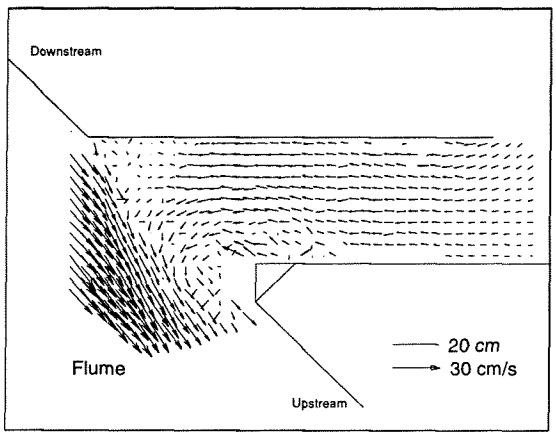

Figure 9.2.a. Surface flow at t=125s

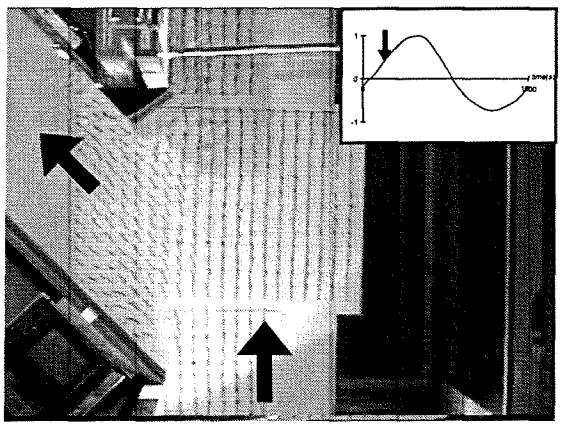

Figure 9.2.b. Bottom flow at t=125s

Dye solution injected downstream near the bottom enters the harbour in several rather large clouds. Much of the injected dye enters the harbour entrance at the downstream corner, as well as further upstream the harbour entrance. This is visible in figure 9.8.a.

Density stratification during rising tide

During the first half of the period of rising tide the water in the flume was stratified vertically. The interface between fresh water and saline water could clearly be made out through the glass side walls of the flume. The picture in figure 9.3, taken at t=990s, shows the flume just downstream of the harbour. The harbour edge, the bottom, and water surface are indicated by the dotted lines. The saline water is light grey, as a consequence of the accumulation of dye in the sea water. Dye solution that was injected when the picture was taken causes the dark grey stream near the bed. The fresh, colourless river water is visible as a white stream near the surface. The interface between the layers is clearly visible. It can be seen that the elevation of the interface increases in the downstream direction. Because the water from the sea is flowing in the upstream direction, the interface at the location of the harbour rises. Eventually it reaches the surface at approximately t=100s. From that moment on the flume is almost completely mixed, and the salinity profile does not change much anymore. These conditions are confirmed by the salinity measurements in the flume, which are depicted in figure 9.11.

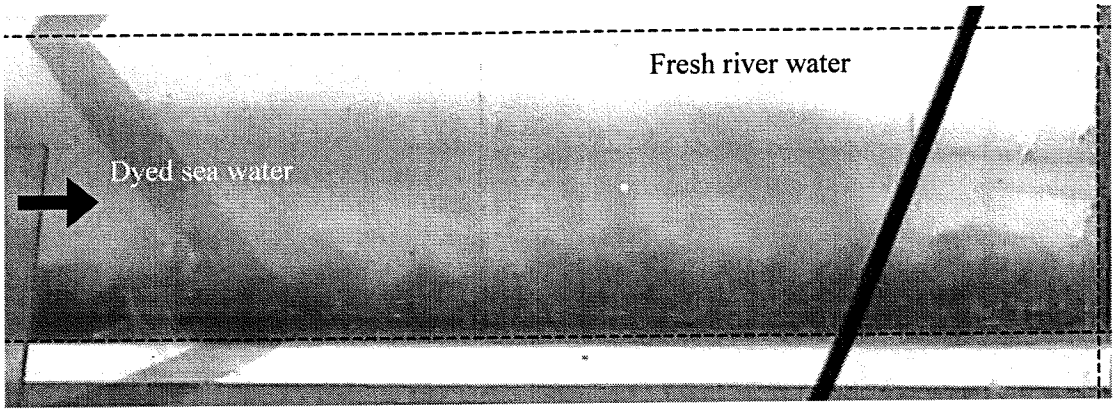

Figure 9.3. Side view of flume just downstream of harbour.

Period 2 (t=250-350s): High water slack

At high slack water (t=320s) water can be seen flowing into the harbour at the surface. This happens quite uniformly over the harbour width. As the tidal filling is negligible at this moment this flow can be attributed entirely to the density differences.

Period 3 (t=350-475s): Falling tide & in-going density current near bottom

After high water slack the density current near the bed is still flowing into the harbour with a rather large velocity because the density difference between river and harbour is still present. The density induced exchange flow reduces quickly however.

Period 4 (t=475-525s): Falling tide & slack density current

After t=320s the flow direction in the flume reverses, the saline water is returning to the sea, and the density in the river starts to decrease. However, the driving force behind the density current into the harbour near the bed only reverses when the density in the river becomes less than the density in the harbour. This happens during period 4.

Period 5 (t=525-800s): Falling tide & outgoing density current near the bed

At about t=540s the density current at the bed is flowing out of the harbour, as can be seen in figure 9.4. This pushes the mixing layer near the bottom into the flume. Little mixing between harbour and flume occurs in the bottom layer.

The time at which the density in the flume and in the harbour are equal and the time at which the flow changes direction are not exactly the same. Tidal emptying has a small influence. The maximum flow velocity caused by it is about 3 mm/s. There is not one density with which the density of the harbour can be characterised. An internal wave in the harbour takes about 35s to reach the back of the harbour, therefore it takes time for the layered system in the harbour to adapt to changing river densities.

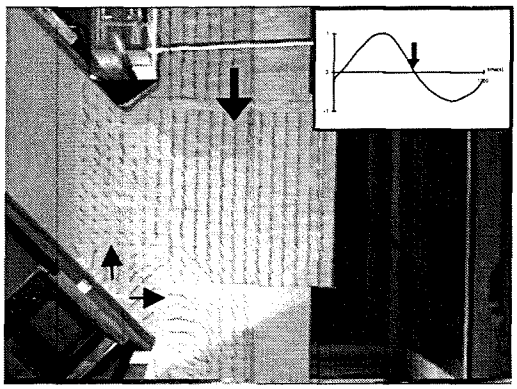

Figure 9.4. Bottom flow at t=540s

Dye was injected near the bottom of the flume halfway falling tide. Until t=545s almost no dye seemed to enter the harbour. At around t=585s more dye starts flowing in at the downstream side of the entrance and after t=605s part of the dye solution enters the harbour right around the upstream corner where the dye solution first appeared. The last situation is shown in figure 9.14.a. Inflow of dye into the harbour at this stage is remarkable because the water in the lower layer of the harbour is flowing outward. Probably this has to do with the rapid decrease of density in the river, which causes the density of the river water near the bottom to be lower than the density of the water in the harbour. The river water now flows over the denser outflow of the harbour. Consequently part of the near-bed water is transported to the upper layer and into the harbour as is indicated in figure 9.5.

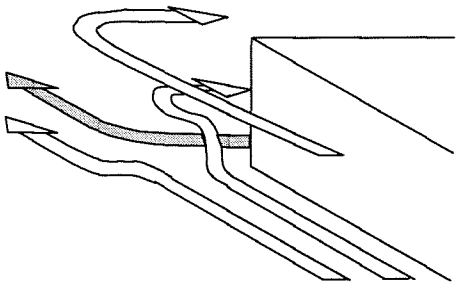

Figure 9.5. During ebb, also river water from the lower parts is entering the harbour.

Narrowing of effective entrance width during rising tide

In figure 9.4 diverging flow can be distinguished at the bottom around the downstream harbour corner. The little arrows that are drawn in the figure indicate this. An explanation of this flow is given next.

Water from the top layer flows into the harbour due to the density current. In a homogeneous situation during rising tide, the mixing layer would be "pushed into the harbour" over the full depth. Water would flow to both left and right of the stagnation point at the downstream harbour side and not so much to the bottom because the pressure gradient over the vertical is not very large. But now a density current is present and the mixing layer is pushed out at the bottom layer. Because of the inflow at the surface there is a large pressure gradient over the vertical and the water from the top layer flows down as well as to the left and the right. When reaching the bottom the flow spreads in all directions. This type of flow is also described in the dissertation of Langendoen (1992). The effect of the diverging flow is that it reduces the effective width of the harbour entrance, which could hamper the inflow or the outflow of the density current.

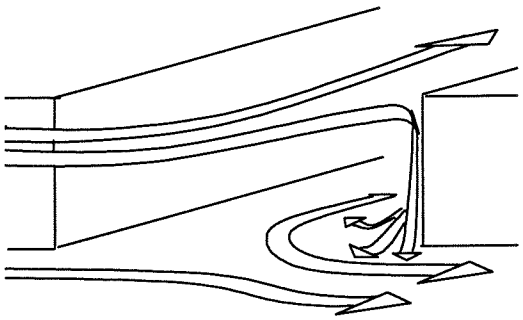

Figure 9.6. Narrowing of the effective entrance width.

Langendoen (1992) concluded that the eddy reduces the effective entrance width of the harbour. Due to the eddy bordering the harbour entrance in the upper layer, the direction of the flow velocity in the upper layer is not only directed into the harbour. At the downstream side of the harbour the flow direction is outwards, thereby partly blocking the harbour entrance.

Whether a decrease of the effective entrance width decreases the density current depends on the conditions at the entrance. When the flow is internally critical, the entrance width influences the inflow, and the inflow will decrease due to a decrease of the effective entrance width. When calculating the discharge due to double-critical flow, B_e in equation 2.7 is equal to the effective entrance width. When salinity changes slowly in the flume, and the salinity in the harbour adapts very quickly to the salinity of the river, then the entrance width is not of influence.

During rising tide this type of flow can also be seen at the upstream harbour wall (figure 9.7.b). When the direction of the density current is reversed, water from the bottom layer starts flowing to the surface. Now the diverging flow is visible in the upper layer.

Period 6: (t=800-900s): Low water slack and beginning of rising tide

During low water slack the flow at the bed that is coming out of the harbour has a big influence on the flow direction at the bed of the river. Dye injected in the harbour entrance even reaches the opposite side of the flume.

At the beginning of rising tide (at about t=800s) the water at the bottom is flowing out of the harbour due to the density differences. Flow velocities in the river are still rather low and the flow near the bottom in the harbour entrance is rather calm with only few and small vortices entering the harbour at the surface.

Period 7: (t=900-1000s): Rising tide with slack density current

When the flood current in the flume starts picking up speed, the flow pattern in the harbour entrance becomes less calm, flow separation is clearer and the mixing zone near the bottom is widening.

At the beginning of each tidal cycle (t=0s) rising tide occurs at the river with velocities almost maximum (approximately -0.20 m/s). Bottom and surface flow are depicted in figure 9.7. The water near the bottom of the harbour is flowing out, but the velocity is small. The density current in the harbour is about to reverse direction. Flow separation at the downstream harbour corner and the forming of a mixing layer in the harbour entrance are clearly visible when flow velocities in the river become higher. The vortices that are generated in the mixing layer enter the harbour at the upstream side. An eddy over the width of the harbour, bordering the entrance, is present. The ratio B/L of this eddy is rather large, about 1:2, which is probably caused by the net inflow of water in the top layer. It was also

observed in phase 1 of the experiments that an increased net discharge through the entrance increased this ratio.

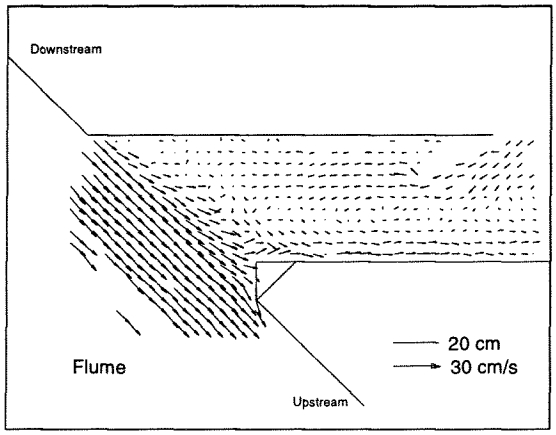

Figure 9.7.a. Surface flow at t=0s

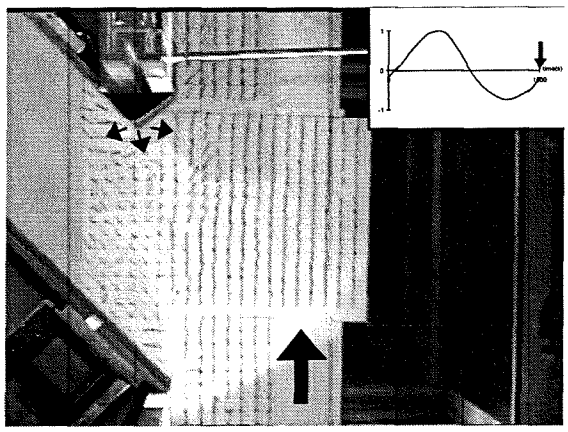

Figure 9.7.b. Bed flow at t=0s

9.4. Description of flow with CDW during a tidal cycle

This section contains the description of flow in the harbour with the CDW present. The CDW is described in section 3.5. During periods 1 and 7 the CDW has the largest influence on the flow. Some effects are still visible after that in periods 2 and 3. When the upstream sill is also added, this changes flow during all periods.

Period 1 (t=0-300s): Rising tide & in-going density current near the bottom

During rising tide the flow pattern near the bottom is much calmer when a CDW is present. The vortices in the entrance are reduced in size and are less distinct. Much less turbulent flow is entering the harbour at the upstream side, as was observed without a CDW present.

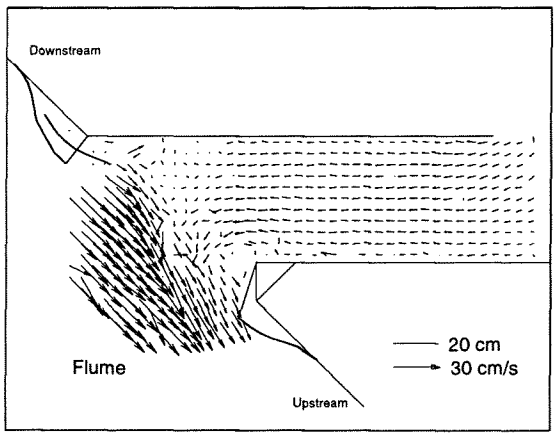

Figure 9.8.a. Surface flow with CDW (C) at t=125s

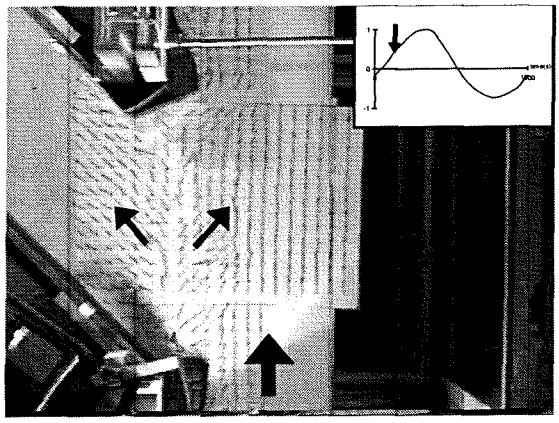

Figure 9.8.b. Bottom flow with CDW (C) at t=120s

Behind the sill near-bed flow diverges over the width of the harbour entrance. This was not present without the CDW (figure 9.2). The arrows in figure 9.8.b emphasise this with part of the flow going into the harbour and part being directed into the flume. The stagnation line in the figure is formed due to water that is flowing down from the upper layers. It is not useful anymore to speak of a mixing layer because the flow pattern is completely different with a

CDW present. This was observed for both configurations B and C, although the dividing flow over the width was stronger with configuration C.

In the situations with CDW (B), and with CDW and sill (C), dye injected near the bottom is flowing past the harbour entrance with only a small part entering the basin. Figure 9.9 shows the differences between the configurations A and B. In contrast to the configuration without CDW, there are no large clouds of dye entering the harbour area. This flow pattern is observed from the beginning of flood onwards until almost the end of the flood period.

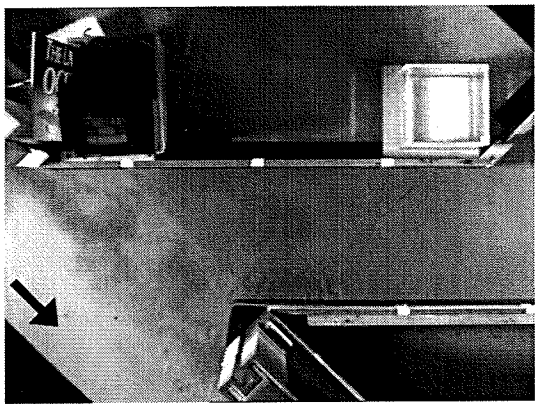

Figure 9.9.a. Situation without CDW at t=180s

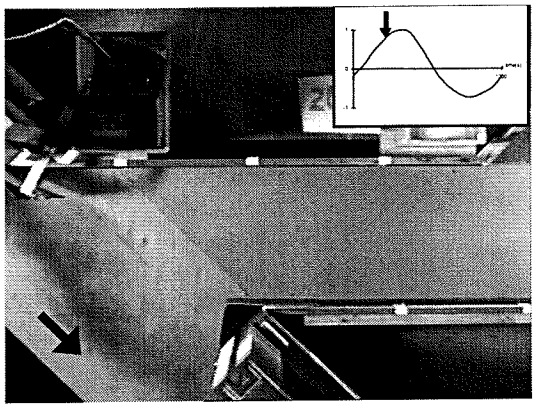

Figure 9.9.b. Situation with CDW at t=180s

Functioning of the CDW during flood

The observations and measurements described above make it possible to form an idea of the complex three-dimensional flow in the harbour entrance. In figure 9.10 the flow situation during flood is schematically depicted. This occurs for both configurations with a CDW.

The top section of the CDW steers the flow into the harbour and against the out-going density current in the top layer. This creates an area with higher pressure behind the CDW in the top layer. Behind the sill near the bed a low-pressure area develops because of the deflected flow. Because of the high-pressure area in the top layer and the low-pressure area near the bed, the water captured by the CDW flows down and diverges at the bed behind the sill. This downward, diverging flow creates a vortex with a horizontal axis in front of the entrance width. At high velocities it covers the entire entrance width. The vortex over approximately half the water depth from the bed was observed during the experiments.

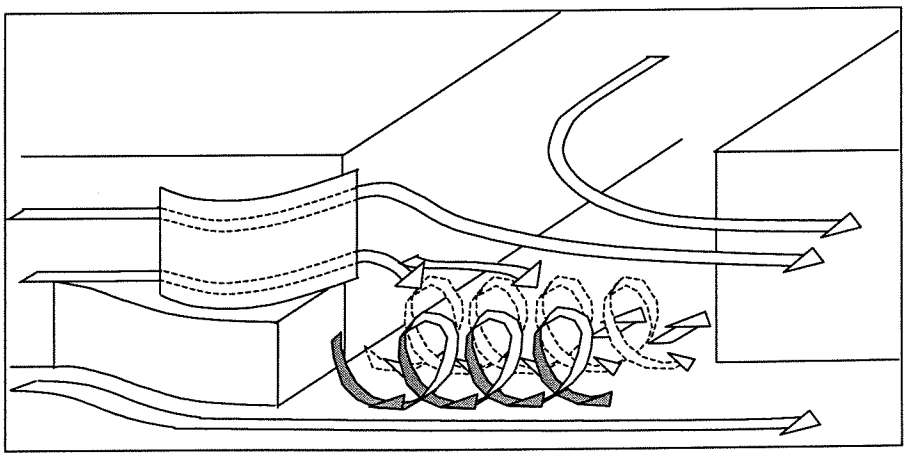

Figure 9.10. Schematic flow pattern in entrance during flood, with CDW present

The vortex explains the existence of the stagnation-line over the width of the harbour entrance that was present behind the sill. Because of the vortex water near the bed of the flume is hardly exchanged into the harbour. For the configuration with sill, the vortex seemed stronger.

A second, counter-rotating vortex is possibly present next to the other one at the inside of the harbour. This was not concluded from the observations. Therefore the counter-rotating vortex is depicted in figure 9.10 by a dotted line. Instead of a second vortex it is possible that behind the first vortex water flows straight into the harbour.

A similar vortex is also observed behind submerged vanes (Odgaard, 1991). Submerged vanes can be compared to the sill in the lower part of the water column, at the downstream side of the harbour entrance. Behind submerged vanes with high angles of attack two counter rotating vortices are observed (Marelius, 1998).

The discharge through the CDW is less than the exchange discharge due to the density current in the harbour (see chapter 3). Water also has to come from the outside of the CDW.

The reduction of the effective entrance width at the surface layer due to water flowing up from the bottom layer is less when a CDW is present. The CDW does reduce the effective entrance width at the downstream side but the reduction of the effective entrance width at the upstream corner is stopped. A considerable reduction of the effective entrance *height* can be said to take place as a consequence of the vortices.

Density distribution during rising tide

In figure 9.11 the density profiles of the various configurations, and the density profiles at the river are depicted. Especially the differences between configurations A and C at t=125s are large. The depth-averaged densities in the harbour with a CDW (B) are lower than the reference densities during the time interval 0 to 400s. The depth-averaged densities in the harbour with CDW and upstream sill (C) are lower during the entire tidal cycle. Each density profile depicted in the figure is the average of 16 recorded density profiles. The accuracy of the results is therefor rather high (± 0.05 kg/m^3).

The lower average densities in the harbour with a CDW can be explained as follows: Because of the CDW in combination with the sill the denser water from the lower layer is to some extent kept out of the harbour, during flood. Instead, the less saline water from the top layer is directed into the harbour. The result is a lower (average) density in the harbour during rising tide.

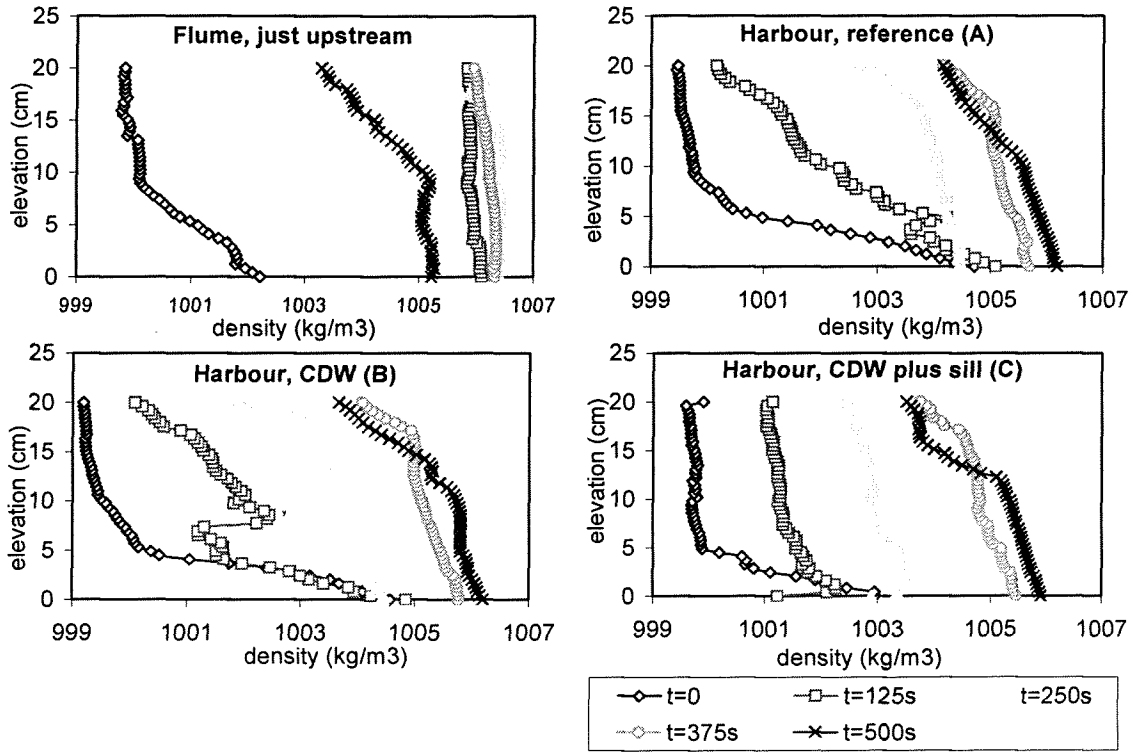

Figure 9.11. Density distributions during first half of tide

Shadow across entrance

When a CDW was present, from t= 40s until t=280s in the flood period a line-shaped shadow was visible across the width of the harbour. This shadow was probably caused by a steep gradient in the interface between fresh and salt water near the entrance. A curved interface works as a lens and could have created this shadow. The reason it was visible more inside the harbour was that an extra lamp was installed across the harbour entrance, shining into the harbour. A steep gradient of the interface could indicate almost critical flow to be present in the entrance.

Period 2 (t=250-350s): High water slack

Nearing high water slack (until approximately t=250s), dye injected near the bottom is being pushed into the river by the downstream sill. Nearing t=250s the flow pattern is less calm compared to the previous stage during flood with the CDW present. Quite some mixing over the width appears but still most of the dye seems to pass the harbour entrance.

At about t=250s flow velocities in the river start to decrease substantially, and quite suddenly the entire stream of river water containing the dye solution enters the harbour basin over the entire entrance width. This is illustrated in the figure 9.12. Dye is flowing in just as it does in the situation without CDW. However, the PTV measurements show that the surface velocities are in fact higher at this moment when a CDW is present, which could indicate that the exchange discharge at this time has increased, compared to the reference configuration.

An increased density exchange discharge can be explained by the increased salinity gradient between the flume and the harbour. The flume velocity has diminished at this time, so the CDW stops functioning and can no longer regulate the flow pattern. Now an extra inflow of saline water into the harbour occurs, as the salinity in the harbour is lower than the salinity at the same time in the reference harbour, which means that the density difference is higher. This is the case for both configurations with CDW (B and C). The difference in density with

the reference harbour diminishes at t=450s for configuration B, but is present during the whole tidal cycle for configuration C, see figure 9.1, 4th graph.

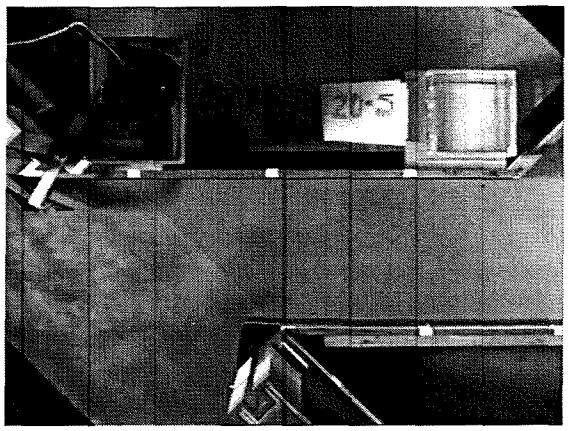

Figure 9.12. Dye injection near bottom, nearing high slack water t=320s

Period 3 (t=350-475s): Falling tide & in-going density current near bottom

During this period no differences are observed in the flow pattern. No exchange measurements were done.

Period 4 (t=475-525s): Falling tide & slack density current

When the upstream sill is present the flow velocities in the eddy in the upper layer are increased (see figure 9.13). This could indicate that more water is exchanged through the upper layer in consequence of the upstream sill.

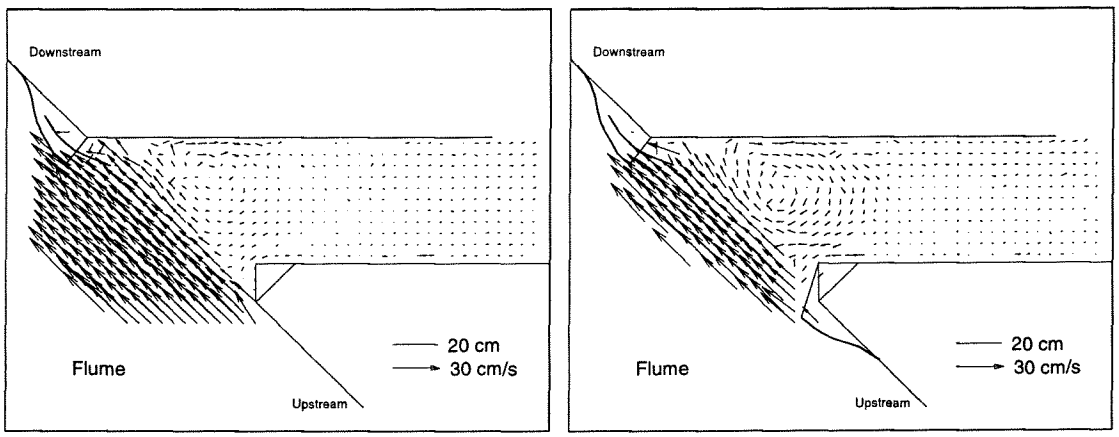

Figure 9.13. Surface velocities without (B) and with (C) upstream sill during ebb t=500s

Period 5 (t=525-800s): Falling tide & outgoing density current near the bed

With CDW (B) the flow pattern near the bottom is very similar to the reference situation and no large vortices occur.

When an upstream sill is present differences are visible. The sill clearly pushes the near-bed flow into the river. However, the amount of near-bed flow entering the harbour does not seem to be large at any configuration.

Secondly, the dye flow at the bottom seems to go around the left-hand side of the downstream CDW instead of flowing partly into the harbour. The mixing layer seems to lie further into the river. See figure 9.14 for a comparison at the end of the ebb period between the reference harbour and the harbour with the CDW and the upstream sill.

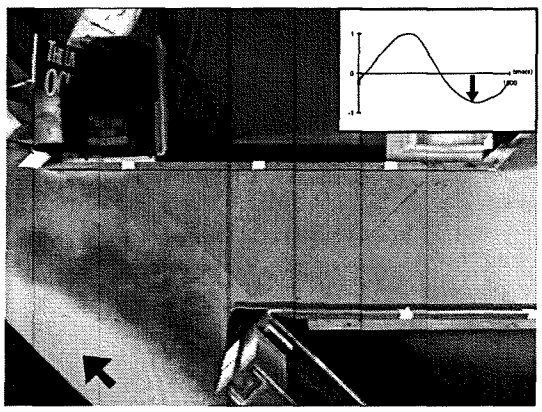

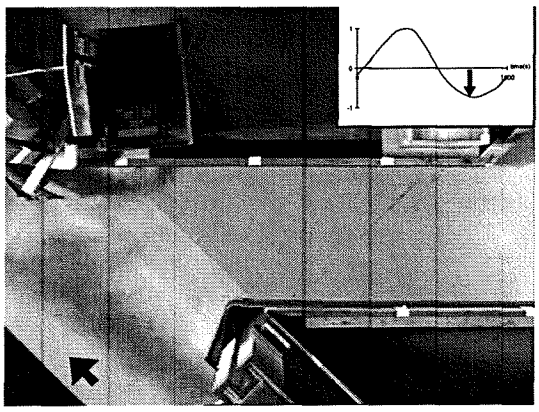

Figure 9.14.a. No upstream sill (A) at t=605sFigure 9.14.b. With upstream sill (C), at t=605s

Period 6: (t=800-900s): Low water slack and beginning of rising tide

No visible changes were observed during this period.

Period 7: (t=900-1000s): Rising tide with slack density current

No visible changes were observed during this period.

9.5. Quantification of exchange discharge

9.5.1 DCM results

Approach

The DCM tests have been focused on the period of the tidal cycle with rising tide, as was discussed in section 6.6.2. With the tangents to the response curves at the beginning of dye exchange between river and harbour, the differences between the configurations were determined.

The next step was to quantify the discharge going in near the bed. This is possible because the amount of water going into the harbour can be linked to the increased dye concentration in the harbour. There are some limitations to this approach however. The calculated in-going discharge near the bed is a result of density currents, tidal filling and mixing. It is impossible to distinguish between the different effects because dye was injected in part of the lower water layer only. Secondly, it is not possible to distinguish between an upper and a lower layer because it is not confirmed that the entire in-going discharge stems from the lower layers of the water column. The last limitation to the approach is that the injected dye has spread over part of the vertical and over part of the width. For an estimate of the exchange discharge this spread is measured and an equal distribution over the spread area is assumed.

Results

As was described in the last section, the calculated discharges are only part of the in-going discharge and only give an indication of the inflow near the bed. The results are presented in table 9.2 and in figure 9.15.

The response curves were to some extent irregular. It was therefore impossible to only take the tangent at the very beginning of dye exchange over the full entrance width as was explained in section 6.2.3. Instead the average trend line through the first 25 seconds after this moment was taken as the tangent. During this interval there is not only dye inflow at the bed but dye outflow in the upper layer as well because of vertical mixing. Therefore the calculated exchange discharges are probably lower than the actual exchange discharges through the lower layer.

Time (s)	$Q_{tidal\ filling}$ (l/s)	A, Reference harbour	B, Harbour with CDW		C, Harbour with CDW & upstream sill	
		Q (l/s)	Q (l/s)	Difference with ref. (%)	Q (l/s)	Difference with ref. (%)
930	0.23	0.15	0.13	-18	0.16	+4
990	0.42	0.29	0.24	-19	0.16	-47
110	0.44	0.81	0.44	-46	0.08	-90
160	0.35	0.81	0.43	-47	0.19	-76
245	0.24	0.33	0.12	-64	0.19	-44
Weighted average		**0.46**	**0.25**	**-41**	**0.17**	**-67**

Table 9.2. In-going discharge at the bed, calculated from the DCM results

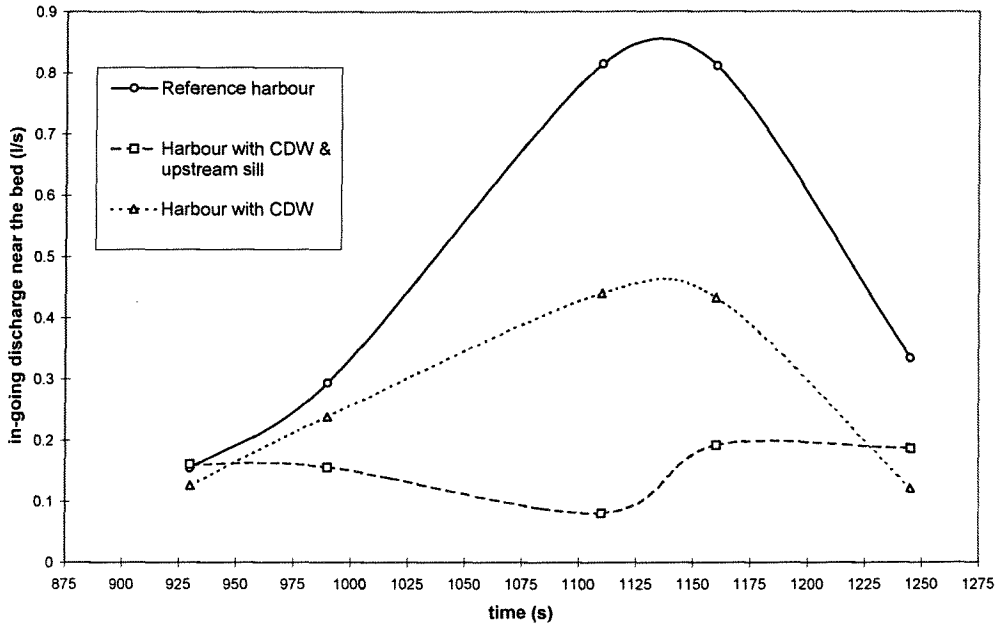

Figure 9.15. In-going discharge near the bed during periods 7 and 1, calculated from DCM results

9.5.2. PTV and EMS measurements

Approach

From the PTV and EMS measurements the exchange discharge can be determined via integration of the velocity profile over a cross section in the harbour. This discharge is the effect of both the density-induced discharge and the tidal filling. The effect of mixing is not visible in the measurements.

From PTV the surface velocities are known, and velocities have been measured at 9 other points in one cross section by EMS. The combined velocities of PTV and EMS measurements are depicted in appendix B.2 for 4 times in the tidal cycle. Although the vertical velocity profile, caused by the density current is clearly visible in these results, the discharges that are determined from these measurements are not very accurate.

It was tried to obtain the exchange discharge more precisely by using the known net discharge and density profiles. The density profiles are related to the vertical velocity profile to some extent (see appendix M). The following kinds of interpolation were tried to quantify the density exchange discharge:

- The velocity profile was assumed linear. A linear trend line was fit through the width-averaged EMS and PTV data. The correlation with the velocity measurements was good, but the net discharge not well reproduced.
- A 3rd order polynomial trend line was fit through the EMS and PTV data. This also gave a good correlation, but the net discharge was not reproduced well.
- A fit was made through the EMS and PTV data. The slope of the velocity profile was related linearly to the slope of the density profile. The relation between the density profile and the velocity profile was chosen in such a way that the net discharge was correct. Now the correlation between the EMS measurements and the velocity was not good.
- A 2 dimensional spline fit was made through all the velocity measurements (EMS and PTV) in the cross sectional area, to get a 2-dimensional velocity profile. The net

discharge, determined by integrating this profile over the cross section, was again not reproduced well.

None of the interpolation methods rendered results that were clearly better than linear interpolation of the EMS and PTV measurements.

Results

Figure 9.16 shows the density exchange discharges calculated by linear interpolation of the EMS and PTV data. The density exchange discharge is determined for the upper and lower layer separately, and corrected for the tidal filling. Now two values for the discharge are available per configuration. This explains the two lines per configuration in figure 9.16. Quite some difference is present between the discharges calculated from both layers. This difference is a measure for the (in-)accuracy of the calculated exchange discharge.

From figure 9.16 the only thing that can be seen is that the discharges are in the same order of magnitude as the discharges calculated with equation 2.8. According to the figure it is likely that the discharge increases with a CDW present. If a CDW decreases the exchange discharge during flood, this will be 15% at maximum.

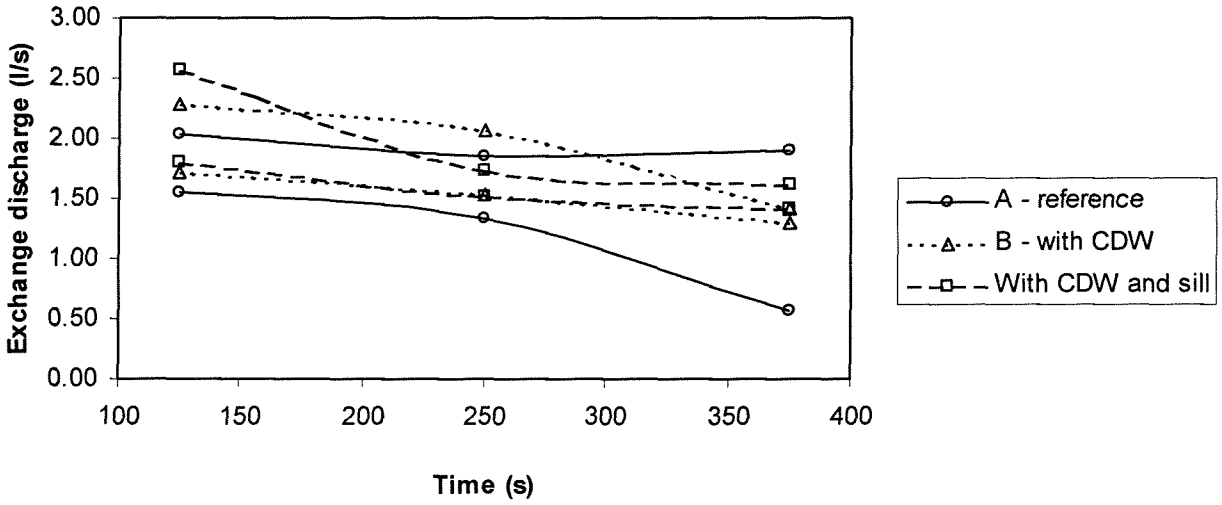

Figure 9.16. Density exchange discharge determined from EMS and PTV measurements for upper and lower layer separately

9.5.3. Density measurements

Another way of quantifying the exchange discharge is making use of the density measurements in the same way as the dye measurements. Salt is now the tracer that is being used. Because the variation in salinity is rather small, conservation of volume is practically true (linear relation between density and volume). This implies that the density can also be used as a tracer.

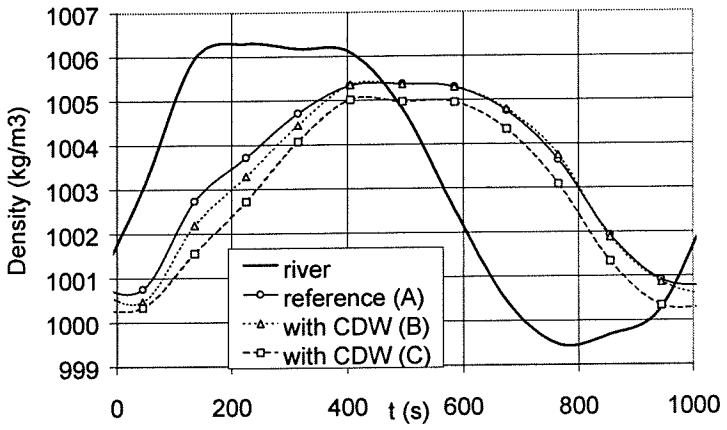

Figure 9.17. Depth-average of density in river and harbour, for all configurations

The magnitude of the density exchange is not calculated entirely correct because the salinity of the outgoing flow is not equal to the average salinity in the harbour, but mostly lower, and because the tidal filling is not taken into account. Despite these shortcomings the results can be compared because the results are influenced in the same way for the various configurations. The discharges calculated from the dye measurements show similar results for the time interval t=900s to t=250s (see figure 9.18).

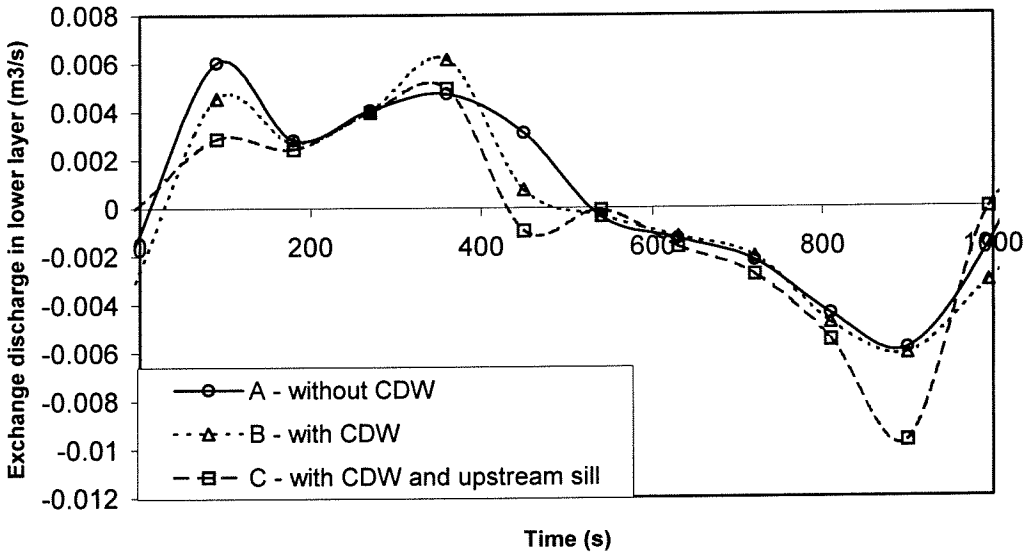

Figure 9.18. The exchange discharge as determined when using the averaged density (salinity)

The density results show a decreased exchange due to the CDW by 20%, and a decrease of 50% due to the CDW plus sill, during upcoming tide and large flow velocities (figure 9.18, t=100s). A negative effect is present during the beginning of falling tide, followed by a positive effect. During the rest of the falling tide the exchange is not altered.

At the beginning of rising tide (t=900s) the exchange for the configuration with a sill present is increased substantially.

9.6. Modelling the effect of a CDW during a tidal cycle

9.6.1. Introduction

It is difficult to predict the influence of a Current Deflecting Wall on the water exchange, because several mechanisms with varying magnitudes interact during a tidal cycle. In order to make an estimate of the influence of the CDW on the flow processes in the model harbour, a model was developed. The outcomes of this model can help with the interpretation of the measurements that were taken.

The main aim is to see what happens during an entire tidal cycle *if* the CDW functions, because an adverse effect is expected after the period in which the CDW functions. The second aim is to see how the CDW works, by modelling in two ways.

First a description of the model will be given. Then the outcomes will be discussed and compared to the measurements.

9.6.2. The model

The model is a very simple description of a tidal harbour. For most parameters like flow velocity, density, and depth, the mean value is used to describe the flow processes. Below the model is illustrated schematically. The velocities are shown in the positive direction.

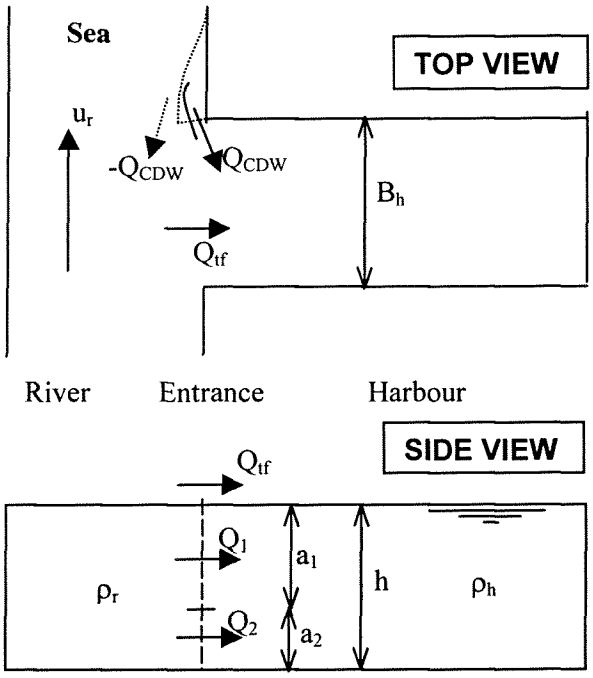

Figure 9.19. Sketch of model, with definition of parameters used.

In the model a two-layer flow is present in the entrance of the harbour. This flow is determined totally by the density in the harbour (which is characterised by the density averaged over the entire harbour volume), and the density in the river in front of the harbour (averaged over the depth). The density in the harbour is influenced by the inflow of water.

The major assumptions in the model are:

- The exchange due to mixing at the entrance is neglected.
- The density in the harbour at a specific time is characterised by one density, averaged over the volume.

- The river in front of the harbour is completely mixed over the vertical.
- Flow in the harbour entrance is quasi-steady.
- Flow in the harbour entrance is doubly critical (or it has the magnitude of a certain proportion of that).

The exchange mechanisms of tidal filling and density driven currents are considered. The tidal filling is the only process that results in a net influx of water to or from the harbour basin at a specific time. The inflow integrated over a tidal cycle is also zero. The density current does not give a net influx of water at a specific time. However, it does give a net influx of salt to or from the harbour at a specific time.

External water movement

The external water movement is given by:

$$h_{river} = h_{harbour} = h(t) \qquad \text{Equation 9.1}$$

This is correct if the harbour is much shorter (<5%) than a tidal wave[1]. With this assumption the net flow in the entrance is also known when applying continuity of volume, this gives the tidal filling:

$$Q_{tf} = A_h \frac{dh}{dt} \qquad \text{Equation 9.2}$$

In which A_h is the surface area of the harbour basin.

Internal water movement

A density difference between the river and the harbour will cause an exchange flow. Double-critical flow is often assumed to be present at the entrance although flow velocities will be lower in reality. The velocities and layer depths become, based on the formulas for double-critical flow (after Kranenburg, 1996):

$$\rho_r > \rho_h: \begin{cases} a_1 = \frac{h}{2} - \frac{Q_{tf}}{2B_h\sqrt{\varepsilon g h}} \\ a_2 = \frac{h}{2} + \frac{Q_{tf}}{2B_h\sqrt{\varepsilon g h}} \end{cases} \qquad \rho_r < \rho_h: \begin{cases} a_1 = \frac{h}{2} + \frac{Q_{tf}}{2B_h\sqrt{\varepsilon g h}} \\ a_2 = \frac{h}{2} - \frac{Q_{tf}}{2B_h\sqrt{\varepsilon g h}} \end{cases} \qquad \text{Equation 9.3}$$

$$\rho_r > \rho_h: \begin{cases} u_1 = -\tfrac{1}{2}\sqrt{\varepsilon g h} + \frac{Q_{tf}}{2hB_h} \\ u_2 = +\tfrac{1}{2}\sqrt{\varepsilon g h} + \frac{Q_{tf}}{2hB_h} \end{cases} \qquad \rho_r < \rho_h: \begin{cases} u_1 = +\tfrac{1}{2}\sqrt{\varepsilon g h} + \frac{Q_{tf}}{2hB_h} \\ u_2 = -\tfrac{1}{2}\sqrt{\varepsilon g h} + \frac{Q_{tf}}{2hB_h} \end{cases} \qquad \text{Equation 9.4}$$

In which ε is the relative density difference, a_1 and a_2 are the layer heights, and u_1 and u_2 are the flow velocities in the layers. The rest of the parameters is depicted in figure 9.19.

A factor *f* is added to the formula for the discharge, to enable not entirely double critical flow in the harbour entrance. Another term is added in order not to change the net discharge. The internal discharges are now described by:

[1] Length of tidal wave = T*c = T(gh) ½ = approximately 1500m. The harbour is about 3 meters long (0.2%).

$$\begin{cases} Q_1 = f \cdot B_h a_1 u_1 + \tfrac{1}{2}(1-f)Q_{tf} \\ Q_2 = f \cdot B_h a_2 u_2 + \tfrac{1}{2}(1-f)Q_{tf} \end{cases}$$ Equation 9.5

The actual in- and outflow are given by:

$$Q_+ = \sum_{n=1}^{2} \begin{cases} Q_n > 0 : \Delta Q_+ = Q_n \\ Q_n < 0 : \Delta Q_+ = 0 \end{cases} \qquad Q_- = \sum_{n=1}^{2} \begin{cases} Q_n < 0 : \Delta Q_- = Q_n \\ Q_n > 0 : \Delta Q_- = 0 \end{cases}$$ Equation 9.8

CDW model 1

The exact way of functioning of the CDW is not known. It is known that it hardly influences the net flow through the entrance of the harbour basin. The CDW also only works during rising tide (flow velocity), as its effect is driven by the flow in the river. The first attempt to describe a functioning CDW was to assume a decrease of the exchange discharge due to the density current. The assumptions were made that the magnitude of this decrease is proportional to the velocity in the flume, and that the decrease of the exchange discharge due to the density current is absent during horizontal ebb.

The flow due to the CDW can now be written as:

$$\begin{array}{l} u_r < 0: \\ (flood) \end{array} \begin{cases} Q_{CDW,1} = +\dfrac{u_r}{u_{r,\max}} Q_{CDW,\max} \\ Q_{CDW,2} = -\dfrac{u_r}{u_{r,\max}} Q_{CDW,\max} \end{cases} \qquad \begin{array}{l} u_r > 0: \\ (ebb) \end{array} \begin{cases} Q_{CDW,1} = 0 \\ Q_{CDW,2} = 0 \end{cases}$$ Equation 9.6.

The maximum CDW-induced discharge ($Q_{CDW,max}$) is assumed to be much smaller than the discharge induced by the density current, as this current was still observed in the experiments. The value of $Q_{CDW,max}$ is roughly based on measurements. The value was determined so that the maximum computed difference in density between configurations A and B was equal to the maximum measured difference. This was 1 l/s.

The discharges in the layers are now calculated as follows:

$$\begin{cases} Q_1 = f \cdot B_h a_1 u_1 + \tfrac{1}{2}(1-f)Q_{tf} + Q_{CDW,1} \\ Q_2 = f \cdot B_h a_2 u_2 + \tfrac{1}{2}(1-f)Q_{tf} + Q_{CDW,2} \end{cases}$$ Equation 9.7

CDW model 2

The second way of modelling the CDW was based more on the observations during the experiments. The assumption is that when the velocity in the flume is directed up-river then the water that is flowing into the harbour flows through the upper part of the CDW. This means that the water comes from the upper part of the water column. Water there is less dense due to buoyancy effects. This can be incorporated in the box model by changing the river density. This decrease is a function of the density-difference between the upper and lower part of the water in the flume and the flow velocity in the flume.

The density of the flume water that is flowing in through the bottom layer when a CDW is present can now be written as:

$$\begin{matrix} u_r < 0 \\ (flood) \end{matrix} : \rho_{r,CDW} = \frac{2}{h} \int_{z=½h}^{h} \rho_r(z)dz ,$$

$$\begin{matrix} u_r > 0 \\ (ebb) \end{matrix} : \rho_{r,CDW} = \overline{\rho}_r \qquad \text{Equation 9.9}$$

The measurements of the average density in the top layer of the river must be added as extra input values. These are given in figure 9.20.

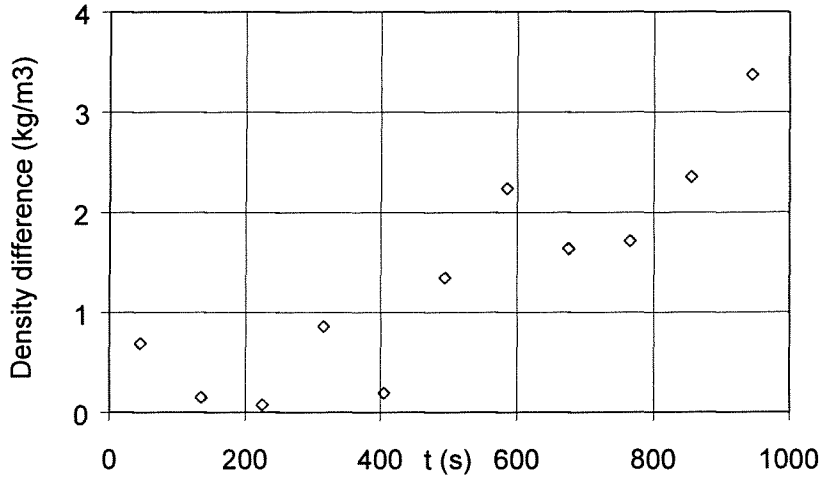

Figure 9.20. Measured density difference between top 25% and lower 25% of flume water

Volume balance

The average density in the harbour is only influenced by the actual inflow (Q_+) because it is assumed that the water flowing out has a density equal to the average density in the harbour. The change of density (9.13) is calculated by substituting the volume balance of water in the harbour (9.11) and the equation of state (9.12) into the mass balance of dissolved salt in the harbour (9.10):

$$\frac{dM_{salt}}{dt} = \frac{dV_h S_h}{dt} = Q_+ S_r - Q_- S_h \qquad \text{Equation 9.10}$$

$$\frac{dV_h}{dt} = Q_+ - Q_- \qquad \text{Equation 9.11}$$

$$S = \frac{\rho - \rho_0}{\alpha} \qquad \text{Equation 9.12}$$

$$\frac{d\rho_h}{dt} = \frac{Q_+}{V_h}(\rho_r - \rho_h) \qquad \text{Equation 9.13}$$

For equation 9.13 to be correct, the salinity variations must be so small, that preservation of volume approximately applies. This is the case in the model harbour of LIP III.

The top layer will always have a lower density than the bottom layer. This could be incorporated in the model by introducing a factor that gives the ratio between the average top

layer density and the average bottom layer density (≤1). This factor will change in time, but when an average value is chosen, the results should improve.

Solving the equations

The equations that were mentioned in the previous section can be substituted into the first order differential equation 9.13. This differential equation can be solved using the Euler method for numerical integration. This was executed in the spreadsheet program Excel. The equilibrium situation is determined by iteration. The starting value of the density in the harbour is changed into the last value of the tide. This is repeated until the harbour density at the end of the tide does not change any more.

9.6.3. Comparison between calculations and measurements

The values for the river velocity, river density, and water level were obtained from the LIP III measurements. In the first three graphs of figure 9.1 these boundary values are shown. Calculations were made without the influence of the CDW, and with the influence, computed with both CDW models.

Measurements vs. computations for configuration without CDW (A)

In figure 9.21 the measured density in the harbour is depicted. The measured density in the harbour was calculated by taking the mean value of the depth-averaged densities at the back and at the middle of the harbour (see chapter 5 for exact positions of density measurements). In figures 9.22 and 9.23 the computed densities in the harbour are depicted. In these two graphs the density for the configuration without CDW is the same. The factor f was chosen to be 1, so double critical flow was assumed. It is seen that the outcome of the model resembles the average density in reality, only the amplitude is 0.4 kg/m^3 smaller. Because the flow in the prototype is not totally doubly critical because of friction, one would expect a larger amplitude. The assumption however, that the outflow has the average density of the harbour is not entirely correct either. Water that flows out at the top has a lower density, and this will cause a smaller amplitude. Because of the fact that the amplitude of the density in the harbour is underestimated, the density difference between the harbour and the river is overestimated. Therefore the flow velocities are about 50% larger than measured (see section 9.5.2). The model can only be used for a qualitative analysis of the flow.

Measurements vs. computations for configuration with CDW (B)

It can be seen that the measured average density is lower when a CDW is applied. The density difference between the cases with and without a CDW is present during the first half of the tide, and negligible during the second half.

The effect that the CDW in both models has on the salinity in the harbour during a tidal cycle, corresponds up to a certain extent to the measured effect. Both CDW models reduce the salinity in the harbour during flood. Both models also show an increased density exchange is after the period of functioning. What happens during the combination of an outgoing density current at the bottom and rising tide (900-1000s) is doubtful for both models. This period is rather short, so it will not have much influence.

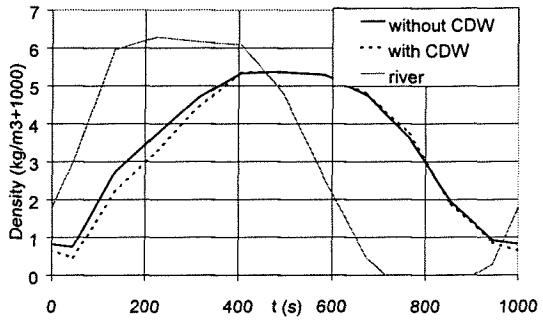

Figure 9.21. Measured density in the harbour, without CDW and with CDW (B)

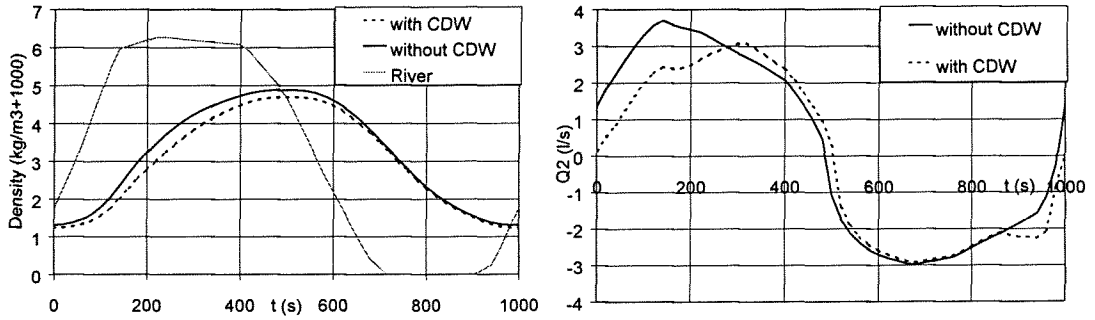

Figure 9.22. Computed density in harbour, and discharge through lower layer, CDW model 1, for configurations without CDW (A) and with CDW (B)

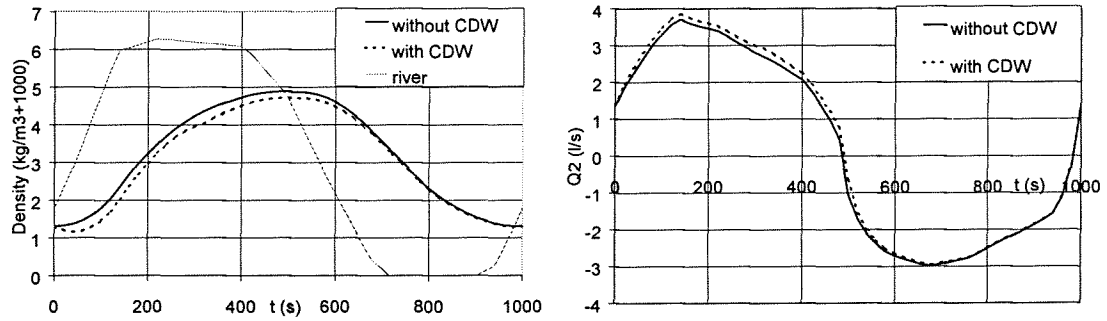

Figure 9.23. Computed density in harbour, and discharge through lower layer, CDW model 2, for configurations without CDW (A) and with CDW (B)

9.6.4. Results CDW model 1

The graphs in figure 9.22 show the computations with CDW model 1. They can be explained as follows: The CDW is especially slowing down the density current during maximum flood (0-300s). A maximum reduction of 35% is achieved. Less salt (mass) enters the harbour basin because of this. This causes the density in the harbour at 300s to be lower when a CDW is present. When the CDW is not working any more (300-900s) the density will draw near to the original density. First (300-500s) the density rises faster due to a larger density difference between river and harbour, which gives an increased inflow. After that (500-900s) the density lowers less fast due to a smaller density difference, which gives a decreased inflow.

Above it is shown that a positive effect of the CDW during 0-300s (less inflow) will cause a negative effect (increased inflow) in the period after that (300-500s). According to the box model the increase of the exchange volume by the negative effect (300-500s) is smaller than the decrease of the exchange volume that was accomplished by the CDW (0-300s). This can be explained by the fact that the salinity of the river at the time of this increased discharge is higher than during the time that the CDW functions. When the extra exchange volume has

brought the same amount of salt into the harbour as the amount of salt that was kept out by the CDW, the driving force (density difference) will be the same, and the exchange flow will by the same again. Because salinity is higher at the moment of the extra inflow (300-500s), this amount of salt can be brought into the harbour with less water, thus a smaller exchange volume is required to make up for the negative effect earlier.

It can also be seen that at 900-1000s, when the CDW starts to function, the density exchange is increased. The CDW is pushing the water in the same direction as the density current. The period over which this occurs is rather small, and the magnitude is not very high. The water that flows in originates from the upper part of the water column, which contains less sediment. The increased inflow implies internally supercritical flow in the harbour entrance when f is chosen close to 1. This is not realistic.

9.6.5. Results CDW model 2

When the second CDW is applied (figure 9.23), the density in the harbour also decreases during flood. This is because the water that flows into the harbour has a lower density. Because of this the density difference is increased. The exchange flow is not influenced directly by the CDW now. Therefore the exchange discharge is already increased during the time of functioning of the CDW (approximately 0-300s) due to this increased density difference. After the time of functioning of the CDW the exchange discharge remains higher than with the reference configuration until the density difference has gone back to its original value (500s).

The CDW model 2 does not influence the exchange discharge as much as model 1. The maximum increase of the exchange discharge is 5%. The time at which the density in the harbour starts to deviate from the reference condition is earlier. These two facts correspond better with the measurements that were described in chapter 9.

For determining the net effect of a CDW the total inflow over a tidal cycle needs to be calculated. The total inflow can be calculated by integrating the influx (Q_+) over one tidal cycle. As the model is not validated enough at the moment, this has not been done. It can be seen that the second model results in a higher total exchange volume due to the density current. The exchange through the lower layer decreases, however. The magnitude of the increased total exchange that is caused by the CDW (model 2) is determined by the density stratification of the river.

9.7. Summary of results phase 2

Flow pattern

All measurements that were executed, combined with visual observations gave a good picture of the flow pattern in the harbour entrance. The flow pattern in the harbour entrance during flood changed drastically when the CDW was applied.

Without CDW, during flood, water near the bottom of the flume flows in due to tidal filling and the density current. Flow near the surface flows out of the harbour. At the river-side of the harbour entrance some water from the bottom layer is flowing up along the side wall.

The flow pattern during flood with CDW is depicted in figure 9.10. At this moment most water that is flowing into the harbour originates from the upper layers of the flume. The downstream CDW creates a vortex with a horizontal axis that covers the lower water layers over the width of the harbour entrance.

WAVO

The tidal filling discharge is calculated from the WAVO measurements with a high level of accuracy and dependency. The amplitude of the tidal filling discharge is 0.45 l/s.

PTV and EMS

The combined results of PTV and EMS render an order of magnitude for the density exchange discharge of approximately 2 l/s. Although the accuracy of the measurements is limited, it seems that with a CDW present the exchange discharge increases 5-10% during flood.

DCM

The DCM results show that when a CDW without an upstream sill is applied, the exchange volume of near-bed water from the flume during flood decreases by 40%. The use of an additional upstream sill increases this reduction to 70%. At the beginning and at the end of the flood period the exchange discharges of near-bed water are of the same order of magnitude for all configurations (with or without CDW).

Density

During the second part of the flood period and the beginning of the ebb period (0-400s), an increased salinity gradient is present between harbour and river due to the CDW. Because the influx of salt is decreased by the CDW during flood, the salinity of the harbour drops. At the end of flood the CDW stops functioning and the increased salinity gradient between river and harbour causes an increased influx of salt into the harbour. This continues until the salinity goes back to its original value without a CDW present. The extra upstream sill decreases the salinity in the harbour during the whole tidal cycle.

At the beginning of rising tide, when the density current reverses (900s), the influx of salt is increased for the configuration with a CDW and an upstream sill. This could indicate an increased exchange at this time.

Mathematical Model

A simple mathematical model has been set up to study the effects that a CDW would have on the exchange at other times in the tidal cycle. Two ways of modelling the CDW were applied. The model that was based on the hypotheses that all water that flows in during flood is captured from the upper layers by the CDW rendered results that were similar to the density and the DCM measurements. Characteristic outcomes of the model on the influence of the CDW were:

- The average density in the harbour was less with a CDW present. This density difference between the configurations with and without a CDW was present during 0-500s.
- A small increase (5%) of the total density exchange volume due to the CDW (from the upper layer) was predicted. This increase commences during the period that the CDW functions (flood period). It's present until the density of the harbour is equal to the reference concentration (500s).

10. Discussion, Conclusions and Recommendations

10.1. Phase 1: homogeneous conditions

Please note that all experiments of Phase 1 were executed during the flood period, at which the CDW functions. Therefore all conclusions of Phase 1 will only deal with this period.

10.1.1. Discussion

The main objective of the Phase 1 experiments was to quantify the effect of a CDW on exchange between harbour and river. In this section the outcome of the experiments will be discussed.

Effect of CDW on exchange

The Dye Concentration Measurements (DCM) of Phase 1 show small differences between most configurations with the same harbour angle and extracted discharge (appendix B.1). This means the effect of the CDW on exchange of water between harbour and river is small as well. Previous research also showed a small influence of the CDW on the mixing effect. Van Schijndel (1997) and Delft Hydraulics (1992) found a reduction of approximately 5%.

For the 45°-harbour angle with an extracted discharge of 1 l/s the differences between configurations are more substantial than for the 2 l/s extracted discharge or for the 90°-harbour angle. Those results show an increase in exchange of water between harbour and river for the situation with CDW. The other DCM results give a similar indication. These differences are however too small in comparison to the accuracy of the results to say anything conclusive about the increasing effect of the CDW on exchange of water between harbour and river.

Main function CDW

The small influence of the CDW on the turbulent exchange through the mixing layer could mean that the most important function of the CDW is capturing water from layers with a small sediment concentration. With higher sediment concentrations near the bed and the combination of a CDW and a sill an unaltered (or maybe even increased) exchange discharge can still mean less siltation in the harbour basin. This is due to the fact that only water from the upper water layer is captured and led into the harbour.

Positioning the CDW

The LIP III conditions of Phase 1 were kept the same as the conditions of the LIP II experiments as much as possible. The same CDW was used as well but for the 45°-harbour of the LIP III experiments the opening between the CDW and the flume side wall was 3 cm wider than that of the optimal CDW of the LIP II experiments. This means that the LIP III CDW probably captured too much water and caused an increase in exchange of water between harbour and river. One of the major conclusions of LIP II was that a slight alteration of the CDW position can have a large impact on the exchange. This could be a reason for an increased exchange caused by the CDW for the 45°-harbour.

Harbour entrance modification and different harbour angles

The effect of a harbour entrance modification and different harbour angles on exchange between harbour and river was investigated as well. DCM results indicated that the harbour entrance modification caused higher exchange discharges in comparison to the reference

harbour and the harbour with the 45° angle rendered higher exchange discharges than the harbour with the 90° angle.

Although the differences are larger than caused by the CDW they are however still too small in comparison to the accuracy of the results to say anything conclusive about the increasing effect on exchange of water between harbour and river.

Low values calculated discharge

The discharges calculated from exponential fits through the DCM response curves are in general lower than the extracted discharges. This in turn renders negative exchange discharges, which is impossible. The question is what the reason is for the low values. It might be that the theoretical approach of section 6.2.2 (with equation 6.4) is not satisfactory for the phase 1 experimental conditions. Secondly, it might be that the error levels for the dye concentrations calculated with DCM software package LOOK&C are too high. This influences the shape of the curves and therefore the exponential fit. The disturbing colour components only add to this last-mentioned problem.

10.1.2. Conclusions

- During flood the CDW's used during Phase 1 had a small effect on exchange of water between harbour and river (under quasi-tidal flow and homogeneous conditions with constant water density and constant discharges through the flume and the harbour).
- The CDW changed the flow pattern in the harbour basin considerably. The primary eddy stretched and flow velocities in the primary eddy decreased.
- When a CDW was applied, most water that flowed into the harbour basin originated from the inside of the CDW (space between the CDW and the harbour entrance corner).
- The DCM results indicate that a smaller harbour angle (at the upstream side) between the flow direction in the flume and the orientation of the harbour leads to larger exchange discharges.
- The blunt upstream harbour entrance corner of the 45°-reference harbour caused flow to separate just inside the harbour basin. This mainly determined the shape of the primary eddy and thus created a fixed length of the primary eddy.
- The DCM results indicated that the upstream harbour entrance corner modification used for the 45°-harbour angle increased the exchange discharge.

10.1.3. Recommendations

- Further research on siltation reduction is needed on the effect of the combination CDW & sill in a harbour with tidal movement and a homogeneous environment. Previous research indicates that the most beneficial effect on siltation reduction is obtained when a sill is added.

10.2. Phase 2: inhomogeneous conditions

10.2.1. Discussion phase 2

Until now the CDW had not been studied under tidal flow and inhomogeneous conditions (salinity gradients). The objective of the Phase 2 experiments was to investigate and quantify the effect of a CDW under these conditions. In this section the outcome of the experiments will be discussed.

Effect of CDW

Before the start of the experiments it was doubted whether a CDW (in combination with a sill) could influence the exchange between harbour and river under tidal flow and a density current present. However with DCM the inflow of near-bed water from the lower 25% of the water column was examined and the results show a substantial reduction in exchange near the bed when a CDW is applied

The CDW causes a vortex near the bed with its axis across the harbour entrance width. Near the bed, this vortex separates the harbour from the river. In the present study the vortex is probably the main cause for reducing exchange in the lower half of the water column between harbour and river.

From the results it can be concluded that the most important function of the CDW is that most water that flows into the harbour during rising tide originates from the upper water layer in the flume. Hereby the influx of near bed water is substantially decreased. It also increases the density difference however, which causes a small extra exchange around high water slack. This effect is only minor when compared to the decrease of exchange of near bed water. The increase of the density difference is influenced by the degree of stratification of the river. When the river would be completely mixed, the CDW could capture water from the upper layers of the river, without changing the driving force of the density discharge. A slight increase in the exchange discharge through the upper layer would not occur now.

Upstream sill

The reduction in near-bed exchange is even larger when the CDW is combined with an upstream sill. The vortex, visualised at the bed by the threads, was also more pronounced when the upstream sill was added to the CDW. The upstream sill probably increases the strength of the vortex that is initiated by the downstream CDW. When compared to the reference situation the decrease in near bed exchange caused by the CDW with an upstream sill is significant, even when a 95% reliability error band is applied.

During the entire ebb period the driving force of the density current (density difference between harbour and river) is increased when a CDW with an upstream sill is applied. Because the density current at the bottom and the tidal emptying are directed outward near the bed, this is not expected to have a large impact on the siltation rate.

Scale factors

It could be that flow velocities in a prototype river are not large enough to be able to make the CDW effective. The vortex that is created will be weaker and probably less efficient. When a depth scale of 50 assumed in this model (the prototype depth is now 12.5 meter, which is a common value), then according to the Froude condition the velocity scale will be $\sqrt{50} = 7.1$. This would mean that the flow velocities in the prototype river will be around 1.4 m/s. This is rather high.

An additional factor, which might hamper the effect of a CDW in a prototype harbour, is the proportion between the water depth to the width of the harbour entrance. For the present study this proportion was approximately 1 : 4. For actual harbours this proportion is around 1 : 15.

Therefore in reality the vortex might not be strong enough to exist over the entire harbour entrance width. The vortex might be artificially prolonged by placing bottom vanes across the harbour entrance in the direction present in the vortex.

Other scale effects must also be examined closely, when comparing the results from these experiments to prototype situations. For extrapolation of the results the undisturbed exchange volumes of the density current, mixing, and tidal filling must have the same proportion to the harbour volume as for the present study. CDW model 1 serves as an illustration on how the extrapolation of these harbour volumes can be performed (appendix K). This extrapolation should be performed using the CDW model 2. This model probably describes the function of the CDW better. The effects of a CDW under different conditions are not known however, so the model results can only give an indication.

Influenced Mixing

The exchange due to turbulent mixing could not be determined in this research, as the DCM results probably underestimated the exchange discharge. This way it is not clear which mechanism contributed to which part of the exchange. A part of the reduction that the CDW caused can be a reduction of the mixing exchange, instead of a reduction of the density current only. When all water that is flowing in must pass over the vortex in the harbour entrance, the mixing layer at that depth will be pulled more into the harbour. This causes a lower exchange due to mixing. The increased acceleration of the water that flows in, which has to flow through a smaller cross section, could also decrease the turbulent mixing.

Siltation

Ultimately the siltation of a harbour must be determined. In order to do this the sediment distribution over the depth must be coupled to the exchange discharge. The mathematical model from section 9.6 could be used for this. The sediment concentration and distribution over the vertical, which change constantly during a tidal cycle, can be coupled to parameters like the flow velocity and salinity. Now the incoming sediment is calculated by equation 2.11. Integrating this over a tidal cycle gives the total influx of sediment (this is the net influx when the trapping efficiency is high).

Although no actual sediment concentration was linked to the inflow of water, it seems likely that a CDW can already decrease the sediment influx when a small gradient of the sediment concentration over the depth is present. The average reduction of 70% of the inflow of near-bed water during flood will probably outweigh the minor increase of 5% of the total water exchange around high slack water (a period with low flow velocities, and therefore low sediment concentrations at the river).

Low values of calculated discharges

From the DCM results the discharges going in through the lower 25% of the water column are calculated. These values are in general lower than findings of other experiments and of the PTV/EMS measurements. This can partly be explained by the rather crude estimate of the dye distribution over the depth that is used in the calculations. Another reason is the dispersion of dye in the flume and the vertical mixing between the two layers the harbour.

10.2.1. Conclusions phase 2

Effect of a CDW on siltation under tidal inhomogeneous conditions

- The application of a CDW can decrease siltation in an estuarine harbour where salinity-driven density currents are present. The CDW can only reduce siltation when a sufficient gradient in the sediment concentration over the depth is present at the river.

Effect of the CDW without upstream sill

- The CDW substantially decreased the inflow of near-bed water during rising tide. The maximum reduction of inflow of near-bed water (through the lower 25% of the water column) was approximately 60% when flow velocities in the flume are high. For the entire flood period the relative decrease of the total exchange volume of near-bed water is approximately 40%.
- When a CDW is present most water that flows into the harbour during rising tide originates from the upper water layer in the flume.
- During rising tide the CDW created a vortex near the bed with its axis across the harbour entrance width (with or without upstream sill). The vortex is probably the main cause for the reduction of near bed influx during rising tide.
- During flood the absolute decrease of the exchange discharge through the lower layer due to the CDW is related to the flow velocity in the flume. A larger reduction occurs when higher flow velocities are present in the flume.
- The total inflow of water during flood does not change much with a CDW present. Measurements indicate that the density exchange (through the higher water layers) increases by 5%, due to an increased density difference between harbour and river.
- At the end of the flood period, after the CDW has stopped functioning, the increased density difference between river and harbour causes an increased density exchange, which lasts until the average density in the harbour is back to the level that was present without CDW.

Effect of an extra upstream sill

- During flood when the CDW is present, an upstream sill reduces the inflow of near-bed water (through the lower 25% of the water column) even further. For this configuration the maximum reduction of inflow of near-bed water was approximately 90%. The decrease of the total exchange volume during rising tide was approximately 70%.
- The salinity level in the harbour is lower during the entire tidal cycle when the upstream sill is added.
- The results indicate that an upstream sill increases the water exchange during falling tide.

Flow without CDW

- The harbour used for the Phase 2 experiments was relatively small. The density exchange discharge into the harbour had an amplitude of approximately 2 l/s and the tidal filling discharge had an amplitude of 0.45 l/s.
- During falling tide, when an outgoing density current at the bottom is present in the harbour, still some near-bed river water enters the harbour. This water flows in through the upper water layers in the harbour entrance. This phenomenon is due to three-dimensional flow effects.

10.2.3. Recommendations phase 2

- The results show that a reduction of siltation in an estuarine harbour is possible. But for a conclusive answer on the magnitude of this siltation reduction the site-specific conditions of a prototype harbour must be taken into account.
- Only a first indication of the flow structure in the harbour entrance due to a CDW was found in this research. For optimising a CDW design more knowledge is needed. The 3D-flow structure can be examined with particle tracking techniques. Dye measurements with injections at several places (different depths, in- and outside of the CDW) could determine the exact origin of the incoming water. Previous research like the research on bottom vanes can be used for a theoretical basis.
- The upstream sill can increase the effect of the downstream CDW but the exact function of the sill is not known and needs further research.
- Not much is known yet about the interaction between the mixing layer and the density current. This interaction between the density current and the mixing layer also has an influence on the total water exchange. Research should be undertaken in order to quantify the interaction between the two mechanisms.
- The CDW in this research was designed to capture the tidal filling discharge plus an additional 10%. In the case of a density current this capture discharge is not necessarily the best choice anymore. Several capture discharges (in the range of 0 to the density exchange discharge) should systematically be examined to investigate the effect on the vortex and on the exchange discharge.
- Increased flow velocities and increased turbulence will occur in the harbour entrance because of the vortex that is caused by the CDW. This will cause erosion. The magnitude of this needs further research. The flow pattern in the entrance could also change due to an altered bathymetry. The impact of this altered bed on the effectiveness of the CDW must be examined.

10.3. Experimental techniques of Phase 1 & 2

10.3.1. DCM

Conclusions

- DCM is a useful aid in quantifying the effect of a CDW on exchange. However in combination with the software package LOOK&C it is also a laborious method.

Recommendations

- The effect of the three colour components (red, blue and green) on the greyscale DCM results needs more investigation.
- The application of DCM (LOOK&C included) is very site specific and careful investigation into the effect of the various parameters is essential.

10.3.2. PTV

Conclusions

- PTV is a reliable and robust way of measuring velocity distributions. Even in an experiment that was not always set up optimally, because of time pressure and other experiments that had to be taken, good results were obtained.
- The time needed for processing PTV results can be decreased drastically when also the pre- and post processing are combined in one program.
- 2-D particle tracking cannot be used for measuring discharges in a complex flow field like the one that was examined in the LIP III research. Additional measurements are still required.
- The variation in flow velocity was the main source of the errors in the median vectors.

Recommendations

- The sample frequency can be taken lower at approximately 5 Hz, when only average velocities are required. The amount of data decreases proportionally with the sample frequency, so attention should be given to the right choice of this value.
- Three dimensional Particle Tracking should be applied for obtaining a clear picture of the complex three dimensional flow structure in the harbour entrance.

11. References

Battjes, J.A., *Fluid mechanics (in Dutch)*,
Lecture notes Delft UT, 1990

Berge, A. van den, Case study Drimmelen,
M.Sc. thesis Delft UT, August 1997 (in Dutch)

Booij, R., *Measurements of exchange between river and harbour*,
Lecture notes Delft UT, 1986 (in Dutch)

Booij, R., *Turbulence*,
Lecture notes Delft University of Technology, 1992 (in Dutch)

Brown, G.L. & Roshko, A., On density effects and large structure in turbulent mixing layers,
Journal of Fluid Mechanics, Vol. 64, Part 4, pp. 775-816

Crowder, R.A., *Flow Control in the entrance to river harbours, embayments and irrigation channels*,
to be published 1999

Crowder, R.A., *LIP II- study on the reduction of siltation in harbours by means of a Current Deflecting Wall*,
Bradford, 1996

Delft Hydraulics, *Description of the flow scheme of the Tidal Flume (in Dutch)*,
version 2, Z0017, 1986

Delft Hydraulics, *Parkhafen in Hamburg model study*,
Delft 1992

Eysink, W.D., *Sedimentation in harbour basins. Small density differences may cause serious effects*,
Delft Hydraulics, 1989

Dursthoff, W., *Über den quantitativen Wasseraustauch zwischen Flusz und Hafen*,
Mitteilungen des Franzius-Instituts für Grund- und Wasserbau der Technischen Universität Hannover, Heft 34, 1970

Graaff, J. Van de, and Reinalda, R., *Horizontal exchange in distorted scale models*,
Delft Hydraulics, June 1977

Headland, J.R. *et all*, *Application of an engineering model for harbour sedimentation*,
PIANC-28th Int. Navigation Congress, 1994

Kranenburg, C., *Density currents*,
Lecture notes Delft UT, 1996 (in Dutch)

Langendoen, E.J., *Flow patterns and transport of dissolved matters in tidal harbours*,
Delft, November 1992

Marelius, F., *Experimental Investigation of Flow Past Submerged Vanes*,
Journal of Hydraulic Engineering, Vol. 124, no. 5, may 1998

Massie, W.W., *Coastal Engineering, Volume I Introduction*,
Delft, revised edition 1982

Odgaard, A.J. and Wang, Y., *Sediment Management with submerged Vanes I: Theory*,
Journal of Hydraulic Engineering, Vol. 117, no. 3, March 1991

Plas, G.A.J. van der, *Description of some FPTV-algorithm parts*,
Eindhoven, April 1998

Plas, G.A.J. van der, *Matching algorithms for particle tracking velocimetry*, Eindhoven 199?

Prooijen, B.C.van, *Large flow structures in a river with outer marches*, M.Sc. thesis Delft UT, May 1999 (in Dutch)

Roelfzema, A., *Harbour studies: study to the influence of a harbour on state of salinity in the river and the exchange between harbour and river*, Delft, October 1977

Roelfzema, A. & Os, A.G. van, *Effect of harbours on salt intrusion in estuaries*, Report No. 204, Delft Hydraulics, 1978

Rohr, F., *Movement of water and sediment in harbours on rivers and seas (in German)*, Ph.D. thesis, Technische Hochschule Karlsruhe, 1933

Schijndel, S.A.H. van, *Siltation of a river harbour*, Final thesis Delft UT, April 1997 (in Dutch)

Volmers, H.J., *Systematik der Maszahmen zur Verringerung der Schwebstoffablagerungen in Binnenhafenmündungen (in German)*, Technische Hochschule Karlsruhe, March 1963

Wallast, I, *Exchange of dissolved matter between groyne field and river*, M.Sc. thesis Delft UT, September 1998 (in Dutch)

Westerweel, J., *Digital Particle Image Velocimetry – Theory and application*, Ph.D. thesis Delft UT, 1993

Winterwerp, C. *et. al.*, *The Current Deflecting Wall: a device to minimise harbour siltation*, The Dock and harbour authority p.243-246, March 1994

Winterwerp, C., *Note on CDW-experiments for inhomogeneous conditions*, Delft 1999 (not published)

12. Acknowledgement

First of all we are indebted to our families and friends for accompanying and supporting us throughout these years of study, in particular Dineke & Frank Hofland, Ine & Willem van Leeuwen, Derske Naafs and Elisabeth Pietermaat.

The European Union provided a large part of the funds for the experiments under the "large scale installations and facilities programme".

The professional experimental team of Delft Hydraulics was of vital importance for the experiments. We highly appreciated the expertise of John Cornelisse and the unremitting dedication of John Coolegem during the experiments. Furthermore, we want to mention Kees Koree, Frans de Vreede, Wim Taal, Erik van Velzen and Rinze Bruinsma from Delft Hydraulics as well as Arie den Toom from Delft University of Technology for their help on various subjects.

The LIP III Steering Group paved the way for the present CDW investigations at the Delft Tidal Flume. The committee consists of Herman Christiansen, Richard Falconer, Robert Kirby, Tim Smith and Han Winterwerp. We are especially grateful to Han Winterwerp for his guidance, Richard Crowder for the pleasant co-operation during the many long test days and Herman Christiansen for inventing such a CDW that we are able to present positive results.

Last but certainly not least we want to thank the thesis committee from Delft University of Technology consisting of professor J.A. Battjes, J.C. Winterwerp, W. Uijttewaal, C. Kranenburg and G.J. Schiereck. Their advise and their comments on our work have guided us throughout the project and have helped us achieve a higher standard of performance. Wim Uijttewaal has been a great help with the application of the experimental measurement techniques and Cees Kranenburg gave us better understanding of flow with inhomogeneous density.

13. Appendices

Appendix A
Coordinates of CDW configurations tested during LIP III

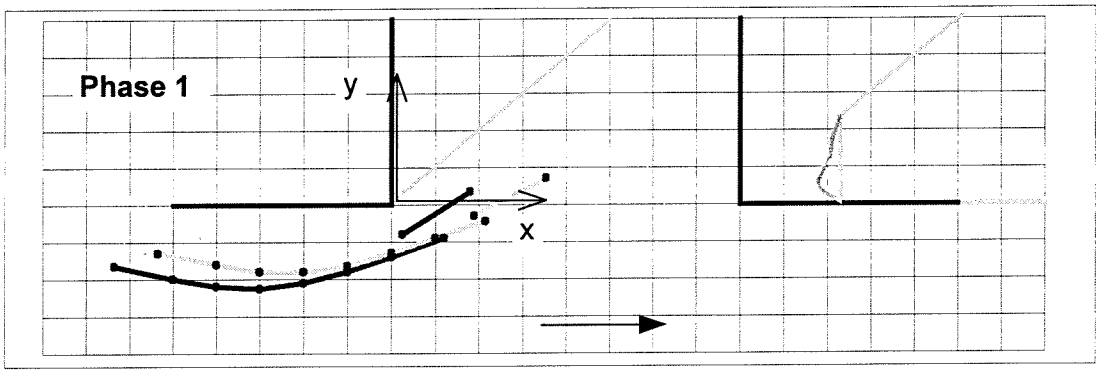

Phase 1

45 degree angle		90 degree angle	
x	y	x	y
First segment		First segment	
0.215	-0.045	0.120	-0.090
0.100	-0.090	0.000	-0.140
0.000	-0.130	-0.100	-0.180
-0.100	-0.165	-0.200	-0.210
-0.200	-0.180	-0.300	-0.225
-0.300	-0.180	-0.400	-0.220
-0.400	-0.160	-0.500	-0.200
-0.535	-0.130	-0.635	-0.165
Second segment		Second segment	
0.354	0.071	0.025	-0.080
0.190	-0.030	0.180	0.035
Entrance modification			
1.030	0.000		
0.984	0.042		
0.977	0.060		
1.007	0.125		
1.014	0.185		
1.030	0.230		

Phase 2

Downstream		Upstream	
x	y	x	y
CDW (above 0.125m)		Sill (lower 0.125m)	
-0.200	-0.063	0.940	0.110
-0.100	-0.080	1.030	-0.107
0.000	-0.075	1.100	-0.100
0.100	-0.040	1.200	-0.070
0.157	-0.015	1.250	-0.035
Sill (lower 0.125m)		1.300	-0.015
-0.400	0.000	1.350	0.000
-0.350	-0.020	Entrance modification	
-0.300	-0.045	1.030	0.230
-0.200	-0.110	0.940	0.120
-0.100	-0.140	1.030	0.000
0.020	-0.155		
0.000	0.000		

- Measures in metres
- All parts cover full water depth, exept when indicated otherwise

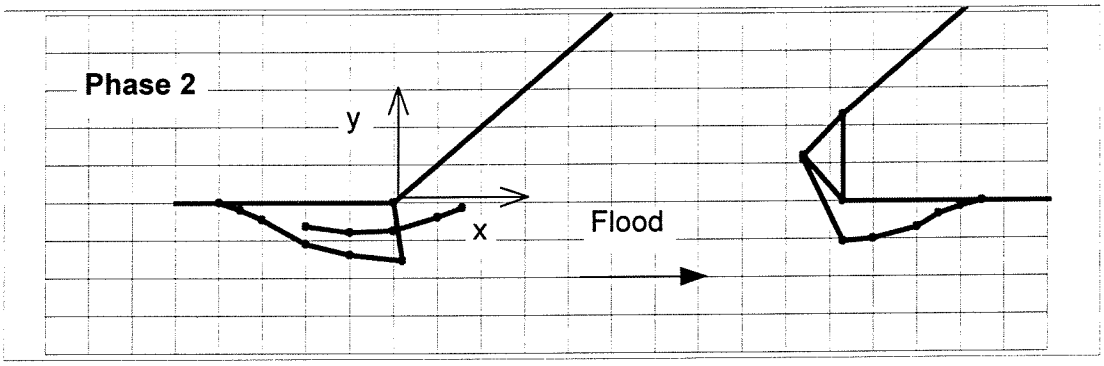

Appendix B.1. DCM Results Phase 1

Relative concentrations from t=0s

Phase 1, 45 degree harbour angle, 1 l/s harbour discharge

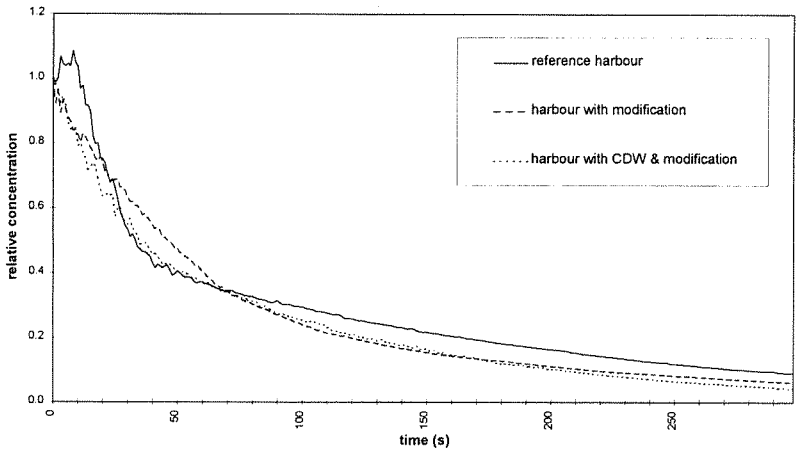

Phase 1, 45 degree harbour angle, 2 l/s harbour discharge

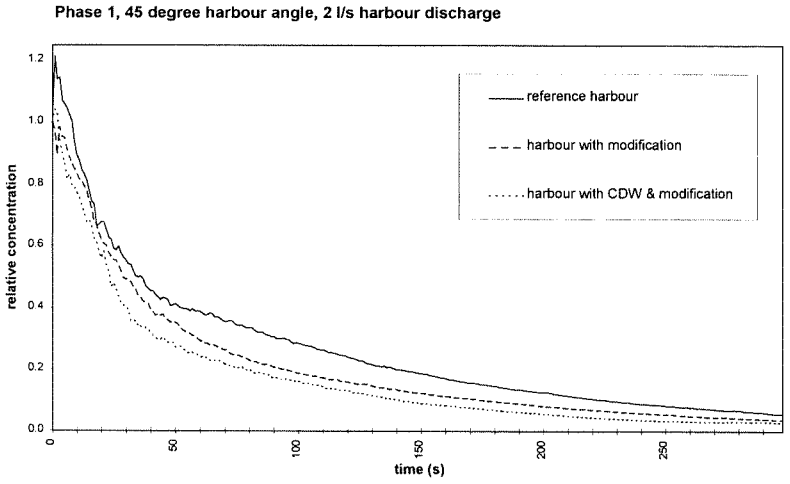

Phase 1, 90 degree harbour angle, 1 l/s extracted discharge

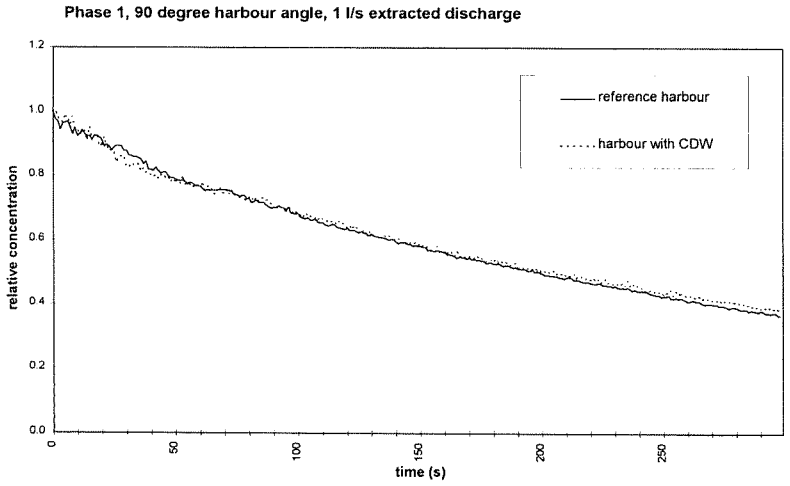

Phase 1, 90 degree harbour angle, 2 l/s harbour discharge

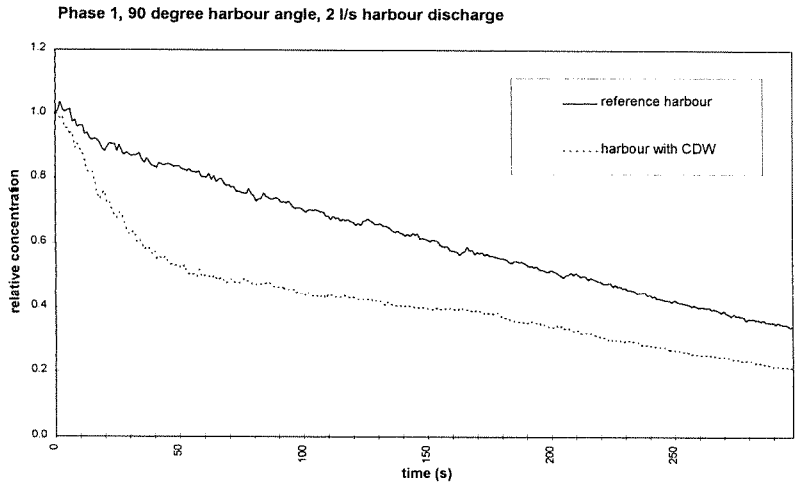

Relative concentrations from t=50s

Phase 1, 45 degree harbour angle, 1 l/s extracted discharge

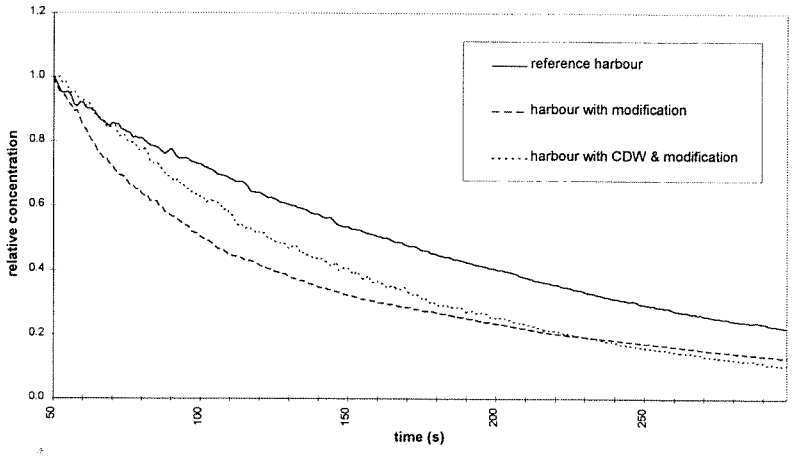

Phase 1, 45 degree harbour angle, 2 l/s extracted discharge

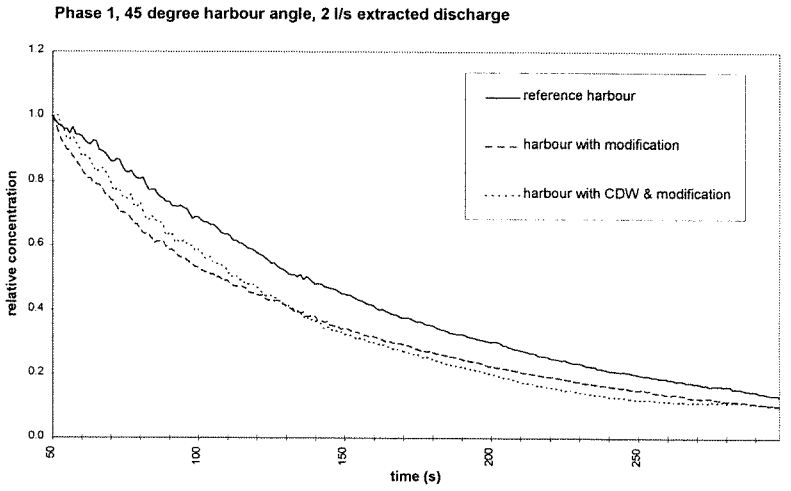

Phase 1, 90 degree harbour angle, 1 l/s extracted discharge

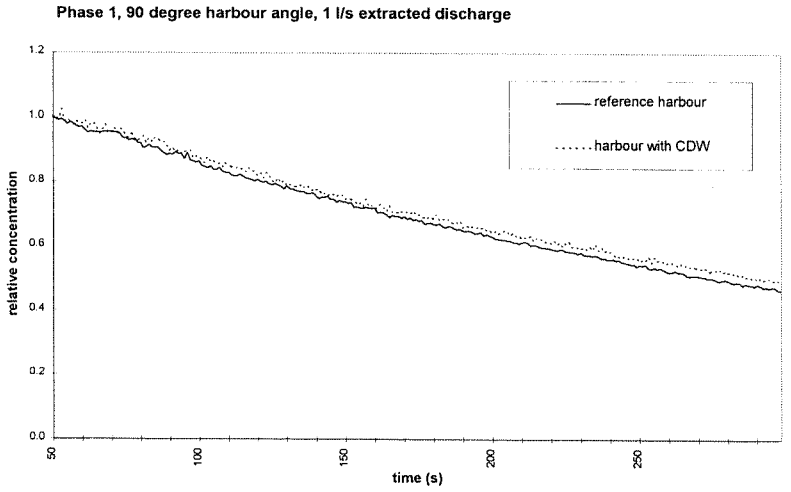

Phase 1, 90 degree harbour angle, 2 l/s extracted discharge

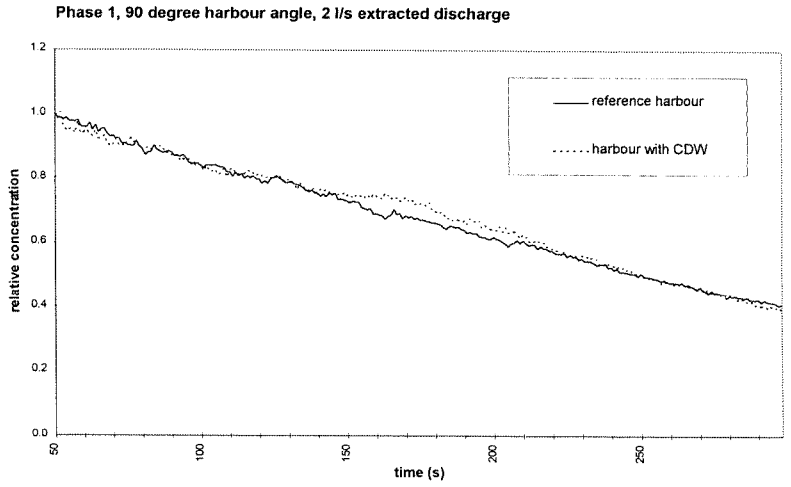

Appendix B.2. PTV Results phase 1

1. Reference, 1l/s discharge

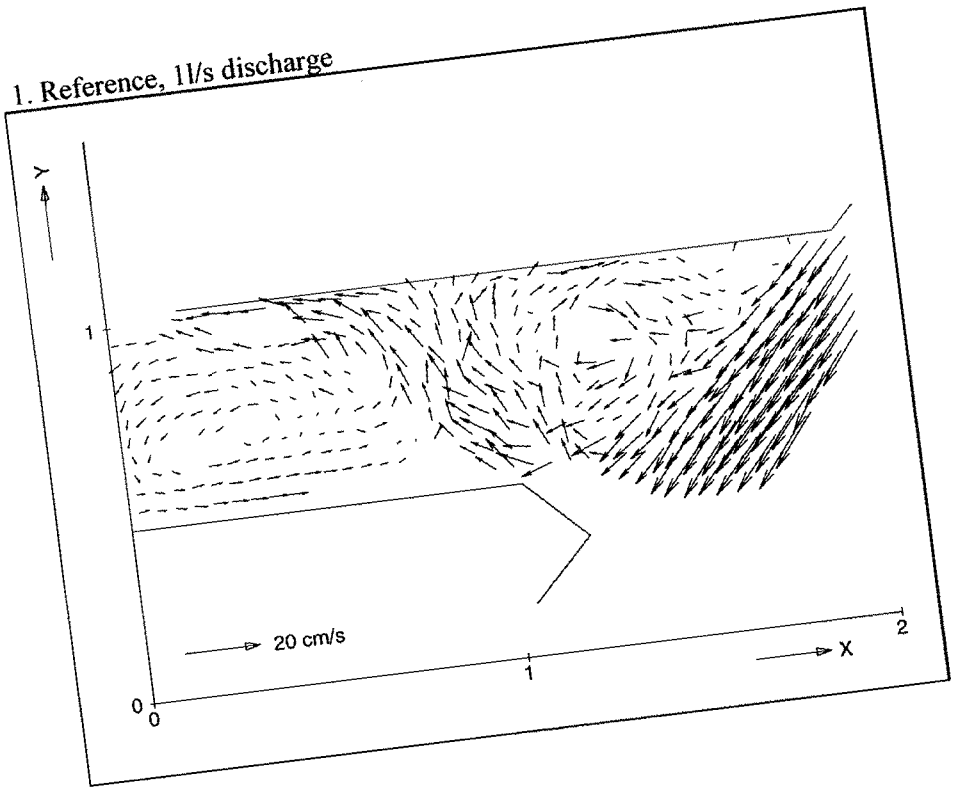

2. Reference, 2l/s discharge

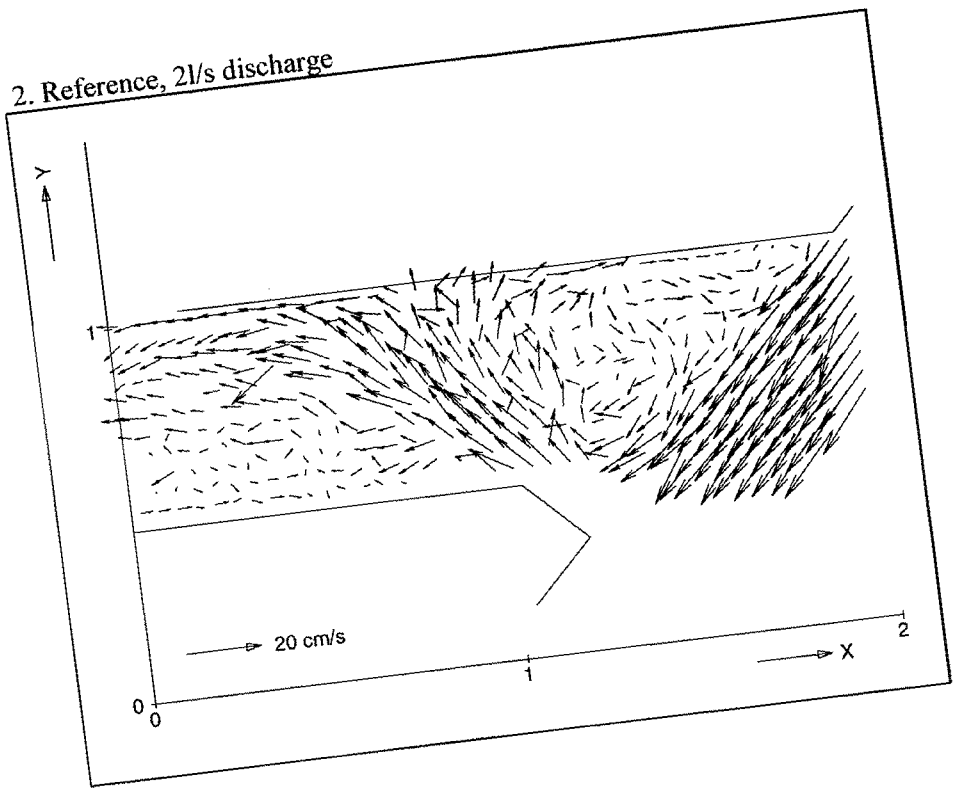

3. Plus Harbour Entrance Modification, 1l/s discharge

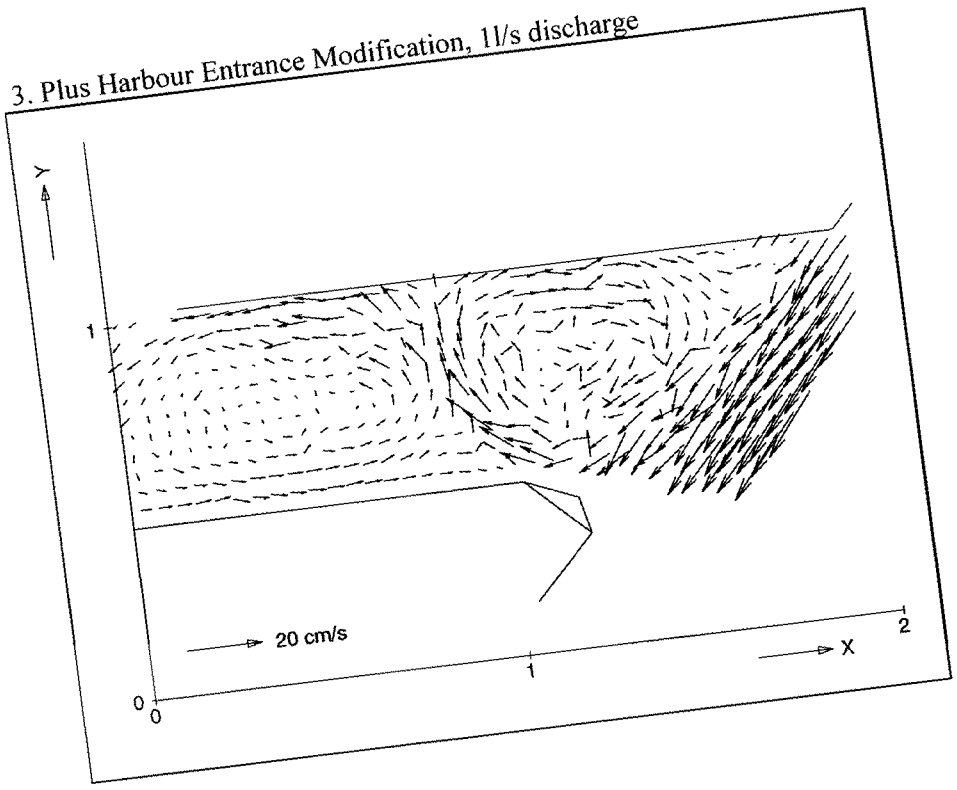

4. Plus Harbour Entrance Modification, 2l/s discharge

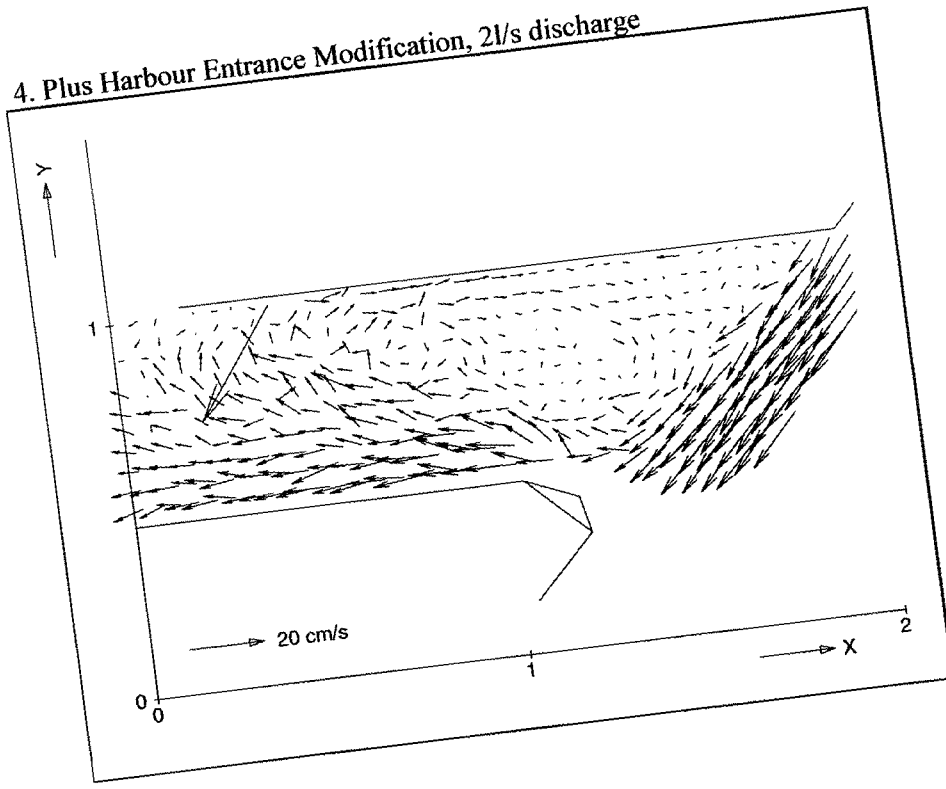

5. Plus CDW, 1l/s discharge

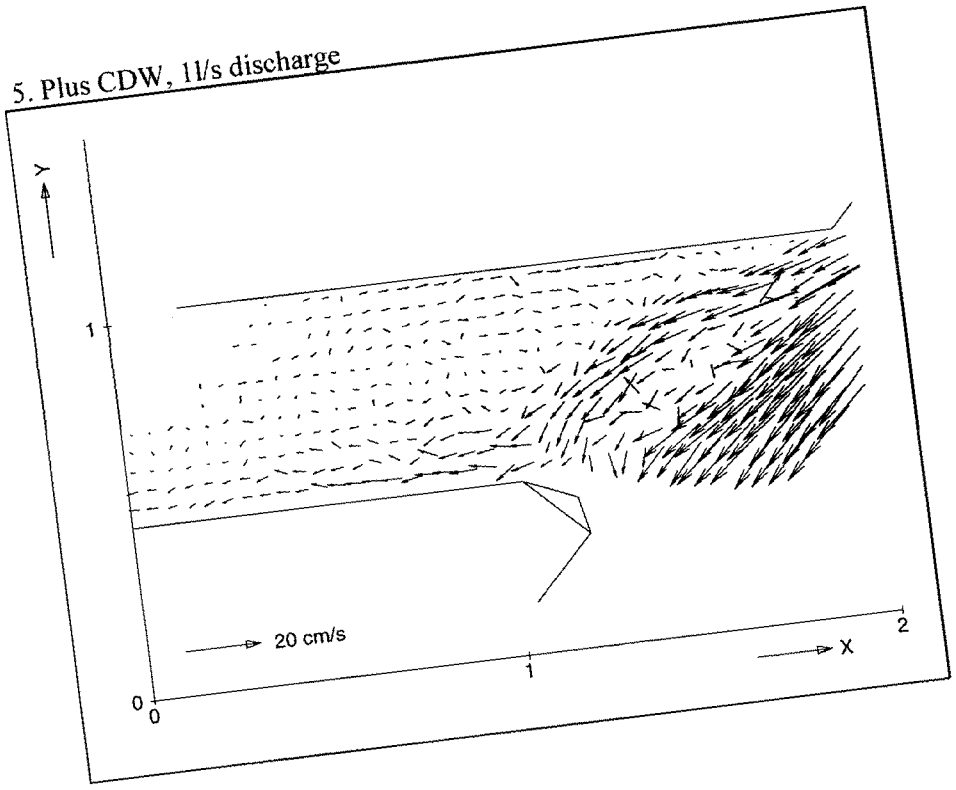

6. Plus CDW, 2l/s discharge

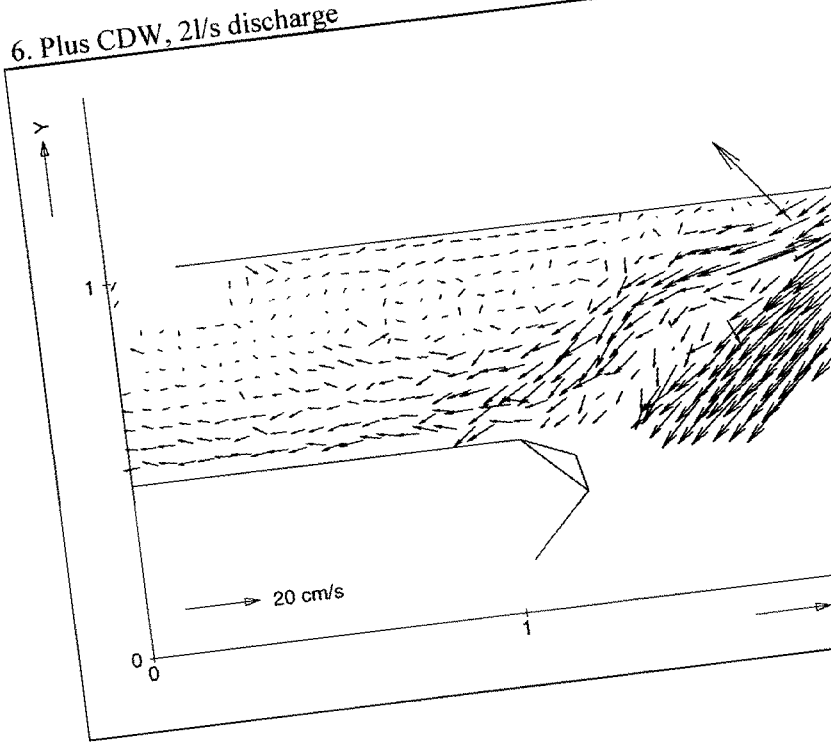

Appendix B.2. PTV Results Phase 1

90° harbour

1. Reference, 1l/s discharge

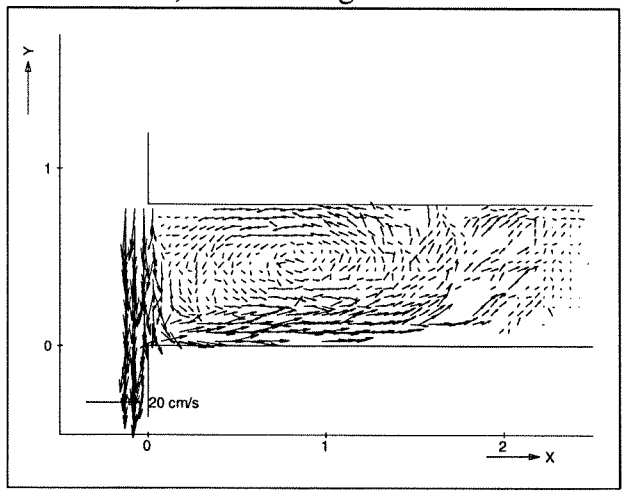

2. Reference, 2l/s discharge

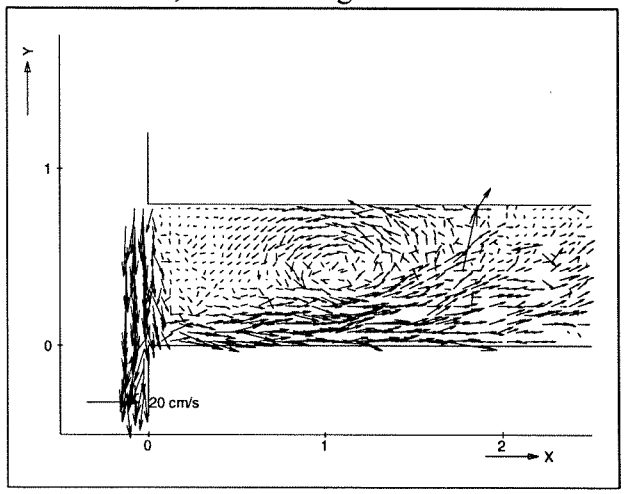

3. Plus CDW, 1l/s discharge

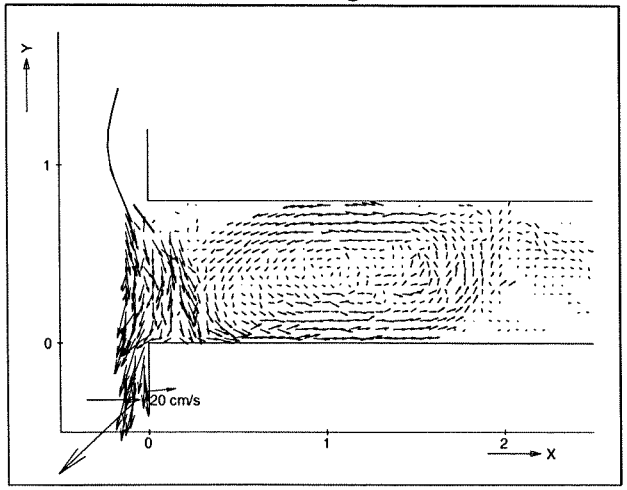

4. Plus CDW, 2l/s discharge

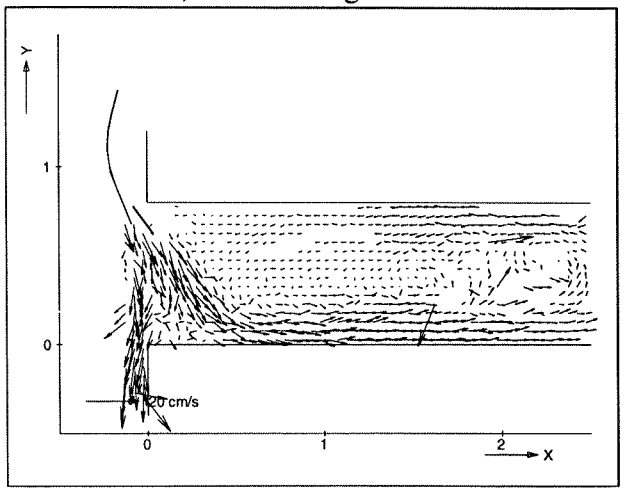

Appendix B.3. EMS results phase 1 45° harbour

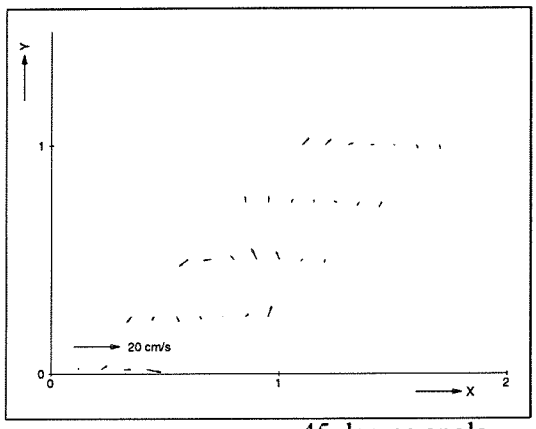

Quasi tidal Homogeneous 45 degree angle
Reference configuration **5 cm elevation**
1l/s discharge from harbour basin

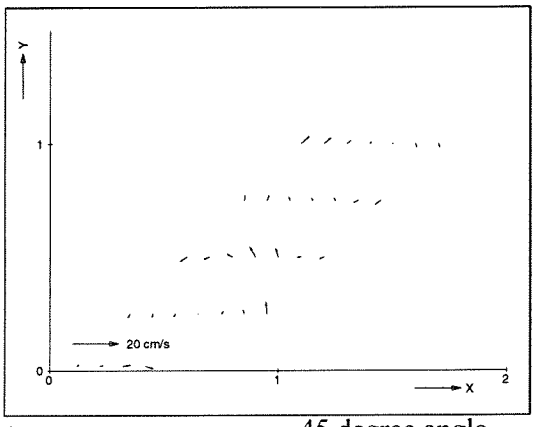

Quasi tidal Homogeneous 45 degree angle
Reference configuration **10 cm elevation**
1l/s discharge from harbour basin

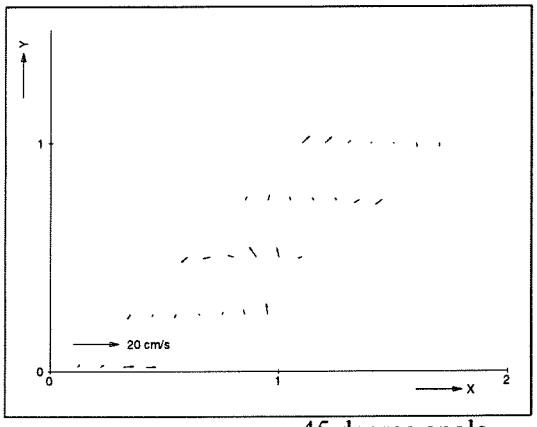

Quasi tidal Homogeneous 45 degree angle
Reference configuration **15 cm elevation**
1l/s discharge from harbour basin

Note: The flume is situated at the bottom of the figures. The sea is situated at the lefthand side. The borders of the harbour are marked by the positions of the EMS measurements.

Appendix B.3. EMS results phase 1 45° harbour

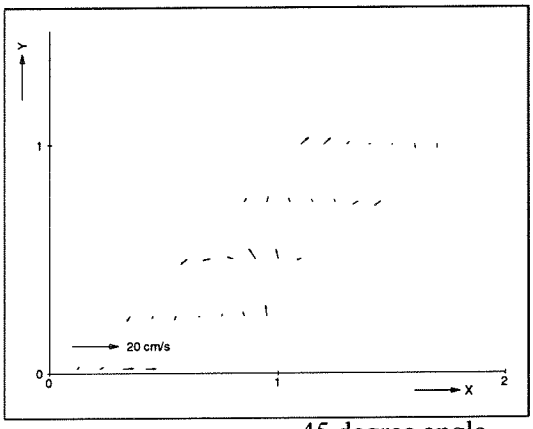

Quasi tidal Homogeneous 45 degree angle
Reference configuration 15 cm elevation
1l/s discharge from harbour basin

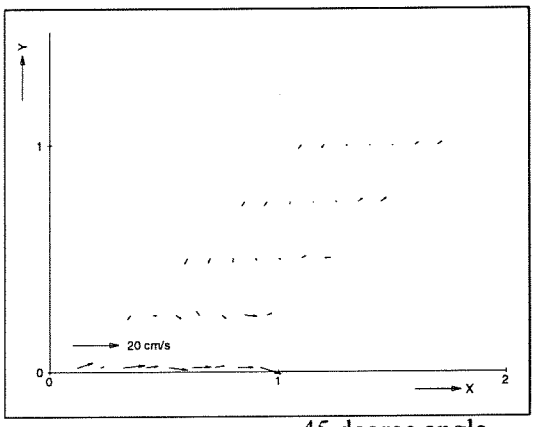

Quasi tidal Homogeneous 45 degree angle
Plus harbour entrance modification 15 cm elevation
1l/s discharge from harbour basin

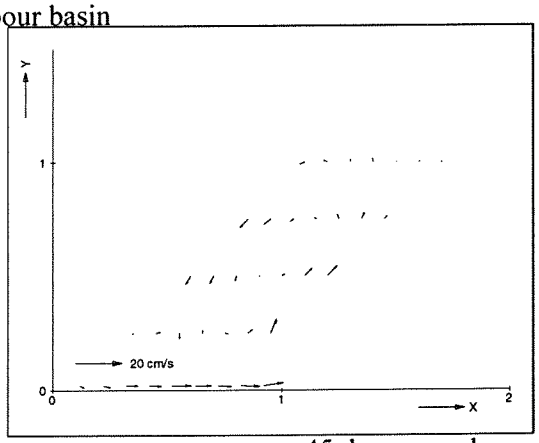

Quasi tidal Homogeneous 45 degree angle
Plus CDW 15 cm elevation
1l/s discharge from harbour basin

Note: The flume is situated at the bottom of the figures. The sea is situated at the lefthand side. The borders of the harbour are marked by the positions of the EMS measurements.

Appendix C.1. DCM Results Phase 2

For a better overview of the DCM results during phase 2 first a graph of the tidal period is given:

Comparison configurations phase 2 during rising tide:

Phase 2, downstream dye injection at t =880s

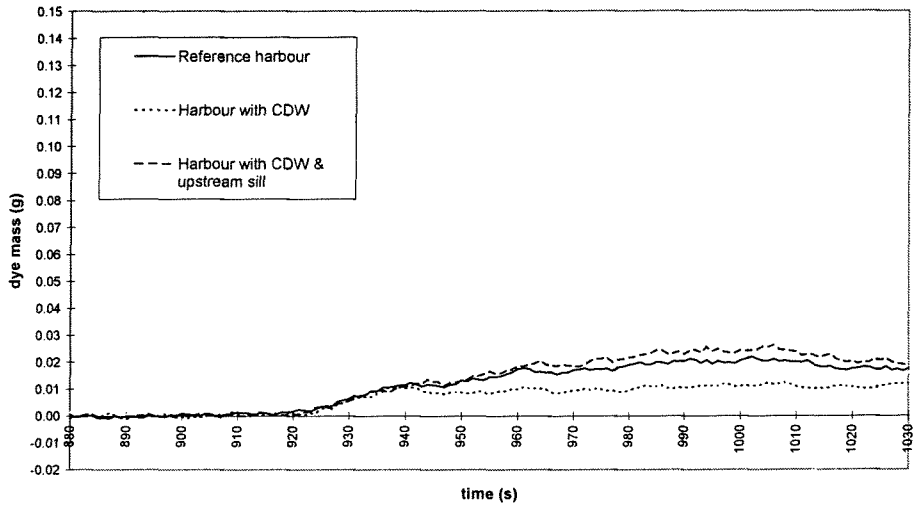

Phase 2, downstream dye injection at t=940s

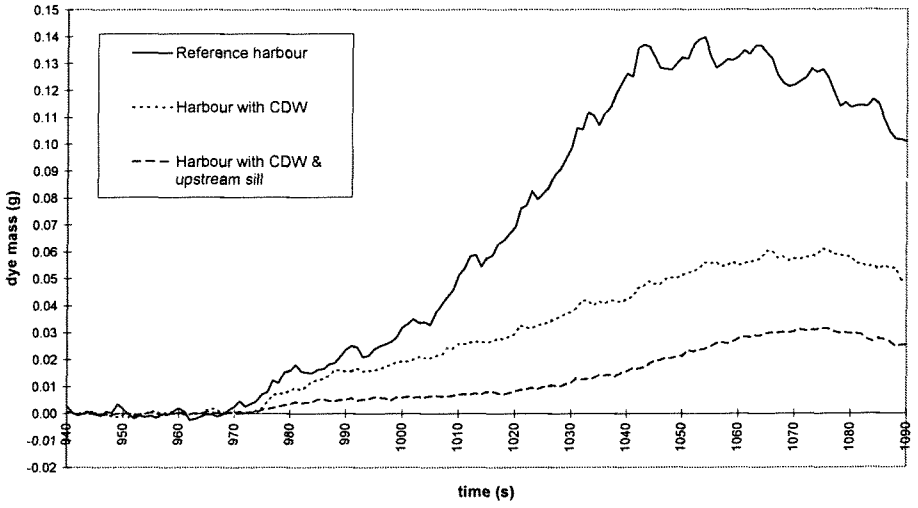

Phase 2, downstream dye injection at t=60s

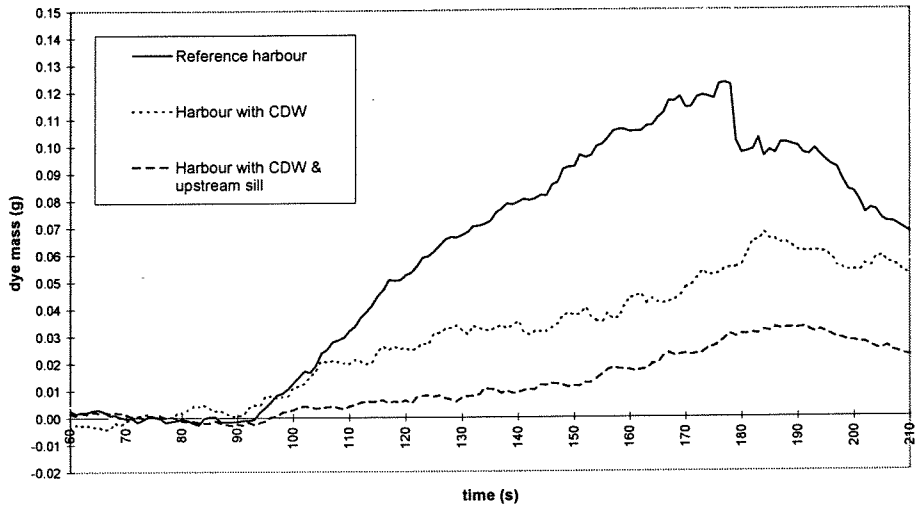

Phase 2, downstream dye injection at t=120s

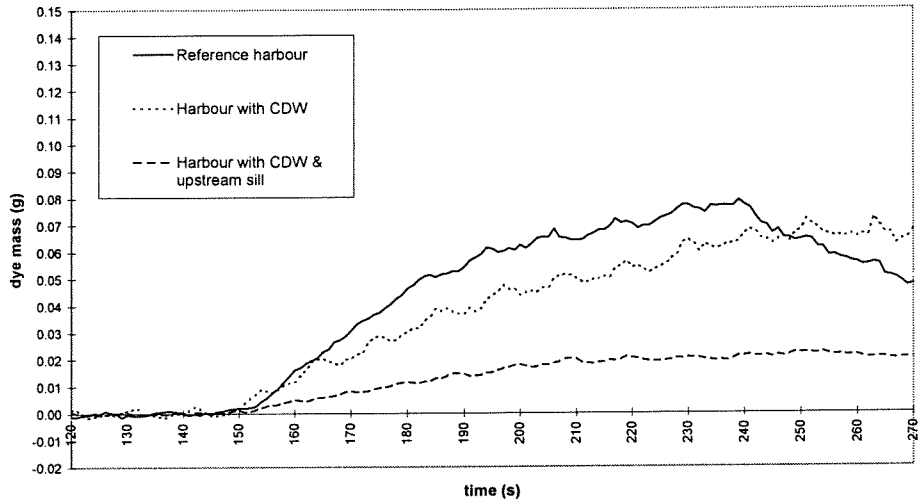

Phase 2, downstream dye injection at t =195s

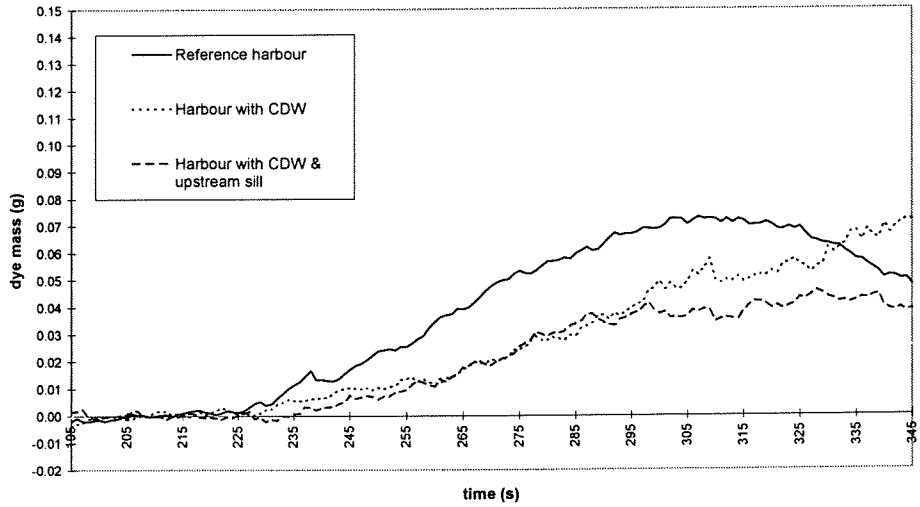

Comparison configurations phase 2 during falling tide:

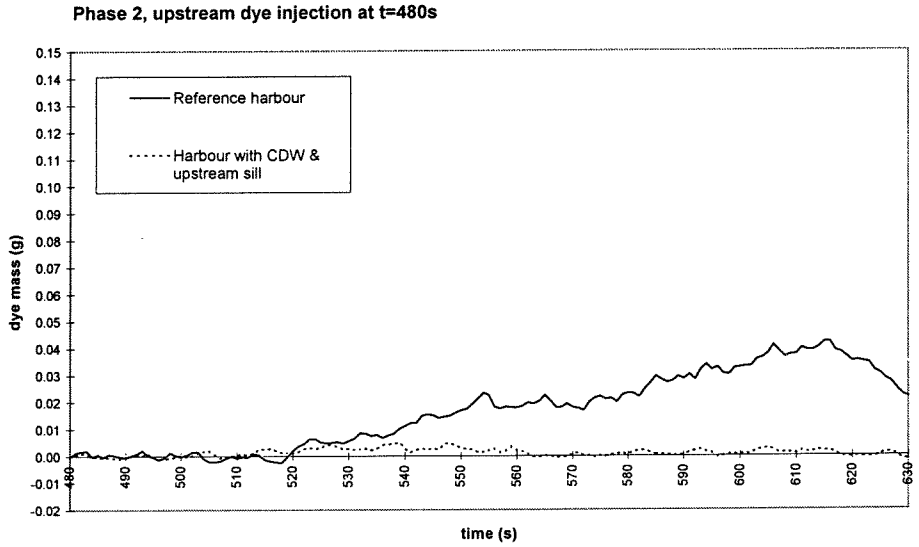

No succesful tests were performed for configuration B (harbour with a CDW).

Appendix C.2. PTV Results phase 2

Configuration A - Reference

1. Time = 125s

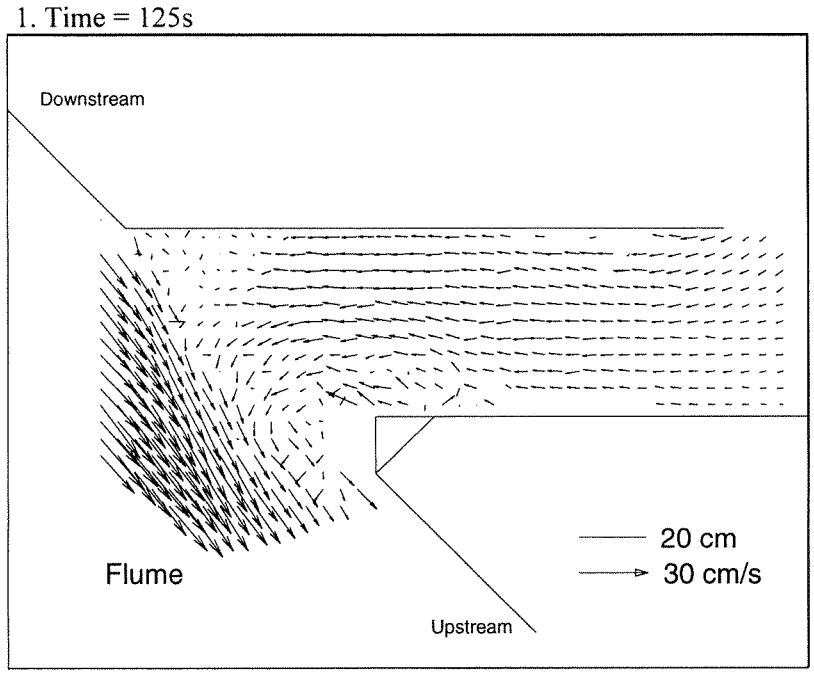

2. Time = 250s

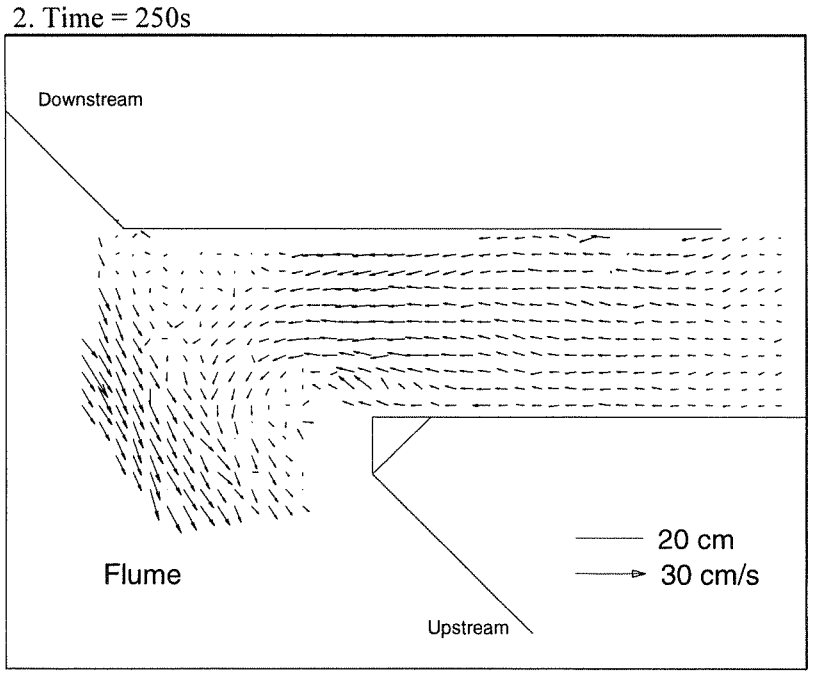

3. Time = 375s

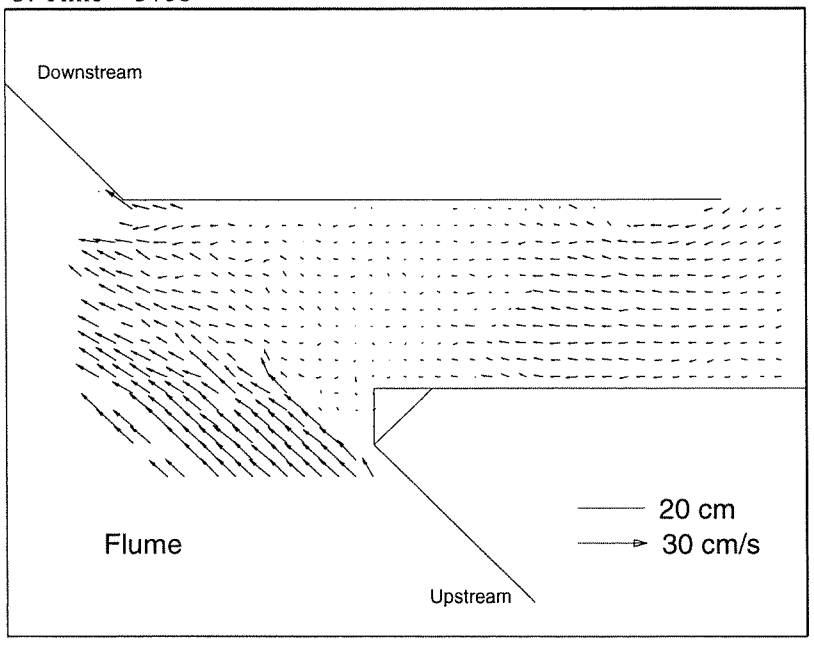

4. Time = 500s

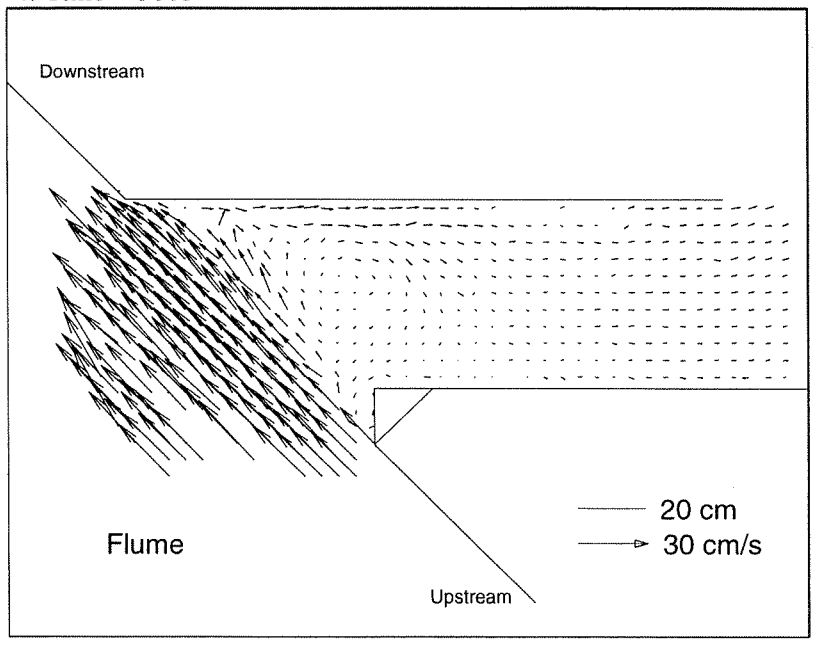

5. Time = 625s

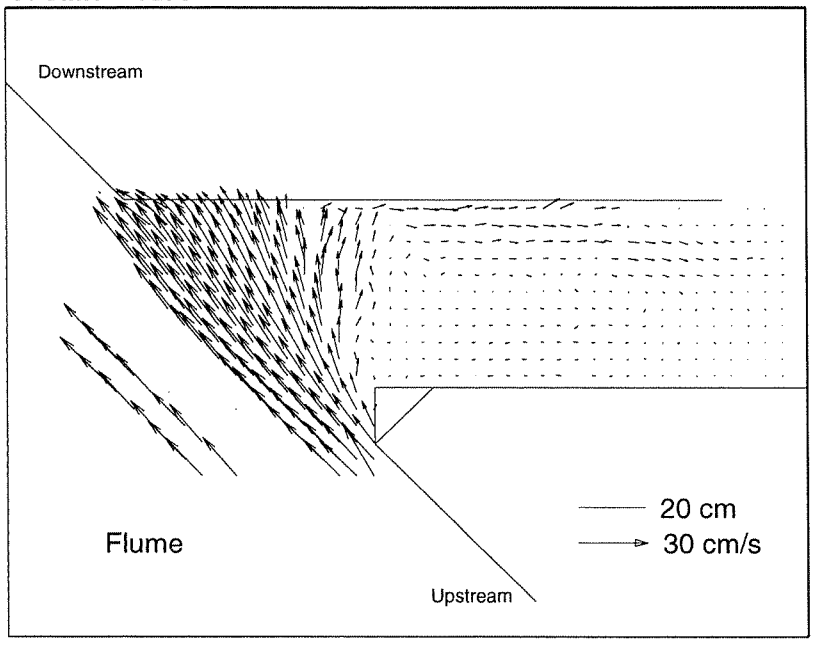

6. Time = 750s

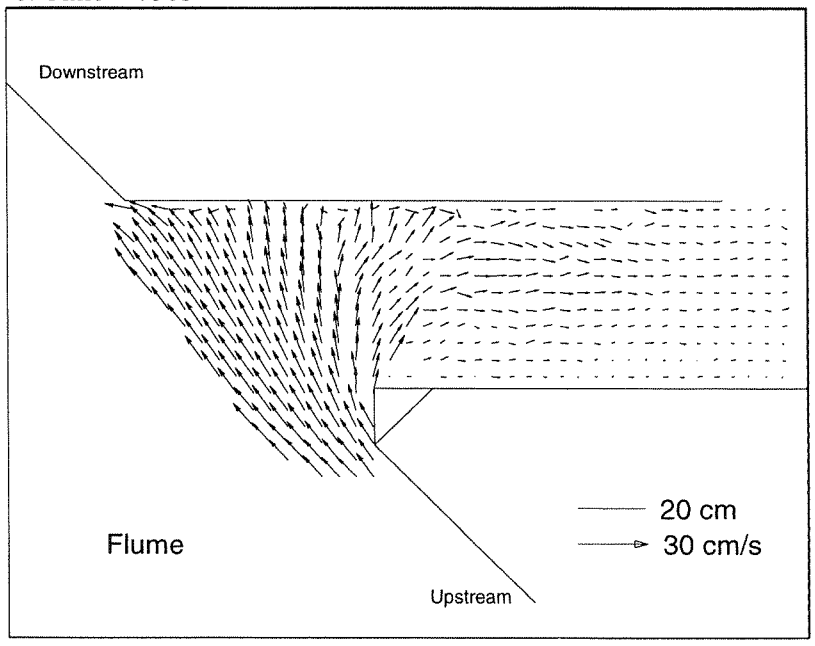

7. Time = 875s

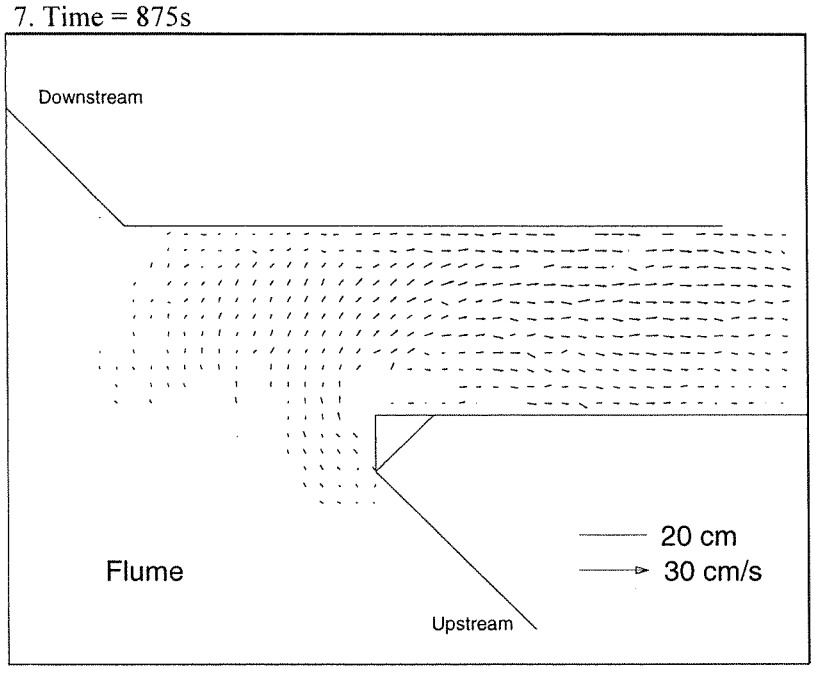

8. Time = 1000s

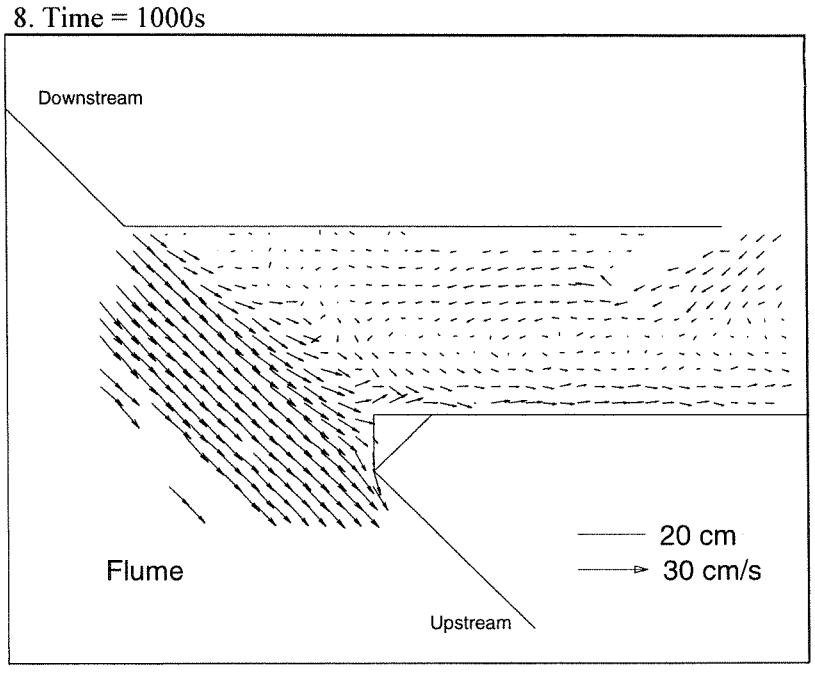

Appendix C.2. PTV Results phase 2

Configuration B – With CDW

1. Time = 125s

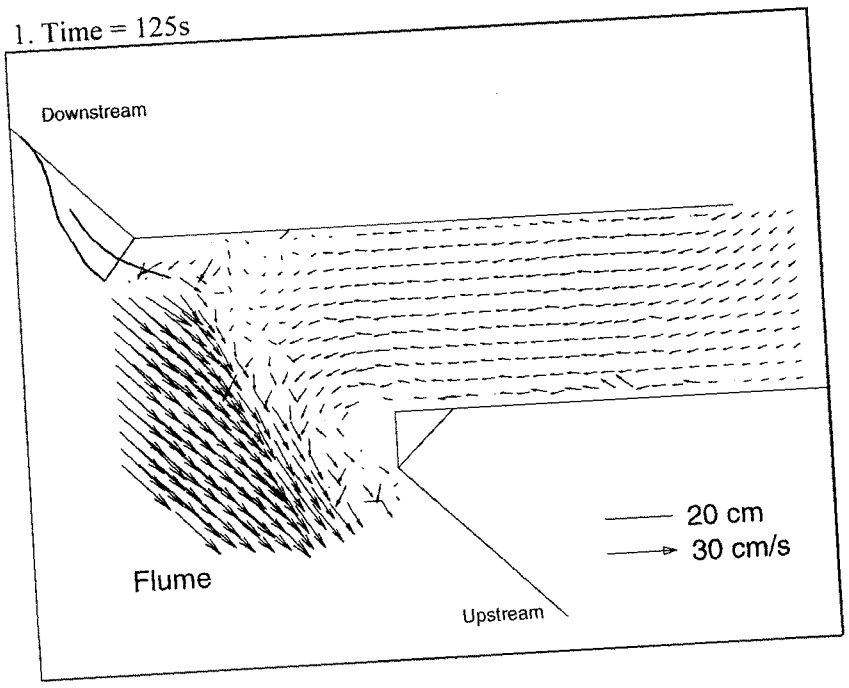

2. Time = 250s

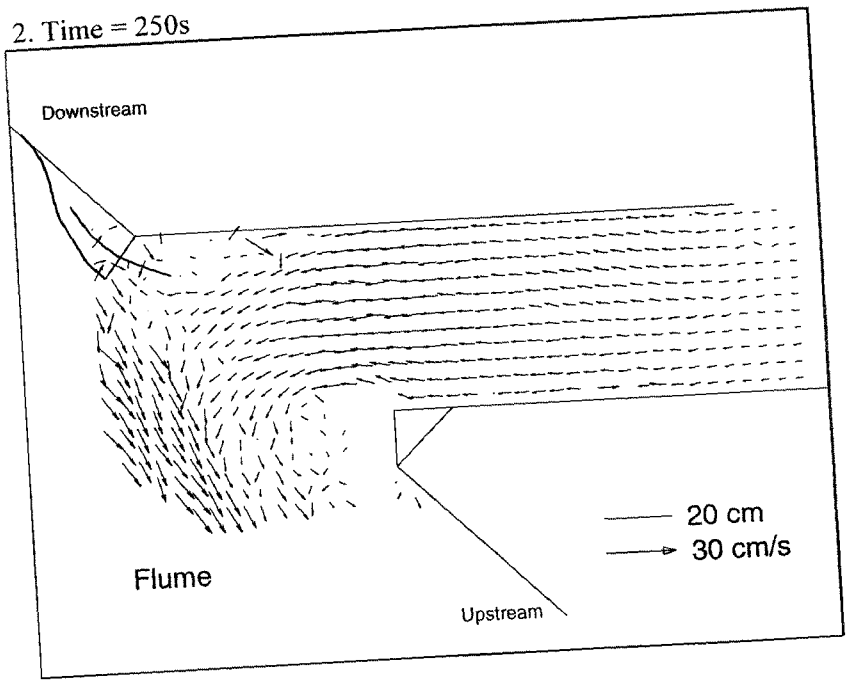

3. Time = 375s

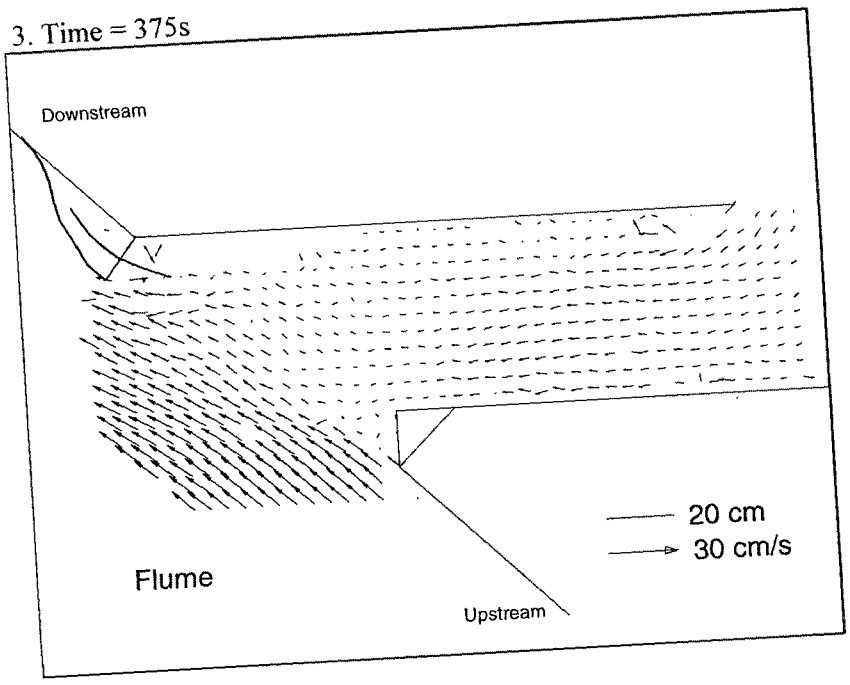

4. Time = 500s

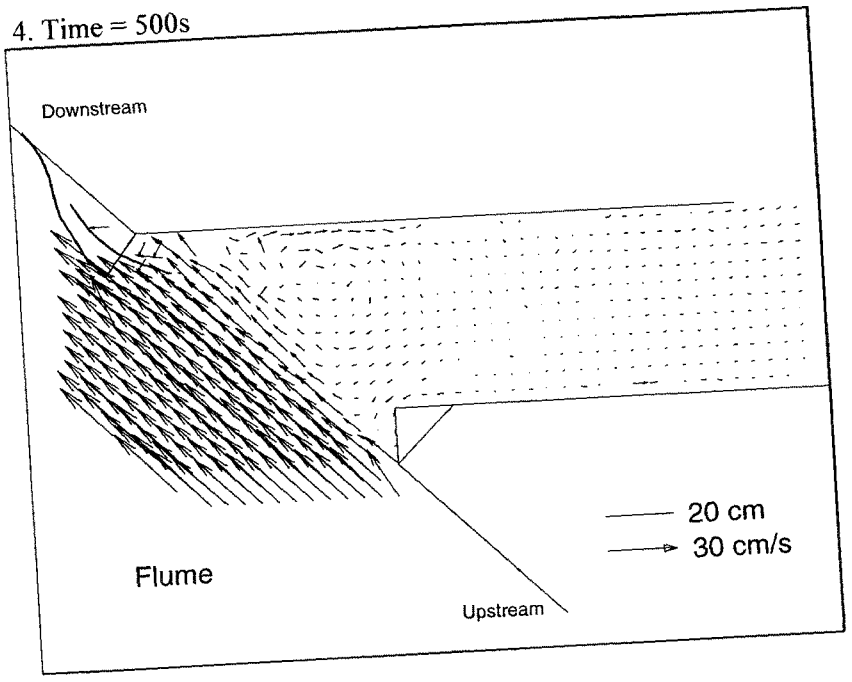

5. Time = 625s

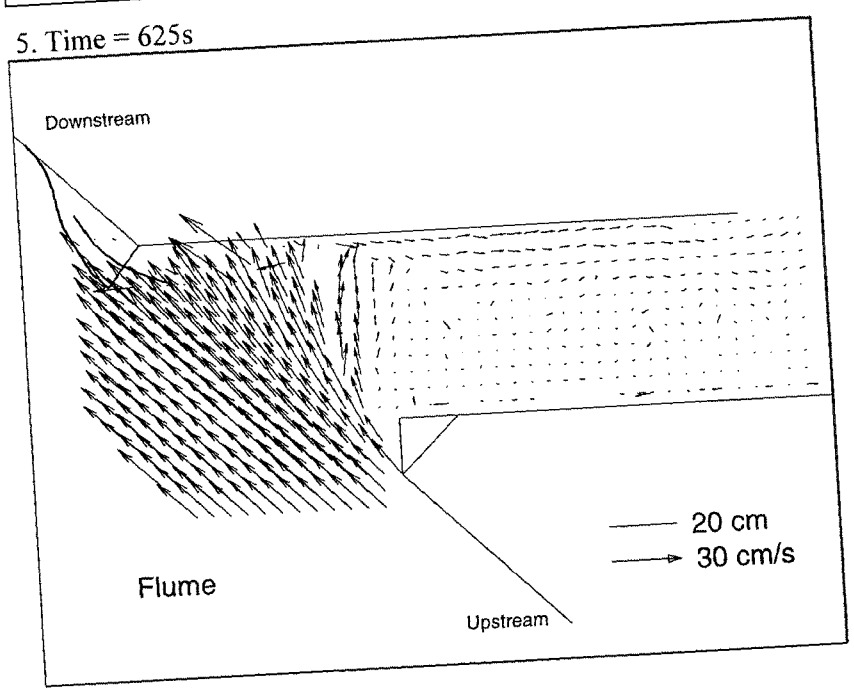

6. Time = 750s

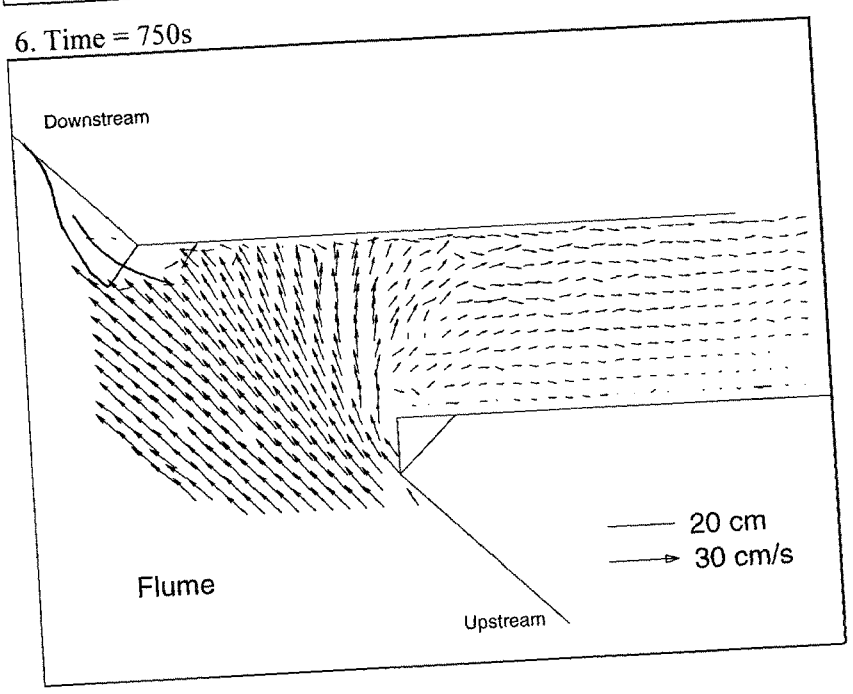

7. Time = 875s

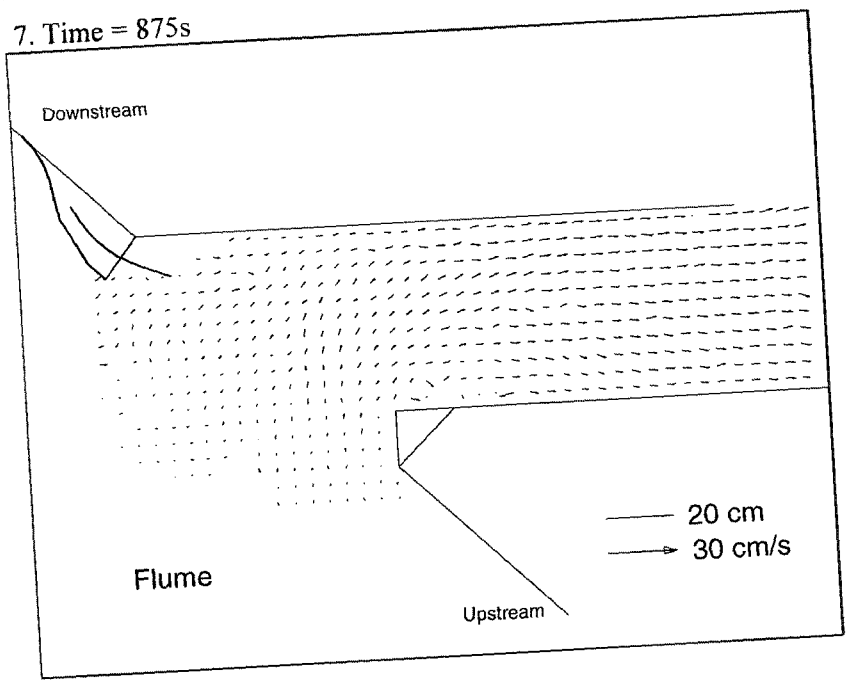

8. Time = 1000s

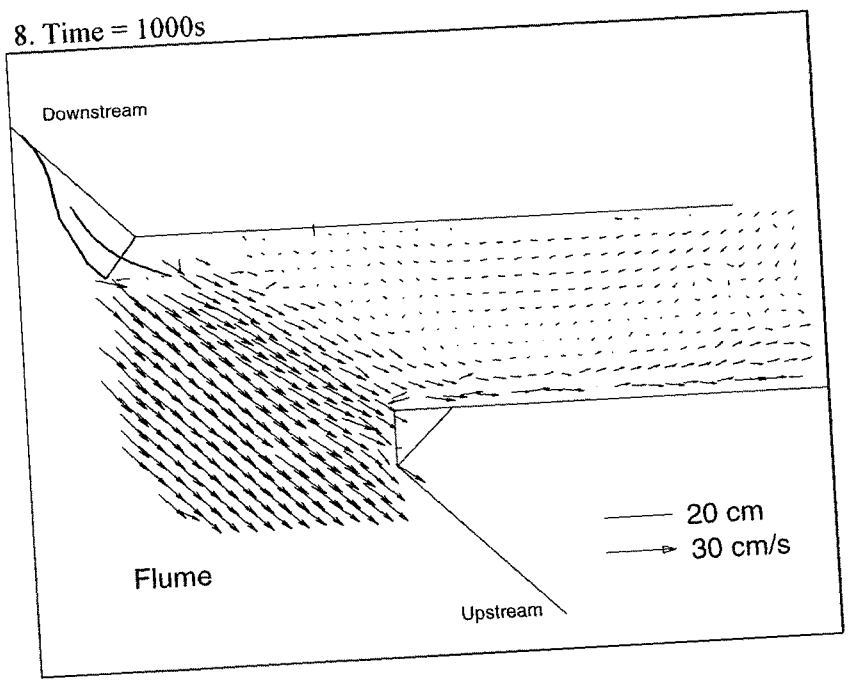

Appendix C.2. PTV Results phase 2

Configuration C – With CDW and sill

1. Time = 125s

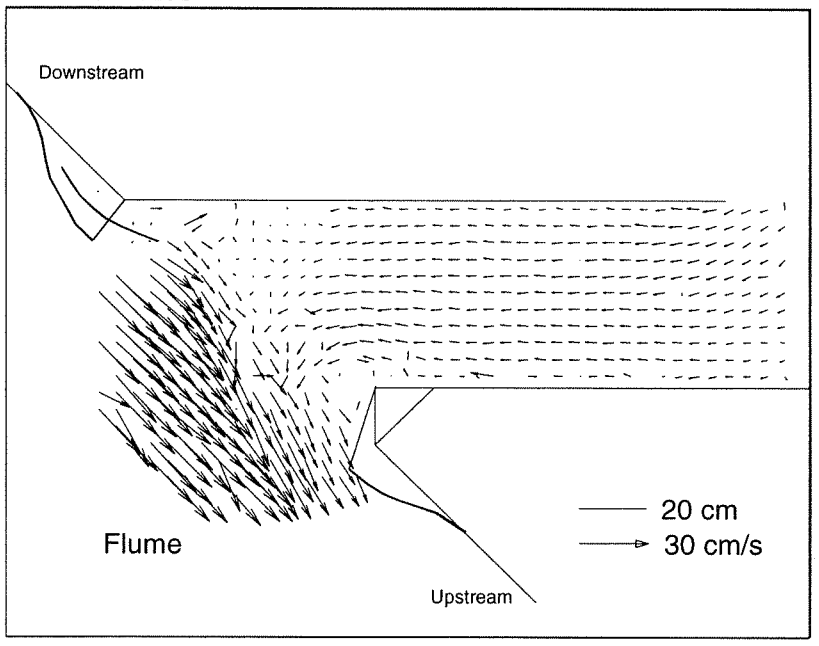

2. Time = 250s

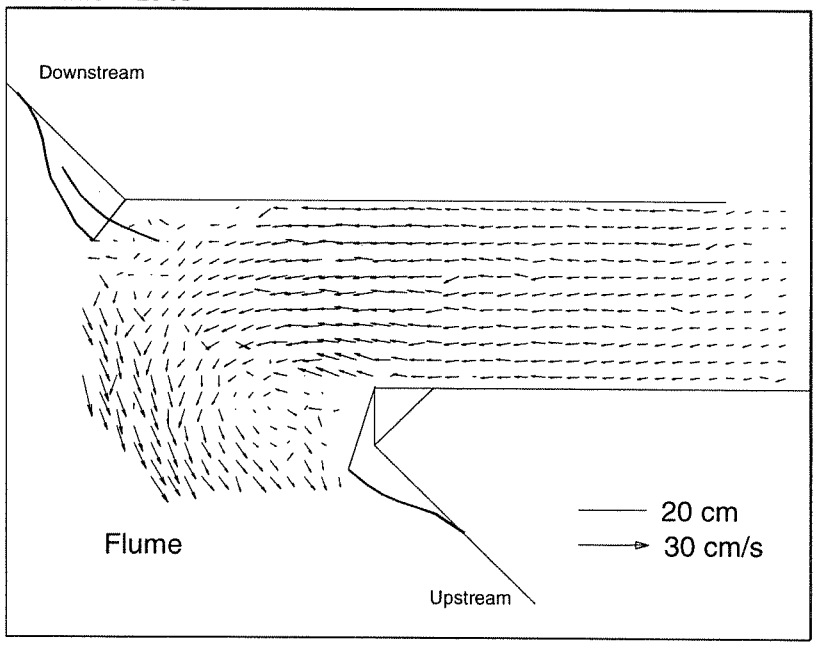

3. Time = 375s

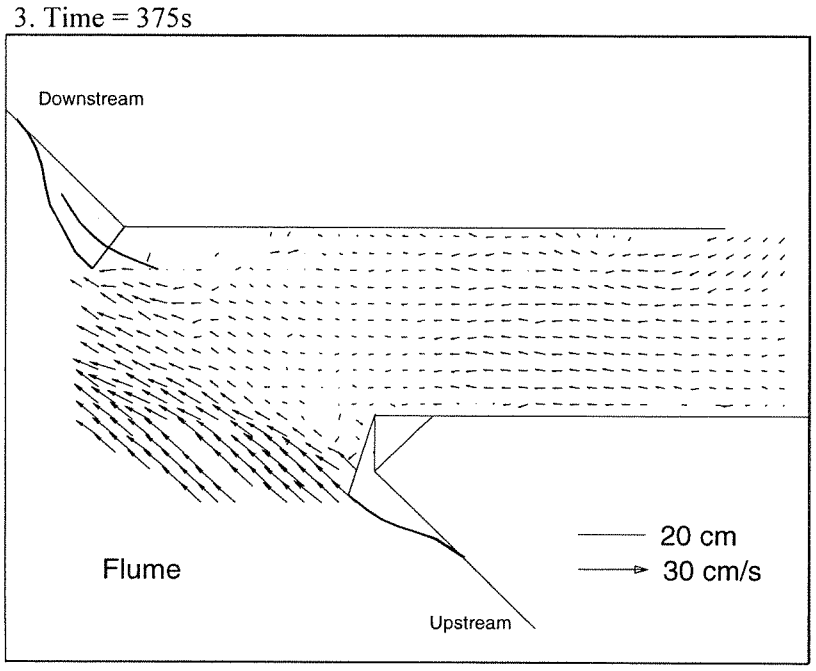

4. Time = 500s

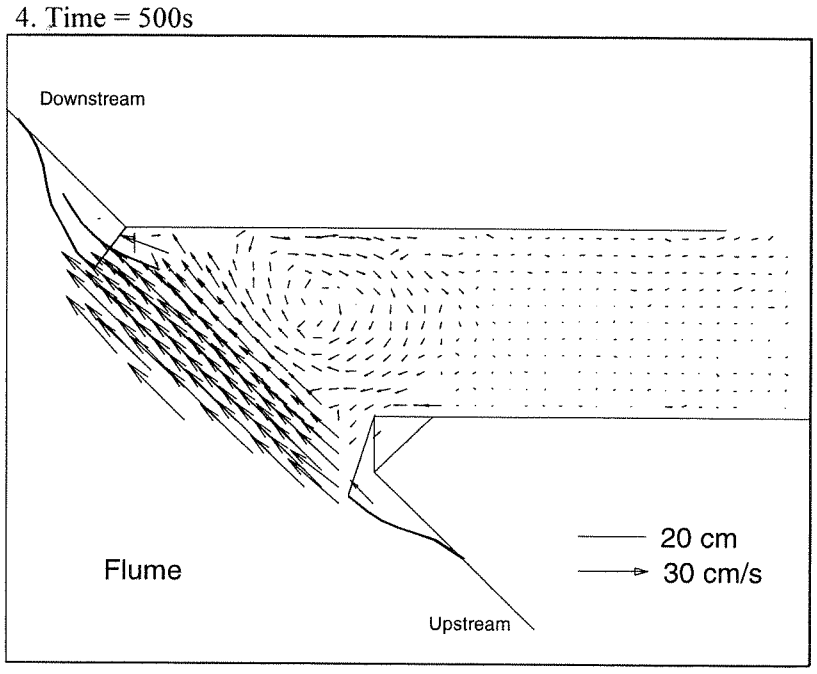

5. Time = 625s

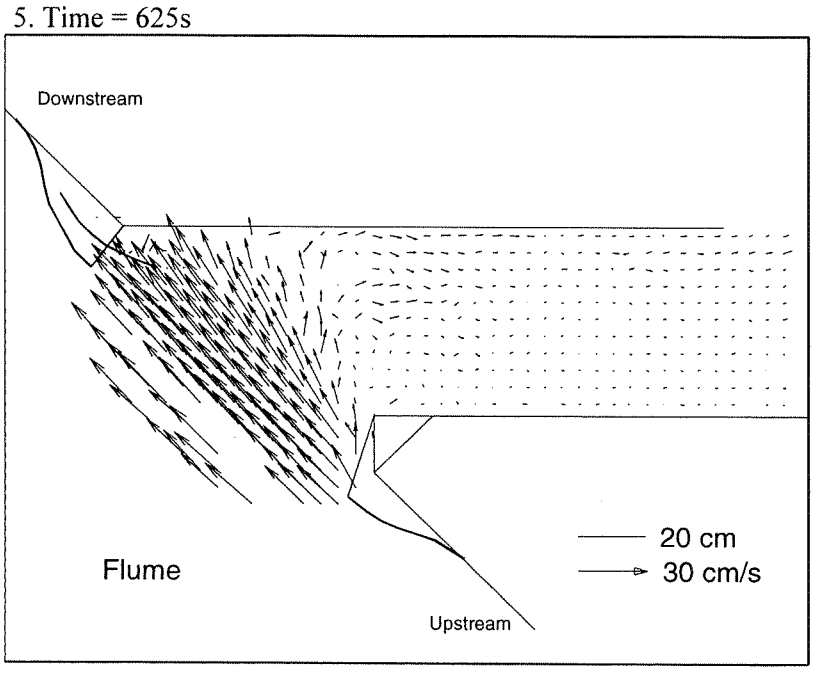

6. Time = 750s

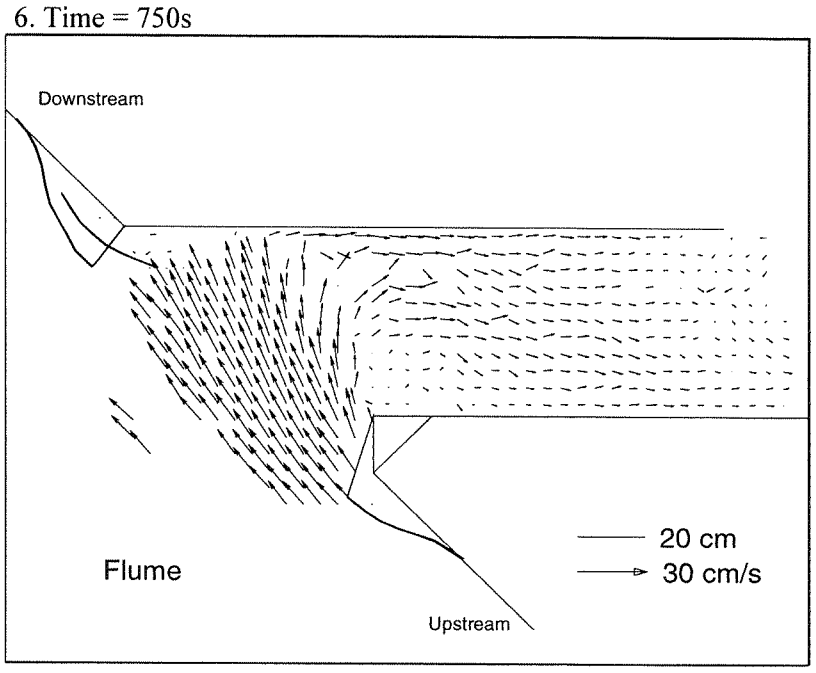

7. Time = 875s

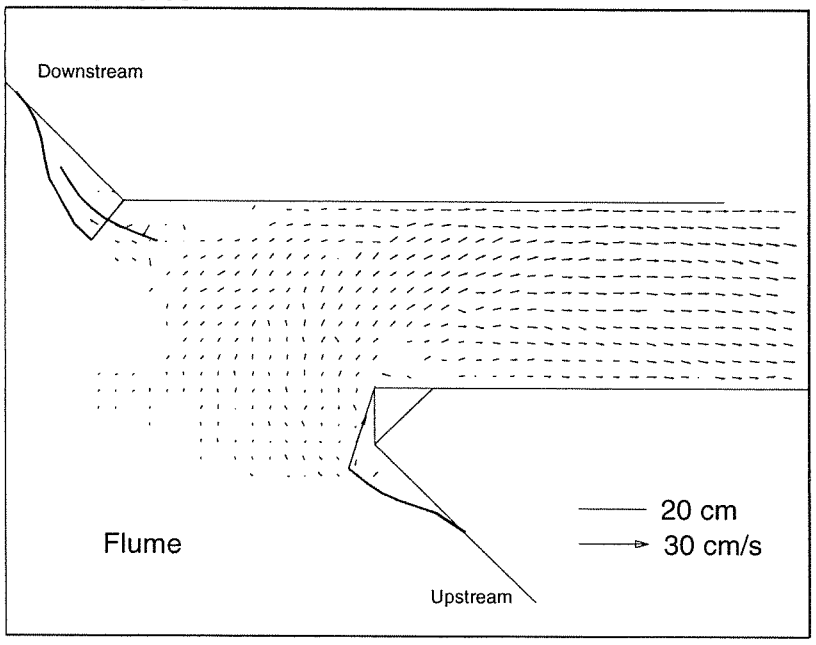

8. Time = 1000s

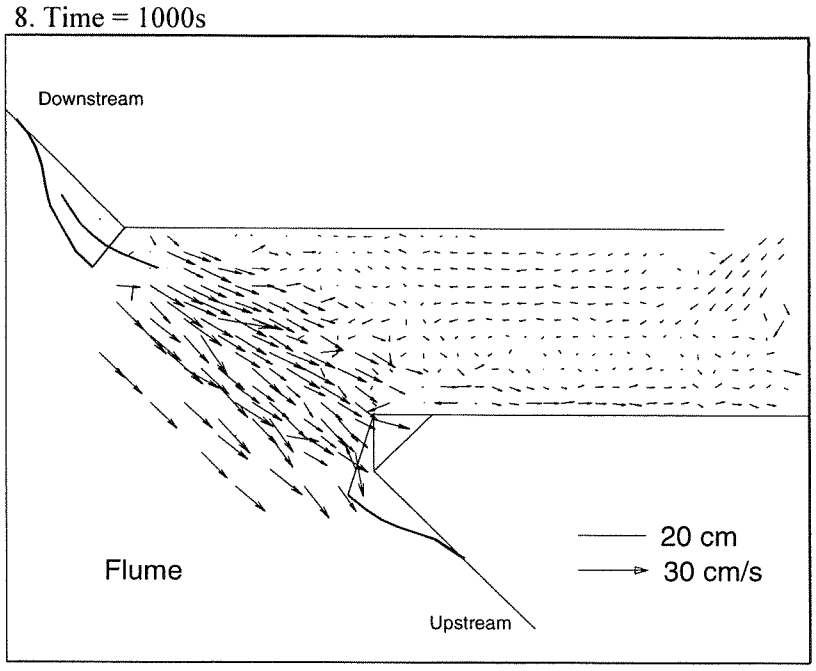

Flow velocities at cross section of harbour, only downstream CDW

125s left middle right

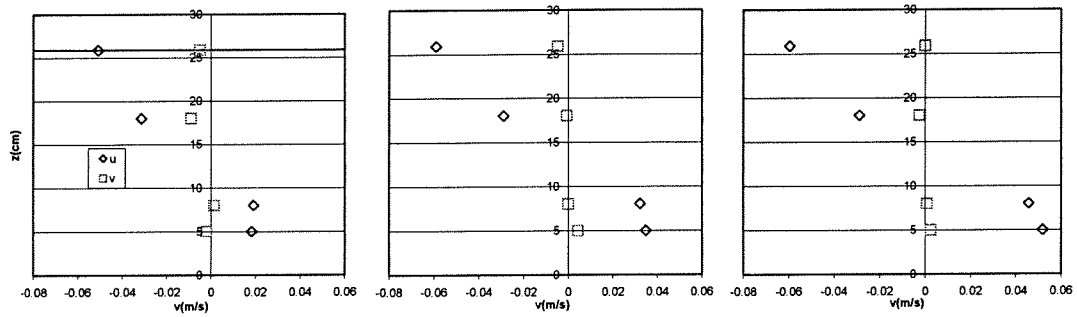

250s

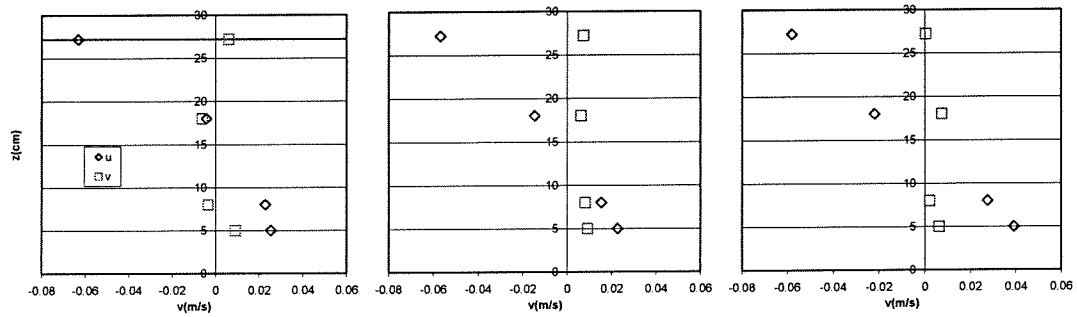

375s

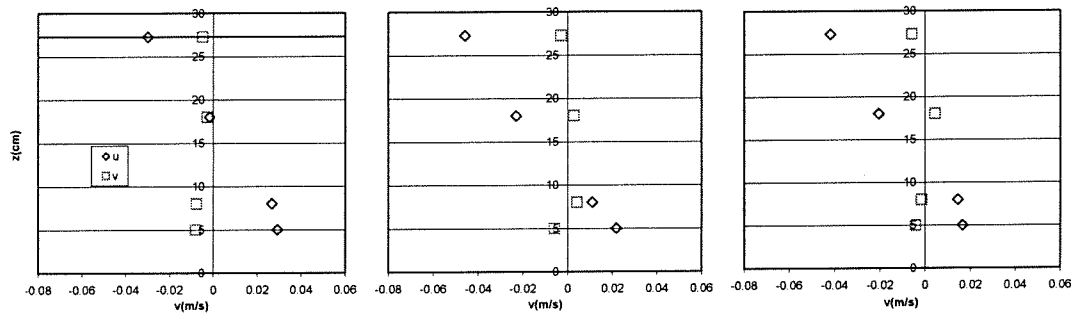

500s

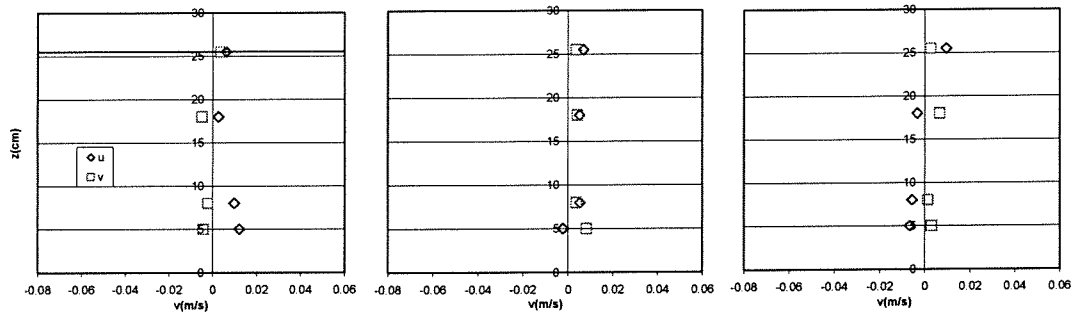

	125 s		250 s		375 s		500 s	
	u (m/s)	v (m/s)	u (m/s)	v (m/s)	u (m/s)	v (m/s)	u (m/s)	v (m/s)
left	-0.051	-0.005	-0.063	0.006	-0.030	-0.005	0.006	0.004
	-0.031	-0.009	-0.004	-0.006	-0.002	-0.003	0.003	-0.005
	0.019	0.001	0.023	-0.003	0.027	-0.008	0.010	-0.002
	0.018	-0.002	0.025	0.009	0.029	-0.008	0.012	-0.004
middle	-0.059	-0.005	-0.057	0.007	-0.046	-0.003	0.007	0.004
	-0.029	-0.001	-0.015	0.006	-0.023	0.003	0.005	0.004
	0.032	0.000	0.015	0.008	0.011	0.004	0.005	0.004
	0.035	0.004	0.023	0.009	0.022	-0.006	-0.002	0.008
right	-0.060	0.000	-0.058	0.001	-0.042	-0.006	0.010	0.003
	-0.029	-0.003	-0.022	0.008	-0.021	0.004	-0.003	0.007
	0.046	0.001	0.028	0.002	0.014	-0.002	-0.006	0.001
	0.052	0.002	0.039	0.006	0.017	-0.004	-0.007	0.003

Appendix C.3. EMS measurements phase 2

Flow velocities at cross section of harbour, no CDW

125s left middle right

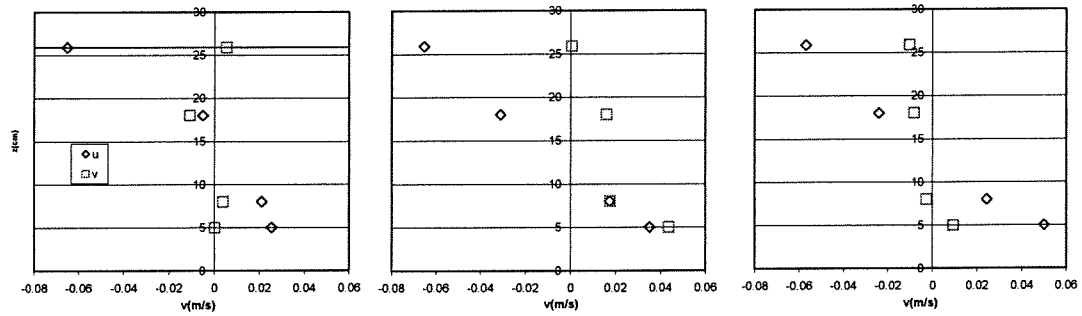

250s

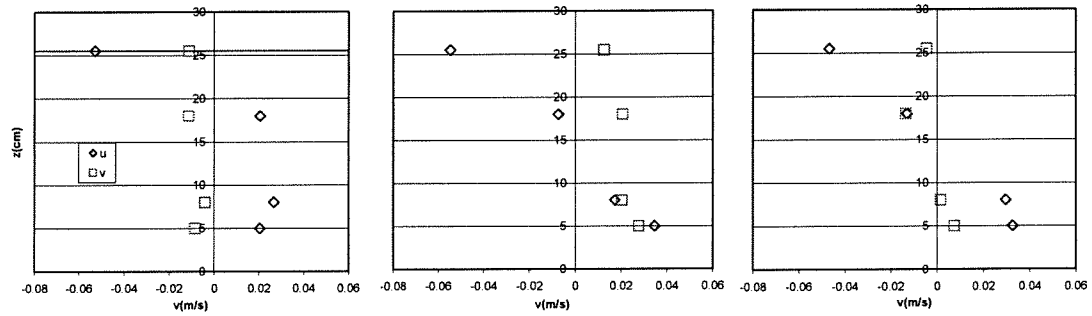

375s

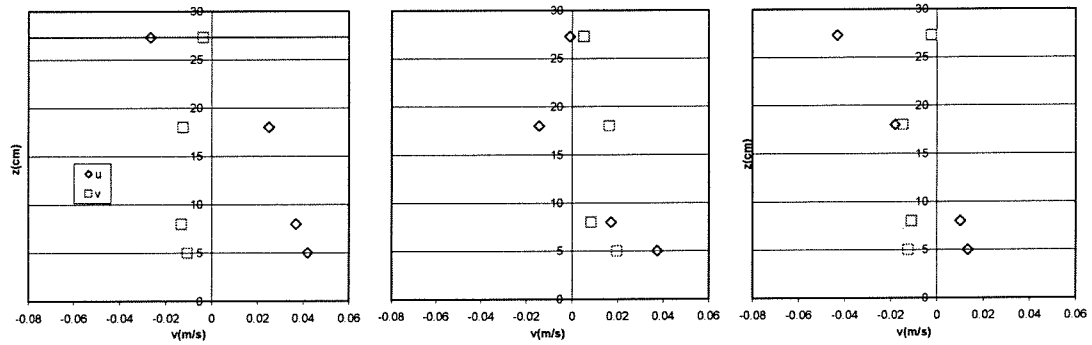

500s

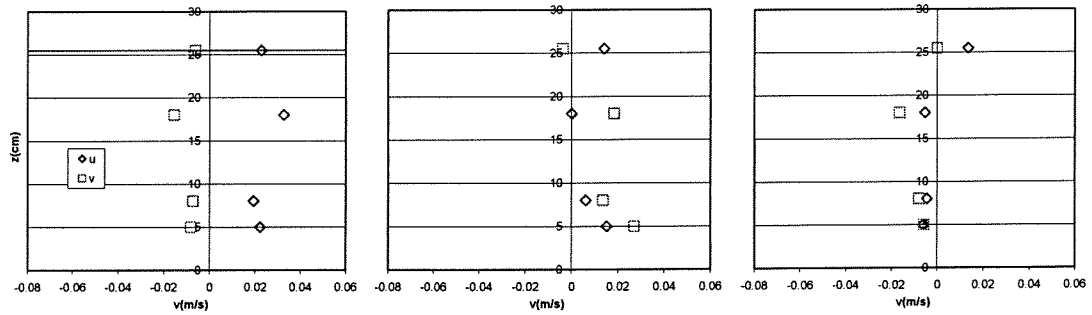

	125 s		250 s		375 s		500 s	
	u (m/s)	v (m/s)	u (m/s)	v (m/s)	u (m/s)	v (m/s)	u (m/s)	v (m/s)
left	-0.065	0.005	-0.053	-0.011	-0.027	-0.004	0.023	-0.006
	-0.005	-0.011	0.020	-0.011	0.025	-0.013	0.033	-0.016
	0.021	0.004	0.026	-0.004	0.037	-0.013	0.019	-0.007
	0.025	0.000	0.020	-0.009	0.042	-0.011	0.022	-0.008
middle	-0.065	0.001	-0.055	0.012	-0.001	0.005	0.014	-0.004
	-0.031	0.016	-0.007	0.021	-0.014	0.016	0.000	0.018
	0.017	0.018	0.017	0.020	0.017	0.008	0.006	0.013
	0.035	0.044	0.035	0.028	0.037	0.020	0.015	0.027
right	-0.057	-0.010	-0.047	-0.005	-0.043	-0.002	0.013	0.000
	-0.024	-0.008	-0.013	-0.014	-0.018	-0.015	-0.005	-0.016
	0.024	-0.003	0.030	0.001	0.010	-0.011	-0.004	-0.008
	0.050	0.009	0.033	0.007	0.013	-0.012	-0.006	-0.006

Flow velocities at cross section of harbour, CDW & upstream sill.

125s left middle right

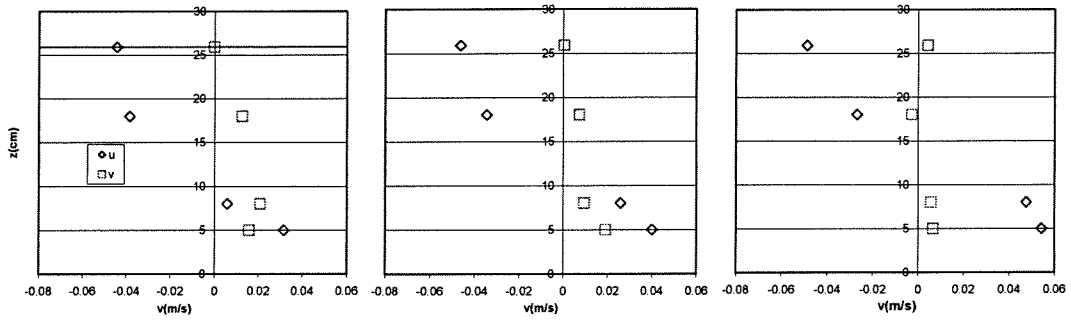

250s

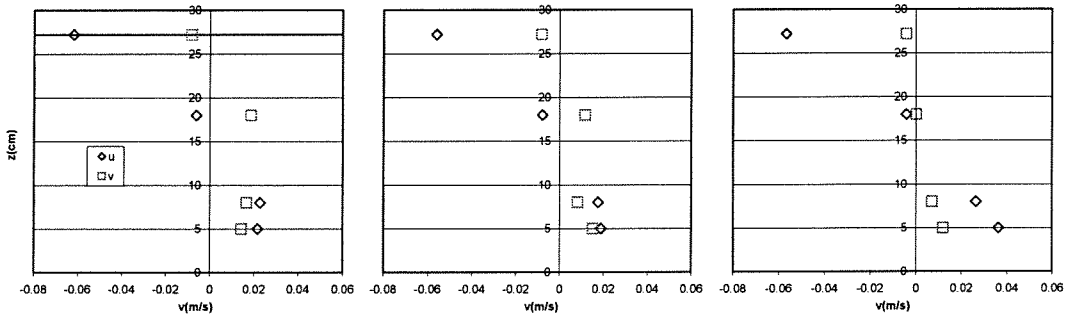

375s

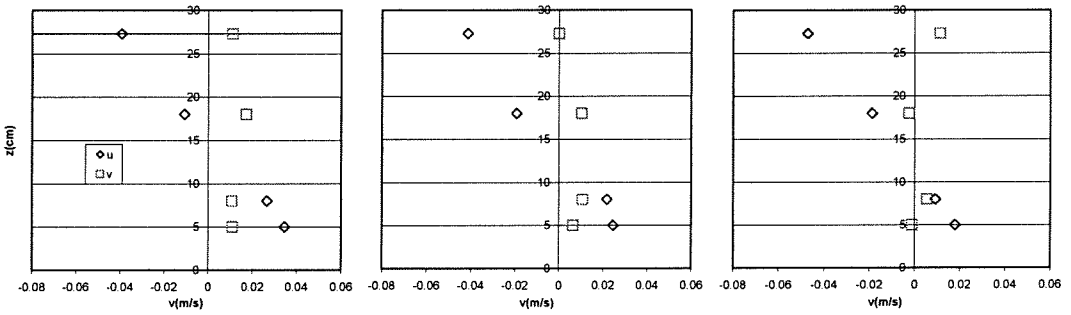

500s

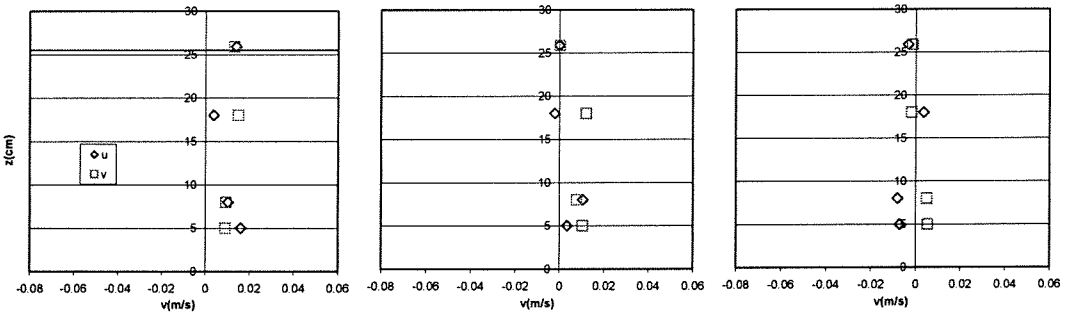

	125 s		250 s		375 s		500 s	
	u (m/s)	v (m/s)	u (m/s)	v (m/s)	u (m/s)	v (m/s)	u (m/s)	v (m/s)
left	-0.045	0.000	-0.062	-0.008	-0.039	0.011	0.014	0.013
	-0.039	0.013	-0.006	0.019	-0.011	0.017	0.004	0.015
	0.006	0.021	0.023	0.017	0.027	0.011	0.010	0.009
	0.032	0.016	0.022	0.014	0.035	0.011	0.016	0.009
middle	-0.046	0.000	-0.056	-0.008	-0.041	0.000	0.000	0.000
	-0.034	0.007	-0.008	0.012	-0.019	0.010	-0.002	0.012
	0.026	0.010	0.018	0.008	0.022	0.011	0.011	0.008
	0.040	0.019	0.019	0.015	0.025	0.006	0.003	0.010
right	-0.049	0.004	-0.057	-0.004	-0.047	0.011	-0.003	-0.001
	-0.027	-0.003	-0.004	0.000	-0.019	-0.002	0.004	-0.002
	0.048	0.006	0.026	0.007	0.009	0.006	-0.008	0.005
	0.054	0.007	0.036	0.012	0.018	-0.001	-0.007	0.005

Threads – Phase 2: Inhomogeneous conditions

Configuration A - Reference

Time=0s

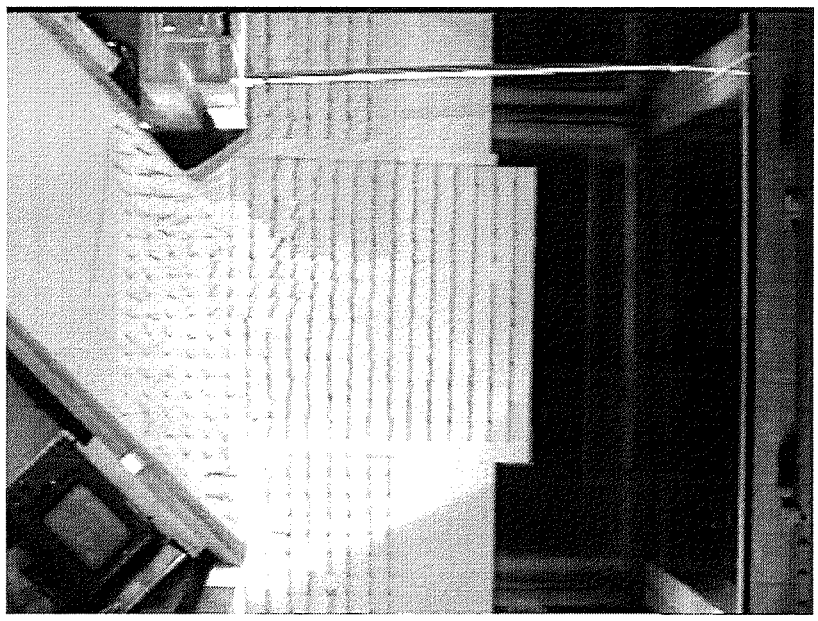

Time=120s

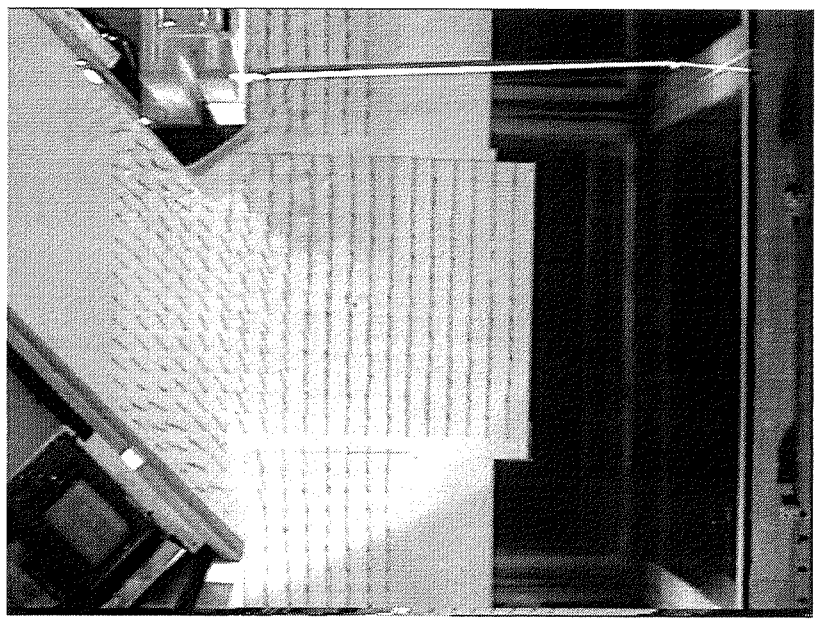

Time=260s

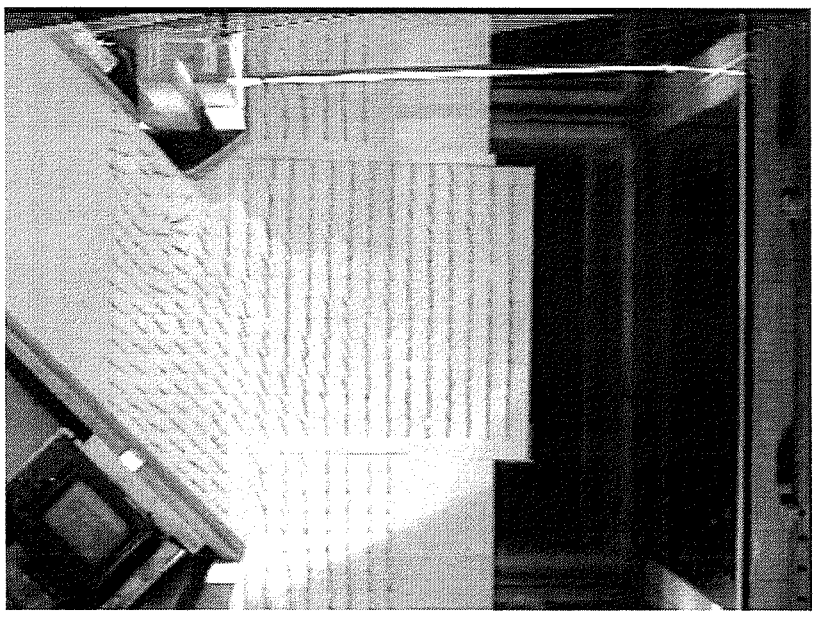

Missing picture

Time=500s

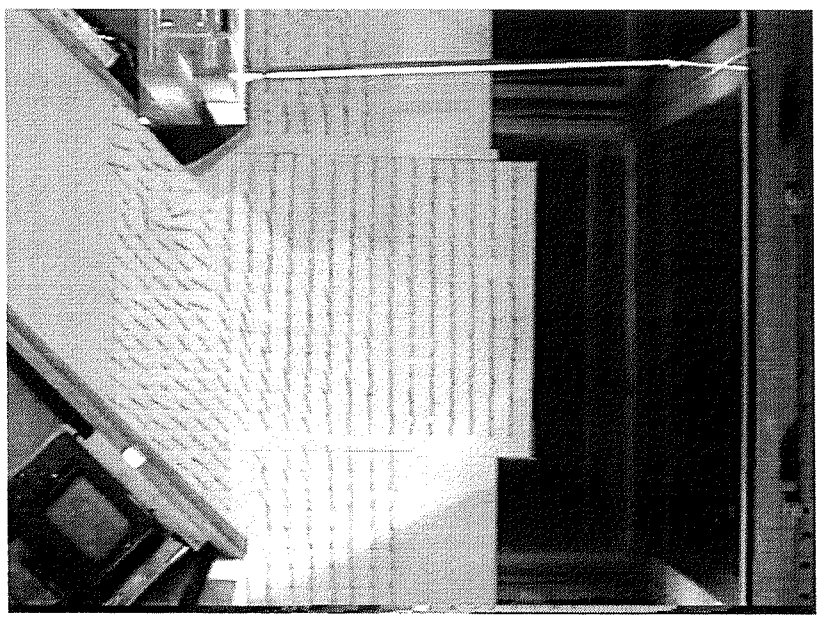

Time=620s

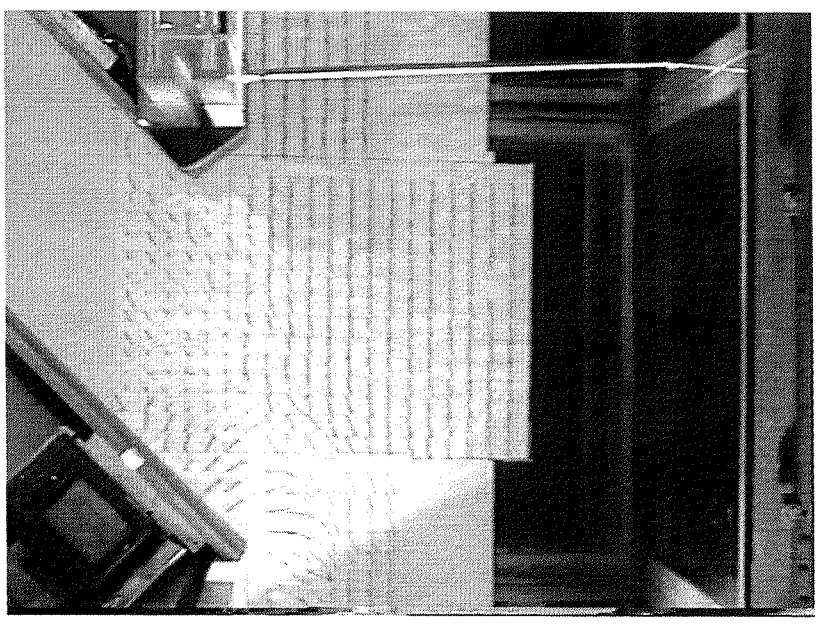

Time=740s

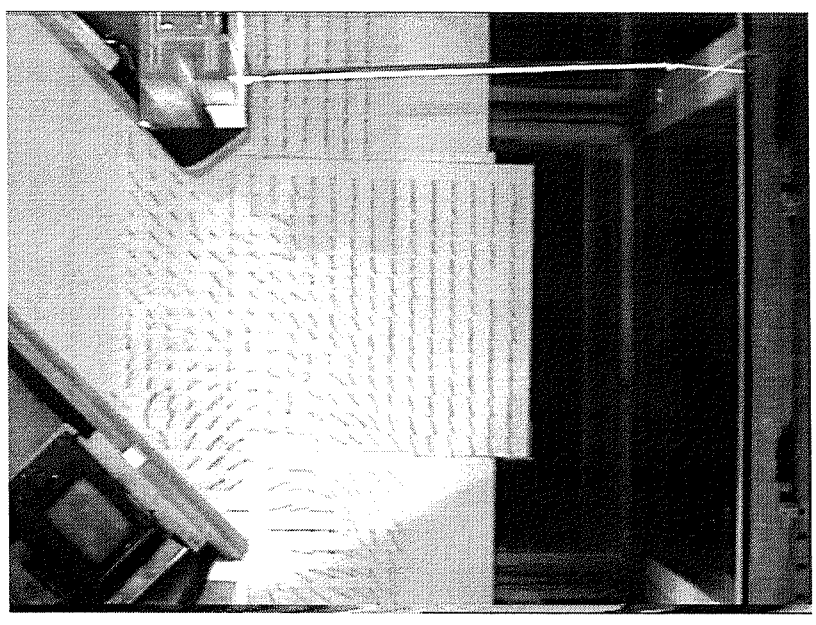

Time=865s

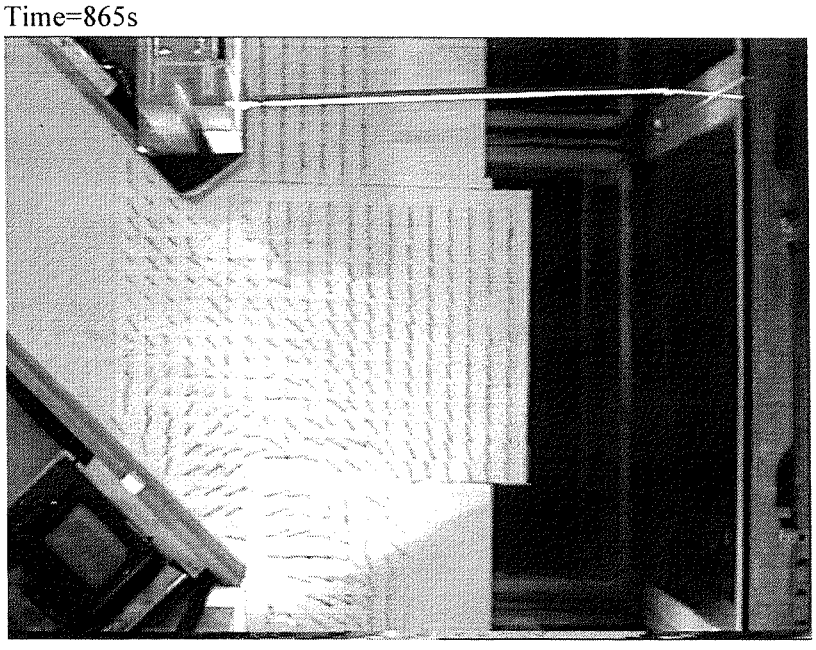

Threads – Phase 2: Inhomogeneous conditions

Configuration B

Time=0s

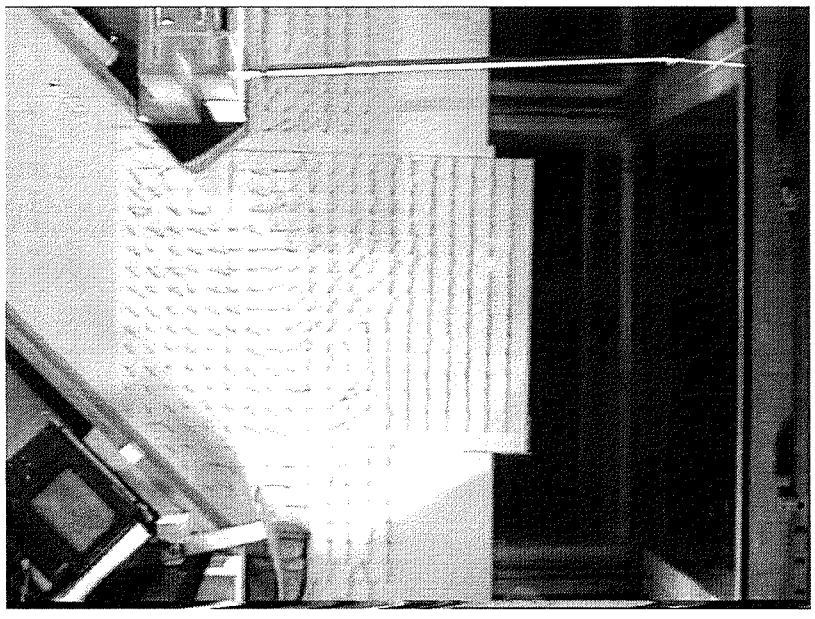

Time=120s

Time=260s

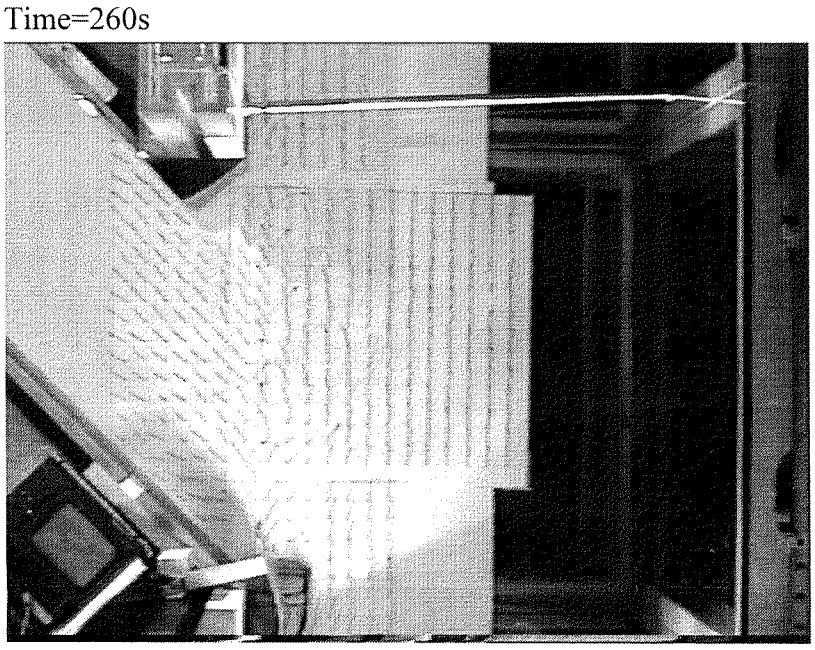

Time=380s

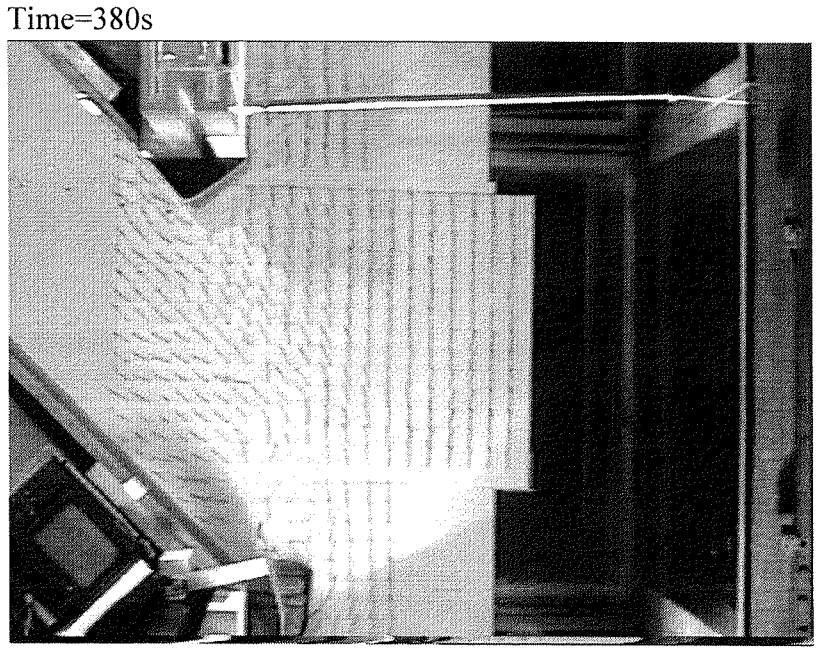

Time=500s

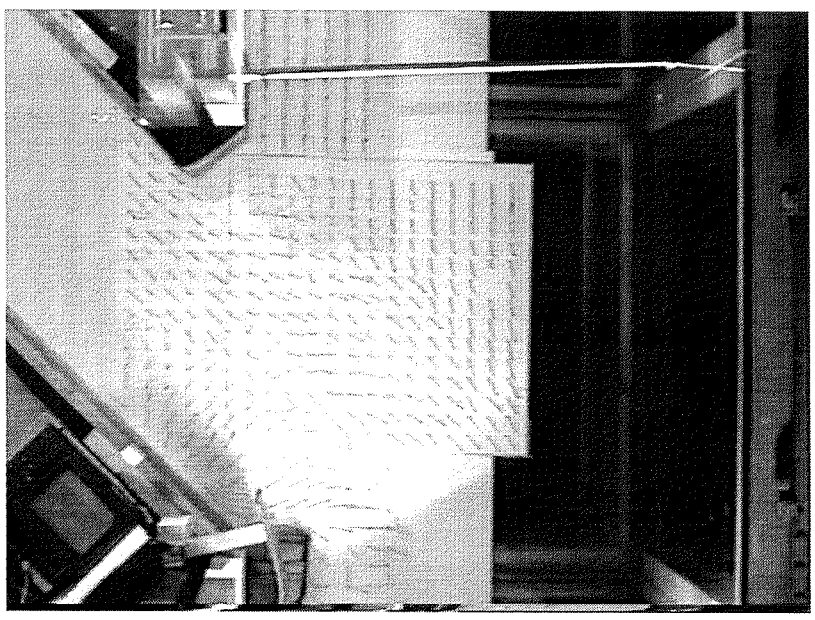

Time=620s

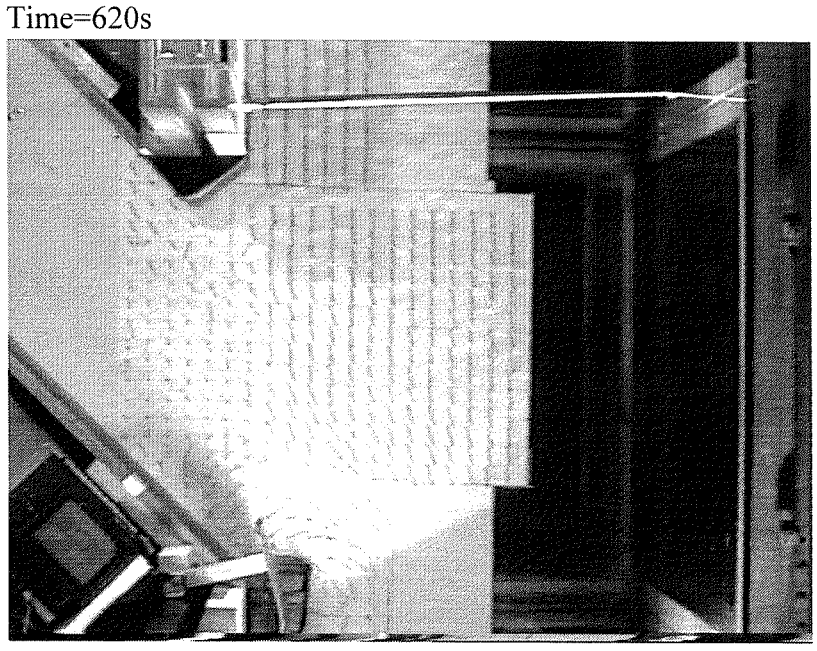

Time=740s

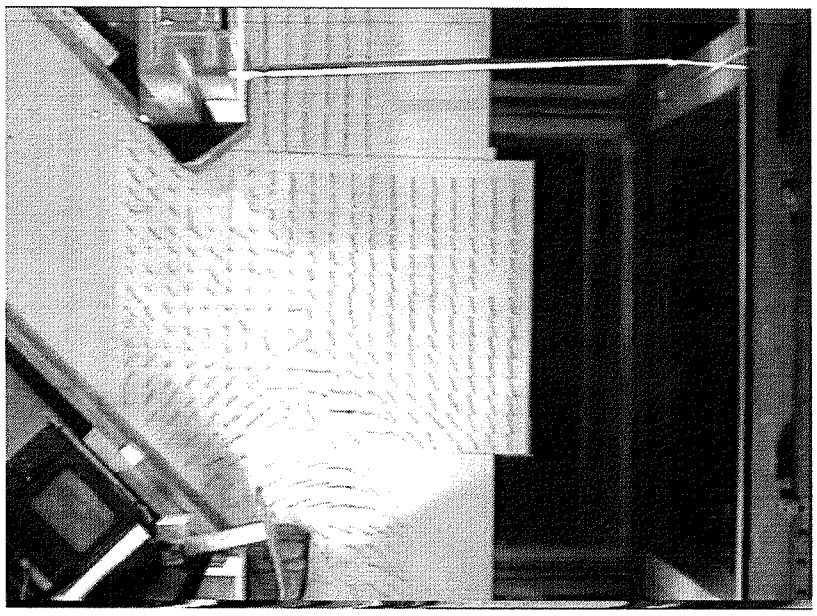

Time=865s

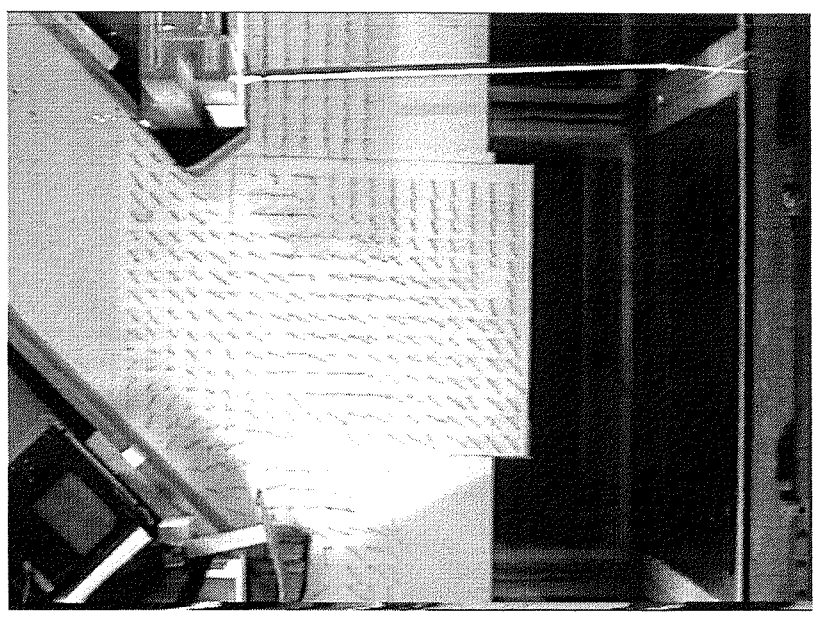

Threads – Phase 2: Inhomogeneous conditions

Configuration C

Time=0s

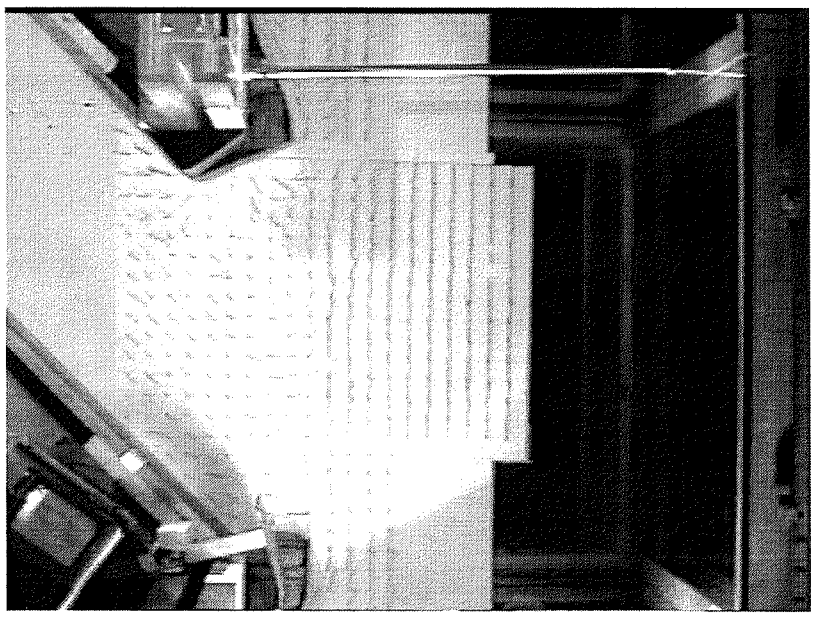

Time=120s

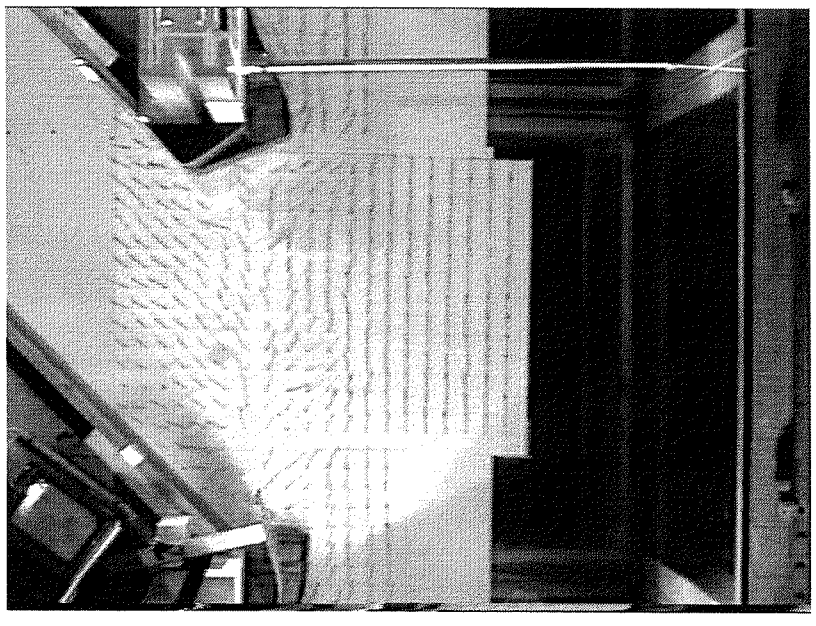

Time=260s

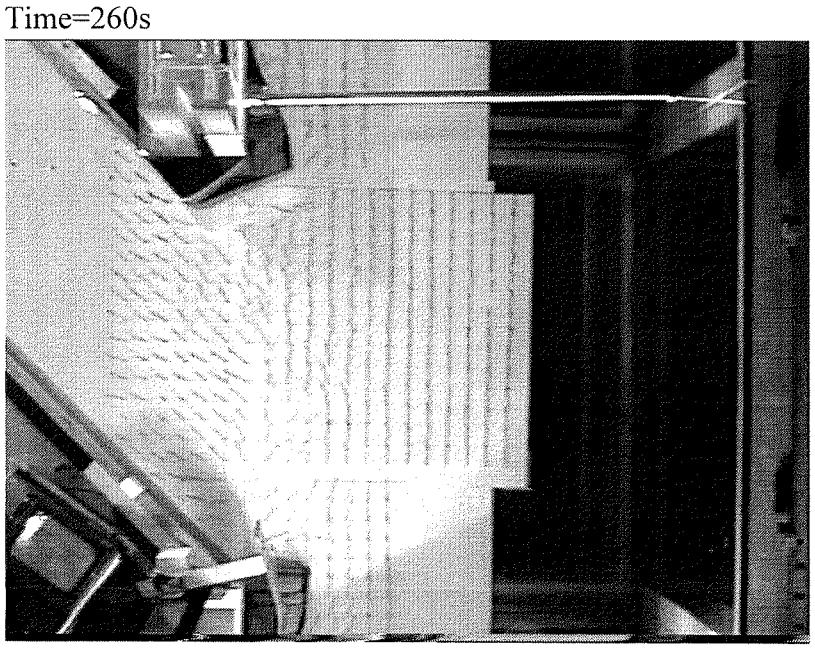

Time=380s

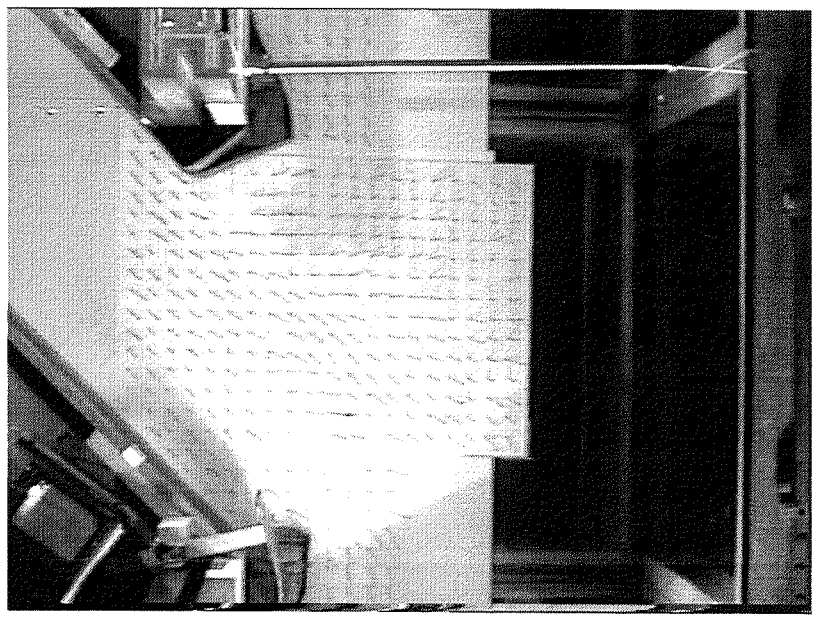

Time=500s

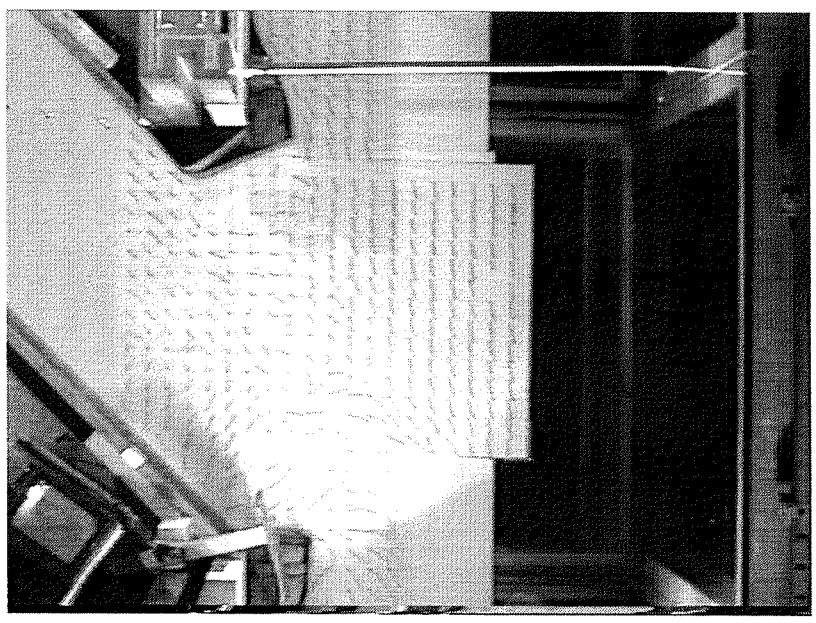

Time=620s

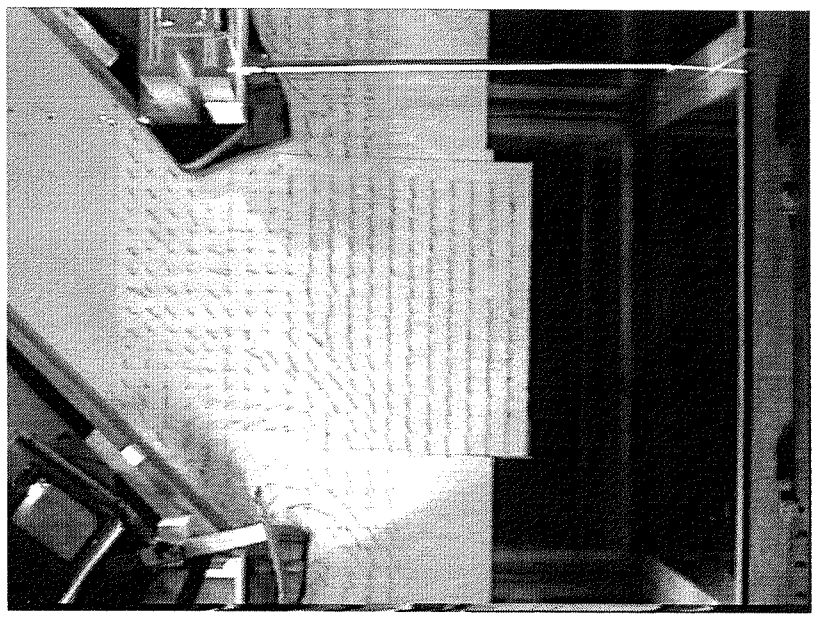

Time=740s

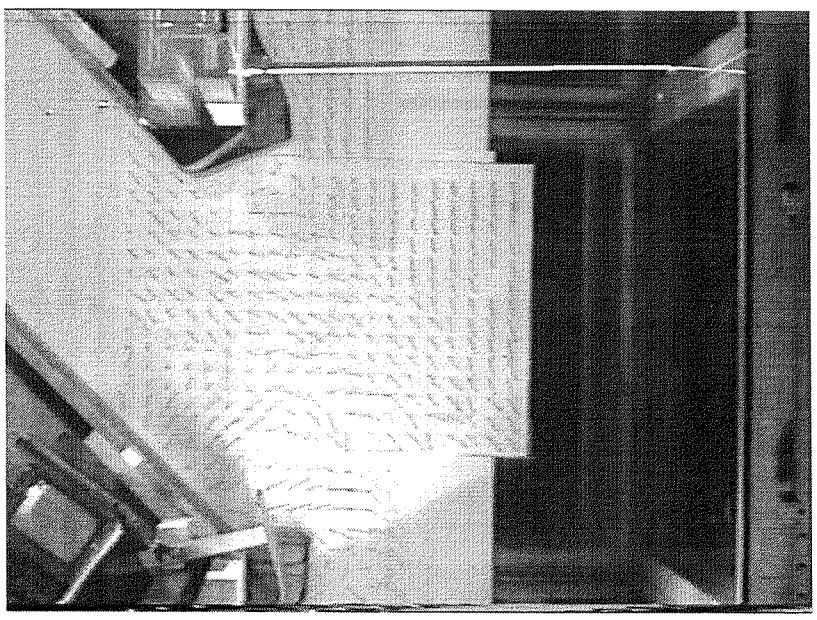

Time=865s

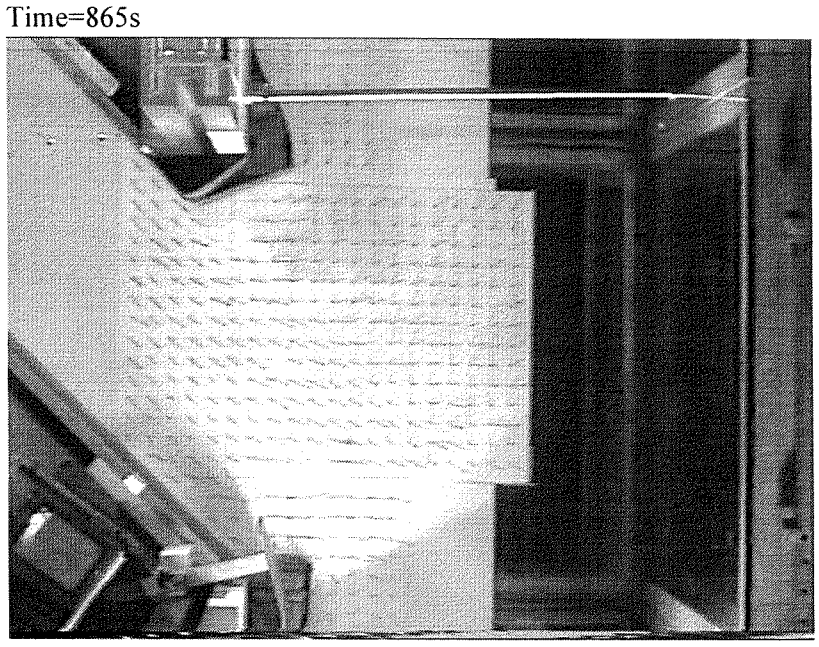

Appendix D. Listing *Borders*

```
Program Borders;
Type
Tarray = array [1..4] of real;

Var
Config, input, output: text;
namec, namein, nameout: string;
Hz    : real;
x_pix : real;
y_pix : real;
alfa  : real;
p1  : Tarray;
p2  : Tarray;
pw  : Tarray;
vectors, i, n : longint;
j : integer;
xtrans: real;
ytrans: real;
Vin, Vout: Tarray;
s: string;

xa,ya: array[1..10,1..4] of real;
numberareas, numberpoints, k: integer;
xvector, yvector, uvector, vvector: real;
OK : boolean;
help: string;
x: real;

Procedure configuration;
Var
l,m : integer;
Begin
  writeln('give name config file');
  readln(namec);
  assign(config, namec);
  reset(config);
  {part1 - filenames}
  readln(config);
  readln(config);
  readln(config, namein);
  readln(config, nameout);
  {part2 - rotate and scale}
  Readln(config);
  Readln(config, Hz);
  Readln(config, x_pix);
  Readln(config, y_pix);
  Readln(config, alfa);
  alfa := alfa/180*pi;
  readln(config);
  Readln(config, p1[1]);
  Readln(config, p1[2]);
  Readln(config, pw[1]);
```

```
 Readln(config, pw[2]);
 {part3 - area}
 readln(config);
 readln(config, numberareas);
 For l := 1 to numberareas do
  Begin;
  readln(config);
  For m := 1 to 4 do
    Begin
    read(config, xa[l,m]);
    readln(config, ya[l,m]);
    End;
  End;
 writeln('reading in configfile complete');
 close(config);
End;

{rotation, scaling, and shifting of coordinates}
Procedure Transform(Vi: Tarray;var Vo: Tarray; tx, ty: real);
Begin
 Vo[1] := cos(alfa)*Vi[1]*x_pix - sin(alfa)*Vi[2]*y_pix + tx;
 Vo[2] := sin(alfa)*Vi[1]*x_pix + cos(alfa)*Vi[2]*y_pix + ty;
 Vo[3] := cos(alfa)*Vi[3]*x_pix*Hz - sin(alfa)*Vi[4]*y_pix*Hz;
 Vo[4] := sin(alfa)*Vi[3]*x_pix*Hz + cos(alfa)*Vi[4]*y_pix*Hz;
End;


{check whether coordinates lie within boundaries}
Procedure Check;
Var
l,m: integer;
y: real;
Begin
 OK := true;
 For l := 1 to numberareas do
  Begin
   If (Vout[1]<xa[l,2]) and (Vout[1]>xa[l,1]) then
    Begin
    y := (ya[l,2]-ya[l,1])/(xa[l,2]-xa[l,1])*(Vout[1]-xa[l,1])+ya[l,1];
    If (y > Vout[2]) then
     Begin
     y := (ya[l,4]-ya[l,3])/(xa[l,4]-xa[l,3])*(Vout[1]-xa[l,3])+ya[l,3];
     If (y < Vout[2]) then
     OK := false;
     End;
    End;
  End;
End;
```

```
{determine shift of known points}
Procedure Rotscalepoint;
Begin
  Transform(p1, p2, 0, 0);
  xtrans := pw[1] - p2[1];
  ytrans := pw[2] - p2[2];
End;

Begin
configuration;
rotscalepoint;
assign(input, namein);
reset(input);
read(input,s);
read(input,vectors);
read(input,x);
assign(output, nameout);
rewrite(output);
n := 0;
writeln('beginning transformation');
For i := 1 to vectors do
  Begin
    read(input, Vin[1],Vin[2],Vin[3],Vin[4]);
    Transform(Vin, Vout, xtrans, ytrans);
    Check;
    If OK = true then
      Begin
      n := n+1;
      Writeln(output, Vout[1]:1:5, ' ', Vout[2]:1:5, ' ', Vout[3]:1:5, ' ', Vout[4]:1:5);
      Writeln(n, ' / ',i);
      End;
  End;
  writeln(100*(vectors-n)/vectors:3:1, ' percent of vectors outside borders');
  writeln('completed writing vectors to output file');
  close(input);
  close(output);
End.
```

Appendix E
Program Listing of *Medians*

```
Program medians; {This program is written in Turbo Pascal 7}

Type
Tarray = array[1..4,1..200] of real;
TGrid = record
      gu : real;
      gv : real;
      gn : integer;
      end;
Var
Select : Tarray;
Grid : array[0..50,0..50] of Tgrid;
i,j,nx,ny,q : integer;
number, n, vectors, totnumb: longint;
totcells: integer;
x,y,u,v,dx,dy: real;
x0,y0: real;
name, namein, nameout: string;
input, output, conf: text;
medianu, medianv: real;
s: string;
maxvec, prec: real;
nreliable: integer;

Procedure configuration; {this procedure imports the paramaters that are needed for the processing of the vector data}
Begin
  writeln('give name configfile ');
  readln(name);
  writeln('opening configfile');
  assign(conf, name);
  reset(conf);
  readln(conf);
  readln(conf);
  readln(conf, namein);
  readln(conf, nameout);
  readln(conf);
  readln(conf, x0);
  readln(conf, y0);
  readln(conf);
  readln(conf, nx);
  readln(conf, ny);
  readln(conf);
  readln(conf, dx);
  readln(conf, dy);
  readln(conf);
  readln(conf, maxvec);
  readln(conf);
  readln(conf, prec);
  readln(conf);
  readln(conf, nreliable);
  close(conf);
  writeln('read in configfile');
End;
```

```
Procedure determinemedian(A: Tarray; num: integer; var median:real; b:integer);
Begin
 if (num/2 - trunc(num/2)) > 0.25 then    {odd or even?}
  Begin
  median := A[b,trunc(num/2+0.5)];
  end
 else
  begin
  median := 0.5*A[b,trunc(num/2)] + 0.5*A[b,trunc(num/2+1)];
  end;
End;

Procedure shuffle(select: Tarray; numb:integer;var median:real; a:integer); {in this procudure all vectors that }
Var                                                                          {are found in a cell are ordered by the size}
max,k,l,m,o,p,q,r:integer;                                                   {of one of the vector components}
maxval,u:real;                                                               {(a=3:u, a=4:v)}
select2: Tarray;
x: real;
Begin
m := 1;
for r := numb downto 1 do
Begin
 maxval := -1000;
 for k:= 1 to r do
  Begin
  if select[a,k] > maxval then
   Begin
   max := k;
   maxval := x;
   end;
  end;
 for o := 1 to 4 do Select2[o,m] := Select[o,max];
 m := m + 1;
 for o := max to r do
  Begin
   for p := 1 to 4 do select[p,o] := select[p,o+1];
  end;
 end;
 determinemedian(Select2, numb, median, a);
end;

Procedure initialisation;
Begin
totnumb := 0; totcells := 0;
for i := 1 to 50 do
 begin
 for j := 1 to 50 do
  begin
  grid[i,j].gn := 0;
  end;
 end;
end;
```

```
Procedure set_to_grid; {per grid cell, all vectors from the .all file that lie in that cell are gathered}
Begin
assign(input, Namein);
for j := 1 to ny do
 Begin
 for i := 1 to nx do
  Begin
  number := 0;
  reset(input);
  read(input,s);
  read(input,vectors);
  read(input,x);
  For n := 1 to vectors do
   Begin
   read(input, x, y, u, v);
   if (x < x0+i*dx) and (x >= x0+(i-1)*dx) then
    Begin
    if (y < y0+j*dy) and (y >= y0+(j-1)*dy) then
     Begin
     if sqrt(u*u+v*v) < maxvec then
      Begin
      number := number+1;
      if number = 201 then number := 200;
      select[1,number] := x; select[2,number] := y;
      select[3,number] := u; select[4,number] := v;
      End;
     End;
    End;
   End;
   If number >= 1 then
    Begin
    Totcells := totcells + 1;
    Totnumb := totnumb + number;
    Shuffle(Select, number, medianu, 3);
    Shuffle(Select, number, medianv, 4);
    Grid[i,j].gu := medianu;
    Grid[i,j].gv := medianv;
    Grid[i,j].gn := number;
    End;
  writeln(100*((j-1)*nx+i)/(ny*nx):5:1, ' %');
  End;
 End;
 close(input);
 writeln('median collection complete');
 writeln(totnumb, ' of ', vectors, ' vectors from ', namein, ' used');
end;
```

```
Procedure check_vectors; {all median vectors that have been based on less vectors than given by the variable}
Var                      {nreliable are compared to the value of the reliable neighbouring vectors}
neighbours: integer;
averageu, averagev: real;
Begin
writeln('starting check of uncertain vectors with ',totcells,' cells filled');
for j := 1 to ny do
 Begin
 for i := 1 to nx do
  Begin
  neighbours:=0; averageu:= 0; averagev:=0;
  If (Grid[i,j].gn<nreliable) and (Grid[i,j].gn>0) then
   Begin
   If Grid[i-1,j].gn>=nreliable then
    Begin
    neighbours := neighbours + 1;
    averageu := averageu + Grid[i-1,j].gu;
    averagev := averagev + Grid[i-1,j].gv;
    End;
   If Grid[i+1,j].gn>=nreliable then
    Begin
    neighbours := neighbours + 1;
    averageu := averageu + Grid[i+1,j].gu;
    averagev := averagev + Grid[i+1,j].gv;
    End;
   If Grid[i,j-1].gn>=nreliable then
    Begin
    neighbours := neighbours + 1;
    averageu := averageu + Grid[i,j-1].gu;
    averagev := averagev + Grid[i,j-1].gv;
    End;
   If Grid[i,j+1].gn>=nreliable then
    Begin
    neighbours := neighbours + 1;
    averageu := averageu + Grid[i,j+1].gu;
    averagev := averagev + Grid[i,j+1].gv;
    End;
    If (neighbours=0) or
      (abs(averageu/neighbours-grid[i,j].gu)>prec) or
      (abs(averagev/neighbours-grid[i,j].gv)>prec) then
     Begin
     totcells:=totcells-1;
     totnumb:=totnumb-grid[i,j].gn;
     grid[i,j].gn:=0;
     grid[i,j].gu:=0;
     grid[i,j].gv:=0;
     End;
   End;
  End;
 End;
End;
```

```
Procedure output_to_file;
Begin
assign(output, Nameout);
rewrite(output);
writeln(output,'AA');
writeln(output, totcells,' 4');
for i := 1 to nx do
 Begin
 for j := 1 to ny do
  Begin
   If Grid[i,j].gn>0 then
   Writeln(output, (x0+i*dx-0.5*dx):9:4,' ',(y0+j*dy-0.5*dy):9:4,
        ' ', grid[i,j].gu:9:4,' ', grid[i,j].gv:9:4,' ', grid[i,j].gn);
  End;
 End;
 Close(output);
 writeln;
 writeln(totcells, ' of ', i*j,' (',100*totcells/(nx*ny):3:0,'%) cells filled');
 writeln('average number of vectors per cell:', totnumb/(totcells):5:1);
End;

Begin; {main program}
configuration;
initialisation;
set_to_grid;
check_vectors;
output_to_file;
End.
```

Appendix F
Program Listing of *Average*

This program was used for determining the ensemble average of a short timespan of data from a series of tides. These files contained all the signals that were measured. The columns 21 to 26 (EMS x and y velocities) are read for 7 tiomes 10 seconds, and the average and the standard deviation are determined and written to a file.

```
c1000*
      program average
c-------------------------------------------------------------
c     average
c     Bas Hofland 11/6/99
c-------------------------------------------------------------
c declaraties
      integer nr,n,i,j,nt
            real totave(6), std(6), ave(6,50)
            character*12 naamin(50), naamuit(3)
            real ems(50,39)
c lees configfile
            open(99,file='files.inv')
      read(99,*) (naamuit(i), i=1,3,1)
      read(99,*) n
            do 10 nt=1, n
      read(99,*) naamin(nt)
 10   continue
            close(99)
            write(*,*) 'invoerfile gelezen'
            write(*,*) 'aantal invoerfiles:'
            write(*,*) n
            write(*,*) 'namen uitvoer bestanden'
            write(*,*) naamuit(1)
            write(*,*) naamuit(2)
            write(*,*) naamuit(3)
            pause
c open resultatenfile
      open(96,file=naamuit(1))
      open(97,file=naamuit(2))
      open(98,file=naamuit(3))
c open datafiles
            do 20 nt=1, n
      open(nt,file=naamin(nt))
 20   continue
c naar eerste punt in file
            do 22 is=1,2400
              do 21 nt=1,n
                read(nt,*) (ems(nt, i), i=1,39,1)
 21     continue
 22   continue
```

```
c begin bewerking
================================================================================
          write(96,*) 'ave(1x)  ','std(1x)  ','ave(1y)  ','std(1y)  '
          write(97,*) 'ave(2x)  ','std(2x)  ','ave(2y)  ','std(2y)  '
          write(98,*) 'ave(3x)  ','std(3x)  ','ave(3y)  ','std(3y)  '
         do 100 nr=1, 7
c initialiseren
           do 30 i=1, 6
             std(i)= 0
       totave(i)= 0
       do 23 j=1,n
        ave(i,j)=0
 23          continue
 30    continue
c inlezen en gemiddelde (over 10 seconden) bepalen
      do 40 nt=1, n
            do 37 is=1,200
                  read(nt,*) (ems(nt, i), i=1,39,1)
              do 35 i=1, 6
                    totave(i)=totave(i) + ems(nt,20+i)/(n*200)
          ave(i,nt)=ave(i,nt) + ems(nt,20+i)/(200)
 35                 continue
 37               continue
 40    continue
c standaarddeviatie bepalen
           do 50 nt=1, n
             do 45 i=1, 6
                  std(i)=std(i)+(ave(i,nt)-totave(i))*(ave(i,nt)-totave(i))
 45               continue
 50    continue
           do 60 i=1, 6
                 std(i) = sqrt(std(i)/(n-1))
 60        continue
c naar volgende punt in file
         do 80 is=1, (115*20)
           do 70 nt=1,n
             read(nt,*) (ems(nt, i), i=1,39,1)
 70    continue
 80  continue
c wegschrijven
         write(96,'(1x,4f10.5)') totave(1),std(1),totave(2),std(2)
         write(97,'(1x,4f10.5)') totave(3),std(3),totave(4),std(4)
         write(98,'(1x,4f10.5)') totave(5),std(5),totave(6),std(6)
100    continue
c
================================================================================
=====
c files sluiten
         do 110 i=1, n
           close(i)
110      continue
         close(96)
         close(97)
         close(98)
c einde
    end
```

Appendix G
Additional User Manual DCM

This appendix is an addition to the user manual of LOOK&C. It will help users through the various steps and can serve as an indication for possible improvement to the software package. The changes made to LOOK&C during the test period are not discussed. Only the matters for possible further improvement of the software package are given attention.

Additional User Manual for LOOK&C

Use of file names

The names of test series are usually formed in such a way that they distinguish between tests, conditions, configurations and days. The problem of LOOK&C is that it cannot handle file-names larger than 3 characters. Larger file-names are cut off with an underscore for the fourth character, followed by the file extension. After each processing step with BM and Mod1 to 3, the file-names have to be manually altered. When processing data series of different settings, this can easily lead to confusion and loss of information.
For every configuration that is substantially different from other configurations, or when the conditions are entirely different, a new calibration has to be performed and new data sets recorded. The co-ordinates of the grid and the reference area are then usually different too. The co-ordinates of grid and reference area are stored in the initial-file of BM, the l&c_bm.ini. It would be convenient if the initial file could be renamed after its specifics but BM only recognises the original name. This can again lead to confusion and loss of data. The same is valid for the concentration file, the conc.dat file, used in Mod2, and for an adjusted concentration fit, *_FIT2.rtf used for Mod3.

Processing with BM

The best way to install a certain grid is to first adjust the x- and y-partitioning in the initial file, the bm_l&c.ini file. Then start BM and with 'select world co-ordinates' one can place the grid in its proper position. When trying to adjust the partitioning under 'properties', this might cause BM to crash on some computers. Other parameters can be adjusted under 'properties' without problems.
When different partitioning is applied to a grid with identical property-co-ordinates, the BM-display shows grid areas of different sizes. Although the property-co-ordinates have remained the same, the property-grid values have changed.

Processing with Mod1

Having picked a zero-concentration file with and without flow, Mod1 shows an error-report twice. When using a fine grid, the error-report is longer than the screen so only part of the error-report can be observed.
Although an error-report is given when a grid cell is selected, it is not clear how this information can be used to ascertain the accuracy of LOOK&C as a whole. It is also not clear which light conditions are preferable for doing tests with LOOK&C. Should they be kept constant or not, and what are the consequences?

Processing with Mod2

Before starting Mod2 one has to make sure the concentrations in the concentration file, conc.dat, range from 0 to 30. The actual concentrations used for the calibration have to be scaled back to the value range 0 to 30. When a different range is used, chances are that Mod3 will crash. When the concentrations range from 0 to 300 or 3000, Module 2 gives an

overflow error. When the concentrations range from 0 to 3, the errors in the fit2 are enormous, from -200% to + 200%.
After starting up Mod2, the property-method and the property-suggestions that have to be chosen are not clearly defined as is explained in appendix H.
In Mod2 two kinds of error-reports are given. The first appears when a grid cell is selected. The second error-report is shown when the button 'error-report' in the heading is selected. This second report is of no use because there is no indication of the importance of the fail-numbers mentioned there. Again the question arises whether and how this information can be used for an insight into the accuracy of results.

Processing with Mod3

The first step in processing with Mod3 is selecting the so-called fit files. It is not made clear which of the two fit1 files to choose: the zero-concentration fit file or the fit file without flow (choose the fit file without flow).
Then a data set has to be selected for processing and the final step is pressing the 'Go!' button. Mod3 then shows the change in concentration over the time span of the test series per grid cell. The general picture is a gradual change in concentration over time. Some grid cells or areas in the grid turn black for a certain time interval. The black cells or areas move over the grid over time and give the impression of a disturbed data set. Although this looks worrisome, the outcome of both Mod2 and Mod3 give no indication of disturbances.
Another item worth mentioning is that with increasing concentrations, the colour blue of the grid cells in the Mod3-display get darker but above a certain concentration, the Mod3-display only gives a light-blue shade for each grid cell although it should give a darker colour still. This can again lead to doubts about the accuracy of the data set but is in itself no reason to worry.
The speed at which Mod3 shows the change in concentration is highly dependent on the grid partitioning. With a fine grid, the changes over time can be clearly monitored. With a less fine grid, Mod3 is too fast to make out anything.
The question is if the Mod3-display in this form is useful or just confusing.

Post-processing

When processing data, the raw outcome of LOOK&C are the numbers in the *_MASS.RTF output file. The first column of the output file gives the concentration relative to the highest concentration found in that particular test series. The second column gives the data that can be calculated back to actual dye masses. The proportion between this data and the actual dye masses is determined by a factor, the average mass factor, which can be calculated from the calibration calculations. By putting the calibration concentrations through LOOK&C as well, and since the injected dye mass per concentration is known, the average mass factor can be determined.

Appendix H. Validation of DCM Results

H.1. Introduction

This appendix contains a report on the extensive tests that have been performed to optimise the DCM results and to investigate the validity of the DCM results. Tests have been performed with the DCM digital recordings (*.avi files) and with the DCM program LOOK&C. The conclusions of this section have already been reported on in the main text.

The tests that have been performed are the following:

Phase 1 tests:	Performing phase 1 tests
	Distinction between different colours
Phase 2 tests:	Background concentration
LOOK&C tests:	Calibration concentrations
	Accuracy dye mass calculations
	Grid partitioning
	Module 2
	Reference area size
General tests:	Grid position in harbour
	Salinity
	Light conditions

The results of the tests will be given in order of appearance.

H.2. Phase 1 tests

The first results for phase 1 hardly showed any differences in dye exchange between the reference configuration and the configurations with the modification and with CDW. Since the PTV results did show significant differences in flow pattern it was concluded that the signals as shown in the results might not be accurate. The first possible problem could be that the flow disturbance caused by the dye input was present throughout the test and therefore disturbed results. The second possible reason was that there might be a different response for different colours. From data analysis with the DCM program KLEUR, that is able to look into the three base colours separately, it appeared that the colours red and blue disturbed the averaged grey scale response. The KLEUR analysis suggested that the best results could be obtained by using the colour green only.

Both matters were looked into and will be discussed in the sections H.2.1 and H.2.2.

H.2.1. Performing phase 1 tests

The reason for this test was to investigate the influence of the method of dye input and the decline in dye concentration for the duration of the test. This was done by analysing separate images over the course of a test. The result is given in figure H.1. For this test a 90-degree harbour with CDW was used with an extracted discharge of 1 l/s (test series SH1abd01).

t=0s

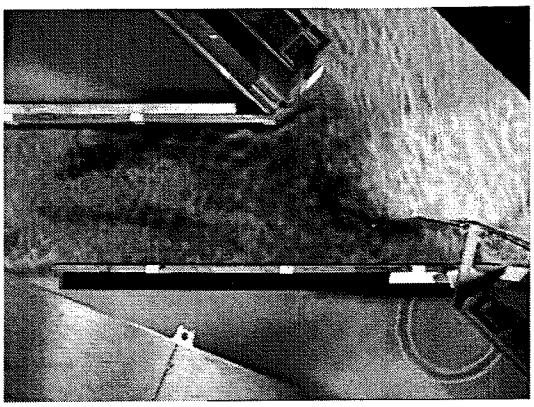

t=25s

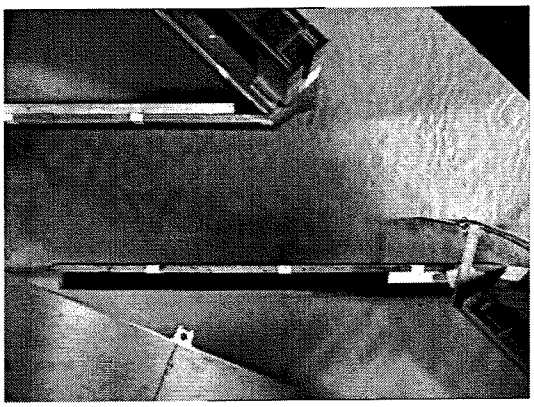

t=50s

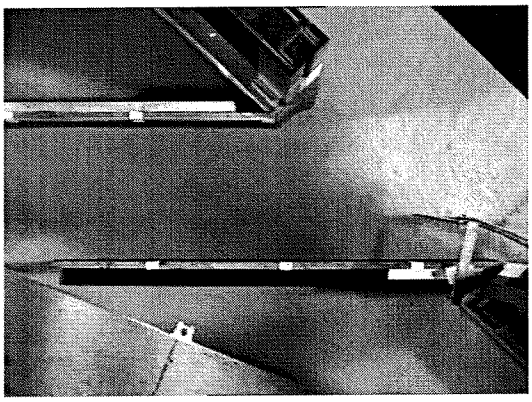

t=100s

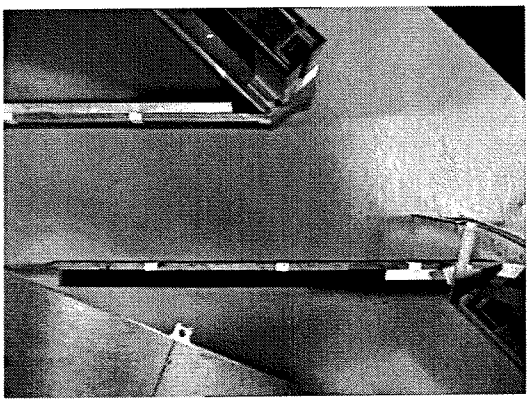

t=150s

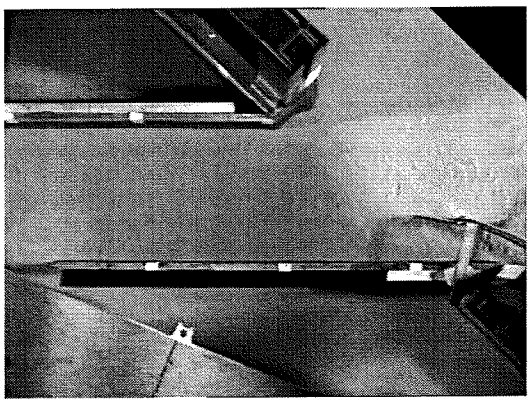

t=275s

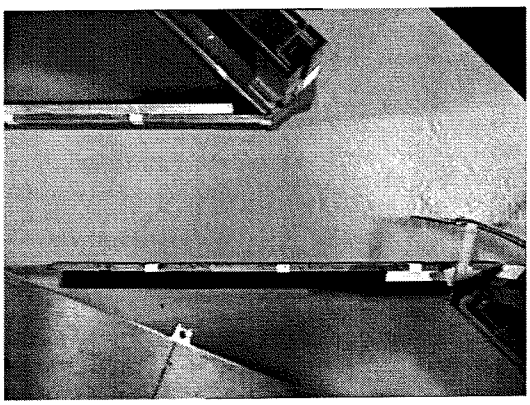

Figure H.1. Decline in dye concentration after dye input at t=0s.

The figure shows the rather large disturbance of flow caused by the input of dye solution at t=0s, as was described earlier. This disturbance is no longer visible at t=50s and the dye solution has spread equally over the control volume. The recording at t=50s further shows the flow adjustment in the harbour entrance by the CDW. Another matter of interest is that despite the rapid decline in concentration at the beginning of the test, the presence of dye in the harbour is visible throughout the test. For the 2 l/s extracted discharge the decline was more rapid.

Neither these images nor the LOOK&C results gave any indication of flow disturbance after t=50s.

H.2.2. Distinction between different colours

When the matter of different responses for the different colours was looked into it became clear that it influenced the shape of the result curve.

The response of the colour grey is the average of the responses of the colours red, green and blue. Normally LOOK&C only works with the grey response. Now LOOK&C was used on data sets containing the separate colours only. The results show there is a substantial difference in the response curve in figure H.2. Red was indeed disturbing the signal because its response curve showed a sharp increase in dye concentration until about t=150s after which there was sharp decrease in dye concentration. With dye solution being added only at t=0s this response does not seem logical.

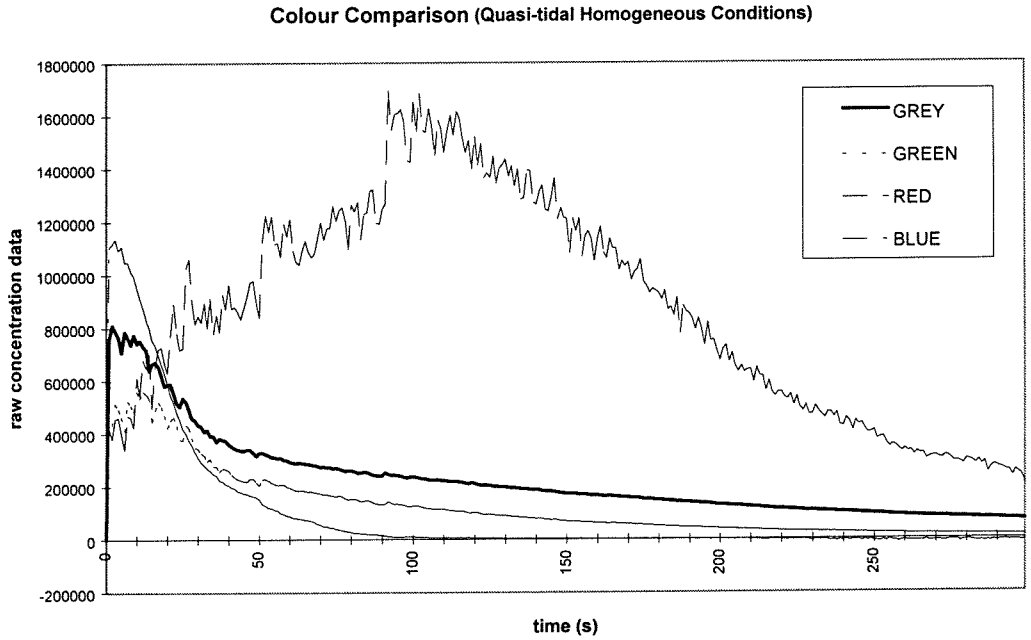

Figure H.2. LOOK&C with different base colours (using the same data set)

The colours red, grey and blue should be equally important for the averaged grey response. However, this cannot be concluded from the figure. This indicates that somewhere during recording or processing the colours of the data sets were adapted. The most logical source for this adaptation is the camera that recorded the experiments or the program Image Robot that was used for filtering out the colours for this particular test. Optical instruments or software is sometimes designed to bring out colours differently for a visual result better suiting the human eye.

From the results it appears that the colours red and blue should be left out of the data processing and that only the colour green should be used.

H.3. Phase 2 tests

H.3.1. Background Concentration

Maintaining the same base conditions throughout the test series is important for the accuracy level of the results. Most conditions could be kept the same but the background dye concentration turned out to be an unavoidable variable.

The varying background concentration posed a problem because the added dye solution gave less contrast with the flume water when the background value was raised. Moreover, different levels of calculated concentrations have different error levels (see section H.4.2). The negative effect of this aspect on the results was instantly visible. With only a slightly varying background concentration, the test results were reproducible to a very large extent. When background concentrations varied, the results were less similar.

Before the tests started it was assumed that the methylene blue (C16H18ClN3S.3H20) would loose its colour in a day or so but it did not. With each test more dye accumulated in the system and the flume turned gradually more blue. An extra factor creating a larger background value was that the dye also stuck to the walls and the bottom.

The background concentration was checked for every set of tests. For phase 1 it did not turn out to be a significant problem. For phase 2 it was a different matter because larger quantities of dye were used over a shorter period of time and because the saline water in the sea did not refresh itself quickly. The 'same' seawater was used several times, each time absorbing part of the injected dye solution. The dye accumulated in the saline water and only slowly disappeared from the system through mixture with fresh water from the river. This brackish water was lead straight into the sewer and not reused. Figure H.3 gives an illustration of the different background concentration levels during phase 2.

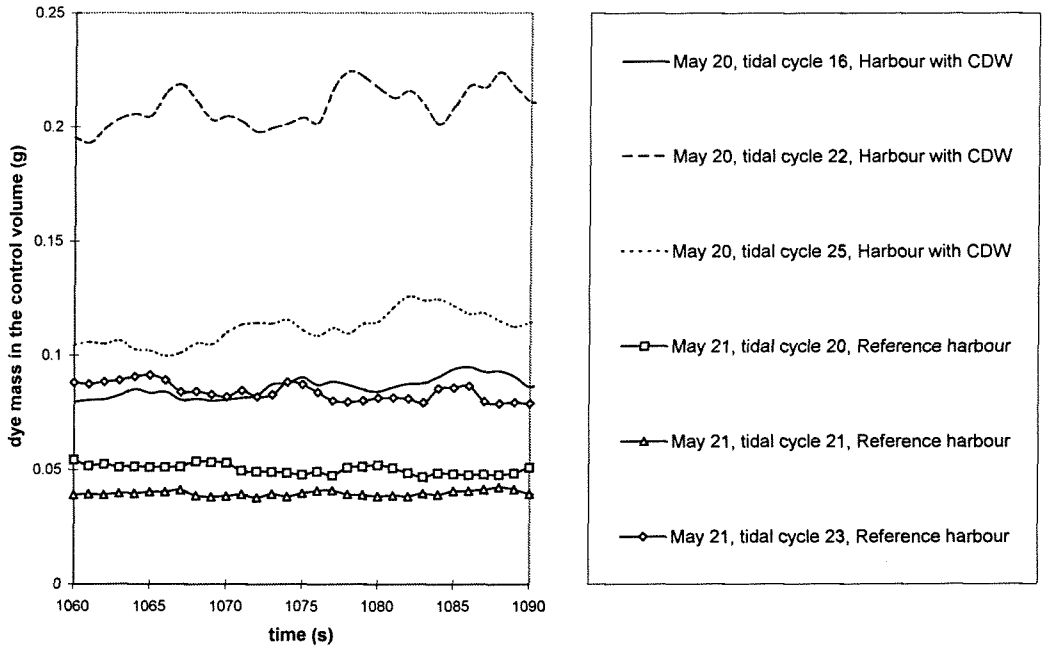

Figure H.3. Different background concentrations during phase 2

The figure shows that there was a substantial difference in background concentration between days and even between test series of one day. These background concentrations are especially large when the increase of dye mass in the control volume per test is taken into consideration. The dye increase for the tests at t=60s was only about 0.04 to 0.12 g while the background concentrations for these tests are in the order of 0.04 to 0.22 g (figure H.3). The figure further

shows that the signal becomes more disturbed when higher background concentrations are present.

It is clear that an increased background value has a negative effect on the accuracy of the results. The extent of that effect is discussed in more detail in section H.4.2.

H.4. LOOK&C tests

The aim of the LOOK&C tests was to investigate the influence of LOOK&C on the accuracy of the results and to investigate the various LOOK&C parameters.

For the tests Grid partitioning, Reference area size and Position grid in the harbour, the same data sets are used (tdbl_1.2, tdbl_1.3). Only one factor was varied per test. For all of these tests the input parameters for Module 2 of LOOK&C were: suggestion (0) = 0.500, suggestion (1) = -0.01.

H.4.1. Calibration Concentrations

The calibration concentrations form the link between the actual concentrations during tests and the concentrations as calculated with LOOK&C. This link, the concentration fit, has great influence on the eventual results. From the calibration tests the following appeared.

The grey value difference between concentration 0 and concentration 1 was considerably larger than the grey value difference between concentration 4 and 5 although equal quantities of dye mass were added for each following concentration. More calibration concentrations were created at lower concentration levels for a better fit for these lower concentrations.

Secondly, with hardly any background concentration, the average concentration in the actual tests never reached the highest concentrations created in the calibration. Therefore it is even more important that the lower concentrations are properly calculated. Leaving the unused higher concentrations out of the concentration fit would improve the accuracy of the results even further. This was not applied for the present study because the varying background concentrations made it impossible to leave out any of the higher calibration concentrations.

Another matter concerning the calibration was that the calibration area was formed by placing a Perspex plate across the harbour entrance and a Perspex plate towards the head of the harbour. In this way only a small area had to be used for the calibration instead of the entire system. This speeded up the calibration process and prevented too much dye from entering the harbour. Especially the Perspex plate across the harbour entrance blocked some of the light that usually entered the harbour basin from the opposite side of the flume. This has a negative impact on the calibration fit because the light conditions during tests were now different from light conditions during the calibration. For practical reasons the calibration could not have been performed otherwise. The effect of an influenced fit will be further discussed in the following sections.

H.4.2. Accuracy dye mass calculations

The concentration fit that was made with the calibration concentrations has a different level of accuracy for different levels of dye concentrations as can be seen in table H.1. It gives an indication of the error that is introduced by using the calibration concentrations (phase 2).

Calibration concentration no.	Concentration (g)	Error (%)
1	0.04	34

2	0.08	11
3	0.12	2
4	0.16	-17
5	0.21	-16
6	0.27	-9
7	0.33	-3
8	0.41	0
9	0.56	-2

Table H.1. Indication of the error introduced by using the calibration concentrations.

From table H.1 it becomes clear that the error introduced by the calibration is substantially different for different levels of concentration.

The error that is introduced by LOOK&C will have an effect on the phase 1 and phase 2 results. For both phases an example is given of the possible influence on the results. First an example is given for phase 1 with an exponential fit that renders negative exchange discharges (see figure H.4).

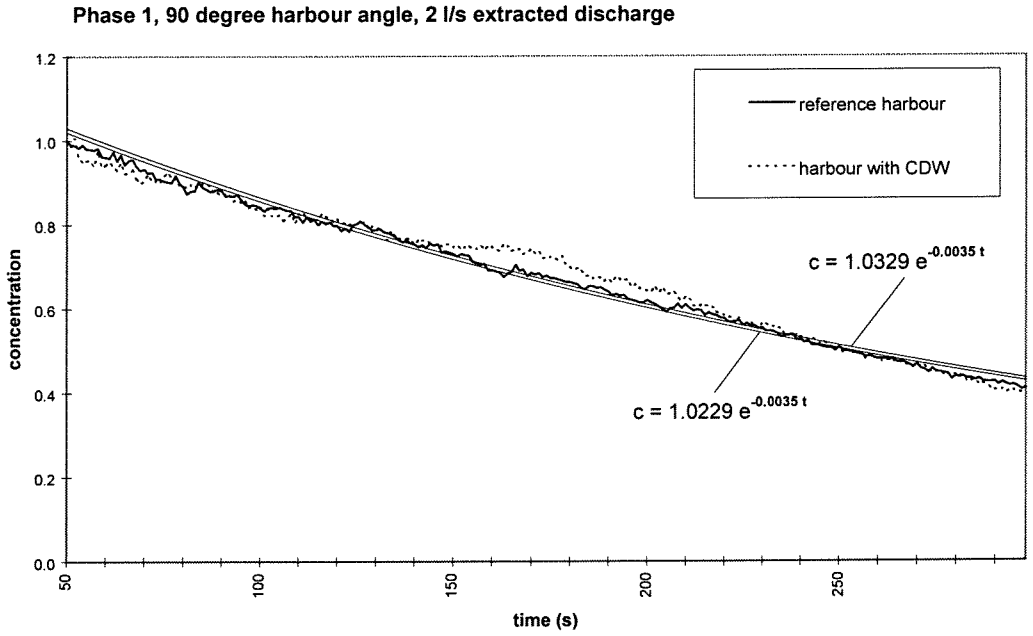

Figure H.4. Exponential fit through phase 1 results

With the use of equation 6.4 and the results from the exponential trendlines in figure H.2: $e^{-\frac{Q}{V}t} = e^{-0.035t}$. With V = 305 l (control volume for the 90 degree harbour basin) then follows that Q = 1.07 l/s for both configurations in figure H.2. This calculated discharge consists of two components: the extracted discharge (net filling effect) and the exchange discharge. The extracted discharge (in this case is 2 l/s) subtracted from the calculated discharge renders a negative value for the exchange discharge of –0.93 l/s. As was discussed chapter 8 this is impossible.

The effect on phase 2 results of the errors when calculating dye masses can best be illustrated with figure H.5. It shows the result of the 95% reliability error band for the configuration A (reference condition) and configuration C (with both the downstream CDW and the upstream

sill). It shows there is still a significant difference between the two configurations. The error band of configuration B results falls over the error band of the other two configurations.

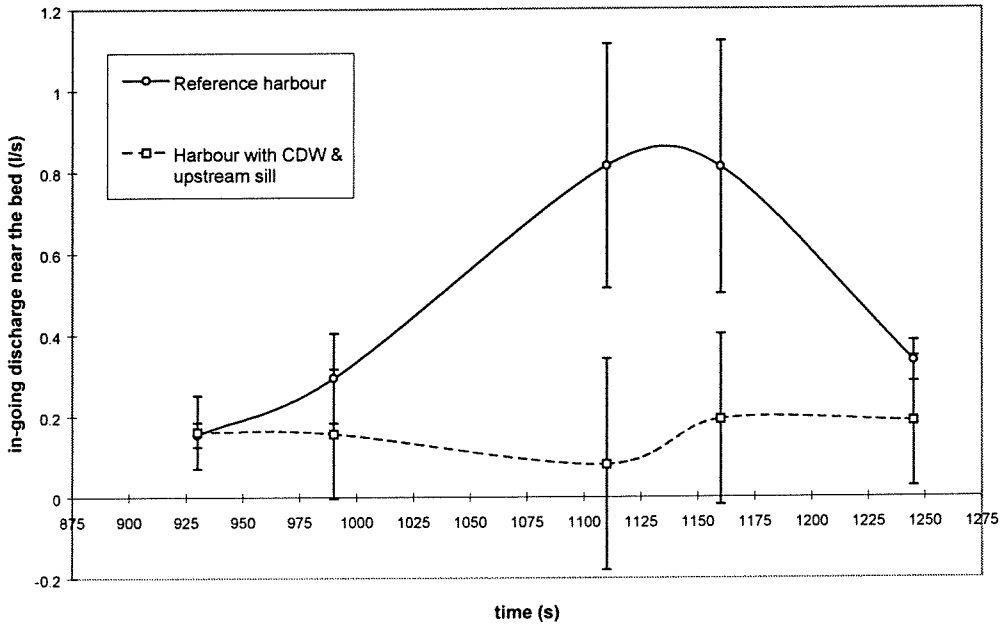

Figure H.5. Error band of 95% reliability for the results of configurations A and C

H.4.3. Grid partitioning

The first phase 2 results showed a rather large disturbance of the response signal. It appeared that the partitioning of the grid had a big impact on this kind of disturbance.

The rectangular grid area used for the LOOK&C calculations can be partitioned in x- and y-direction with a maximum of 50 grid cells is both directions. For an investigation of the influence of partitioning on the results, 3 different partitioning sets were used on one data set. The grids were 1x1, 15x5 and 50x50. The surface of each of the grid areas has remained the same: 1.75m x 0.50m. See figure H.5 for the results.

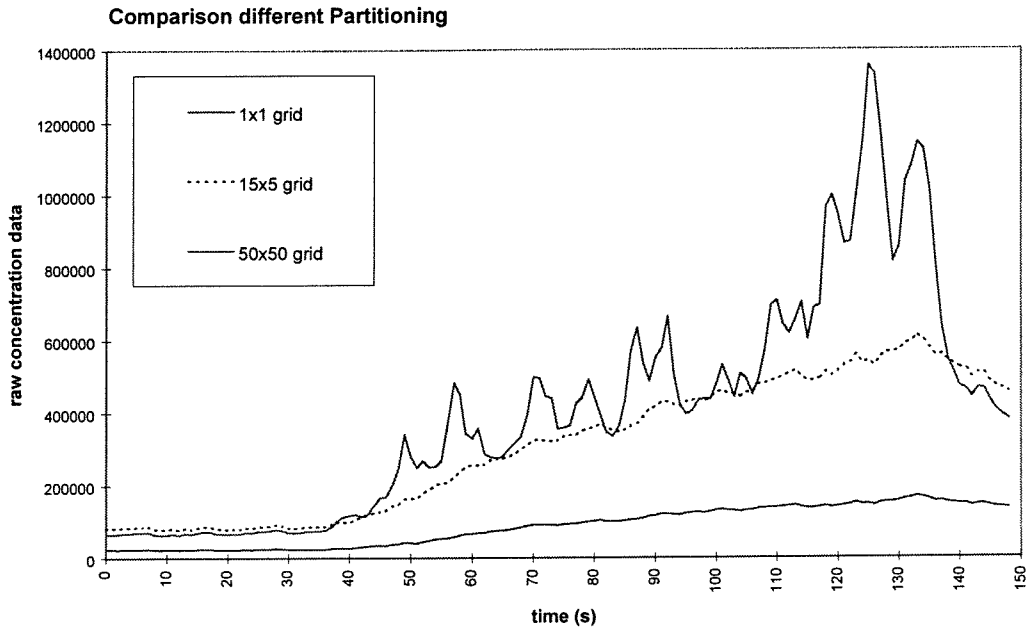

Figure H.5.

From the tests the following appeared:

1. Using the partitioning 1x1 to approximately 15x5 should give smooth results. When a finer grid is used the result graph is very likely to consist mainly of big spikes.
2. Using fewer grid cells renders lower values for the calculated dye masses although the surface area of the grid is kept the same.
3. The basic response of the different grid partitioning used is generally the same.

The property-suggestions in Mod2 are probably the cause of the spikes found when using a fine grid. The next section explains.

H.4.4. Module 2

The influence of Module 2 on the accuracy of the results is explained in this section. First of all an explanation is given on the steps in data processing with Mod2.

When starting processing with Mod2 one has to choose property-method 0, which stands for robust processing. After having used the original property-suggestions, the output files of Mod2 give an indication what the values for the suggestions should have been. The fourth last column and the third last column of the *_DAT2.RTF file give an indication of what suggestion 0 and 1 should have been respectively. These values should be used for obtaining a good concentration fit.

However, there can be a spread in the indication given in the *_DAT2.RTF file. The appearance of large values belonging to individual grid cells is a sign of large spikes in the final results. When using a less fine partitioning there is no big spread in what the value for suggestion 0 should be. With a fine partitioning the spread for suggestion 0 is huge. The output file of Mod2 is used for processing all data and with the high values big spikes in the final results are created.

Mod2 gives the possibility to leave out certain grid cells for the mass calculation. This is sometimes needed to make the grid area fit a harbour shape that is not rectangular or to leave out grid cells that fall outside the calibration area. After having selected all calibration files in

Mod2, an overview of the entire grid area indicates which cells should not be used. Those grid cells are a lighter or darker shade of red. The red cells should be left out of the mass calculation. For a less fine grid this red indication works and the high values for suggestion 0 (causing the spikes) are eliminated. For a fine grid this indication with the colour red is not good enough. Still very high numbers for suggestion 0 are included into the final result although no red indication is given for all these cells.

H.4.5. Reference area size

For the data processing a rather narrow strip was used as a reference area in BM. The results with this reference area showed what seemed to be a disturbance over the actual signal as was described in the previous section. The size of the reference also seemed to have an effect on this disturbance. To check the influence of the size of the reference area, its size was increased. The larger reference area gave a much smoother signal. Although the calculated dye mass was 17.5% less with the bigger reference area this was to be preferred over the ragged signal. For a comparison see figure H5.

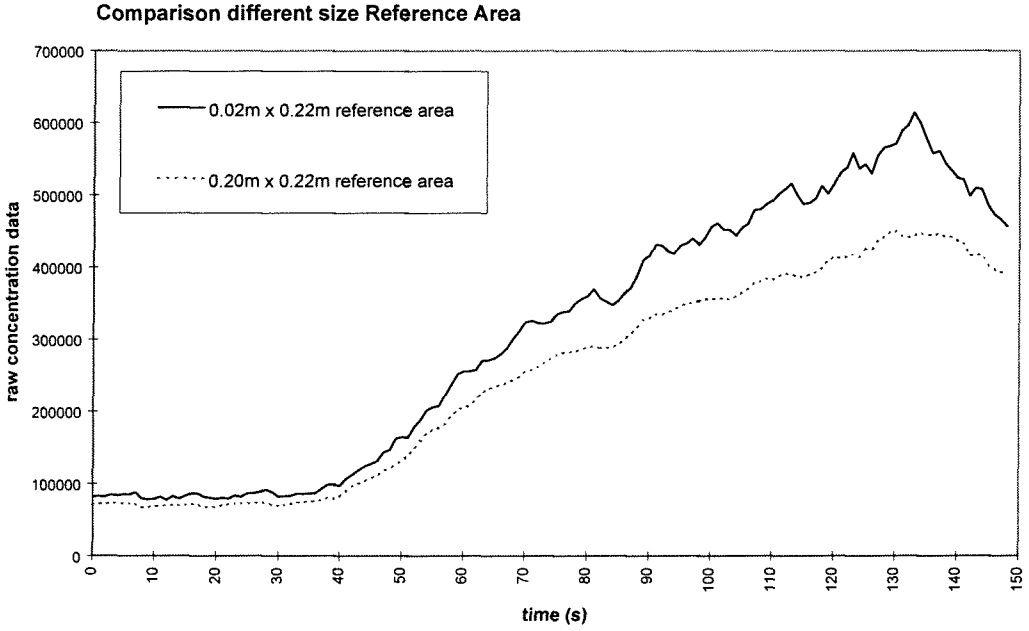

Figure H.5.

The two different reference area surfaces used were 0.02m x 0.22m and 0.20m x 0.22m, both in the same corner of the harbour basin. The size of the grid area was 1.75m x 0.50m for both tests.

H.5. General tests

H.5.1. Grid position in harbour

The grid areas used for data processing all directly bordered the river with the flume sides of the grid only just inside the harbour basin. As was indicated before the results of phase 1 did not show much difference between tests. One of the ideas was that this might have been caused by the place of the grid directly adjacent to the river. Because of this, part of the grid covered the harbour entrance. Part of the mixing layer or part of the CDW-induced flow pattern were the cause of a very rapid exchange in this area. In a short time span almost

nothing of the injected dye solution in this area was still visible. By placing the grid more to the head of the harbour the exchange might be more gradual and more comparable to exchange for the reference configuration.

Placing the grid area 0.47-cm away from the direct harbour entrance tested this. The recorded harbour area had a length of 1.75m. Figure H.6 shows the relative result.

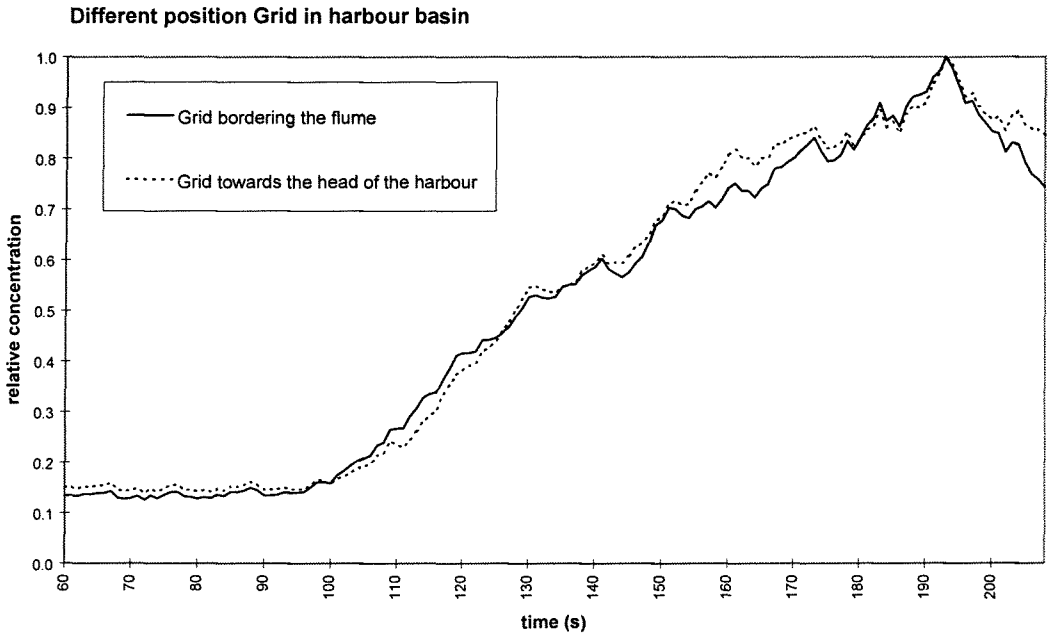

Figure H.6.

Although the grid not bordering the river is situated quite far inside the basin, there seems to be no phase lag in the response curve. It was therefore concluded that there was no difference in the response of a grid area in the vicinity of the harbour entrance. A second conclusion might be that there is almost instantaneous mixing in the harbour basin and that the harbour is homogeneously mixed.

H.5.2. Salinity

When performing the calibration dye solution was added to the closed-off harbour area and well mixed to avoid an unequal spread of dye over the area.

For phase 2 tests dye was only injected in the lower half of the water column and dye only entered the harbour in the lower half of the water column. The camera might pick up these concentrations over the lower half of the water column differently than it would when the same concentration was evenly distributed over the depth. This possible effect was not studied.

Secondly, for phase 2 a saline dye solution was used while the calibration was performed under fresh conditions. The salinity might have an influence on the light conditions as seen by the camera. This, in turn, has an effect on the calculated dye mass.

H.5.3. Light conditions

The light intensity plays an important role because one grey value (= one fixed concentration) can be seen by the camera as a different value under different light intensities. In relation to the light intensity there were several matters to be reckoned with:

- For a recording with more contrast between the system and the added dye extra lights were put up;
- Too much light gave a distorted camera view in which changes in dye concentrations could not be distinguished;
- Reflections in the camera image of the lights shining down were to be avoided;
- Lights attached to the sides of the harbour and shining under a slight angle gave shadows of the mixing zone and waves on the bottom. Secondly, the reflections of waves on the bottom were better visible than the flow disturbance itself. Therefore the disturbance could be seen in a spot next to the place were the disturbance was created instead of under the disturbance. This phenomenon confused visual observations;
- Some debris or a small stagnant shadow in the water does not have a significant effect on the results. LOOK&C checks the colour difference for one grid cell over time and the size of the grid cell is much bigger than the piece of debris. Stagnant shadows in the grid area only render a higher background concentration at the beginning of each test. Changing light conditions or shadows over the entire area, including the reference area, are compensated for in Mod1.

The best results were obtained with several halogen lights shining in the length direction of the harbour entrance, from both sides.

Appendix J
Tests undertaken during phase 2

Date	config.	Relevant tidal cycles	test no.	Kind of measurement	Remarks	CD no.
30-mrt	various			video tape	H. Christiansen optimizes CDW	
31-mrt	various			video tape	H. Christiansen optimizes CDW	
14-apr	X	12-14,20-21	TDAA	PTV		
22-apr	A		TDBA	Density	Density measurements in harbour were faulty	
23-apr	A	9-11,13-15	TDBB	EMS PTV		
27-apr	A			EMS		
28-apr	A			EMS		
29-apr	A			Density		
03-mei	A	20-22,24-27	TDBF	Density EMS		
04-mei	A		TDBG	Density		
05-mei	A		TDBH	EMS/Density	Determining undisturbed signal	
06-mei	A		TDBI	EMS/Density	Determining undisturbed signal (before tests harbour was fixed)	
07-mei	C	4-7,14-17,21-23	TDCA	PTV	Dens. Meas in harbour was faulty	
10-mei	A	6-17, 20-22, 24-26, 28-30	TDBJ	Density	Plus three positions in harbour	
11-mei	C	6-17, 20-22, 24-26, 28-30	TDCB	Density	Plus three positions in harbour	
12-mei	B	6-12, 15-17, 19-21, 23-25	TDDA	Density	Plus three positions in harbour	
17-mei	A		TDBK	Dye		
18-mei	B	7-9, 11-13, 15-17, 19-21, 23-25, 27-29	TDDB	EMS		
19-mei	C	6-8, 10-12, 14-16, 18-20,22-24,26-28 29-end	TDCC	EMS Dye		
20-mei	C B	6-25,26-35	TDCD TDDC	Dye PTV		
21-mei	C B A C A	7 8 10 11 13 14		Video Threads Video Threads Video Threads Dye Dye		

Configurations:

X Blunt harbour entrance
A No CDW - modified harbour entrance
B Downstream CDW
C Downstream CDW and upstream sill

Appendix K
Extrapolating model results

The influence of the various parameters in the model on the performance of a CDW can be examined by systematically changing them. Although the results cannot be trusted very much, as the model is validated on only one test. The model used for these calculations was model 1. The other model can be used in the same manner. Important parameters that can vary for various harbours are:

- Harbour area
- Phase lag between water level variation and flow velocity
- The "strength" of the CDW.
- The amplitude of the density in the river
- Width and depth of entrance.

Most of these parameters influence both the density current and the tidal filling. It is therefore difficult to predict what the effect of changing one of them will be. In the figure 9.6.8 the influence of some of these parameters on the relative reduction of exchange due to the CDW is depicted. These graphs give the following conclusions:

Harbour area

A CDW will reduce exchange very much in a harbour with a small surface area. This is probably because the density current is smaller in a small harbour. The density difference between harbour and river decreases, when the density in the harbour follows the density on the river better.

When the harbour area increases very much, the harbour area the CDW functions the same during flood. The negative effect just after the functioning of the CDW is less, because the density in the harbour will be affected less.

Phase lag water level variations and flow velocities

The phase difference does not have much effect, surprisingly. One would expect an increasing exchange, with an increasing phase-lag. The moment of functioning of the CDW overlaps more with the time the density current takes place, when the time-lag increases. Other effects (tidal filling?) probably also have an effect.

Magnitude of CDW effect

When the magnitude of the CDW-effect increases, the total inflow over the bottom layer is increased almost proportionally. The total inflow also increases, but the increase of the total inflow does get less for increased CDW discharges. This is probably because of the negative effect caused by a functioning CDW: After the CDW stops functioning the density difference has increased, so the exchange increases.

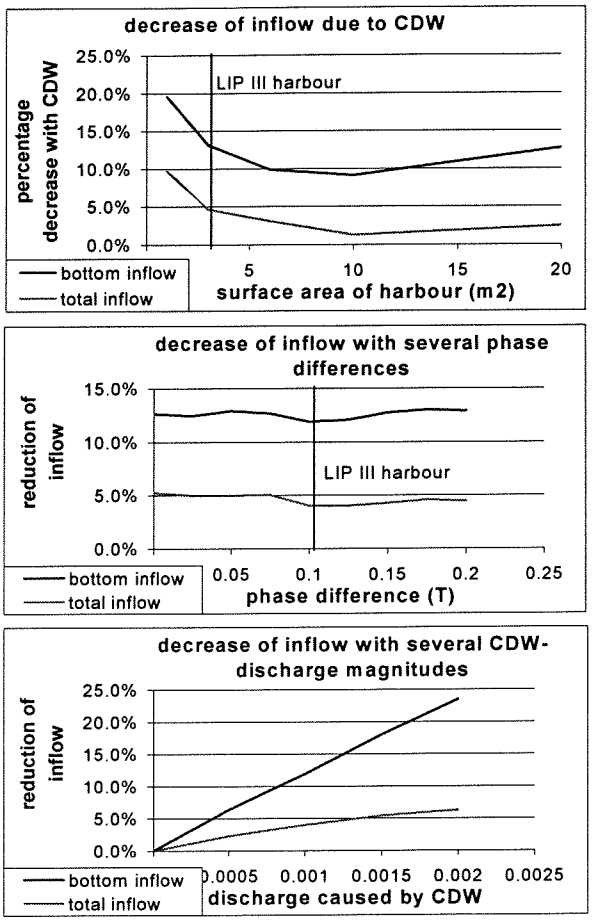

Figure K.1. Computed decrease of exchange, as a function of certain parameters, when applying a CDW.

Appendix L
Determination of undisturbed density exchange volume

When the harbour volume (V_h) is infinitely large, the density in the harbour does not change due to the inflow caused by the density current during a tidal cycle (V_d). When V_h decreases, the density in the harbour will adapt over the tidal cycle, the average density difference will be smaller, and the exchange volume due to the density current will decrease. The maximum volume of water due to the density current ($V_{d,o}$) is exchanged when: $V_h >> V_{d,0}$.
This maximum volume of exchanged water due to the density current is now calculated.

The flow in the entrance is:

$$u_d = f_3\sqrt{\frac{\Delta\rho}{\rho}gh}$$

$$Q_d = \tfrac{1}{2}Bhf_3\sqrt{\frac{\Delta\rho}{\rho}gh} \qquad [1]$$

$$f_3 \approx 0.45$$

In which:

B = width of harbour entrance
h = depth of entrance
g = gravitational acceleration
Δρ = difference in density between harbour and river

The following assumptions are made in order to determine the discharge:

$$\rho_r = \overline{\rho}_r + \hat{\rho}_r \sin\left(2\pi/T\, t\right)$$

$$\rho_h = \overline{\rho}_r$$

$$h(t) = \overline{h}_0 \qquad [2]$$

In which:

ρ_h = density of harbour water
ρ_r = density of river water
h_0 = average depth in entrance

The density discharge is integrated over a tidal cycle in order to get the exchange volume due to the undisturbed density current:

$$V_{d,0} = 2\int_0^{\frac{1}{2}T} \tfrac{1}{2}h_0 B \cdot u_d dt = 2\int_0^{\frac{1}{2}T} \tfrac{1}{2}h_0 B\sqrt{\frac{\Delta\rho}{\rho}gh_0}\,dt =$$

$$2\int_0^{\frac{1}{2}T} \tfrac{1}{2}h_0 Bf_3\sqrt{\frac{\hat{\rho}_r \sin\left(2\pi/T\, t\right)}{\rho}gh_0}\,dt = f_3 h_0 B\sqrt{\frac{\hat{\rho}_r}{\rho}gh_0}\cdot\int_0^{\frac{1}{2}T}\sqrt{\sin\left(2\pi/T\, t\right)}dt \qquad [3]$$

Let $2\pi t/T = x$, then

$$\int_0^{\frac{1}{2}T} \sqrt{\sin\left(2\pi/T\, t\right)}dt = \frac{T}{2\pi}\int_0^{\pi}\sqrt{\sin x}dx \qquad [4]$$

$$\int_0^{\pi}\sqrt{\sin x}dx = 2\int_0^{\frac{1}{2}\pi}\sqrt{\sin x}dx = \mathrm{B}\left(\tfrac{3}{4},\tfrac{1}{2}\right) = \frac{\Gamma\left(\frac{3}{4}\right)\Gamma\left(\frac{1}{2}\right)}{\Gamma\left(1\frac{1}{4}\right)} \approx 2.3963 \qquad [5]$$

In which:

Γ = Gamma function, $\Gamma(z) = \int_0^{\infty} t^{z-1}e^{-t}dt$

B = Beta function, $\mathrm{B}(z,w) = 2\int_0^{\pi/2}(\sin t)^{2z-1}(\cos t)^{2w-1}dt = \frac{\Gamma(z)\Gamma(w)}{\Gamma(z+w)}$

Combining [3], [4], and [5] yields for the exchange discharge $V_{d,0}$:

$$V_{d,0} = f_{4,\max}h_0 B\sqrt{\frac{\hat{\rho}_r}{\rho}gh_0}T$$

$$f_{4,\max} = \frac{2.3963 f_3}{2\pi} \approx 0.172$$

(notes C. Kuijper, after Eysink (1989))

Appendix M
Relation between velocity profile and density profile

Attempts were made to link the density profiles that were measured to the velocity profiles. This way the shape of the velocity profile could be determined with less velocity measurements.
When one looks at the vorticity equation (Kranenburg, 1996):

$$\frac{D\xi}{Dt} = \frac{1}{\rho^2}\left(\frac{\partial\rho}{\partial x}\frac{\partial p}{\partial z} - \frac{\partial\rho}{\partial z}\frac{\partial p}{\partial x}\right)$$

Equation M.1

and the definition of vorticity:

$$\xi = \frac{\partial w}{\partial x} - \frac{\partial u}{\partial z}$$

Equation M.2

and one assumes that the vertical profiles of velocity density are constant in the harbour mouth , the vorticity in the river is constant, and all particles in a cross section travel from the entrance of the harbour to the cross section in approximately the same time span, then integrating M.1 to t, and substituting M.2 in this equation forms:

$$\frac{\partial u}{\partial z} = K_1\frac{\partial\rho}{\partial z} + K_2$$

Equation M.3

With K is a constant.

For parallel flow with constant density profiles the following equation can be derived (Benjamin, 1981):

$$\frac{du^2}{dz} = \frac{g}{\rho_0} z \frac{d\rho}{dz}$$

Equation M.4

In which z is the vertical co-ordinate, g is the gravitational acceleration, ρ is the density, u is the velocity, and ρ_0 is the reference density.

Both equations indicate that the density profile and velocity profile can be related under certain circumstances.